Towards the development of novel *Aspergillus fumigatus* targeted antifungals with an in-depth analysis of Sfp-PPTase, PptA

A thesis submitted to The University of Manchester for the degree of Doctor of Philosophy in the Faculty of Medicine and Human Sciences

2015

Anna Elisabeth Johns

School of Medicine

Table of Contents

Table of Contents 2
List of Figures 5
List of Tables 6
List of Supplementary Figures 7
List of Supplementary Tables 7
Abbreviations 8
Abstract 11
Declaration 12
Copyright Statement 12
Acknowledgements 13
1. Introduction and Aims 14
1.1. Overview of Thesis 15
1.2. Fungi 18
1.3. Fungal Pathogens 19
1.4. Treatment of mycoses 24
1.4.1. Pyrimidine Analogues 25
1.4.2. Polyenes 25
1.4.3. Triazoles 26
1.4.4. Echinocandins 27
1.4.5. Allylamines 27
1.4.6. Combination Therapy 28
1.4.7. Novel Antifungals 28
1.5. Approaches to Antifungal Drug Discovery 30
1.5.1. Target Based Drug Discovery 30
1.5.2. *In Silico* Comparative Genomics 30
1.5.3. Essential Gene Identification 30
1.5.4. Haploinsufficiency screens 31
1.5.5. Large Scale Fitness Profiling 34
1.6. Potential Drug Targets 37
1.6.1. Phosphopantetheinyl Transferase A 37
1.6.2. Phosphatases 39
1.8. Aims 41
1.9. References 42
2. PptA, a drug target for *Aspergillus fumigatus* infection 49
2.1. Introduction 51
2.2. Materials and Methods 54
2.2.1. Identification of sequences used in this study 54
2.2.2. Strains 54
2.2.3. Generation of strains 55
2.2.4. Phylogenetic analysis 55
2.2.5. Phenotypic analysis 55
2.2.6. Secondary metabolite assay 56
2.2.7. Host response assays 56
2.2.7.1. Dendritic cell challenge 56

2.2.7.2. Phagolysosomal acidification assay 57
2.2.8. Virulence studies 58
2.2.8.1. Insect infection 58
2.2.8.2. Murine intranasal infection 58
2.2.8.3. Murine intravenous infection 59
2.2.8.4. Cortisone acetate treated murine intranasal infection 59
2.2.8.5. Histological analysis 60
2.2.9. Preparation of recombinant PptA 60
2.2.9.1. Assay for PptA activity 60
2.3. Results 62
2.3.1. PPTases form 3 distinct evolutionary clades 62
2.3.2. Type II PPTases are phylogenetically diverse 62
2.3.3. PptA is required for normal growth 66
2.3.4. PptA is required for the production of secondary metabolites in *A. fumigatus* 67
2.3.5. PptA an important factor in host response 69
2.3.6. PptA is vital for virulence of *A. fumigatus* 70
2.3.7. A high throughput screen to determine PptA activity 73
2.4. Discussion 75
2.5. Acknowledgements 78
2.6. References 79
2.7. Supplementary data 83
3. Inducible cell fusion in the human pathogenic fungus *Aspergillus fumigatus* permits use of parallel fitness analyses to determine the mechanism of action of antifungal compounds 91
3.1. Introduction 93
3.2. Materials and Methods 95
3.2.1. Strains 95
3.2.2. Strain construction 95
3.2.3. Assessment of cell fusion 96
3.2.4. Parallel fitness profiling 96
3.2.5. Real time PCR fitness assessment 98
3.2.6. Individual growth assays for fitness assessment 98
3.3. Results 100
3.3.1. Conidial anastomosis tubes are not produced by *A. fumigatus* 100
3.3.2. Cell fusion is enhanced between complementing auxotrophic mutants 101
3.3.3. Cell fusion was not observed in shake flask culture 103
3.3.4. Cell fusion is induced by exposure to antifungal stress 103
3.3.5. Low levels/absence of cell fusion in *A. fumigatus* permits parallel fitness profiling of heterozygous diploid strains 105
3.4. Discussion 110
3.5. Acknowledgements 113
3.6. References 114
3.7. Supplementary data 117
4. Exploring the *Aspergillus fumigatus* phosphatome for potential drug targets 122
4.1. Introduction 124
4.2. Materials and Methods 126
4.2.1. Bioinformatics 126

4.2.2. Phylogenetic Analysis 126
4.2.3. Phosphatase knockout generation 126
4.2.4. Parallel Fitness Profiling 127
4.2.5. NGS library preparation 127
4.2.6. Ion Personal Genome Machine (PGM) system preparation 129
4.2.7. NGS data processing 129
4.2.8. Individual growth rate assessment 130
4.3. Results 131
4.3.1. There is high similarity between phosphatase types in fungal species 131
4.3.2. Fungal specific phosphatase groups are found in many phosphatase families 133
4.3.2.1. Phosphoprotein Phosphatases (PPP) 133
4.3.2.2. Metal-dependent protein phosphatases (PPM) 135
4.3.2.3. Aspartate based phosphatases 135
4.3.2.4. Protein tyrosine phosphatases (PTP) 137
4.3.2.5. Dual-specificity phosphatases (DSP) 139
4.3.2.6. MTM and PTEN phosphatases 139
4.3.3. Parallel fitness profiling in *A. fumigatus* allows high throughput drug target identification 141
4.4. Discussion 144
4.5. Acknowledgements 147
4.6. References 148
4.7. Supplementary Data 151
5. Conclusions and Future Work 163
5.1. References 167
6. Appendix 168
6.1. Introduction 170
6.2. Methods and Materials 173
6.2.1. Sfp-PPTase identification 173
6.2.2. Strains 173
6.2.3. Deletion of pptA 173
6.2.4. Radial growth rate 174
6.2.5. Determination of grow rates in liquid cultures 174
6.2.6. Coomassie (Bradford) protein assay 175
6.2.7. Clearance zone assay 175
6.3. Results 176
6.3.1. Identification of a Sfp-PPTase in *T. reesei* 176
6.3.2. Sfp-PPTase is required for normal growth in all species 177
6.3.3. *T. reesei* Δ*pptA* exhibits an increased growth rate in the presence of lysine 179
6.3.4. Sfp-PPTases have a significant effect on total protein production under certain conditions 181
6.3.5. An increase cellulase production is caused by Sfp-PPTase deletion 183
6.4. Discussion 184
6.5. Acknowledgements 185
6.6. References 186

Total word count: 54,321

List of Figures

Figure 1.1:	Top 4 prevailing fungal pathogens	19
Figure 1.2:	Haploinsufficiency screen	32
Figure 1.3:	Heterozygote deletion construct	33
Figure 1.4:	Schematic of conditional mutant generation using the GRACE method	34
Figure 1.5:	Two Step Fusion PCR	36
Figure 1.6:	Phosphopantetheinylation	39
Figure 2.1:	Molecular Phylogenetic analysis of Sfp-PPTases by Maximum Likelihood method	64
Figure 2.2:	Sequence alignments Sfp-PPTases	65
Figure 2.3:	Dose response of a *pptA* null isolate to increasing concentrations of TAFC or Lysine	66
Figure 2.4:	Analysis of secondary metabolite production	68
Figure 2.5:	Immune response to different Aspergillus mutant strains	69
Figure 2.6:	Detection of conidia in acidified compartments after phagocytosis by RAW264.7 macrophages	70
Figure 2.7:	The effects of A) a series of KO mutants of *A. fumigatus* on the mortality of the larvae and B) an iron treatment on the pathogenicity of Δ*pptA* and Δ*sidA* in a larvae model	71
Figure 2.8:	Kaplan-Meier curve and histology for murine survival	72
Figure 2.9:	PptA-GST and AarA-pManHis protein expression and purification	73
Figure 2.10:	A) Fluorescence polarization (FP) Schematic. B) Titration of PptA (0-200ng per reaction) in the fluorescent polarisation assay	74
Figure 3.1:	Static liquid co-culture of RFP and GFP expressing strains (AfRFP and AfGFP) in AMMNO3	100
Figure 3.2:	Co-localisation of GFP and RFP strains when co-inoculated on solid AMMNO3	101
Figure 3.3:	Static liquid co-culture of nitrogen starved RFP and GFP expressing strains (AfRFPniaD and AfGFPcnx) in $AMMNO_3$ liquid medium	102
Figure 3.4:	Co-localisation of GFP and RFP strains when co-inoculated on solid AMMNO3 in the presence of stress	104
Figure 3.5:	Schematic representation of the chemical genomics methodology employed in this study	106
Figure 3.6:	Alligned scatter diagram of relative change in fitness (Log 2)	107
Figure 3.7:	Real-time PCR quantitative analysis of the DNA analysed by en mass sequencing	108
Figure 3.8:	Fitness assessment of strains in growth assays on solid $AMMNO_3$ agar medium (A and B) and (C) liquid RPMI 1640 media in the presence and absence of drug	109
Figure 4.1:	Schematic of DNA preparation for NGS	128
Figure 4.2:	Comparison of the protein phosphatase in different fungal species	132
Figure 4.3:	Phylogram of PPP	134
Figure 4.4:	Phylogram of PPM	136
Figure 4.5:	Phylogram of PTP	138
Figure 4.6:	Phylogram of DSPs	140
Figure 4.7:	33 non-essential phosphatase knockout strains generated	141
Figure 4.8:	Pairwise comparisons of A) technical and B) biological replicates	142
Figure 4.9:	Alligned scatter diagram including all the Log2 data points from the parallel fitness and the individual growth rate studies	143

Figure 6.1: Phosphopantetheinylation 171
Figure 6.2: Sequence alignment of *A. fumigatus* PptA and the *A. niger* and *T. reesei* orthologues. 176
Figure 6.3: Photographs of parental and Δ*pptA* strains 178
Figure 6.4: Radial growth rates of parental and Δ*pptA* strains 179
Figure 6.5: Growth rate measurements in 96 well plate 180
Figure 6.6: Coomassie (Bradford) protein assay 182
Figure 6.7: Protein gel of *A. fumigatus* supernatants 182
Figure 6.8: Cellulose clearance assay 183

List of Tables

Table 1.1: Different types of aspergillosis including symptoms, diagnostic criteria and treatments 23
Table 2.1: Fungal strains used during this study 54
Table 6.1: Strains used in this study 173
Table 6.2: Primers used to generate gene deletion cassette 174
Table 6.3: List of Clustal W pairwise alignment scores and BLASTp analysis between *A. fumigatus* PptA, *A. niger* PptA and *T. reesei* (protein ID 41504) 177

List of Supplementary Figures

Figure S2.1: Phosphopantetheinylation 85
Figure S2.2: Southern blot analysis was used to confirm single intergration of knock out and reconstitution cassettes in mutant strains 85
Figure S2.3: Molecular Phylogenetic analysis by Maximum Likelihood method 86
Figure S2.4: Fungal Sfp-PPTases signature 87
Figure S2.5: Partial sequence alignment of a selection of fungal A) AcpS-type, B) Sfp-type and C) FAS-type PPTases 88
Figure S2.6: Spot analysis of deleted genes 89
Figure S2.7: Growth rate measurements in 96 well plate 90
Figure S2.8: Repeatability determination of AFPptA assay over 384 well plate 90
Figure S3.1: Shake flask co-culture of nitrogen starved RFP and GFP expressing strains (AfRFPcnx and AfGFPniaD) in liquid AMMNO3 medium 121
Figure S3.2: Real-time PCR quantitative analysis of the DNA analysed by en mass sequencing 121
Figure S4.1: 2 families of phosphatases; A) tyrosine-specific phosphatases (PTP) and B) serine/threonine phosphatases (STP). 158
Figure S4.2: Two Step Fusion PCR 159
Figure S4.3: PCR validation of phosphatase null mutants 160
Figure S4.4: Phylogram of aspartate based phosphatases 161
Figure S4.6: Phylogram of MTM and PTEN phosphatases 161
Figure S4.5: Fitness assessment of strains in growth assays on solid VMM 162

List of Supplementary Tables

Table S2.1: Primers for pptA, aarA, sidA and pksP gene knock out and reconstitution constructs 83
Table S2.2: Primers for host response RT-PCR 84
Table S2.3: Primers for recombinant protein production 84
Table S2.4: List of Clustal W pairwise alignment scores and BlastP analysis against *A. fumigatus* PptA 84
Table S3.1: Strains used in this study 117
Table S3.2: Experimental indexing sequences used in this study 119
Table S3.3: Unique strain identifier 119
Table S3.4: Real-time PCR primers used to quantify strain abundance in parallel fitness studies. 120
Table S4.1: Primers used to generate knockout cassette 151
Table S4.2: Unique index that identifies the condition of the experiment 155
Table S4.3: Unique strain identifier 155
Table S4.4: Table of phosphatase mutants generated. 156
Table S4.5: Essential phosphatases identified in *A. fumigatus* and orthologues 157

Abbreviations

5-FC	Flucytosine
AASDHPTT	L-aminoadipate-semialdehyde dehydrogenase-phosphopantetheinyl transferase
ABPA	Allergic bronchopulmonary aspergillosis
ACPs	Acyl carrier protein
ACTβ	Beta-actin
ADP	Adenosine diphosphate
AF/f	*Aspergillus fumigatus*
AIDS	Acquired immune deficiency syndrome
AMB	Amphotericin B
AMM	Aspergillus Minimal Medium
AN	*Aspergillus nidulans*
an/An	*Aspergillus niger*
Arf	ADP Ribosylation Factors
ATP	Adenosine triphosphate
Bar-Seq	Barcode Analysis by Sequencing
BLASTp	Basic local alignment search tool protein-protein
bleo	Bleomycin resistant gene
CA	*Candida albicans*
CADRE	Central Aspergillus Resource
CaFT	*Candida albicans* fitness test
CATs	conidial anastomosis tubes
CCPA	Chronic cavitary pulmonary aspergillosis
CDC14	Cell division cycle 14
CDC25	Cell division cycle 25
CFPA	Chronic fibrosing pulmonary aspergillosis
CMC	Carboxymethyl cellulose
CoA	Coenzyme A
CPA	Chronic pulmonary aspergillosis
Ct	Cycle threshold
CTAB	Cetyl trimethyl ammonium bromide
CV	Coefficient of variation
CYP	Cytochrome P
DCs	Dendritic cells
DEPOD	DEPhOsphorylation Database
DHN	1,8-Dihydroxynaphthalene
DSP	Dual specificity phosphatases
EDTA	Ethylenediamine tetra-acetic acid
FAS	Fatty acid synthases
FC	Fusarinine C
FCP	TFIIF-associating C-terminal domain phosphatase
FDA	Food and Drug Administration
FP	Fluorescence polarization
GFP	Green fluorescent protein
GM-CSF	Granulocyte-macrophage colony-stimulating factor
GRACE	Gene replacement and conditional expression
GST	Glutathione S-transferase
GTP	Guanosine triphosphate

GTPase	Guanosine triphosphatase
HAD	Haloacid dehalogenase
HcsA	Homocitrate synthase
HEPA	High-efficiency particulate arrestance
His	Histidine
HIV	Human immunodeficiency virus infection
HS	*Homo sapiens*
HTS	High throughput screening
IA	Invasive aspergillosis
IL	Interleukin
IMPase	Inositol monophosphatase
IPTG	Isopropyl β-D-1-thiogalactopyranoside
ISP	Ion sphere particle
JTT	Jones-Taylor-Thornton
LC-MS	Liquid chromatography–mass spectrometry
LMW	Low molecular weight
lys	Lysine
MEGA 6	Molecular Evolutionary Genetics Analysis version 6.0
MES	2-(*N*-morpholino)ethanesulfonic acid
Mptp	Mycobacterium tuberculosis protein tyrosine phosphatase
MTM	Myotubularin
NGS	Next generation Sequencing
NI-NTA	Nickle-nitrilotriacetic acid
NRPS	Nonribosomal peptide syntheases
PBMCs	Peripheral blood mononuclear cells
PBS-T	Phosphate buffered saline - tween
PCR	Polymerase chain reaction
PEG	Polyethylene glycol
PFA-DSPs	Plant and Fungi Atypical dual specificity phosphatases
PGM	Personal Genome Machine
PK	Polyketide synthases
PksP	Polyketide synthase P
PP2B	Serine/threonine-protein phosphatase 2B catalytic subunit
P-pant	Phosphopantetheine group
PPM	Metal-dependent protein phosphatases
PPP	Phosphoprotein phosphatases
PptA	Phosphopantetheinyl transferases A
PPTase	4' Phosphopantetheinyl transferases
PRL	Phosphatase of regenerating liver
PTEN	Phosphatase and tensin homolog
PTP	Tyrosine-specific phosphatases
pyrG	Orotidine-5'-phosphate decarboxylase gene
QRT-PCR	Quantitative real-time polymerase chain reaction
R^2	Coefficient of determination
rec	Reconstituted
REST	Relative Expression Software Tool
RFP	Red fluorescent protein
SAB	Sabouraud
SAFS	Severe asthma with fungal sensitisation

SC	*Saccaharomyces cerevisiae*
SCP	Small TFIIF-associating C-terminal domain phosphatase
Sfp	Surfactin synthetase
STP	Serine/threonine phosphatases
Sup	Supplementation
TAFC	Triacetylfusarinine C
TMR	Tetramethylrhodamine
TPR	Tetratricopeptide repeat
TR	*Trichoderma reesei*
TRI	Trizol
VMM	Vogel's minimal media

Abstract

The University of Manchester
Anna Elisabeth Johns
Doctor of Philosophy
Towards the development of novel Aspergillus fumigatus targeted antifungals with an in-depth analysis of Sfp-PPTase, PptA
2015

Humans are continuously confronted by the threat of fungal infection. Estimates put the number of individuals infected by superficial fungal disease at about 1.7 billion. Additionally there are a significant proportion of invasive infections which are difficult to treat and lead to an estimated 1.5 million deaths each year. *Aspergillus fumigatus* is an opportunistic, fungal pathogen which can lead to a variety of disease manifestations, generally termed aspergillosis and account for more than 200,000 life threatening infections annually with mortality rates of up to 95%. The occurrence of fungal disease has increased significantly due to the expansion of the immune deficient population, particularly those who receive immunosuppressive therapies. This combined with the problems surrounding current therapeutic options for fungal disease such as a rise in the incidence of antifungal resistance, adverse side effects in patients and drug-drug interactions has led to an urgent need to discover and develop an innovative class of antifungal agents. This thesis will address this requirement by validating a potential drug target, PptA, for combating *A. fumigatus* infection and explore methods to identify novel antifungal target identification.

PptA is a Sfp-type 4'-Phosphopantetheinyl transferase required for transfer and covalent tethering of 4'-phosphopantetheine from coenzyme A to a conserved serine residue within a peptidyl carrier domain of a protein substrate. This project outlines the many critical roles PptA plays within *A. fumigatus*, such as; involvement in the production of many virulence factors as well as the biosynthesis of the essential amino acid, lysine. Furthermore, it is demonstrated that PptA is vital for secondary metabolite production in *A. fumigatus*, growth in iron limiting conditions and virulence. Finally, the design of a high-throughput screening assay capable of identifying inhibitors of PptA enzymatic activity further demonstrate the suitability of this target. It is the combined effect of all these characteristics that makes PptA such a suitable candidate for an antifungal target.

Additionally two validation methods are included which can be used to identify novel drug targets. The first method utilises chemically induced haploinsufficiency profiling, a technique which has been proven successful for drug target identification and determining mode of action of drugs in *S. cerevisiae* and *C. albicans.* The project has shown this technology can be successfully used in *A. fumigatus.* Furthermore, a new technique for *in vitro* parallel fitness screening using next generation sequencing was validated with a library of phosphatase deletion mutants. Bioinformatic analysis against strains exhibiting severe fitness defects allowed the identification of three phosphatases that have the potential of becoming successful antifungal drug targets.

Declaration

The co-localisation and the generation of the 46 diploid knockouts referred to in chapter 3 of this thesis has been submitted in support of an application for another degree or qualification of this or any other university or other institute of learning.

Copyright statement

Acknowledgements

Firstly, I would like to thank my family and friends for their continued care and guidance, especially my mum and dad who have offered much encouragement and support during my studies. They have made me who I am today and always inspire me to do my very best. I would also like to mention my grandma, who sadly passed away just before completion of this thesis, but she had continuously offered love and support throughout my PhD. I would also like to thank Matthew Rowland for his encouragement and for his ability to always put a smile on my face.

I would also like to take this opportunity to offer my sincerest gratitude to my supervisor Dr Mike Bromley for the expertise and knowledge he has provided me as well as offering excellent guidance throughout my PhD. He has pushed me farther than I thought I could go and the skills I have developed throughout the last 4 years will be invaluable to my future career. Furthermore I would like to thank Dr Paul Bowyer for his knowledge and assistance and my advisor Dr Lydia Tabernero for her ideas and positive input.

Finally, I would like to show my appreciation for the rest of the Manchester Fungal Infection Group members who have offered help throughout my PhD, especially the members who have shown me kindness and friendship.

Chapter 1

Introduction and Aims

1.1. Overview of Thesis

The thesis has been written in an alternative format; chapter 1 will provide the biological context of the study, with chapters 2 to 5 written as manuscripts which are either in the process of being submitted for publication or are soon to be submitted. Chapter 6 presents conclusions and future work for the projects. The manuscripts' formats have been changed to ensure consistency throughout the thesis with figures and tables placed near to where they have been cited. The contribution of each author to the manuscripts is listed below:

Chapter 2: PptA, a drug target for *Aspergillus fumigatus* infection
Anna Johns, Daniel Sharf, Bharat Rash, Elaine Bignell, Michael Bromley

Target Journal: PLOS Pathogens

Abstract:

Fungal diseases are estimated to kill between 1.5 and 2 million people each year which exceeds global mortality estimates for either tuberculosis or malaria. Aspergillus fumigatus is the leading cause of invasive aspergillosis, a globally distributed fungal disease which causes 200,000 life threatening infections annually with mortality rates of up to 95%. It poses as a common threat to patients with a compromised immune system due to disorders such as leukaemia, HIV, AIDS and also persons undergoing chemotherapy treatments or transplantation. Problematic issues surrounding the standard treatment protocol for this infection include fungal drug resistance and serious adverse side effects. There is an urgent need to discover and develop an innovative class of drugs that possess new mechanisms of action against novel drug targets. We have identified a potential drug target, PptA that plays a key role in A. fumigatus secondary metabolism. PptA is a sfp-type phosphopantetheinyl transferase and is required to activate non-ribosomal peptide synthases, polyketide synthases and a protein required for lysine biosynthesis, aminoadipate reductase (AarA). Disruption of *pptA* renders the fungus avirulent in both insect and murine infection models. It also appears that the loss of PptA affects the immune recognition of spores, similar to other melanin deficient strains leaving fungal spores more vulnerable to host detection. Furthermore the PptA recombinant protein has been produced and proven active in a high throughput fluorescence polarisation assay which can be used for screening purposes to find potential inhibitors.

Authors' Contribution:

Anna Johns: Bioinformatic analysis, phenotypic analysis, virulence studies, dendritic cell assay, protein productions and purification, design of PptA protein assay, PptA assay optimisation

Daniel Sharf: Secondary metabolism assay, acidification of phagolysosomes assay

Bharat Rash: Technical support with assay optimisation

Elaine Bignell: Support with murine infection models

Michael Bromley: Project supervisor

Chapter 3: Inducible cell fusion in the human pathogenic fungus Aspergillus fumigatus permits use of parallel fitness analyses to determine the mechanism of action of antifungal compounds

Anna Johns, Darel Macdonald , Adriana Contreras Valenzuela, Jane Mabey Gilsenan, Max Erble, Paul Bowyer, David Denning, Nick Read, Michael Bromley

Target Journal: Eukaryotic cell

Abstract:

Aspergillus fumigatus is the leading cause of invasive aspergillosis, a disease that causes life threatening infections in the immunocompromised population. Due to the pharmacological shortcomings surrounding the current therapeutic options to treat fungal disease such as; toxicity, drug-drug interactions and poor bioavailability, combined with the increasing incidence of antifungal resistance, there is an urgent need to develop a novel class of antifungal drugs. This study validates the use of a chemical genomics approach based on chemically induced haploinsufficiency profiling in A. fumigatus to identify either novel drug targets or the mechanism of action of antifungal compounds. We have combated several issues that have previously prevented this technology being used with A. fumigatus, including; developing a stable diploid as well as a high throughput gene knockout methodology to generate a suitable library of deletion mutants. Furthermore we have shown that vegetative cell fusion, which would be detrimental to this technology, occurs infrequently under normal cultural conditions in A. fumigatus. This study demonstrates the use of parallel fitness profiling along with next generation sequencing based barcode strategy to confirm the mechanism of action of the antifungal agents, itraconazole and brefeldin A.

Authors' Contribution:

Anna Johns: Parallel fitness studies, optimisation and development of parallel fitness studies, Next generation sequencing data processing

Darel Macdonald and Adriana Contreras Valenzuela: Co-localisation studies

Jane Mabey Gilsenan: Development of next generation sequencing data processing pipeline

Max Erble: Knock out mutant library generation

Paul Bowyer and David Denning: Support and advice in manuscript preparation

Nick Read and Michael Bromley: Project supervisors

Chapter 4: Exploring the Aspergillus fumigatus phosphatome for the identification of potential drug targets

Anna Johns, Lydia Tabernero, Michael Bromley

Abstract:

Aspergillus fumigatus is the leading cause of invasive aspergillosis a fungal disease which poses as a serious threat to patients with a weakened immune response due to disorders such as leukaemia, HIV, AIDS and also persons undergoing chemotherapy treatments. In *Aspergillus fumigatus* and all other fungal species phosphatase mediated reversible protein phosphorylation is an important regulatory mechanism of cell cycle and homeostasis maintenance. Therefore phosphatase genes are considered to be an attractive target for novel drugs. In this study we used an ontology based classification tool and published literature to identify 38 phosphatases in the genome of *A. fumigatus*. Bioinformatic analysis allowed the identification of several fungal specific enzymes. Deletion strains were generated for all phosphatase genes and phenotypic analysis was carried out. A method to assess parallel fitness using next generation sequencing was validated and used to identify strains exhibiting reduced fitness. Our analyses show there are three candidates; NimT, NemA and PtcB, which have the potential of becoming novel antifungal targets for the pathogen *A. fumigatus.* These phosphatases have both significant effects on fungal fitness but are also highly divergent from human proteins.

Authors' Contribution:

Anna Johns: All bioinformatical and experimental data

Lydia Tabernero and Michael Bromley: Project supervisors

1.2. Fungi

Fungi are unlike plant or animal, distinguished by non-motile bodies called thalli which consist of hyphae, they are classified within their own kingdom, the Myceteae. 1.5 million species of fungi were 'conservatively' estimated to exist in 1991 (1) however newer estimates have predicted species numbers ranging from 3.5 - 5.1 million (2). As only a small fraction of fungal species have been identified and scientifically described, the number of species will continue to be an area of debate. The Myceteae are composed of a wide diversity of organisms ranging in lifecycles, ecology, morphology and size from single celled yeast to multinucleated, filamentous moulds. Fungi can replicate asexually or sexually, methods include: budding, fission, hyphae fragmentation or sporulation. Fungi play a useful part in the natural ecosystem, as they are the principal decomposer of organic matter and therefore have a vital role in both the carbon and nitrogen cycles. However some species can cause a direct threat to human health.

Mycoses are fungal infections that affect both humans and animals. 400 species of fungi are known to be responsible for causing mycoses (3) and rapid rise in incidence of fungal infection in humans (4) is becoming an increasing concern. This dramatic increase has been due to enhanced numbers of immunosuppressed individuals (5). Immunosuppression is caused by numerous factors including but not limited to; induction chemotherapy for acute leukaemia, human immunodeficiency virus/AIDS, hematopoietic stem cell transplant recipients or organ transplant patients. There are five main classifications of clinical fungal infection; superficial, cutaneous, subcutaneous, systemic and opportunistic.

Superficial infections are restricted to the outermost layer of the skin known as the epidermis consisting of dead cells that lack nuclei and organelles. These infections tend to be cosmetic problems only as they rarely result in an inflammatory response (6). Tinea versicolor is a globally distributed pigmentary disorder caused by superficial infection of *Malassezia* spp (7) and is a prevailing problem in the tropics showing up to 40% incidence in that region (8). The infection occurs when fungi comes into contact with the skin and a transition from dimorphic state of the yeast into mycelia state follows. Clinical characteristics of this infection take the form of slightly scaling macules and patches, commonly covering large areas of the body (7).

Cutaneous infections involve the epidermis, hair and nails and the infecting agent generally elicits some form of inflammatory response. Dermatophytes are the general name given to organisms that cause this type of infection. One of the most common forms is Tinea pedis (athlete's foot) affecting a 15% of the population (9). Subcutaneous infections are associated

with the dermis and subcutaneous tissue. This type of infection usually results from implantation of a fungal organism through the skin. One of the main forms of this type of infection is sporotrichosis which results from the implantation and inoculation of *Sporothrix schenkii.* Symptoms include small, red lumps that develop at the site of infection, these then turn into ulcers. The fungi travel up the lymphatic channel causing lines of ulcers to develop (10). Systemic infection occurs when the fungi reach the bloodstream and end up invading deep into tissue, the consequences of which can be life-threatening.

1.3. Fungal Pathogens

The number of fungal infections increases every year with the current number of estimated infection at 1.2 billion (5, 11) and the number of associated deaths surpassing those caused my malaria or tuberculosis (5). The majority of deaths caused by fungal infections result from species in the genera Cryptococcus, Candida, Aspergillus, and Pneumocystis and of greater concern is the mortality rates associated with these infections which all exceed 70% (Figure 1.1).

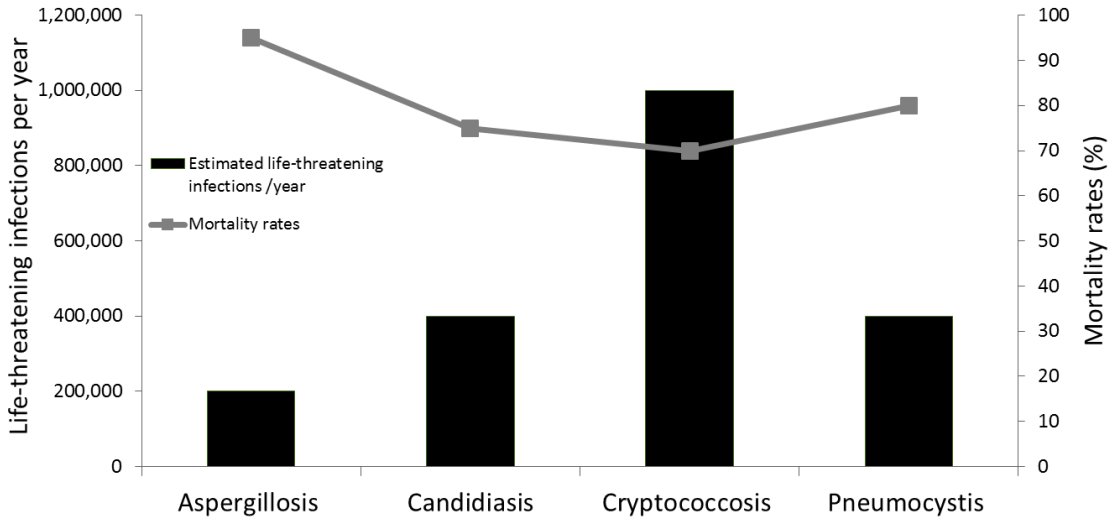

Figure 1.1: Top 4 prevailing fungal pathogens. Associated estimated life-threatening infections/year and mortality rates. Adapted from (5).

Candida species are a major cause of opportunistic mycoses on a global scale with 72.8 million cases per year (12, 13). *Candida* species are ubiquitous and opportunistic yeast pathogens that frequently colonise human skin and mucous membranes of the respiratory, gastrointestinal, and female genital tracts (14). The overgrowth of this yeast leads to candidiasis. There are more than 150 species of *Candida*, however only 15 are recognized as frequent human pathogens, of which the most clinically significant member is *C. albicans* (14). Invasive candidiasis is very problematic with one study finding an associated mortality rate of up to 61% among nosocomial *Candida* blood stream infection patients compared to 12% in patients

with no history of the same infection, giving an attributed mortality of 49% (15). It has a range of clinical manifestations including the most common form, candidemia this manifests when *Candida spp* are isolated in one or more blood cultures. Symptoms of candidemia include an acute septic syndrome or fever of unknown origin. The use of intravascular catheters, parenteral hyperalimentation, and broad-spectrum antibiotics are the major risk factors that increase the likelihood of candidemia (16).

Cryptococcosis is a disease that can manifest as asymptomatic to severe, life threatening meningitis and is caused mainly by the fungal pathogens *Cryptococcus neofomans* and *C. gattii*. More than 1 million life threatening infections occur globally per year (5). *C. neofomans* is commonly found in soil contaminated with pigeon guano whereas *C. gattii* is more likely found in eucalyptus trees and decaying wood (17). Infection normally derives from inhalation of airborne organisms into the lungs. Once inside the lungs it is either; cleared by the human immune system; left in its dormant form or disseminates to cause systemic infection (17). The fungal pathogen has a predilection for invading the central nervous system which relates to the most common clinical cases of human cryptococcosis presenting as meningoencephalitis (5). A major risk factor of *Cryptococcus* is AIDS with associated mortality rates of 15- 20% in the United States and 55-70% in Latin America and sub-Saharan Africa even after treatment (18)

Pneumocystis is a genus of opportunistic fungal pathogens that can cause fatal pneumonia in hosts with compromised immune systems (19). It is a common infection in patients with HIV and is considered as a AIDS-defining illness (20). *Pneumocystis* has neither a known environmental niche nor a long-term *in vitro* culture system (19) and it is postulated that Individuals colonised with *Pneumocystis* may cause the transmission to others (21). The global incidence of *Pneumocystis* pneumonia is estimated to be greater than 400,000 per annum with possible mortality rates of up to 80% (5).

This thesis will focus on the human pathogen *Aspergillus fumigatus,* a saprophytic, filamentous fungus which is ubiquitous in the environment. It produces green-greyish hydrophobic conidia (2–3.5µm) (22) from specialized multicellular structures called conidiophores. These then become widely distributed in the environment due to air currents and disturbances. Inevitably human individuals come into contact with *A. fumigatus* conidia and estimates predict that each individual inhales hundreds daily (23). The small size of the conidia enables them to travel through the terminal respiratory airways to the pulmonary alveoli (22). In healthy individuals this does not cause a problem as the conidia are removed by the acquired or innate immune system (24). A problem arises when the individual is immunosuppressed as their immune system is incapable of successfully removing the conidia, allowing them subsequently to

germinate. Germination involves both isotropic and polar growth and initiates the *A. fumigatus* asexual development program. The unicellular conidia eventually develop into hyphae, which are able to invade tissue (22) and in turn can lead to the development of a variety of life threatening pulmonary disease, generally termed aspergillosis (25).

There are several manifestations of aspergillosis (table 1.1). One form is triggered by an allergic reaction to fungal conidia, known as allergic bronchopulmonary aspergillosis (ABPA) (26). Individuals with atopic asthma or cystic fibrosis are most susceptible to ABPA which is due to an increased sensitivity to *A. fumigatus* allergens (26). Symptoms include coughing, wheezing and amplified classic asthma symptoms. Another allergic reaction associated with all fungi as well as *Aspergillus spp* is "severe asthma with fungal sensitisation" (SAFS). This occurs in patients with severe asthma who are immunologically sensitised to any type of fungi (determined by skin prick test or radioallergosorbent test) (27). Nasal symptoms such as runny nose, sneezing and hay fever-like symptoms are common with SAFS. Chronic persistence of asthma symptoms that are difficult to control by multiple medications is also a distinguishing factor, with hospitalisation commonly resulting from this. *A. fumigatus*, *Penicillium notatum*, *Cladosporium herbarum, Alternaria alternata* or *Candida albicans* are common culprits (27).

Chronic pulmonary aspergillosis (CPA) is a long-term aspergillus infection of the lung. There are different types of CPA including aspergilloma, chronic cavitary pulmonary aspergillosis (CCPA) and Chronic fibrosing pulmonary aspergillosis (CFPA). CPA can occur in immunocompetent patients and even following treatment can have a mortality rate of 20-33% in the short term and up to 50% over a 5 year period (28). The majority of CPA patients have an underlying lung disease. It is estimated that 1.2 million people in the world have CPA as a sequel to as pulmonary tuberculosis (28). The most commonly recognised form of CPA is pulmonary aspergilloma which occurs when a fungus ball develops within pre-existing pulmonary cavities (29). Cavities usually arise from previous illnesses such as tuberculosis, sarcoidosis, bronchiectasis, bronchial cysts and bullae, ankylosing spondylitis, neoplasm, or pulmonary infarction. The ball consists of a clump of fungal mycelia, inflammatory cells, fibrin, mucus, and tissue debris (29). A similar form of aspergillosis, CCPA, involves multiple cavities as opposed to just one. It occurs in damaged lung tissues and results in fibrosis and chronic inflammation of the lungs (30). Symptoms include weight loss, chronic cough, haemoptysis, fatigue and shortness of breath. Finally CFPA occurs when pulmonary aspergillosis has been left untreated subsequently leading to chronic lung scarring, which does not improve over time (30).

Invasive aspergillosis (IA) is considered the most serious and devastating form of disease (31, 32). It not only affects patients with compromised immune system but also critically ill patients and those with chronic obstructive pulmonary disease (33). Factors such as infection site, treatment regime and the host immune response influence the severity of the disease. Mortality rates of 95% are observed even with treatment (5, 32). The rate of IA incidence is rapidly increasing due to a rise in individuals exhibiting high risk factors as previously described (34, 35). Symptoms can include; fever, cough, sputum production and chest pain, however are often unspecific.

There are several rarer but emerging fungal infections worldwide, such as zygomycosis predominately found in tropical and subtropical regions. Zygomycosis is caused by fungi in the orders Mucorales and Entomophthorales (36) and it is a common opportunistic fungal infection in patients with diabetic ketoacidois or those that are immunosuppressed with stem cell transplant recipients especially at risk. Manifestations of zygomycosis include rhinocerebral, pulmonary, cutaneous, gastrointestinal and allergic diseases (36). Another uncommon mycosis known as Scedosporiosis is caused by fungi in the genus *Scedosporium* with two species being medically significant *S. apiospermum* and *S. prolificans* (37). *S. apiospermum* causes three types of infection; mycetoma, deeply invasive infection and saprophytic involvement. Immunosuppressed patients are most at risk from developing a deeply invasive infection especially in the lungs due to spore inhalation. A fungal ball can also develop in a manner similar to an aspergilloma. Immunocompetent patients that have been involved in near drowning accidents are also at risk of developing fatal pulmonary and disseminated infection (37). *S. prolificans* can cause deeply invasive infection in immunosuppressed patients however infection is restricted to soft tissue and bone in immunocompetent patients (37).

Table 1.1: Different types of aspergillosis including symptoms, diagnostic criteria and treatments (Adapted from; http://www.aspergillus.org.uk/).

Illness	Type	Symptoms	Diagnostic Criteria	Treatment
evere Asthma and Fungal Sensitisation (SAFS)	Allergy	Significant nasal symptoms with runny nose, sneezing and hay fever- like symptoms	Severe asthma (British Thoracic Society step 4 or worse), Exclusion of ABPA (total IgE <1000 IU/ml), Evidence of sensitisation to one or more fungi, by skin prick test or RAST test	Long-term inhaled and frequent courses of oral corticosteroids combined with short or long-acting beta-2 agonists, or leukotriene antagonists, oral doses of itraconazole
Invasive Pulmonary Aspergillosis (IPA)	Invasive	Chest pain, cough, fever, joint pain, shortness of breath, unintentional weight loss	Patient will be severely immunosuppressed, detection of aspergillus species by biopsy, culture and microscopy of tissue samples, chest CT scans, detection of aspergillus antigens in body fluids	Antifungal drugs; voriconazole, caspofungin, itraconazole, posaconazole, or amphotericin B
Allergic Bronchopulmonary Aspergillosis (ABPA)	Non-invasive	Shortness of breath, coughing and wheezing, intermittent episodes of feeling unwell, produce brown plugs of sputum	Elevated total serum IgE, together with evidence of *Aspergillus* sensitisation as seen by either the presence of Aspergillus antibodies, or identification from respiratory fluid	Oral, long-term, high-dose steroids, Itraconazole used in conjunction with steroids

Aspergilloma	Semi-invasive	Chest pain, cough, coughing up blood, fever, malaise, unintentional weight loss, shortness of breath, wheezing, many patients experience no symptoms	Chest X-rays showing a lung cavity with a fungal ball present, symptoms lasting more than 3 months, blood test or tissue fluid test positive for *Aspergillus* species	No treatment is necessary unless patient is coughing up blood, surgery to remove the aspergilloma, pre- and post-operative antifungal drugs, orally administered itraconazole, voriconazole or posaconazole
Chronic Cavitary Pulmonary Aspergillosis (CCPA)	Semi-invasive	Chest pain, cough, coughing up blood, fever, malaise, unintentional weight loss, shortness of breath, wheezing, many patients experience no symptoms	Chest X-rays showing cavities are present in the lung but not necessary with a fungal ball, symptoms lasting more than 3 months, a blood test or tissue fluid test positive for *Aspergillus* species	No treatment is necessary unless patient is coughing up blood, surgery to remove the fungal ball if present, pre-and post-operative antifungal drugs, orally administered itraconazole, voriconazole or posaconazole
Chronic Fibrosing Pulmonary Aspergillosis (CFPA)	Semi-invasive	Chest pain, cough, coughing up blood, fever, malaise, unintentional weight loss, shortness of breath, wheezing, many patients experience no symptoms	Chronic scarring of the lungs, chest X-rays showing cavities are present in the lung but not necessary with a fungal ball, symptoms lasting more than 3 months, a blood test or tissue fluid test positive for *Aspergillus* species	No treatment is necessary unless patient is coughing up blood, surgery to remove the fungal ball if present, pre-and post-operative antifungal drugs, orally administered itraconazole, voriconazole or posaconazole

1.4. Treatment of mycoses

There are two types of antifungals; topical and systemic. Topical antifungals are applied directly on the skin surface. The objective of this thesis is to progress the development of treatments for systemic infections and hence topical antifungal agents will not be discussed further. Systemic antifungals are used to treat deep tissue fungal infections; they can be administered orally or intravenously. Currently there are only four classes of drugs available

for systemic fungal infection treatment: pyrimidine analogues, polyenes, triazoles and echinocandins in the human antifungal therapeutics market worth $11.8 billion in 2013 (38). Mortality rates associated with invasive diseases remain high due to a range of problems accompanying each drug class (5). Drug toxicity, drug:drug interactions, bioavailability in select tissues, emerging resistance and a limited range of targets make identifying novel antifungal targets of upmost importance (39, 40).

1.4.1. Pyrimidine Analogues

Flucytosine (5-FC) is a fluorinated pyrimidine analogue, it was originally investigated as an antitumor therapy before its antifungal properties were discovered and was used to treat candidosis and cryptococcosis murine infection in 1968 (41-43). Once inside the fungi 5-FC is deaminated by cytosine deaminase into 5-fuorouracil and then is converted into 5-fuorouracil-ribose monophosphate. This then follows one of two metabolic pathways resulting in either 5-fluorouridine triphosphate or 5-fluoro-2'-deoxyuridine-5'-monophosphate (42). The former inhibits protein synthesis by incorporating into RNA whereas the latter inhibits thymidiate synthetase (an enzyme involved in DNA synthesis) (44). There are problems surrounding the use of 5-FC, it can cause gastrointestinal issues (such as nausea, vomiting and diarrhea), hepatotoxicity, and myelosupression (44). 5-FC shows activity against yeasts, including *Candida*, T*orulopsis* and *Cryptococcus spp*., as well as *Phialophora*, *Cladosporium* and *Aspergillus spp.* (42). However 5-FC has demonstrated rapidly developing resistance incidence. This is exemplified in *Candida albicans* which has a resistance incidence of 7-8% and rises to 22% when considering other *Candida spp* (42). *S*ubsequently it is often used in combination with other drugs (44). For example, it is used mainly with amphotericin B (AMB) for cryptococcal meningitis and has been proven to sterilise the cerebral spinal fluid faster than AMB monotheraphy (45-47).

1.4.2. Polyenes

The only systemic fungal infection polyene treatment that has proven successful is amphotericin B (AMB); it was discovered in 1955 and due to its high potency it was developed into an antifungal. Although a number of polyenes have been discovered since their pharmacokinetic properties have prevented further development. It is postulated to work by binding to ergosterol in the fungal cell membrane creating pores which change the membrane's permeability allowing cellular components to escape leading to cellular dysfunction and finally destruction and death (48). Problems with toxicity may arise due to the similarity between fungal ergosterol and the human cholesterol (44). It has activity against

Candida spp, Aspergillus spp and *Cryptococcus neoformans* amongst others (6). Infusion related reactions and renal dysfunction are common when the deoxycholate solubilised formulations are used (6). The FDA has approved the use of lipid formulations of AMB which have improved tolerability and has allowed increased daily dosage of the parent drug.

1.4.3. Triazoles

This class is the most widely used antifungal treatment and includes fluconazole, itraconazole, posaconazole and voriconazole. The newest triazole, isavuconazole was approved in the US in March 2015. The triazoles prevent the synthesis of ergosterol by targeting and inhibiting the cytochrome P-450 (CYP450) dependent 14α-demthylase. This causes changes to normal cell membrane function, resulting in methylsterol accumulation and eventually cell lysis (6, 44). There has been a trend in the incidence of triazole resistant *Aspergillus* clinical isolates reported which is believed to be a result of excessive use of environmental fungicides (49). The 4 members of this class currently used in treatment elicit different adverse properties such as toxicity, drug:drug interactions and level of fungal resistance.

Fluconazole was the first triazole approved for use and is still widely used. Reasons for this include; its low cost (it is now off patent), water solubility, high absorption from the gastrointestinal tract and lack of inactivation by gastric pH. It exhibits high activity against *Candida* spp. (except *Candida glabrata* and *krusei*), *Cryptococcus neoformans, Blastomyces dermatitidis, Coccidioides* spp., *Histoplasma capsulatum,* and *Sporothrix schenckii* however it is not active against *Aspergillus* spp (50). The second triazole to be approved for use, itraconazole, is not well tolerated in patients and shows problems of erratic oral absorption resulting in a decline of use over the years. It is still frequently used to treat chronic pulmonary aspergillosis, allergic syndromes related to *Aspergillus spp*., onychomycosis, histoplasmosis and blastomoycosis and sporotrichosis (50). It is also fungi-static for *Candida* spp. (6). Voriconazole was next to be approved, it is structurally similar to fluconazole and generally well tolerated within patients. It has a high bioavailability of 96%, which is reduced if taken with food. Voriconazole is active against most *Candida* and *Aspergillus* spp and has been used to treat invasive aspergillosis since 2002, thereby replacing AMB (50). The fourth triazole is posaconazole which shows activity against *Candida* and *Aspergillus spp. in vitro*. It also shows activity against *Scedosporium* spp., *Fusarium* spp., *Histoplasma* spp., *Coccidioides* spp., *Penicillium marneffei, Sporothrix schenckii*, *Blastomyces dermatitidis, Trichosporon* spp., and *Cryptococcus neoformans* as well as several dematiaceous molds (50). Finally, this year the latest triazole, isavuconazole was approved in the US which can be administered orally and

intravenously. It will be used to treat invasive aspergillosis and mucormycosis but also shows promising activity against *Candida spp*., *Cryptococcus neoformans* and *Trichosporon spp* (51). Fluconazole exhibits low levels of toxicity to human patients (chapped lips and dry skin observed if treated with ≥400mg/day) whereas itraconazole exhibits more serious adverse effects. It has been associated with hypertension, hypokalemia, peripheral edema and has negative inotropic effects which may lead to congestive heart failure (6, 44, 52). Furthermore the oral solution can lead to nausea and diarrhoea (53).

Triazoles are responsible for many drug:drug interactions which can result in increased metabolism or decreased solubility leading to treatment failure. This is due to their ability to inhibit human CYP450 dependent enzymes, particularly 2C19, 2C9 and 3A4 (44). CYP450 enzymes are responsible for the metabolism of drugs therefore inhibition of these enzymes can lead to a toxic accumulation of co-administered drugs within the body. Voriconazole exhibits the most CYP450 interaction as it acts as both substrate and inhibitor of CYPs 2C19, 2C9 and 3A4 whereas posaconazole is the most tolerable as it acts only as an inhibitor of CYP34A (53, 54). Therefore when prescribing any of the triazoles a patient's drug regime must be thoroughly checked to avoid any adverse effects occurring.

1.4.4. Echinocandins

Three USA FDA-approved agents belong to echinocandins class; caspofungin, micafungin and anidulafungin (55). They non-competitively inhibit the enzyme UDP-glucose β-(1,3)-D-glucan-β-(3)-D-glucosyltransferase, which synthesises 1,3-β-D glucan, an essential component of select fungal cell walls, (44, 55, 56), resulting in cell wall damage and eventually cell death. This mechanism of action means echinocandins are only effective against fungi that depend on these specific glucan polymers. They have fungicidal effects against many *Candida spp.* and fungistatic effects against *Aspergillus* (56). Echinocandins are generally well tolerated, the main adverse effect is associated with a histamine-mediated infusion-related reaction but is easily treated with antihistamines (57).

1.4.5. Allylamines

Allylamines prevent ergosterol synthesis by inhibiting squalene epoxidase (58). Well known agents belonging to this class include Amorolfin, Butenafine, Naftifine and Terbinafine. These compounds are commonly used as topical treatments for superficial fungal diseases such as jock's itch, athlete's foot and fungal nail infections (59). However Terbinafine has also been shown to be as effective as amphotericin B and Itraconazole in the treatment of bronchopulmonary aspergillosis (60). Allylamines are generally well tolerated but mild adverse

effects can include dryness to site of application, skin irritation and burning/tingling sensation (59).

1.4.6. Combination Therapy

In an attempt to reduce adverse side effects, to increase efficacy and spectrum of the current antifungals on the market combination therapy has been investigated. In 2002 immunosuppressed guinea pig models with invasive aspergillosis were used to investigate the effect of caspofungin acetate in combination with voriconazole. Combination treatment reduced colony counts in tissues and resulted in no mortality however the results showed no difference in mortality rate or mean time of survival when compared to the mono-therapy of voriconazole (61). Nevertheless combination therapy was proven to be successful when liposomal amphotericin B and caspofungin treatment were combined and compared to liposomal amphotericin B treatment only. The combinational group showed 100% survival compared to 80% survival in the mono-therapy group (62). However only 30 subjects were included in this study, a further study including more subjects will be required for a more inclusive result. Although combinational therapy could potentially lead to advances in IA treatment, currently no study has proven a definite plausible strategy. Another successful strategy was the combined treatment of amphotericin B with itraconazole, 82% of patients receiving combined treatment were cured compared to just 50% who received amphotericin only (63).

1.4.7. Novel Antifungals

Researching the current pipelines' of top pharmaceutical companies highlight the lack of attention fungal infection has in relation to other diseases such as central nervous system and cardiovascular related diseases, cancer or bacterial infections. However there are a modest number of novel antifungal agents emerging from smaller pharmaceutical companies which will now be discussed in this section.

Only 3 known antifungal compounds are in active clinical development, and another 2 projected to enter clinical development this year (39). It was announced in 2014 that F2G LTD, a UK based company, would start Phase I clinical trials of their antifungal agent, F901318. The intravenous/oral administered drug would be used on patients suffering with aspergillosis or other debilitating fungal infections (http://www.f2g.com/news). Valley Fever Solutions, Inc is in the process of developing their agent, Nickkomycin Z to tackle the disease valley fever (coccidioidomycosis). This drug works by inhibiting chitin synthesis an important component of fungal cell walls. They hope to enter phase IIa clinical trials in 2015 and so far have

experienced no safety concerns in mammals (http://valleyfeversolutions.com/index.html). The final antifungal agent in clinical trials is SCY-078 from Scynexis. The rights to SCY-078 were transferred from Merck (MK-3118) in 2013 after they altered the prioritisation of their infectious disease portfolio. SCY-078 is a enfumafungin antifungal and targets beta 1,3 D glucan synthesis in the fungal cell wall. It has been shown *in vitro* to have antifungal activity against *Aspergillus* and *Candida spp* including strains exhibiting resistance against azoles and/or echinocandins (64, 65). Currently it is in phase II trials for the oral treatment of *Candida* infections, with the prospect of starting intravenous trials this year (http://www.scynexis.com/pipeline/pipeline.php). Furthermore, Cidara Therapeutics has a series of antifungal agents in its pipeline with their lead compound, CD101 IV predicted to enter phase I trials in 2015. It belongs to echinocandin class of antifungals and will target systemic *Candida* infections (http://www.cidara.com/cd101-iv/). Viamet is carrying out investigational new drug studies on VT1129, which targets the essential component of the cell wall, CYP51. It shows promising activity against *Cryptococcus spp* (http://www.viamet.com/pipeline/vt-1129.php).

There are also emerging targets that are still in the earlier pre-clinical stages of drug discovery. Tsukuba Laboratories discovered a glycosylphosphatidylinositol (GPI) – anchor inhibitor, and after medicinal chemistry optimisation, candidate E1210 emerged (66). E1210 has shown to be well tolerated *in vivo* and active orally against *Candida, Aspergillus*, *Fusarium* and *Scedosporium* species (67). Daiichi Sankyo identified a pyridobenzimidazole derivative antifungal candidate during high throughput screening, this compound inhibits glucan synthase and thus prevents fungal cell wall formation. It show a narrow spectrum of activity with only *Candida* species effected (68). Vical also has an antifungal in pre-clinical tirals, VL-2397, which shows activity against *Aspergillus* species including azole resistant strains. It is thought to enter the cells via an iron channel but currently has an undefined mode of action (http://www.vical.com/products/ASP2397/default.aspx). Finally ASP9726 is an investigational echinocandin discovered by Astellas. It has been shown to be well tolerated *in vivo* and efficacious against invasive pulmonary aspergillosis (69).

It is clear that although there are emerging novel antifungals in the market it is likely that the pace of development will not match the needs of patients within clinics especially as the rate of resistance of current antifungals is being reported far more regularly. Therefore it is essential that work is carried out to identify novel targets and improve existing development timelines of antifungal targets.

1.5. Approaches to Antifungal Drug discovery

The majority of current antifungal drugs have been identified either by screening large numbers of small molecules or natural products for their *in vitro* ability to affect fungal growth or through serendipitous identification of antifungal activity of existing drugs. A target based screening approach has been adopted by many companies as an alternative and perhaps more focussed method of identifying novel drugs.

1.5.1. Target Based Drug Discovery

A molecular drug target can be defined as a protein whose function is critical for viability or pathogenicity. A drug target can be identified in numerous ways. Prior exemplification of a biochemical pathway or gene could infer its usefulness as a drug target. Alternatively several groups have used rational approaches to identify novel drug targets including; *in silico* comparative genomics, essential gene identification, haploinsufficiency screening and large scale fitness profiling.

1.5.2. *In Silico* Comparative Genomics

The most straightforward way of achieving this is to perform *in silico* comparative genomics studies. In 2005, a BLASTp analysis between the whole genome sequence of *A. fumigatus* and 131 single-member eukaryotic orthologous groups (consists of conserved essential genes derived from 7 different fully sequenced eukaryotic genomes) was performed (70). This comparative approach is limited in its success due to the diversity found between different fungal species especially when more distant fungal relations are used as models. As demonstrated when a comparison was made between the essential gene complement of pathogenic *C. albicans* and the non-pathogenic model organism *S. cerevisiae*. 1105 genes were identified as essential in *S. cerevisiae* at 30°C of which 864 share significant homology to *C. albicans* genes (71). Analysis of these genes using a system termed GRACE^{TM} (gene replacement and conditional expression) showed only 61% of these genes to be essential for *C. albicans* (72). Therefore to identify novel drug targets in *A. fumigatus* one must use either *A. fumigatus* or a very closely related organism.

1.5.3. Essential Gene Identification

Two separate studies have attempted to identify essential gene targets in *A. fumigatus*. In an attempt to identify and prioritise essential genes *in vivo* and *in vitro* a conditional promoter replacement technology was developed which used the nitrogen-regulated NiiA promoter

found in *A. fumigatus* (73). They replaced the endogenous gene promoter of 54 *A. fumigatus* genes with the NiiA promoter allowing the control of expression. Essentiality of 35 genes was confirmed by this technology. However this will fail to identify essential genes when the endogenous gene promoter expression levels are naturally lower than the repressed NiiA promoter expression levels. Another molecular technique successfully used with filamentous fungi is transposon mutagenesis. *Impala 160* has been identified to efficiently transpose in *Fusarium* species, *A. nidulans*, *Magnaporthe grisea* and *A. fumigatus* (74-77). As a class II transposable element of the TC1-mariner family, *impala 160* can be used to generate a collection of random heterozygous diploids. Firon*, et al* (2003) used the selective marker, *pyrG*, to create an *imp160::pyrG* transposable element. Using *imp160::pyrG* with 2,386 heterozygous diploid strains allowed the characterisation of 20 essential genes in *A. fumigatus* (76). A more recent study found the viability of using *imp160::pyrG* is improved by first exposing the element to prolonged low temperatures (78). The temperature activates mobilisation of impala and exploitation of this allowed the identification of 96 essential loci, which include; genes required for RNA metabolism, organelle organisation, protein transport and transcription. The insertion of transposons at the nucleotide and chromosomal localisation levels appeared to be random however it was found that it frequently occurred in non-coding regions leading to phenotypically silent mutants (76). However, it has been reported that the use of a transposon often led to DNA rearrangements if the transposition event uses inverted terminal repeats of separate transposons organised in direct orientation (79).

1.5.4. Haploinsufficiency Screens

Another challenge that faces drug target discovery is the use of isolated assays instead of whole-cell screens that determine function and potential inhibitors of the target (80). Due to the isolated nature of the assay it will exclude properties that a potential inhibitor may need to be a successful, for example it may not have the means to travel through cytoplasmic membrane which is essential to reach an intracellular target (81). To overcome this issue uniquely tagged heterozygote mutants are screened for chemically induced phenotypes in a large scale – genome wide growth assay known as a haploinsufficiency screen (figure 1.2). This process allows high-quality drug targets to be singled out from the vast quantity of potential targets. Haploinsufficiency occurs in diploid organisms which have experienced a loss of function to one gene copy (often due to a deletion mutation) which results in the remaining gene unable to produce sufficient protein to assure that the cell functions normally. The outcome of this phenomenon is usually identified by the development of an abnormal phenotype. There have been two postulated theories regarding haploinsufficiency, the first is

known as the “Balance hypothesis” (82). This theory states that differences to the normal stoichiometry of protein-protein complexes cause haploinsufficiency and the associated phenotype would be the same as an over expression phenotype. The second theory assumes that the haploinsufficient phenotype is due only to the reduction of protein levels, furthermore over expression of such proteins should rescue the abnormal phenotype restoring it back to the wild type state (83). Haploinsufficiency is a rare occurrence, for example, only 0.4% of coding loci in *Drosophila melanogastar* are haploinsufficient and lead to a recognisable effect to the organism (84). Despite its rarity haploinsufficient loci allow the identification of genes that are critical to the organism’s growth and development. Therefore these genes can be exploited in the drug target development process.

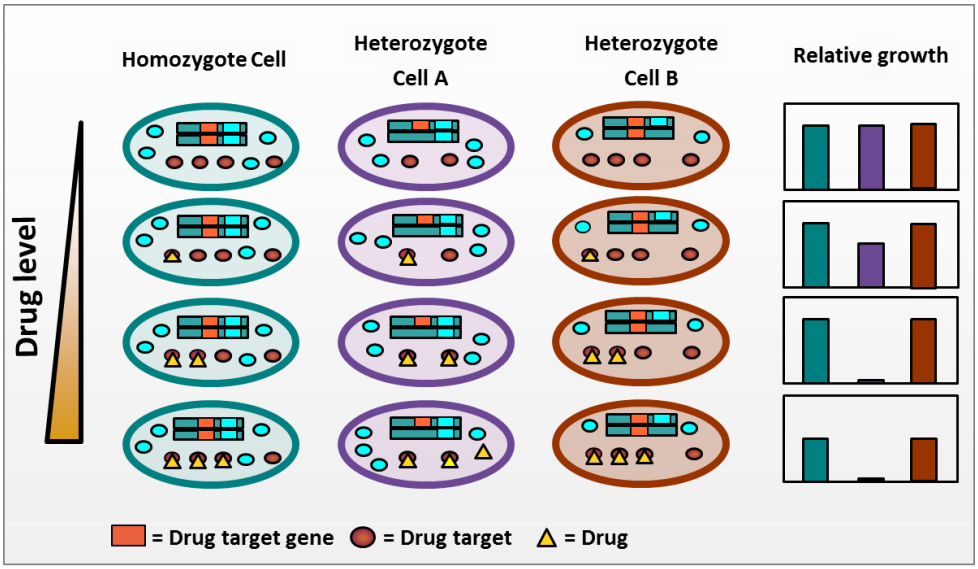

Figure 1.2: Haploinsufficiency screen. A loss of function to 1 gene copy results in the remaining gene unable to produce sufficient protein in the presence of drug targeting that specific gene to assure that the cell functions normally.

Giaever*, et al* (1999) performed a haploinsufficiency screen using *S. cerevisiae* to identify drug sensitivities. They created a set of 6 mutant strains that possess a deleted copy of a known drug target gene plus a unique DNA tag (Figure 1.3). Subsequently each strain was grown with sub-lethal concentrations of the drug that targets the protein encoded by the effective gene set. The growth rate of the mutant compared to the wild type provides a scale of sensitivity in the presence of the particular drug (85). Therefore increased sensitivity of the mutant would indicate specific induced haploinsufficiency. This was demonstrated in all the strains tested. This experiment can be expanded and adapted into drug-sensitivity profiling, where a vast number of labelled heterozygous strains are grown in the presence of drug. Strains showing higher levels of sensitivity compared to wild type possess the deleted gene that could

potentially become a drug target. This type of drug target selection does not need prior knowledge of the target and also due to the *in vivo* nature of this process only cell entering drugs that remain significantly un-metabolised are identified. Xu, *et al* (2007) performed a chemical genetic profiling study of 2,868 heterozygous *C. albicans* mutants using 35 compounds to investigate which of these led to chemically induced haploinsufficiency (86). This method allowed the mechanism of action of these compounds to be identified. Further to this study Jiang, *et al* (2008) used the same library to screen against crude natural-product fermentation extracts. The study successfully discovered parnafungin, a natural product that inhibits poly(A) polymerase (87). Parnafungin shows activity against a broad spectrum of clinically important fungal pathogens including; *C. albicans* and *A. fumigatus* (87).

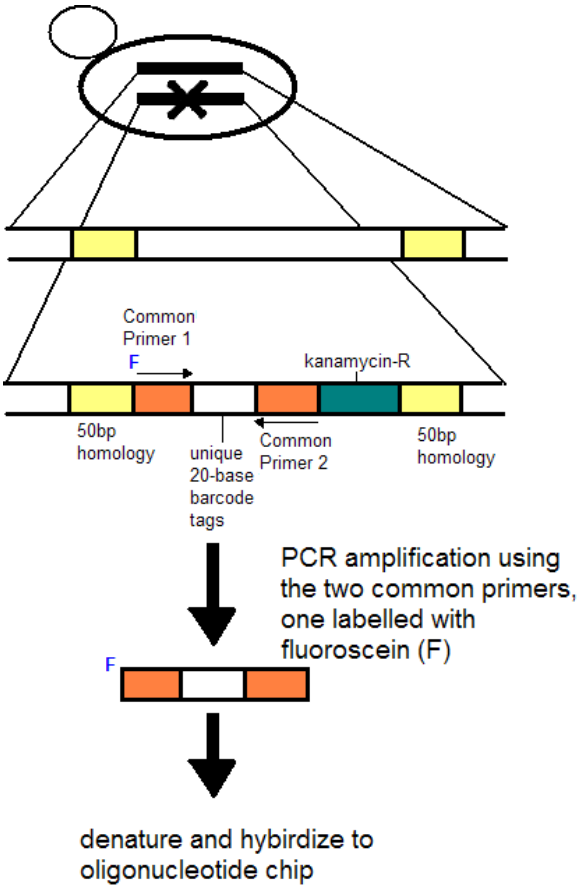

Figure 1.3: Heterozygote deletion construct. Gene knock out cassettes were generated to contain unique barcodes, 5' – fluoroscein label and a selective marker (kanamycin). 50 base pair sequences homologous to the upstream and downstream flanking regions of the ORF of the target gene are included at either end of the cassette to ensure precise site specific miotic recombination. The barcodes used are flanked by two common primer sites allowing a single PCR reaction to produce products that can be hybridised to an oligonucleotide array containing the complement of each tag. Subsequently the relative abundance of each strain in the pool can be calculated (adapted from (85)).

1.5.5. Large Scale Fitness Profiling

A comprehensive, large scale – genome wide screen in *C. albicans* was developed using a method known as GRACE (72). GRACE creates conditional mutants and involves two steps; firstly a heterozygous mutation of the gene of interest is derived using a PCR-generated disruption cassette containing a selectable marker. Secondly 250bp portion of the native promoter upstream of the ATG codon is replaced by a regulatable tetracycline (Tet) promoter, subsequently allowing controllable expression of the remaining allele (Figure 1.4). This method has allowed 1152 genes in *C. albicans* to be evaluated of which 567 have been experimentally identified as essential for growth. The genes identified using this approach can be used to compare against other fungal pathogens that have had their whole genome sequenced, which would enable the essential genes in *C. albicans* to be classified as either broad or narrow spectrum target sets (72).

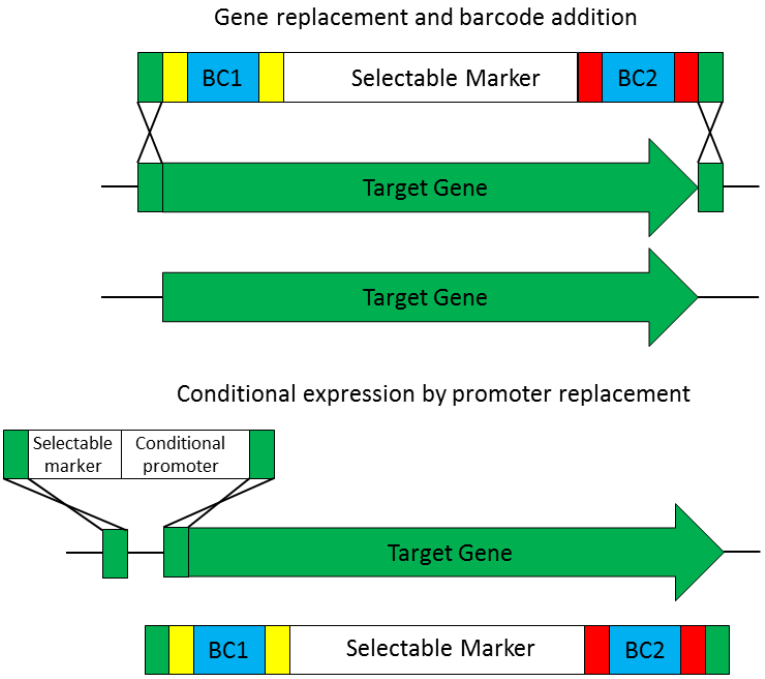

Figure 1.4: **Schematic of conditional mutant generation using the GRACE method**. The *C. albicans* strain CaSS1 was used as the parental strain. A knock out cassette with a selective marker and two unique barcodes (BC1 and BC2) was designed and PCR amplified to replace one copy of a gene at a single loci. These cassettes were transformed into the CaSS1 strain and the presence of the barcodes allowed the different heterozygote to be uniquely identified. A conditional promoter replacement cassette containing a dominant selectable marker (engineered for expression in *C. albicans*) was designed and amplified by PCR. The cassette was designed with homologous flanking sequences to ensure the endogenous promoter of the single remaining gene was replaced by the cassette after transformation. (adapted from (72)).

Another large scale comprehensive screen was achieved by the development of a transposon mutagenesis method known as “signature-tagged mutagenesis” (88). A unique DNA sequence is tagged to each mutant to allow the correct identification of those with reduced fitness from a mixed population. The major advantage to this method is that gene disruption, mutant selection and analysis can be carried out in parallel however the number of strains that can be assayed is limited and the random nature associated with transposon mutagenesis means that cloning and DNA sequencing are required to successfully identify the disrupted genes. Avoidance of these problems was achieved with two novel approaches “quantitive phenotypic analysis” and “molecular bar-coding” (89). Targeting of genes is achieved by a PCR method which creates a large volume of mutant strains, each of which is labelled with a unique 20 base pair molecular tag. Selective growth conditions are used to identify and analyse vast quantities of tagged mutants (>6000). PCR is used to amplify the molecular tags which are subsequently hybridised to a high density microarray containing complementary DNA sequences. The hybridisation signals are measured for intensity which correlates to the relative abundance of specific mutated strains present in the pool. The relative fitness of the mutant strain can be determined by measuring the abundance of tags at certain time intervals. A disadvantage to this method is that the microarrays had to be redesigned for each type of organism, cell or re-engineered strain used to ensure they contained the correct corresponding barcodes (90).

The development of next-generation DNA sequencing technologies has allowed this method to be enhanced into an even faster process. Smith*, et al* (2009) designed a protocol called Barcode Analysis by Sequencing (Bar-Seq) which uses DNA sequencing to “count” each barcode in a sample directly. They demonstrated sensitivity; dynamic range and detection limits all outperformed the original barcode microarray technique (91). It has also allowed genome wide screens to quickly and efficiently identify essential genes at a higher rate than previous techniques. Furthermore, Bar-Seq was able to assess and rescue sequence errors within the barcodes which were previously undetectable. Bar-Seq was further enhanced into a highly multiplexed bar-seq (90) the validation of which consisted of 96 pooled yeast growth assays which were multiplexed so that each sample contained 6200 barcoded mutant strains. This improved method has led to cost reductions as the sample size increases whereas the microarray based techniques costs are always fixed.

Until recently fitness profiling developments have been hampered by the low throughput of knock out mutations in *A. fumigatus*. However a technique has been developed to increase this. Baudin*, et al*, (1993) describe a simple approach for generating null alleles for directed gene deletion in *S. cerevisiae*. They use a one-step PCR amplification in which the construct

(with two distinct regions; the first allowing homologous recombination and known as the deleting sequence and the second permitting the PCR amplification) is inserted between the 5' and 3' flanking sequences of the gene of interest (92). This method has evolved over the years into "Fusion PCR" which is a two-step process resulting in a selection cassette flanked by two amplified, genomic DNA fragments unique to the gene of interest (93) (Figure 1.5).

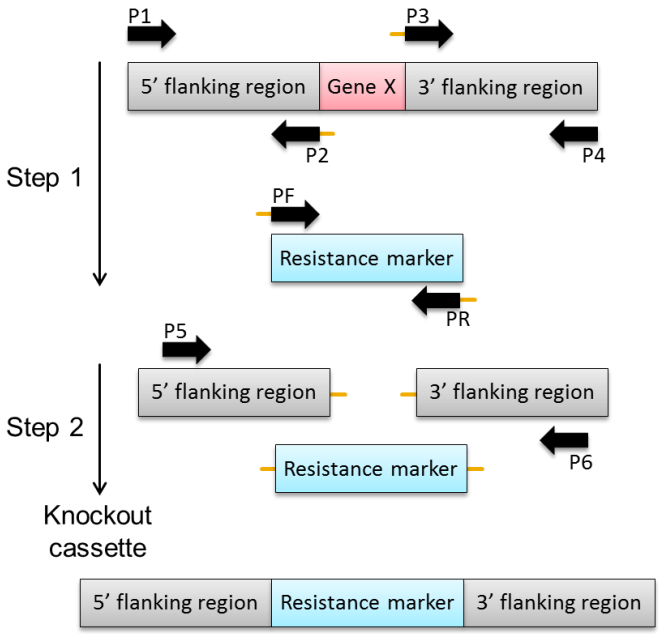

Figure 1.5: Two Step Fusion PCR. Step 1, Using primers P1 and P2 in one reaction and P3 and P4 in another, two PCR products of the regions flanking the chosen insertion site are produced. These products contain "tails" which were embedded in P2 and P3. An additional PCR reaction is used to amplify a resistance marker, primers in this reaction contain complementary "tails" to those found in P2 and P3. Excess primers and nucleotides from this reaction are then removed. Step 2, Nested primers P5 and P6 are used to amplify the two flanking regions together with the pre-amplified resistance marker. The PCR product is a linear transforming DNA fragment.

The non-homologous recombination nature of *A. fumigatus* is another limiting factor challenging the application of large scale drug target discovery in this species. DNA double strand repair makes it possible for a DNA cassette to be ligated into a different organism's genome so it can be successfully replicated. Non-homologous recombination joins DNA ends without homology in turn making directed mutagenesis a lengthy and monotonous procedure because the DNA integrates ectopically at high frequency (94). Non-homologous repair is mediated by the Ku70-Ku80 heterodimer and by IV-Xrcc4 complex (95). In an effort to replace this type of repair with homologous recombination a deletion mutation on the *A. fumigatus*

Ku80 gene to generate akuB^{KU80} mutant was performed (94). The study found that this caused the rate of homologous recombination to increase from 5% to 80% making this mutant a very useful tool for high-throughput gene replacement, especially as the gene deletion has no proven effect on fungi virulence.

1.6. Potential Drug Targets

As there are issues such as resistance, adverse side effects, etc. surrounding the treatment with current antifungal classes, work must be carried out to determine a novel class of drugs that possess a new mechanism of action against drug targets. A target can be a variety of biological entities including proteins, genes or RNA that are essential to an organisms viability or virulence. The most important property of a successful target is that it is "druggable" i.e. it must be reachable and once bound by the putative drug molecule it must incur a measurable biological response (96). Availability of the complete genome sequence of *A. fumigatus* (70) has stimulated the search for such novel drug targets within the fungus. This project will investigate the potential drug target PptA and a group of possible targets (*A. fumigatus* phosphatases). Bioinformatic comparison as well as critical functions required for fungal viability and virulence will be explored. PptA was chosen as a potential drug target as it has been shown to be essential to virulence in a range of pathogenic bacterial species and plant pathogens however this target has yet to be explored in a human fungal pathogen. This protein's involvement in the production of secondary metabolites, many of which have been identified as virulence factors, as well as an essential amino acid make it a very interesting and diverse target.

1.6.1. Phosphopantetheinyl Transferase A

Phosphopantetheinyl transferases (PPTase) are important enzymes involved in post-translation modification of a range of targets including polyketide synthases (PKs), nonribosomal peptide syntheases (NRPSs) and fatty acid synthases (FAS). They have been discovered in bacteria, archae and eukaryote where they are responsible for catalysing a magnesium ion dependent reaction known as phosphopantetheinylation (figure 1.6). This reaction involves the transfer of the phosphopantetheine group (P-pant) from Coenzyme A to a conserved serine residue on a carrier protein coverting it from the inactive apo form to the active holo form. The p-pant group attached to the carrier protein allows thioester tethering of elongation intermediates and substrates which in turn allows further enzyme modification (97).

There are three distinct classes of PPTases; type I Acp-PPTases, type II Sfp-PPTases and type III Fas-PPTases. Type 1 Acp-PPTases modify acyl carrier protein domains found in FAS and PKs,

where they supply a link for a growing fatty acyl or amino acid chain. Acp was first purified from *Escherishia coli* in 1968 (98), it was reported that this protein activates FAS ACP into its holo-form. Since this discovery many more Acp-PPTases have been identified other organisms including *A. fumigatus*. The *A. fumigatus* Acp is known as PptB, it has a low molecular mass of 16.8 kD, localised in the mitochondria with predicted target mitochondrial Acp and was found to be essential to viability (99). Type II Sfp-PPTase, were first characterised in 1996 during a study involving *Bacillus subtilis*, sfp and *E. coli* entD. Sfp was reported to be responsible for surfactin synthetase activation and EntD activates enterobactin synthetase. Surfactin and enterobactin are both siderophores used by organisms to sequester iron from their external environment. Sfp-PPTases have a broad range range of substrates including NRPSs, PKs and an enzyme involved in lysine biosynthesis. Sfp-PPTases are the only type of PPTases found in mammals. In humans this protein is called L-aminoadipate-semialdehyde dehydrogenase-phosphopantetheinyl transferase (AASDHPTT) which is used for all posttranslational 4'-phosphopantetheinylation modifications including; lysine catabolism, cytosolic and mitochondrial fatty acid biosynthesis (100) and 10-formyl-tetrahydrofolate catalysis (101). It is localised in the cytoplasm where it is postulated all 4'-phosphopantetheinylation occurs. The crystal structure of the human PPTase has been determined and appears very similar to the *Bacillus subtilis* SFP structure as both possess a 2-fold pseudo-symmetry (102, 103). It has been hypothesised that mutations in AASDHPTT may lead to pipecolic acidemia due to secondary accumulation of pipecolic acid. This is thought to occur because a-aminoadipate semialdehyde cyclises rapidly to form D1-piperideine 6-carboxylic acid (104). The final type of PPTase is found in yeast and fungi as an integral domain at the C-terminal end of cytosolic type I FAS. They are responsible for the modification of cytosolic apo-ACP to allow the assembly of fatty acid megasynthases.

Investigations have begun into using PPTases as drug targets for bacterial infections. The Sfp-PPTase PPTT found in *Mycobacterium tuberculosis* has recently been validated as a potential drug target against the bacterial pathogen. PPTT was found to be essential to bacterial viability and persistence in a murine model and a high throughput screening (HTS) assay was developed to screen for inhibitors (105). Plant pathogens *Colletotrichum graminicola* and *Magnaporthe oryzea* have also displayed a lack of virulence in Sfp-PPTase null mutants (106). Interestingly, potential inhibitors have already been discovered for the Acp-PPTase of *B. subtilis* with a series of small molecule anthranilate 4H-oxazol-5-one showing potent Acp inhibition (107).

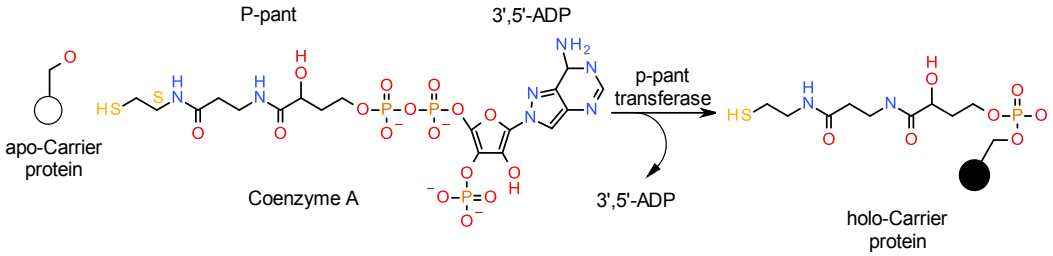

Figure 1.6: Phosphopantetheinylation. The 4'-phosphopantetheine (P-pant) group within Coenzyme A is transferred to a conserved serine residue in the peptidyl carrier domain of the inactive apo-carrier protein to create an active holo-carrier protein. This process is facilitated by 4'-Phosphopantetheinyl transferase (4'-PPTase) (adapted from (97)).

1.6.2. Phosphatases

Cycles of post-translational, reversible, protein phosphorylation occur in eukaryotes as a method to either propagate or terminate internal or external cellular signals. The mechanism involves the removal by phosphatases or the addition by kinases of a negatively charged phosphate at a specific amino acid such as; serine, threonine, and tyrosine residues on the target protein (108). Subsequently, the structural arrangement or the interactions of the target protein become altered. A variety of cellular processes can result from phosphorylation and dephosphorylation cycles including; signal proliferation, differentiation, arrest or cell death (109). The correct regulation of localisation and timing of phosphatases and kinases is vital to ensure equilibrium of phosphorylation cycles is maintained and which in turn is necessary for cellular homeostasis (110).

Phosphatases have been categorised into 2 families based on their substrate specificity; serine/threonine phosphatases (STP) and tyrosine-specific phosphatases (PTP) (108). Serine/threonine phosphatases (STP) can be classified into 3 distinct groups depending on their requirements for metal ions; phosphoprotein phosphatases (PPPs) and metal-dependent protein phosphatases (PPMs). Another STP family are aspartate based phosphatases which consist of the transcription factor IIF–interacting C-terminal domain phosphatase (FCP/SCP). PTP also form subgroups including; classical PTPs, dual specific PTPs (DSPs), low molecular weight (LMW) PTPs, lipid based phosphatases and CDC25 like phosphatases.

As phosphatases are an essential component in the maintenance of cellular homeostasis they have been identified as potential drug targets for many human diseases such as; diabetes, obesity and cancer (108, 111, 112). However the only FDA approved phosphatase targeting drugs are cyclosporine A and FK506 which both inhibit the PPP phosphatase, PP2B, and lead to immunosuppression (108). Phosphatases are also being recognised as virulence factors in a number of pathogenic organisms.

MptpA and MptpB have been classified as essential virulence factors for the bacterial pathogen, *M. tuberculosis.* MptpA is a secreted LMW-PTP, associated in Vacuolar-type H+-adenosine triphosphatase trafficking inhibition and phagosome-lysosome fusion blocking. Reduced survival in human macrophages is observed when MptpA is inhibited (113). MptpB is triple specificity phosphatase show activity towards tyrosine, Serine/Threonine residues and several phosphoinositides (114). It promotes host cell survival by activating the AKT pathway, it also blocks the production of p38 mediated IL-6 and ERK1/2. It has shown to be vital to bacterial viability in macrophages and guinea pigs (115). Many potent inhibitors have been identified for MptpA and MptpB which prove promising for future drug targets (116). The pathogen responsible for bubonic plague, *Yersinia pestis*, has also been shown to secrete a phosphatase (YOPH) that has an effect on virulence. YOPH has been shown to be responsible for phagocytosis and oxidative burst inhibition (117, 118). LipA a lipid and tryrosine phosphatase found in *Listeria monocytogenes*, the cause of listeriosis infection, has an unknown function but causes drastically reduced pathogenicity in mice (119). *Trypanosoma brucei* the causative agent of African sleeping sickness possesses a phosphatase PTP1 that prevents sporadic differentiation of life cycle forms which is vital for transmissibility of the parasite (120). *Salmonella typhimurium*, a bacterial pathogen responsible for causing typhoid infections, secretes a phosphatase, SPTP, into its host cells which causes the reversal of actin cytoskeletal changes induced by the bacterium (121). Phosphatases are critical for virulence in many pathogens therefore are excellent candidates for potential drug targets.

1.7. Aims

Aims of this thesis:

1. To fully characterise PptA as a potential drug target for *A. fumigatus* infection. Proving it an essential component to *A. fumigatus* viability and virulence. To explore the effect PptA has on host response. A high throughput assay will be developed to enable inhibitor screening. Furthermore bioinformatics analysis will be used to predict the antifungal spectrum of a PptA inhibitor and to show whether it is likely to interfere with the human orthologue.

2. To validate a chemical genomics approach in *A. fumigatus* to identify mechanism of action of drugs. This project will show that vegetative cell fusion occurs infrequently under normal cultural conditions in *A. fumigatus*. A library of 46 heterozygous knockouts of essential genes will be generated in a diploid isolate of A. fumigatus. The library will be used to conduct parallel fitness profiling along with an NGS-based barcode-sequencing strategy to confirm the mechanism of action of the antifungal agents; itraconazole and brefeldin A.

3. A comprehensive bioinformatic analysis to identify all the phosphatase encoding genes in *A. fumigatus* will be undertaken and used to identify fungal specific phosphatases. Systematic deletion of all the phosphatases encoding genes will be used to generate a library of mutants and a method involving next generation sequencing to assess the parallel fitness of this library *in vitro* will be validated.

1.8. References

1. Hawksworth DL. The Fungal Dimension of Biodiversity - Magnitude, Significance, and Conservation. Mycological Research. 1991;95:641-55.
2. O'Brien HE, Parrent JL, Jackson JA, Moncalvo JM, Vilgalys R. Fungal community analysis by large-scale sequencing of environmental samples. Applied and Environmental Microbiology. 2005;71(9):5544-50.
3. Romani L. Overview of the Fungal Pathogens. Immunology of Infectious Diseases: American Society of Microbiology; 2002.
4. Fisher MC, Henk DA, Briggs CJ, Brownstein JS, Madoff LC, McCraw SL, et al. Emerging fungal threats to animal, plant and ecosystem health. Nature. 2012;484(7393):186-94.
5. Brown GD, Denning DW, Gow NA, Levitz SM, Netea MG, White TC. Hidden killers: human fungal infections. Science translational medicine. 2012;4(165):165rv13. Epub 2012/12/21.
6. Chapman SW, Sullivan DC, Cleary JD. In search of the holy grail of antifungal therapy. Transactions of the American Clinical and Climatological Association. 2008;119:197-215; discussion -6. Epub 2008/07/04.
7. Schwartz RA. Superficial fungal infections. The Lancet. 2004;364(9440):1173-82.
8. Savin R. Diagnosis and treatment of *tinea versicolor*. The Journal of Family Practice. 1996;43(2):127-32.
9. Bell-Syer SEM, Khan SM, Torgerson DJ. Oral treatments for fungal infections of the skin of the foot. Sao Paulo Medical Journal. 2014;132(2):127-.
10. Kauffman CA, Hajjeh R, Chapman SW, Grp MS. Practice guidelines for the management of patients with sporotrichosis. Clinical Infectious Diseases. 2000;30(4):684-7.
11. Vos T, Flaxman AD, Naghavi M, Lozano R, Michaud C, Ezzati M, et al. Years lived with disability (YLDs) for 1160 sequelae of 289 diseases and injuries 1990–2010: a systematic analysis for the Global Burden of Disease Study 2010. The Lancet. 2012;380(9859):2163-96.
12. Pfaller MA, Diekema DJ. Epidemiology of invasive candidiasis: a persistent public health problem. Clinical microbiology reviews. 2007;20(1):133-63. Epub 2007/01/16.
13. Rees JR, Pinner RW, Hajjeh RA, Brandt ME, Reingold AL. The epidemiological features of invasive mycotic infections in the San Francisco Bay area, 1992-1993: results of population-based laboratory active surveillance. Clinical infectious diseases : an official publication of the Infectious Diseases Society of America. 1998;27(5):1138-47. Epub 1998/11/25.
14. Pappas PG. Invasive candidiasis. Infectious disease clinics of North America. 2006;20(3):485-506. Epub 2006/09/21.
15. Gudlaugsson O, Gillespie S, Lee K, Vande Berg J, Hu J, Messer S, et al. Attributable mortality of nosocomial candidemia, revisited. Clinical infectious diseases : an official publication of the Infectious Diseases Society of America. 2003;37(9):1172-7. Epub 2003/10/15.
16. Cheng MF, Yang YL, Yao TJ, Lin CY, Liu JS, Tang RB, et al. Risk factors for fatal candidemia caused by *Candida albicans* and non-albicans *Candida* species. BMC infectious diseases. 2005;5:22. Epub 2005/04/09.
17. Lin XR, Heitman J. The biology of the *Cryptococcus neoformans* species complex. Annual Review Microbiology. 2006;60:69-105.
18. Park BJ, Wannemuehler KA, Marston BJ, Govender N, Pappas PG, Chiller TA. Estimation of the current global burden of cryptococcal meningitis among persons living with HIV/AIDS. Aids. 2009;23(4):525-30.
19. Carmona EM, Limper AH. Update on the diagnosis and treatment of *Pneumocystis pneumonia*. Therapeutic Advances in Respiratory Disease. 2011;5(1):41-59.

20. Jones JL, Hanson DL, Dworkin MS, Alderton DL, Fleming PL, Kaplan JE, et al. Surveillance for AIDS-defining opportunistic illnesses, 1992-1997. Archives of Dermatology. 1999;135(8):897-902.
21. Morris A, Wei K, Afshar K, Huang L. Epidemiology and clinical significance of *Pneumocystis* colonization. Journal of Infectious Diseases. 2008;197(1):10-7.
22. Ben-Ami R, Lewis RE, Kontoyiannis DP. Enemy of the (immunosuppressed) state: an update on the pathogenesis of *Aspergillus fumigatus* infection. British journal of haematology. 2010;150(4):406-17. Epub 2010/07/14.
23. Hospenthal DR, Kwon-Chung KJ, Bennett JE. Concentrations of airborne *Aspergillus* compared to the incidence of invasive aspergillosis: lack of correlation. Medical Mycology. 1998;36(3):165-8. Epub 1998/10/20.
24. Filler SG, Sheppard DC. Fungal invasion of normally non-phagocytic host cells. PLoS pathogens. 2006;2(12):e129. Epub 2007/01/02.
25. Chandrasekar PH, Alangaden G, Manavathu E. *Aspergillus*: an increasing problem in tertiary care hospitals? Clinical infectious diseases : an official publication of the Infectious Diseases Society of America. 2000;30(6):984-5. Epub 2000/07/06.
26. Gupta RK, Chandr A, Gautam PB. Allergic bronchopulmonary aspergillosis--a clinical review. Journal of the Association Physicians India. 2012;60:46-51.
27. Denning DW, O'Driscoll BR, Hogaboam CM, Bowyer P, Niven RM. The link between fungi and severe asthma: a summary of the evidence. European Respiratory Journal. 2006;27(3):615-26.
28. Denning DW, Pleuvry A, Cole DC. Global burden of chronic pulmonary aspergillosis as a sequel to pulmonary tuberculosis. Bulletin of the World Health Organisation. 2011;89(12):864-72.
29. Soubani AO, Chandrasekar PH. THe clinical spectrum of pulmonary aspergillosis. Chest. 2002;121(6):1988-99.
30. Denning DW, Riniotis K, Dobrashian R, Sambatakou H. Chronic Cavitary and Fibrosing Pulmonary and Pleural Aspergillosis: Case Series, Proposed Nomenclature Change, and Review. Clinical Infectious Diseases. 2003;37(Supplement 3):S265-S80.
31. Denning DW. Invasive Aspergillosis. Clinical Infectious Diseases. 1998;26(4):781-803.
32. Dagenais TR, Keller NP. Pathogenesis of *Aspergillus fumigatus* in Invasive Aspergillosis. Clinical microbiology reviews. 2009;22(3):447-65. Epub 2009/07/15.
33. Kousha M, Tadi R, Soubani AO. Pulmonary aspergillosis: a clinical review. European Respiratory Review. 2011;20(121):156-74.
34. McNeil MM, Nash SL, Hajjeh RA, Phelan MA, Conn LA, Plikaytis BD, et al. Trends in mortality due to invasive mycotic diseases in the United States, 1980–1997. Clinical Infectious Diseases. 2001;33(5):641-7.
35. Chamilos G, Luna M, Lewis RE, Bodey GP, Chemaly R, Tarrand JJ, et al. Invasive fungal infections in patients with hematologic malignancies in a tertiary care cancer center: an autopsy study over a 15-year period (1989-2003). Haematologica. 2006;91(7):986-9. Epub 2006/06/08.
36. Ribes JA, Vanover-Sams CL, Baker DJ. *Zygomycetes* in human disease. Clinical microbiology reviews. 2000;13(2):236-301. Epub 2001/02/07.
37. Walsh TJ, Groll A, Hiemenz J, Fleming R, Roilides E, Anaissie E. Infections due to emerging and uncommon medically important fungal pathogens. Clinical Microbiology and Infection. 2004;10:48-66.
38. Antifungal Drugs: Technologies and Global Markets. BCC Research, 2014 PHM029E.
39. Denning DW, Bromley MJ. How to bolster the antifungal pipeline. Science. 2015;347(6229):1414-6.
40. Denning DW, Hope WW. Therapy for fungal diseases: opportunities and priorities. Trends in microbiology. 2010;18(5):195-204. Epub 2010/03/09.

41. Hope WW, Tabernero L, Denning DW, Anderson MJ. Molecular Mechanisms of Primary Resistance to Flucytosine in *Candida albicans*. Antimicrobial Agents and Chemotherapy. 2004;48(11):4377-86.
42. Vermes A, Guchelaar HJ, Dankert J. Flucytosine: a review of its pharmacology, clinical indications, pharmacokinetics, toxicity and drug interactions. The Journal of antimicrobial chemotherapy. 2000;46(2):171-9. Epub 2000/08/10.
43. Tassel D, Madoff MA. Treatment of *Candida* sepsis and *Cryptococcus meningitis* with 5-fluorocytosine. A new antifungal agent. Jama. 1968;206(4):830-2. Epub 1968/10/21.
44. Pound MW, Townsend ML, Dimondi V, Wilson D, Drew RH. Overview of treatment options for invasive fungal infections. Medical Mycology. 2011;49(6):561-80.
45. Bennett JE, Dismukes WE, Duma RJ, Medoff G, Sande MA, Gallis H, et al. A comparison of amphotericin B alone and combined with flucytosine in the treatment of cryptoccal meningitis. The New England journal of medicine. 1979;301(3):126-31. Epub 1979/07/19.
46. Bicanic T, Wood R, Meintjes G, Rebe K, Brouwer A, Loyse A, et al. High-dose amphotericin B with flucytosine for the treatment of cryptococcal meningitis in HIV-infected patients: a randomized trial. Clinical infectious diseases : an official publication of the Infectious Diseases Society of America. 2008;47(1):123-30. Epub 2008/05/29.
47. Brouwer AE, Rajanuwong A, Chierakul W, Griffin GE, Larsen RA, White NJ, et al. Combination antifungal therapies for HIV-associated cryptococcal meningitis: a randomised trial. Lancet. 2004;363(9423):1764-7. Epub 2004/06/03.
48. Brajtburg J, Bolard J. Carrier effects on biological activity of amphotericin B. Clinical microbiology reviews. 1996;9(4):512-31. Epub 1996/10/01.
49. Verweij PE, Snelders E, Kema GHJ, Mellado E, Melchers WJG. Azole resistance in *Aspergillus fumigatus*: a side-effect of environmental fungicide use? Lancet Infectious Diseases Dis. 2009;9(12):789-95.
50. Zonios DI, Bennett JE. Update on azole antifungals. Seminars in Respiratory and Critical Care Medicine. 2008;29(2):198-210.
51. Pettit NN, Carver PL. Isavuconazole: A New Option for the Management of Invasive Fungal Infections. Annals of Pharmacotherapy. 2015;49(7):825-42.
52. Sharkey PK, Rinaldi MG, Dunn JF, Hardin TC, Fetchick RJ, Graybill JR. High-dose itraconazole in the treatment of severe mycoses. Antimicrobial Agents and Chemotherapy. 1991;35(4):707-13.
53. Ashley ESD, Lewis R, Lewis JS, Martin C, Andes D. Pharmacology of systemic antifungal agents. Clinical Infectious Diseases. 2006;43:S28-S39.
54. Lipp HP. Antifungal agents--clinical pharmacokinetics and drug interactions. Mycoses. 2008;51 Suppl 1:7-18. Epub 2008/05/28.
55. Denning DW. Echinocandins: a new class of antifungal. Journal of Antimicrobial Chemotherapy. 2002;49(6):889-91.
56. Morris MI, Villmann M. Echinocandins in the management of invasive fungal infections, part 1. American Journal of Health-System Pharmacy. 2006;63(18):1693-703.
57. Vazquez JA. Anidulafungin: a new echinocandin with a novel profile. Clinical therapeutics. 2005;27(6):657-73. Epub 2005/08/25.
58. Ryder NS, Dupont MC. Inhibition of squalene epoxidase by allylamine antimycotic compounds. A comparative study of the fungal and mammalian enzymes. Biochemical Journal. 1985;230(3):765-770.
59. Wolverton, SE. Comprehensive Dermatologic Drug Therapy, 3rd ed. Philadelphia, United States: Elsevier - Health Sciences Division; 2012

60. Schiraldi GF, Colombo MD, Harari S, Cicero SL, Ziglio G, Ferrarese M, Rossato D, Soresi E. Terbinafine in the treatment of non-immunocompromised compassionate cases of bronchopulmonary aspergillosis. Mycoses 1996; 39(1-2)
61. Kirkpatrick WR, Perea S, Coco BJ, Patterson TF. Efficacy of caspofungin alone and in combination with voriconazole in a Guinea pig model of invasive aspergillosis. Antimicrobial Agents and Chemotherapy. 2002;46(8):2564-8. Epub 2002/07/18.
62. Caillot D, Thiebaut A, Herbrecht R, de Botton S, Pigneux A, Bernard F, et al. Liposomal amphotericin B in combination with caspofungin for invasive aspergillosis in patients with hematologic malignancies: a randomized pilot study (Combistrat trial). Cancer. 2007;110(12):2740-6. Epub 2007/10/18.
63. Popp AI, White MH, Quadri T, Walshe L, Armstrong D. Amphotericin B with and without itraconazole for invasive aspergillosis: A three-year retrospective study. International Journal of Infectious Diseases. 1999;3(3):157-60.
64. Pfaller MA, Messer SA, Motyl MR, Jones RN, Castanheira M. Activity of MK-3118, a new oral glucan synthase inhibitor, tested against *Candida* spp. by two international methods (CLSI and EUCAST). Journal of Antimicrobial Chemotherapy. 2013; 68: 858–863
65. Pfaller MA, Messer SA, Motyl MR, Jones RN, Castanheira M. *In vitro* activity of a new oral glucan synthase inhibitor (MK-3118) tested against *Aspergillus* spp. by CLSI and EUCAST broth microdilution methods. Antimicrobial Agents and Chemotherapy. 2013; 57: 1065–1068.
66. Tsukahara K, Hata K, Nakamoto K, Sagane K, Watanabe NA, Kuromitsu J, Kai J, Tsuchiya M, Ohba F, Jigami Y, *et al*. Medicinal genetics approach towards identifying the molecular target of a novel inhibitor of fungal cell wall assembly. Molecular Microbiology. 2003; 48: 1029–1042
67. Hata K, Horii T, Miyazaki M, Watanabe NA, Okubo M, Sonoda J, Nakamoto K, Tanaka K, Shirotori S, Murai N, *et al*. Efficacy of oral E1210, a new broad-spectrum antifungal with a novel mechanism of action, in murine models of candidiasis, aspergillosis, and fusariosis. Antimicrobial Agents and Chemotherapy. 2011; 55: 4543–4551
68. Takeshita H, Watanabe J, Kimura Y, Kawakami K, Takahashi H, Takemura M, Kitamura A, Someya K, Nakajima R. Novel pyridobenzimidazole derivatives exhibiting antifungal activity by the inhibition of β-1,6-glucan synthesis. Bioorganic & Medicinal Chemistry Letters. 2010; 20(13): 3893-3896.
69. Wiederhold NP, Najvar LK, Matsumoto S, Bocanegra RA, Herrera M, Wickes BL, Kirkpatrick WR, Patterson TF. Efficacy of the Investigational Echinocandin ASP9726 in a Guinea Pig Model of Invasive Pulmonary Aspergillosis. Antimicrobial Agents and Chemotherapy. 2015; 59(5): 2875-2881.
70. Nierman WC, Pain A, Anderson MJ, Wortman JR, Kim HS, Arroyo J, et al. Genomic sequence of the pathogenic and allergenic filamentous fungus *Aspergillus fumigatus*. Nature. 2005;438(7071):1151-6.
71. Giaever G, Chu AM, Ni L, Connelly C, Riles L, Veronneau S, et al. Functional profiling of the *Saccharomyces cerevisiae* genome. Nature. 2002;418(6896):387-91. Epub 2002/07/26.
72. Roemer T, Jiang B, Davison J, Ketela T, Veillette K, Breton A, et al. Large-scale essential gene identification in *Candida albicans* and applications to antifungal drug discovery. Molecular microbiology. 2003;50(1):167-81. Epub 2003/09/26.
73. Hu W, Sillaots S, Lemieux S, Davison J, Kauffman S, Breton A, et al. Essential gene identification and drug target prioritization in *Aspergillus fumigatus.* PLoS pathogens. 2007;3(3):e24.

74. Hua-Van A, Pamphile JA, Langin T, Daboussi MJ. Transposition of autonomous and engineered impala transposons in *Fusarium oxysporum* and a related species (vol 264, pg 734, 2001). Molecular and General Genetics. 2001;264(5):734-.
75. Villalba F, Lebrun MH, Hua-Van A, Daboussi MJ, Grosjean-Cournoyer MC. Transposon *impala*, a novel tool for gene tagging in the rice blast fungus *Magnaporthe grisea*. Molecular Plant Microbe Interactions Journal. 2001;14(3):308-15.
76. Firon A, Villalba F, Beffa R, d'Enfert C. Identification of essential genes in the human fungal pathogen *Aspergillus fumigatus* by transposon mutagenesis. Eukaryotic Cell. 2003;2(2):247-55.
77. Nicosia MGL, Brocard-Masson C, Demais S, Van AH, Daboussi MJ, Scazzocchio C. Heterologous transposition in *Aspergillus nidulans*. Molecular microbiology. 2001;39(5):1330-44.
78. Carr PD, Tuckwell D, Hey PM, Simon L, d'Enfert C, Birch M, et al. The Transposon impala is activated by low temperatures: use of a controlled transposition system to identify genes critical for viability of *Aspergillus fumigatus*. Eukaryotic Cell. 2010;9(3):438-48.
79. Hua-Van A, Langin T, Daboussi MJ. Aberrant transposition of a Tc1-mariner element, impala, in the fungus *Fusarium oxysporum*. Molecular Genetics and Genomics. 2002;267(1):79-87.
80. Payne DJ, Gwynn MN, Holmes DJ, Pompliano DL. Drugs for bad bugs: confronting the challenges of antibacterial discovery. Nature Reviews Drug Discovery. 2007;6(1):29-40.
81. Jones D. The antibacterial lead discovery challenge. Nature Reviews Drug Discovery. 2010;9(10):751-2.
82. Papp B, Pal C, Hurst LD. Dosage sensitivity and the evolution of gene families in yeast. Nature. 2003;424(6945):194-7.
83. Deutschbauer AM, Jaramillo DF, Proctor M, Kumm J, Hillenmeyer ME, Davis RW, et al. Mechanisms of haploinsufficiency revealed by genome-wide profiling in yeast. Genetics. 2005;169(4):1915-25.
84. Lindsley DL, Sandler L, Baker BS, Carpenter AT, Denell RE, Hall JC, et al. Segmental aneuploidy and the genetic gross structure of the *Drosophila* genome. Genetics. 1972;71(1):157-84. Epub 1972/05/01.
85. Giaever G, Shoemaker DD, Jones TW, Liang H, Winzeler EA, Astromoff A, et al. Genomic profiling of drug sensitivities via induced haploinsufficiency. Nature genetics. 1999;21(3):278-83. Epub 1999/03/18.
86. Xu D, Jiang B, Ketela T, Lemieux S, Veillette K, Martel N, et al. Genome-wide fitness test and mechanism-of-action studies of inhibitory compounds in *Candida albicans*. PLoS pathogens. 2007;3(6):e92. Epub 2007/07/03.
87. Jiang B, Xu D, Allocco J, Parish C, Davison J, Veillette K, et al. PAP inhibitor with *in vivo* efficacy identified by *Candida albicans* genetic profiling of natural products. Chemistry & biology. 2008;15(4):363-74. Epub 2008/04/19.
88. Hensel M, Shea JE, Gleeson C, Jones MD, Dalton E, Holden DW. Simultaneous identification of bacterial virulence genes by negative selection. Science. 1995;269(5222):400-3. Epub 1995/07/21.
89. Shoemaker DD, Lashkari DA, Morris D, Mittmann M, Davis RW. Quantitative phenotypic analysis of yeast deletion mutants using a highly parallel molecular bar-coding strategy. Nature genetics. 1996;14(4):450-6.
90. Smith AM, Heisler LE, St Onge RP, Farias-Hesson E, Wallace IM, Bodeau J, et al. Highly-multiplexed barcode sequencing: an efficient method for parallel analysis of pooled samples. Nucleic acids research. 2010;38(13):e142. Epub 2010/05/13.
91. Smith AM, Heisler LE, Mellor J, Kaper F, Thompson MJ, Chee M, et al. Quantitative phenotyping via deep barcode sequencing. Genome research. 2009;19(10):1836-42. Epub 2009/07/23.

92. Baudin A, Ozier-Kalogeropoulos O, Denouel A, Lacroute F, Cullin C. A simple and efficient method for direct gene deletion in *Saccharomyces cerevisiae*. Nucleic acids research. 1993;21(14):3329-30. Epub 1993/07/11.
93. Szewczyk E, Nayak T, Oakley CE, Edgerton H, Xiong Y, Taheri-Talesh N, et al. Fusion PCR and gene targeting in *Aspergillus nidulans*. Nature protocols. 2006;1(6):3111-20. Epub 2007/04/05.
94. Krappmann S. Gene targeting in filamentous fungi: the benefits of impaired repair. Fungal Biology Reviews. 2007;21(1):25-9.
95. da Silva Ferreira ME, Kress MRVZ, Savoldi M, Goldman MHS, Härtl A, Heinekamp T, et al. The akuBKU80 Mutant Deficient for Nonhomologous End Joining Is a Powerful Tool for Analyzing Pathogenicity in *Aspergillus fumigatus*. Eukaryotic Cell. 2006;5(1):207-11.
96. Hughes JP, Rees S, Kalindjian SB, Philpott KL. Principles of early drug discovery. British journal of pharmacology. 2011;162(6):1239-49. Epub 2010/11/26.
97. Walsh CT, Gehring AM, Weinreb PH, Quadri LE, Flugel RS. Post-translational modification of polyketide and nonribosomal peptide synthases. Current opinion in chemical biology. 1997;1(3):309-15. Epub 1998/07/17.
98. Elovson J, Vagelos PR. Acyl Carrier Protein: X. Acyl carrier protein synthetase. Journal of Biological Chemistry. 1968;243(13):3603-11.
99. Allen G, Bromley M, Kaye SJ, Keszenman-Pereyra D, Zucchi TD, Price J, et al. Functional analysis of a mitochondrial phosphopantetheinyl transferase (PPTase) gene *pptB* in *Aspergillus fumigatus*. Fungal genetics and biology. 2011;48(4):456-64. Epub 2011/01/05.
100. Joshi AK, Zhang L, Rangan VS, Smith S. Cloning, Expression, and Characterization of a Human 4'-Phosphopantetheinyl Transferase with Broad Substrate Specificity. Journal of Biological Chemistry. 2003;278(35):33142-9.
101. Strickland KC, Hoeferlin LA, Oleinik NV, Krupenko NI, Krupenko SA. Acyl carrier protein-specific 4'-phosphopantetheinyl transferase activates 10-formyltetrahydrofolate dehydrogenase. The Journal of biological chemistry. 2010;285(3):1627-33. Epub 2009/11/26.
102. Bunkoczi G, Pasta S, Joshi A, Wu XQ, Kavanagh KL, Smith S, et al. Mechanism and substrate recognition of human holo ACP synthase. Chemistry & biology. 2007;14(11):1243-53.
103. Reuter K, Mofid MR, Marahiel MA, Ficner R. Crystal structure of the surfactin synthetase-activating enzyme sfp: a prototype of the 4'-phosphopantetheinyl transferase superfamily. The EMBO journal. 1999;18(23):6823-31. Epub 1999/12/03.
104. Praphanphoj V, Sacksteder KA, Gould SJ, Thomas GH, Geraghty MT. Identification of the α-Aminoadipic Semialdehyde Dehydrogenase-Phosphopantetheinyl Transferase gene, the human ortholog of the yeast LYS5 Gene. Molecular Genetics and Metabolism. 2001;72(4):336-42.
105. Leblanc C, Prudhomme T, Tabouret G, Ray A, Burbaud S, Cabantous S, et al. 4'-Phosphopantetheinyl transferase PptT, a new drug target required for *Mycobacterium tuberculosis* growth and persistence *in vivo*. PLoS pathogens. 2012;8(12):e1003097. Epub 2013/01/12.
106. Horbach R, Graf A, Weihmann F, Antelo L, Mathea S, Liermann JC, et al. Sfp-Type 4'-Phosphopantetheinyl transferase Is indispensable for fungal pathogenicity. The Plant Cell. 2009;21(10):3379-96.
107. Gilbert AM, Kirisits M, Toy P, Nunn DS, Failli A, Dushin EG, et al. Anthranilate 4H-oxazol-5-ones: novel small molecule antibacterial acyl carrier protein synthase (AcpS) inhibitors. Bioorganic & medicinal chemistry letters. 2004;14(1):37-41. Epub 2003/12/20.
108. McConnell JL, Wadzinski BE. Targeting protein serine/threonine phosphatases for drug development. Molecular Pharmacology. 2009;75(6):1249-61.

109. Brenchley R, Tariq H, McElhinney H, Szoor B, Huxley-Jones J, Stevens R, et al. The TriTryp Phosphatome: analysis of the protein phosphatase catalytic domains. Bmc Genomics. 2007;8.
110. Bauman AL, Scott JD. Kinase- and phosphatase-anchoring proteins: harnessing the dynamic duo. Nature cell biology. 2002;4(8):E203-6. Epub 2002/08/01.
111. Nunes-Xavier C, Roma-Mateo C, Rios P, Tarrega C, Cejudo-Marin R, Tabernero L, et al. Dual-specificity MAP kinase phosphatases as targets of cancer treatment. Anti-Cancer Agent in Medicinal Chemistry. 2011;11(1):109-32.
112. Ríos P, Nunes-Xavier CE, Tabernero L, Köhn M, Pulido R. Dual-specificity phosphatases as molecular targets for inhibition in human disease. Antioxidants & Redox Signaling. 2013;20(14):2251-73.
113. Bach H, Papavinasasundaram KG, Wong D, Hmama Z, Av-Gay Y. *Mycobacterium tuberculosis* virulence is mediated by PtpA dephosphorylation of human vacuolar protein sorting 33B. Cell and Host Microbe. 2008;3(5):316-22.
114. Beresford N, Patel S, Armstrong J, Szoor B, Fordham-Skelton AP, Tabernero L. MptpB, a virulence factor from *Mycobacterium tuberculosis*, exhibits triple-specificity phosphatase activity (vol 406, pg 13, 2007). Biochem Journal. 2007;406:527-.
115. Singh R, Rao V, Shakila H, Gupta R, Khera A, Dhar N, et al. Disruption of mptpB impairs the ability of *Mycobacterium tuberculosis* to survive in guinea pigs. Molecular microbiology. 2003;50(3):751-62.
116. Silva AP, Tabernero L. New strategies in fighting TB: targeting *Mycobacterium tuberculosis*-secreted phosphatases MptpA & MptpB. Future medicinal chemistry. 2010;2(8):1325-37. Epub 2011/03/24.
117. Bliska JB, Black DS. Inhibition of the Fc receptor-mediated oxidative burst in macrophages by the *Yersinia-Pseudotuberculosis* tyrosine phosphatase. Infection and immunity. 1995;63(2):681-5.
118. Rosqvist R, Bolin I, Wolf-Watz H. Inhibition of phagocytosis in *Yersinia* pseudotuberculosis: a virulence plasmid-encoded ability involving the Yop2b protein. Infection and immunity. 1988;56(8):2139-43. Epub 1988/08/01.
119. Kastner R, Dussurget O, Archambaud C, Kernbauer E, Soulat D, Cossart P, et al. LipA, a tyrosine and lipid phosphatase involved in the virulence of *Listeria monocytogenes*. Infection and immunity. 2011;79(6):2489-98.
120. Szoor B, Wilson J, McElhinney H, Tabernero L, Matthews KR. Protein tyrosine phosphatase TbPTP1: a molecular switch controlling life cycle differentiation in *trypanosomes*. Journal of Cell Biology. 2006;175(2):293-303.
121. Fu Y, Galan JE. A salmonella protein antagonizes Rac-1 and Cdc42 to mediate host-cell recovery after bacterial invasion. Nature. 1999;401(6750):293-7. Epub 1999/09/28.

Chapter 2

PptA, a drug target for *Aspergillus fumigatus* infection

Anna Johns, Daniel Sharf, Bharat Rash, Elaine Bignell, Michael Bromley

2. PptA, a drug target for *Aspergillus fumigatus* infection

Anna Johns, Daniel Sharf, Bharat Rash, Elaine Bignell, Michael Bromley

Target Journal: PLOS Pathogens

Abstract:

Fungal diseases are estimated to kill between 1.5 and 2 million people each year which exceeds global mortality estimates for either tuberculosis or malaria. *Aspergillus fumigatus* is the leading cause of invasive aspergillosis, a globally distributed fungal disease which causes 200,000 life threatening infections annually with mortality rates of up to 95%. It poses as a common threat to patients with a compromised immune system due to disorders such as leukaemia, HIV, AIDS and also persons undergoing chemotherapy treatments or transplantation. Problematic issues surrounding the standard treatment protocol for this infection include fungal drug resistance and serious adverse side effects. There is an urgent need to discover and develop an innovative class of drugs that possess new mechanisms of action against novel drug targets. We have identified a potential drug target, PptA that plays a key role in *A. fumigatus* secondary metabolism. PptA is a sfp-type phosphopantetheinyl transferase and is required to activate non-ribosomal peptide synthases, polyketide synthases and a protein required for lysine biosynthesis, aminoadipate reductase (AarA). Disruption of *pptA* renders the fungus avirulent in both insect and murine infection models. It also appears that the loss of PptA affects the immune recognition of spores, similar to other melanin deficient strains leaving fungal spores more vunerable to host detection. Furthermore the PptA recombinant protein has been produced and proven active in a high throughput fluorescence polarisation assay which can be used for screening purposes to find potential inhibitors.

2.1. Introduction

Humans are constantly challenged by the threat of fungal infection. Estimates put the number of individuals infected by superficial fungal disease at about 1.7 billion (1). There is also a significant proportion of invasive infections which are difficult to treat and lead to an estimated 1.5 million deaths each year (2). The incidence of fungal disease increased significantly in the latter part of the 20th century and this has been attributed to the expansion of immune deficient population, particularly those who receive immunosuppressive therapies (3). *Aspergillus fumigatus* is a filamentous fungal pathogen and is the leading cause of aspergillosis, an invasive fungal disease that causes more than 200,000 life threatening infections annually with mortality rates of up to 95% (2). The problems associated with the medications used to treat fungal disease such as adverse side effects in patients, drug-drug interactions and increasing antifungal resistance (4) are significant. This coupled with the limited number of agents currently in development (5) highlight the need to identify novel classes of antifungals.

4'-Phosphopantetheinyl transferase (4'-PPTase) mediates the transfer and covalent tethering of 4'-phosphopantetheine (P-pant) from coenzymeA (CoA) to a conserved serine residue within a peptidyl carrier domain of a protein substrate (6, 7) (figure S2.1). This process modifies the target protein from an inactive apo-enzyme into an active holo-enzyme allowing attachment of substrates and intermediates for a range of enzymes involved in both primary and secondary metabolism.

Proteins of the PPTase superfamily can be categorised into 3 families based on their sequence, structure and targets (8). The type I class of enzymes, are typified by the acyl carrier protein synthase class (ACPs-type PPTases), they are on average 120 aa and prime acyl carrier proteins (ACPs) by covalently attaching a loading site for intermediates. Type II include surfactin phosphopantetheinyl transferases (Sfp), and are thought to have evolved due to a gene duplication of the ACPs-type PPTases (8). They are on average 240 aa and exist as pseudo-homodimers. Each pseudo-homodimer closely resembles ACPs-type PPTases monomers. It has one active site that falls at the pseudo-dimer interface and has much broader specificity than ACPs-type PPTase. The final group, type III, exist as integral domains of the C-terminal of type 1 fatty acid synthases (FAS). They catalyse apo-ACPs to allow assembly of megasynthatase complexes (9).

In most filamentous fungi 3 PPTases have been described, 1 from each family and include an ACPs-type which interacts with the mitochondrial FAS, a Sfp-type enzyme and an integral ACPs-type enzyme which is found in FAS alpha-subunit. In *Aspergillus nidulans* the Sfp-type 4'-PPTase gene is known as *npgA* (10). NpgA has been well characterised and shows a wide array

of activity (11) and is responsible for the phosphopantetheinylation of enzymes involved in primary and secondary metabolism including polyketide synthase, required for melanin pigment synthesis (12), α- aminoadipate reductase (AarA) required for lysine biosynthesis, NRPS SidC and SidD, components of intracellular and extracellular siderophore biosynthesis and NRPS δ-(L-α-aminoadipyl)-L-cysteinyl-D-valine synthetase required for penicillin biosynthesis (11, 13, 14). Without supplementation of the siderophore triacetylfusarinine C (TAFC) and lysine an *npgA* null mutant will not grow (11), making this gene conditionally essential in *A. nidulans*. The *A. fumigatus* orthologue of *npgA* is *pptA*. As in *A. nidulans* a *pptA* null mutant is auxotrophic for lysine and PptA has been shown to activate AarA *in vitro* assay (15). In contrast to the situation in *A. nidulans* however, *A. fumigatus* is able to acquire free iron without the need for siderophores due to the action of an operative reductive iron assimilatory system (16). Stains lacking *pptA* also have albino conidia rather than the normal green colouration. This is due to the lack of phosphopantetheinylation of the polyketide synthase, PksP/Alb1, which is required for the biosynthesis of WA pigment intermediate which is in turn necessary for the synthesis of PK-derived 1,8-Dihydroxynaphthalene (DHN)-melanin pigment (15).

The pathogenic success of *A. fumigatus* includes its ability to produce potent secondary metabolites as part of its defence system (17). Some of the biosynthesis pathways involving PptA activity have already been associated with fungal virulence such as NRPS/PKS dependent siderophore and DHN-melanin synthesis. The ability for pathogens to sequester iron from their host is essential to successful colonisation (18). It was found that siderophore-mediated iron uptake alone was essential for *A. fumigatus* virulence in a murine model (16). DHN-melanin is also known to contribute to the virulence of fungi that attack both humans and plants. The virulence of the former is achieved by quenching oxygen radicals and by providing hyphae with protection against human monocytes (19). For plant attacking fungi melanin is also required to generate appressorial turgor pressure an essential component of their pathogenicity (19-21). Melanin has also been proven to be an important factor in host invasion (22). It effectively hides several *A. fumigatus* pattern-associated molecular patterns, prevents apoptosis by macrophages, provides protection from reactive oxygen species and inhibits acidification of phagolysosomes (23-27). Furthermore, PptA is required for the production of the essential amino acid, lysisne. *A. fumigatus* lysine auxotrophs have also shown to have an effect on virulence. Homocitrate synthase (HcsA) and homoaconitase LysF deletion mutants are both essential in lysine biosynthesis. Both mutations cause strongly attenuated virulence in murine models of bronchopulmonary aspergillosis (28, 29).

PptA involvement in the production of many virulence factors as well as essential amino acid biosynthesis makes it a potential candidate for an antifungal drug target. Here we validate

PptA as a candidate target by demonstrating a critical role for this enzyme in the production of secondary metabolites in *A. fumigatus*, growth in iron limiting conditions and virulence. We further demonstrate the suitability of this target by developing a high-throughput screening assay capable of identifying inhibitors of PptA enzymatic activity.

2.2. Materials and Methods

2.2.1. Identification of sequences used in this study

All *A. fumigatus* DNA sequences were downloaded from the Central Aspergillus REsource (CADRE) database (http://www.cadre-genomes.org.uk/index.html). The following sequences were used in this study; *pptA* (AFUB_024520A), *aarA* (AFUB_068270A), *sidA* (AFUB_023720A) and *pksP* (AFUB_033290A).

2.2.2. Strains

An A1160 ΔKu80 pyrG+ strain, referred to as A1160p+ (30) served as a parental strain for all gene deletion mutants. Strains used are listed in table 2.1. *A. fumigatus* was cultured on Sabouraud (SAB) agar at 37°C in the dark. Lysine auxotrophs were supplemented with 10 mM Lysine. Strains auxotrophic for iron were supplemented with either 1.5 mM $FeSO_4$ or 10 µM TAFC. TAFC was extracted from *A. fumigatus* in iron-deprived liquid cultures. Desferri-TAFC in the supernatant was saturated with iron and subsequently extracted using chloroform (31).

Table 2.1: Fungal strains used during this study

Strain	Description	Source
A1160p+	Derived from CEA10, $Ku80^{\Delta}$, pyrG+	(30)
Δ*pptA*	Derived from A1160p+, *hph*+, *pptA*-	This study
pptA rec	Reconstitued Δ*pptA*, *hph*-	This study
Δ*aarA*	Derived from A1160p+, *hph*+, *aarA*-	This study
aarA rec	Reconstitued Δ*aarA*, *hph*-	This study
Δ*pksP*	Derived from A1160p+, *hph*+, *pksP*-	This study
pksP rec	Reconstituted Δ*pksP*, *hph*-	This study
Δ*sidA*	Derived from A1160p+, *hph*+, *sidA*-	This study
sidA rec	Reconstituted Δ*sidA*, *bleo*+, *sidA*-	This study

2.2.3. Generation of strains

Gene knockout cassettes were generated using a modified PCR fusion approach (30, 32). All primers used to generate the cassettes can be found in table S2.1. Primers P1 and P2 were used to amplify the 5' and P3 and P4 were used to amplify the 3' non-coding regions of the gene Hygromycin B phosphotransferase gene (*hph*) was amplified from pAN7-1 (33) using primers HPHF and HPHR. To facilitate gene fusion, primers P2 and P3 incorporated regions

complementary to the terminal regions of the hph primers. PCR primer design software Primer 3 (http://frodo.wi.mit.edu/) was used to aid primer design and all primers were supplied by Eurofins MWG Operon. The process consists of 3 rounds of PCR reactions previously published by Frazeck, *et al* (2013).

A. fumigatus mycelia were treated with a 5% glucanex solution (made up in 0.6M KCl/50mM $CaCl_2$ solution) for 2–3 h at 30°C to produce protoplasts. DNA was transformed into protoplasts by PEG-mediated transformation. 200µg/ml hygromycin was used for selection.

Reconstituted isolates *pptA* rec, *aarA* rec, *pksP* rec were generated by restoring the named genes back to their original locus using fragments amplified with associated primers P1 and P4. The *pptA* rec isolate was obtained by selection on Vogel's minimal media (VMM) (34) lacking supplemental lysine and iron, the *aarA* rec isolate on VMM lacking supplemental lysine and the *pksP* rec isolate was identified as a green sporulating colony.

For the reconstituted isolate *sidA* rec approximately 1 kb of 5' flanking region in addition to the coding sequence and 3' flanking regions of gene of interest were amplified by PCR from fungal genomic DNA using long amp DNA polymerase. Primers P1 and P2 were used to amplify the 5' region and the gene itself and P3 and P4 were used to amplify the 3' non-coding region of the gene (table S2.1). The bleomycin resistant gene (*bleo*) was amplified from pPICZaA (Life Technologies) incorporating regions complementary to the P2 and P3 using primers HPHF and HPHR. Reconstituted isolates were selected on VMM containing 40µg/ml bleomycin.

All mutant and reconstituted strains were screened for homologous recombination by PCR and confirmed by Southern blotting (figure S2.2).

2.2.4. Phylogenetic analysis

Phylogenetic analyses were conducted using MEGA 6 (35). All sequences were aligned using ClustalW software provided by MEGA 6. Phylogenetic trees were prepared by the maximum likelihood method using the distance estimation models Jones-Taylor-Thornton (JTT) (36). Bootstrap values were calculated from 1000 replications of the bootstrap procedure using programs within MEGA 6 package.

2.2.5. Phenotypic analysis

RPMI-1640 with L-glutamine and $NaHCO_3$ (Sigma) containing either 10 µM TAFC, 10 mM lysine or both supplements was inoculated with $2.5x10^5$ spores/ml from Δ*pptA*, *pptA*rec and A1160p+. 200µl of the media/spore mixture was transferred into a well of a 96-well plate to give $5x10^4$ spores per well. 8 replicates of each strain were included in the plate as well as 20

replicates of a negative control of just media. The plate was sealed with a "breathe easy" covering membrane (Sigma-Aldrich) and placed on a microplate scanning spectrophotometer (BIO TEK® Synergy HT). The plate was incubated at 37°C and the optical density measured at 600 nm every 10 minutes over a 48 hour time period. Fungal growth was determined by calculating the velocity of the linear phase of the growth curve. A Student's T-test was used to determine the statistical significance between the growth rates of the different strains of *A. fumigatus.*

A dose response assay was used to determine optimum concentration of TAFC or lysine. For TAFC dose response RPMI media containing 10 mM lysine was used with a 1 in 2 serial dilution of TAFC ranging from 10 µM to 0 µM. The lysine dose response used RPMI media containing 10 µM TAFC with a 1 in 2 serial dilution of lysine ranging from 10 mM to 0 mM.

2.2.6. Secondary metabolite assay

$1x10^7$ spores Δ*pptA*, *pptA*rec and A1160p+ were grown in 100 ml Czapek-dox medium or SAB medium for 7 days. The culture supernatant was extracted with an equal volume of ethyl acetate. The organic phase was recovered and dried. The residuum was dissolved in 1 ml methanol and analysed by LC-MS.

2.2.7. Host response assays

2.2.7.1. Dendritic cell challenge

Peripheral blood mononuclear cells (PBMCs) were isolated from healthy donors by Ficoll-Hypaque density gradient centrifugation and cultured in growth media (RPMI + 1% penstrep + L-glutamine + 10% FBS). Dendritic cells (DCs) were derived by separating monocytes by magnetic enrichment with anti-CD14 beads. DC differentiation occurred after 5 days culture in the presence of GM-CSF (50 ng/ml) and recombinant IL-4 (25 ng/ml). Fresh media was supplied on day 3.

A. fumigatus strains; Δ*pptA*, *pptA* rec, Δ*pksP* and A1160p+ were streaked onto SAB agar, after 3 days growth at 37°C the spores were harvested through glass wool into PBS. The spores were fixed by incubating in paraformaldehyde (2.5%, v/v) overnight at 4°C. These were washed 3 times in PBS and suspended in growth media. They were counted and normalised to required concentration.

The human cells were challenged for 24 hours with a 2:1 ratio (spores:cells). After the required time RNA was extracted from the cells for quantitative real-time PCR (QRT-PCR) analysis.

Human total RNA was extracted from the dendritic cells by a modified phenol and guanidine thiocyanate protocol (37). Cells were harvest and pelleted by centrifugation for 5 minutes at

300 g. The pellet was resuspended in 10 µl of supernatant and mixed with 1 ml of TRI-reagent (Sigma). 3 cycles of 10 second vortexing and placing samples on ice followed. RNase was added and samples left at room temperature for 5 minutes. 200 µl of chloroform was added and the homogenate was mixed and then centrifuged at 12000 g, the upper aqueous layer was transferred to a clean Eppendorf and 500 µl of isopropanol was added. RNA was pelleted by centrifugation and washed with 1 ml of 75% ethanol. Finally the RNA was resuspended in molecular grade water, quantified and stored at -80°C prior to use.

Brilliant II SYBR green QRT-PCR master mix, 1 step kit was used to synthesise cDNA and to perform PCR amplification using primers in table S2.2 (38). Transcripts for IL-1β and IL-6 genes were quantified using Relative Expression Software Tool (REST) 2009 software. Quantification of the PCR signals was performed by comparing the cycle threshold (Ct) value of the gene of interest with the Ct value of the reference gene ACTβ. A two-sided, student-t test was used for statistical analysis to compare wild type response to other strains. P-value <0.05 was considered significant (P-value <0.05 * and <0.01 **).

2.2.7.2. Phagolysosomal acidification assay

A. fumigatus strains; Δ*pptA*, *pptA* rec, Δ*pksP* and A1160p+ were streaked onto Aspergillus minimal media (AMM) (39) supplemented with 1.5 mM $FeSO_4$ and 10 mM lysine, after 5 days growth at 37°C conidia were harvested.

Murine Alveolar Macrophages (ATCC® TIB-71) were cultured in Dulbecco's Modified Eagle's Medium supplemented with 10 % fetal calf serum (Lonza), 1 % ultraglutamine (Lonza) and 27.5 µg/mL gentamicin (Lonza) at 37 °C and 5 % CO2 to confluence.

RAW264.7 macrophages were cultured overnight on microscopy cover slips in a 24-well plate. Prior to infection with fungal strains cells were pre-stained with 50 nM Lysotracker (Red DND-99, Thermo Fischer Science) for 1 hour at 37 °C in a CO_2 incubator. Another 50 nM Lysotracker were added with the infection of the macrophages. Fungal spores were stained with 100 µg/mL calcofluor white and administered at a MOI = 2. Plates were spun down 5 minutes, 100 x g, 37 °C to synchronize phagocytosis. Cells were co-incubated for 2 hours at 37 °C in a CO2 incubator.

Samples were washed once with PBS and fixed for 10 minutes at room temperature with 4 % formaldehyde. Cells were washed 3 times for 5 minutes with PBS and cover slips applied on glass slides for CLSM analysis.

Images were acquired with an inverted confocal laser scanning microscope (Carl Zeiss AG) and analysed using ZEN software (Carl Zeiss AG). Conidia surrounded by a ring-like Lysotracker signal were considered as residing in an acidified phagolysosome and counted as 'acidified conidia'. The ratio of 'acidified conidia' to the total number of ingested conidia was determined to give the 'acidification ratio'. All values represent mean ± SD values of three experiments. Significance of the results was calculated with the student's t-test.

2.2.8. Virulence studies

2.2.8.1. Insect infection

Sixth stage instar larval *Galleria mellonella* (15-25 mm in length) were ordered from the Live Foods Company (Sheffield, England). Prior to use the larvae were stored in the dark at 4˚C in wood shavings. The larvae were used within 3 weeks of delivery. Randomly chosen groups of 30 *G. mellonella* were inoculated by injecting 10 µl of $1x10^6$ spores/ml suspension into their last, left pro-leg. This injection procedure ensured that the spores reached the haemocoel BBraun Omnican® 50 U-100 0.5 ml insulin syringes with integrated needles were used. The needle was 12 mm in length and had a diameter of 0.3 mm. To ensure that the injection method or the original health status of the larvae were not responsible for any mortality observed, 3 control groups were included. These groups consisted of 30 larvae each, the first group was left untouched, the second were pierced with the needle and the third were injected with 10 µl phosphate buffered saline with 0.05% tween 80 (PBS-T). Post infection the larvae were kept in petri-dishes at 37˚C in the dark and survival monitored daily for 7 days. End points were characterised by a lack of movement or lack of response to stimulation and a blackening discolouration caused by melanisation of the cuticle. Where stated the larvae were treated with an iron source post infection. 10 µl of 1.5 mM $FeSO_4$ was injected into the last, right pro-leg of the larvae immediately after initial fungal inoculation. The treatment continued once a day for the following 5 days. Each treatment was given into a different pro-leg. An additional control group of 30 larvae were included in the treatment study, in which the larvae were injected with 1.5mM $FeSO_4$ once daily. After infection the larvae were kept in petri-dishes at 37˚C in the dark and survival monitored daily for 5 days post infection.

2.2.8.2. Murine intranasal infection

The experiment was performed under UK Home Office project license PPL70/7324 and approved by The University of Manchester Ethics Committee. *A. fumigatus* was cultured on SAB agar at 37°C for 4 days before conidia were harvested by flooding with PBS-T. Viable counts from administered inocula were determined, following serial dilution, by growth for 24–48 hours on SAB agar. Male CD1 mice weighing from 30 to 34g (Charles River Ltd) were stored as groups of 5 in vented HEPA-filtered cages with free access to food and water ad

libitum. All mice were given 1g/L tetracycline hydrochloride (Sigma T8032) and 62.5mg/L ciprofloxacin (Pharmacy Ciproxin) in their drinking water throughout the course of the study. Mice were rendered leukopenic by administration of cyclophosphamide (150 mg/kg, intraperitoneal) on days −3, −1, +2 and every subsequent third day, and a single subcutaneous dose of hydrocortisone acetate (250 mg/kg) administered on day −1.

Leukopenic male CD1 mice (25-30g) were anaesthetized by halothane inhalation and infected by intranasal instillation of spore suspensions of 5.0×10^5 conidia/ml in 40 µl of PBS-T solution. Mice were weighed every 24 hours from day of first immunosuppression and visual inspection made twice daily. In the majority of cases the end-point for survival experimentation was due to sickness, at which point mice were sacrificed.

2.2.8.3. Murine intravenous infection

The experiment was performed under UK Home Office project license PPL40/3101 and approved by The University of Manchester Ethics Committee. *A. fumigatus* was cultured on SAB agar at 37°C for 4 days before conidia were harvested by flooding with phosphate buffered saline containing PBS-T. Viable counts from administered inocula were determined, following serial dilution, by growth for 24–48 hours on SAB agar. Male CD1 mice weighing from 30 to 34g (Charles River Ltd) were stored as groups of 5 in vented HEPA-filtered cages with free access to food and water ad libitum. Mice were rendered neutropenic by a single dose of cyclophosphamide (200 mg/kg, intraperitoneal) on day −3.

Neutropenic male CD1 mice (25-30 g) were infected by intravenous injection via lateral tail vein of spore suspensions of 6.5×10^5 conidia/ml in 200 µl of PBS-T solution. Mice were weighed every 24 hours from day of first immunosuppression and visual inspection made twice daily. In the majority of cases the end-point for survival experimentation was due to sickness, at which point mice were sacrificed.

2.2.8.4. Cortisone acetate treated murine intranasal infection

Female CD1 mice weighing from 18 to 20g (Charles River Ltd) were stored under standard conditions in individually ventilated cages with free access to food and water ad libitum. All animals were cared for in accordance with the European animal welfare regulation and approved by the responsible federal/state authority and ethics committee in accordance with the German animal welfare act (permit no. 03-001/12). Mice were immunosuppressed with two single doses of 25 mg cortisone acetate (Sigma -Aldrich), which were injected intraperitoneally 3 days before and immediately prior to infection with conidia (day 0). Mice were anesthetized by an intraperitoneal anesthetic combination of midazolam, fentanyl, and medetomidine and infected by intranasal instillation of spore suspensions of 2×10^5 conidia/ml

in 20 µl PBS. Anesthesia was terminated by subcutaneous injection of flumazenil, naloxon and atipamezol. Infected animal were monitored twice daily to check weight loss.

2.2.8.5. Histological analysis

For histological analysis, the lungs were fixed in buffered formalin and embedded in paraffin; 4-µm sections were stained using Periodic acid-Schiff

GraphPad Prism was used to interpret all survival data. Kaplan Meier survival analysis was used to create a population survival curve and to estimate survival over time and *p* values were calculated through Log Rank analysis (for comparative survival).

2.2.9. Preparation of recombinant PptA

The complete PptA and AarA coding sequences were amplified from *A. fumigatus* cDNA by PCR using LongAmp^{TM} DNA polymerase using primers found in table S2.3. PCR primer design software Primer 3 (http://frodo.wi.mit.edu/) was used to aid primer design and all primers were supplied by Eurofins MWG Operon. Purified products were cloned into pManHis vector (modified pET16b vector obtained from Dr Eddie McKenzie, University of Manchester). Subsequently PptA coding was excised from pManHis using restriction enzyme BamH1 and sub-cloned into pGEX-6P-1 (GE Healthcare Life Sciences), a vector that contains an N-terminal GST-tag designed to improve solubility of the product. Cloning sites of plasmids were sequenced to ensure accurate amplification and correct insertion. *E.coli* BL21 (DE3) cells were used for transformation of vectors. Expression was induced by the addition of isopropyl β-D-thiogalactoside at 0.5 mM. Cultures were then incubated for 16 hours at 18°C. Cells were harvested and pelleted by centrifugation. Cell lysis was performed by sonication in lysis buffer (MES 50 mM (pH 6), NaCl 500 mM, Tween 20 0.1%, phenylmethanesulfonylfluoride 1 mM, Lysozyme 1 mg/ml). Cell debris was removed by centrifugation at 16000 g for 20 min at 4 °C.
Proteins cloned into pManHis vector underwent purification using a NI-NTA His Bind resin by immobilised metal affinity chromatography. Protein was eluted from the resin using 1 M imidazole in 50 mM MES pH 6, 500 mM sodium chloride and 0.1% Tween 20. PptA cloned into pGEX-6P-1 was purified using glutathione sepharose resin affinity chromatography and was eluted by the addition of excess reduced glutathione (GST Buffer Kit, GE Healthcare Life Sciences). All purified proteins were desalted into the appropriate assay buffer with Sephadex G-25 (PD10 columns, GE Healthcare Life Sciences).

2.2.9.1. Assay for PptA activity

The phosphopantetheinyl transferase activity of PptA was assessed in a fluorescence polarization (FP) assay. The assay monitored the transfer of the phosphopantethiene (p-pant) group from coenzyme A to a target protein, AarA. The p-pant group of CoA was labelled with

BODIPY-TMR iodoacetamide as previously described (15). Titration of PptA (0-200ng per reaction) was perfomed with 750 ng AarA, 1 µl of BODIPY-TMR labelled CoA and assay buffer (62.5 mM BisTris, 12.5 mM MgCl, pH 6.5). This was incubated at room temperature in the dark. The reaction was stopped at various time points by the addition of stop buffer (1 M EDTA, pH 8). FP was measured in a Synergy 2 microplate reader (excitation 530/25, emission 590/35, gain: 1000). Results were plotted into a scatter graph using Microsoft Excel software. Repeatability of the assay over 384 well plate was determined by mixing 100 ng PptA with 750 ng AarA, 1 µl of BODIPY-TMR labelled CoA and assay buffer (62.5 mM BisTris, 12.5 mM MgCl, pH 6.5) in the presence or absence of 1 M EDTA. This was incubated at room temperature in the dark for 30 minutes. This was plotted in an aligned scatter graph using Microsoft Excel software and the Z' value calculated following procedures laid out in Brooks, *et al* (2012) (40).

2.3. Results

2.3.1. PPTases form 3 distinct evolutionary clades

To gain a better understanding of the diversity of the PPTase families, a phylogram was constructed using sequences homologous to PptA, PptB and the PPTase subunit of FasA from other fungi and where present a selection of bacterial species including *Mycobacterium tuberculosis*, *Escherichia coli* and *Bacillus subtilis* and 2 mammalian species *Mus musculus* and *Homo sapiens.* Three distinct and well-supported clades of PPTase sequences, corresponding to the three classes of PPTase were identified (figure S2.3).

The type I cluster contains all representatives of the AcpS-type PPTases. A sub-group of highly conserved fungal AcpS-type PPTases (see dashed box; figure S2.3), including *A. fumigatus,* PptB, are found amongst these proteins, they show relatively high ClustalW alignment scores ranging from 54.6% to 75.4% when compared to the *A. fumigatus* enzyme. The type III PPTases show relatively low evolutionary divergence, with the majority of branch lengths <0.1. This group is far more closely related as a whole than the other two types of PPTases with ClustalW scores ranging from 61.2% to 92.5% when compared to the *A. fumigatus* FasA subunit.

2.3.2. Type II PPTases are phylogenetically diverse

Anti-infective drug targets that lack similarity to their human orthologues are preferred as this indicates a reduced potential for both enzymes to be inhibited by the same compound, reducing the likelihood of drug toxicity. It is also preferable that a target shares high similarity over a broad range of pathogens, indicting the potential to develop a drug with a broad spectrum of activity.

To explore the clustering of Sfp-type PPTases further, phylograms were constructed using additional sequences homologous to mammalian, bacterial and fungal proteins. Five separate clusters were identified (figure 2.1). Cluster A contains highly conserved mammalian PPTases with very short branch lengths (<0.12) while clusters B and E consists of enzymes from Firmicutes and Proteo/Actinobacteria respectively. Interestingly fungal enzymes form 2 distinct clades representing Ascomycota (cluster C) and Basidiomycota (cluster D). It is particularly evident that the PPTases in the Ascomycota group are highly divergent. This is exemplified by *in silico* analysis; no significant similarity is found when the *A. fumigatus* PptA enzyme is used in BlastP analysis against the *Candida albicans* genome and a low identity of 31% (24% coverage) is observed against the *Saccharomyces cerevisiae* PPTase. However there does appear to be a distinct, relatively well conserved grouping within this cluster which includes *Aspergilli* PPTases as well as enzymes from other pathogenic fungi including *Histoplasma capsulatum*, *Arthroderma benhamiae*, *Coccidioides immitis* and *Coccidioides*

posadassi (dashed box, figure 2.1). Proteins found in this cluster have short branch lengths (<0.15), alignment scores >50% and percentage identities ranging from 47 to 72% (table S2.4).

The human and *A. fumigatus* proteins share a common ancestor however they have diverged into 2 separate clusters (A and C respectively). *In silico* analysis showed that the PptA protein shared only 26% identity (61% coverage) and had a low Clustal W pairwise alignment score of 21% with the human orthologue, L-aminoadipate-semialdehyde dehydrogenase-phosphopantetheinyl transferase (AASDHPPT) (http://blast.ncbi.nlm.nih.gov/) (figure 2.2). PptA compares favourably when placing it in context with the azole drug target Cyp51A, which shares 38% identity (92% coverage) and a Clustal W pairwise alignment score of 35.19% to human lanosterol 14-alpha demethylase.

Bacterial Sfp-PPTases have a conserved characteristic signature within their sequence (I/V/L)G(I/V/L/T)D(I/V/L/A)(x)n(F/W)(A/S/T/C)xKE(S/A)h(h/S)K(A/G) (where 'x' are chemically disparate amino acids, n is 38–41 aa, and 'h' is an amino acid with a hydrophobic side chain) (41). We found the signature of the fungal Sfp-PPTases analysed in this study diverges somewhat from this: (I/V/L)G(I/V/A/T)D(I/V/L)(x)n(F/W)(A/S/T/C)x (K/R)E(S/A)h(h/S)K(M/L/A/F) where n is 41-107 aa (figure S2.4) for the collection of fungal .

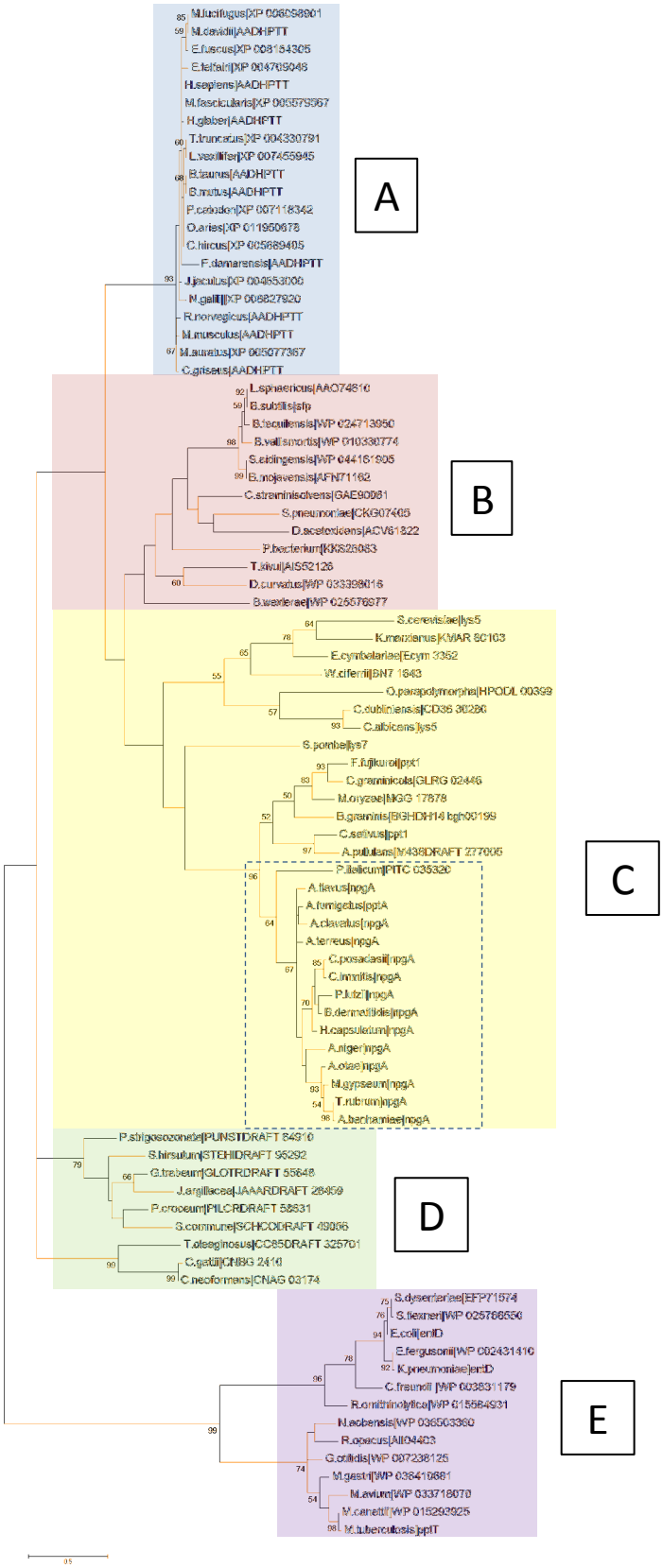

Figure 2.1: Molecular Phylogenetic analysis of Sfp-PPTases by Maximum Likelihood method. The evolutionary history was inferred by using the Maximum Likelihood method based on the JTT matrix-based model. The percentage of trees in which the associated taxa clustered together is shown next to the branches. Initial tree(s) for the heuristic search were obtained by applying the Neighbor-Joining method to a matrix of pairwise distances estimated using a JTT model. The tree is drawn to scale, with branch lengths measured in the number of substitutions per site. Evolutionary analyses were conducted in MEGA6.

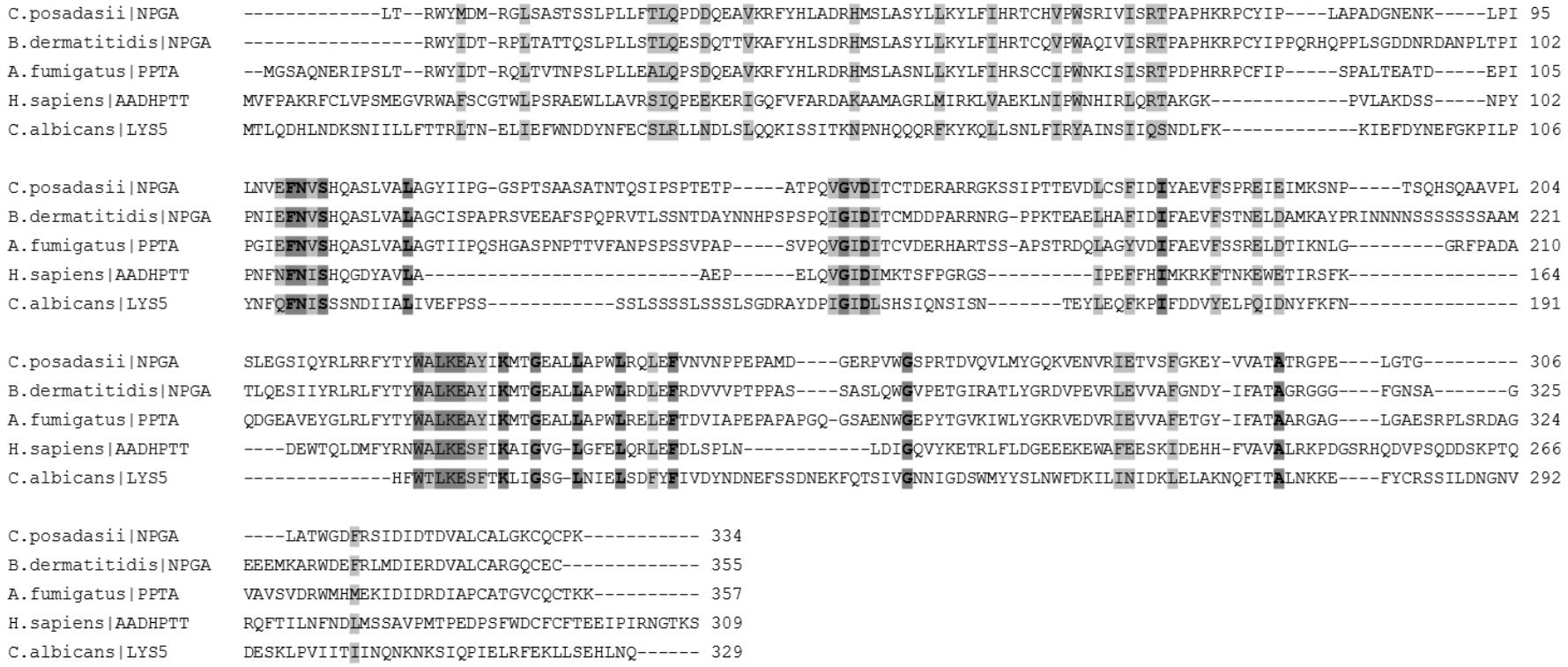

Figure 2.2: Sequence alignments Sfp-PPTases. Sequence alignments of *Aspergilus fumigatus* PptA, the human orthologue AASDHPPT and fungal pathogen orthologues; *Candida albicans* LYS5, *Coccidioides posadassii* NPGA and *Blastomyces dermatitides* NPGA. Dark grey shading and bold lettering indicates positions which have a single, fully conserved residue. Light grey shading indicates conservation between groups of strongly similar properties - scoring > 0.5 in the Gonnet PAM 250 matrix. Boxes indicated the conserved signature used to distinguish PPTases.

2.3.3. PptA is required for normal growth

Previous studies have shown that *A. fumigatus* strains lacking *pptA* require supplementation with both lysine and iron and have white conidia. We confirmed this observation by generating a *pptA* null (named Δ*pptA*) in the CEA10 derived ku80 isolate A1160p+ (figure S2.6/7). To assess the minimum requirement of this strain for both lysine and the extracellular siderophore TAFC, as a source of free iron, growth rate was assessed in RPMI media with varying levels of both supplements (figure 2.3). A minimum of 1.25 mM lysine was required to restore the growth rate of the *pptA* null to wild-type levels, however growth was evident (approximately 10% compared to the parental strain) at 0.16 mM. It is noteworthy that levels of the free amino acid in human plasma can reach up to 0.28 mM (42, 43). The minimal requirement of the *pptA* null mutant for TAFC was $6.3x10^{-4}$ mM. This is significantly above free iron levels found in human hosts, where the iron is under strict homeostasis and is mostly found tightly bound to hemoglobin, transferrin, lactoferrin and ferritin. It is estimated that the concentration of free iron in human secretions and serum is approximately 10^{-15} mM and 10^{-21} mM (44, 45). If this information is taken in isolation, it would suggest that iron limitation in host tissues would prevent Δ*pptA* survival in the human host.

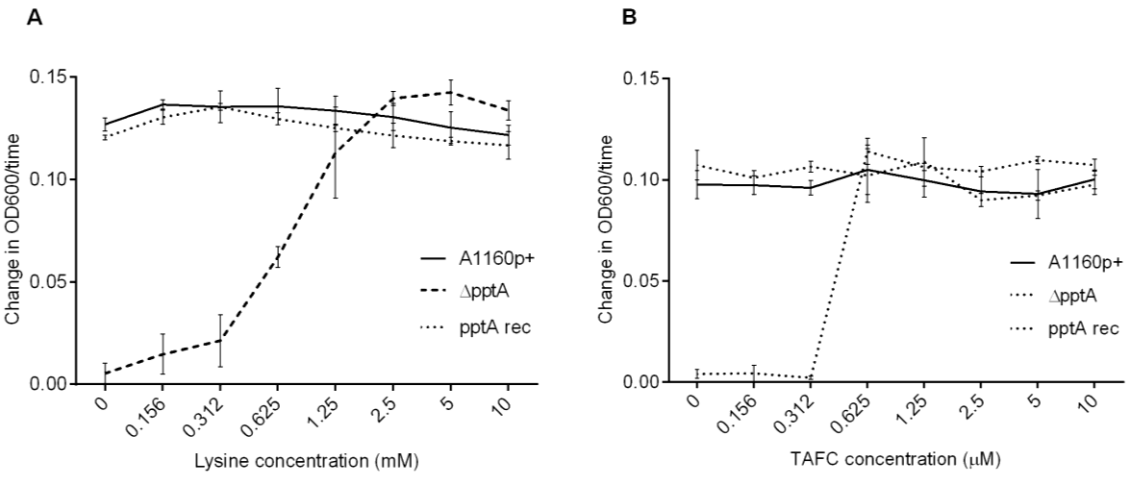

Figure 2.3: Dose response of a *pptA* null isolate to increasing concentrations of TAFC or Lysine. (A) RPMI media supplemented with TAFC (10 μM) and an increasing concentration of lysine. (B) RPMI media supplemented with lysine (10 mM) and and an increasing concentration of TAFC. 2.5 mM lysine and 0.63 μM TAFC is required to restore to parental phenotype.

2.3.4. PptA is required for the production of secondary metabolites in *A. fumigatus*

Márquez-Fernández *et al* (2007) (46) have previously defined a role for *npgA* in the production of NRPS and PKS derived secondary metabolites in *A. nidulans*. As secondary metabolites are thought to play a key role in fungal virulence (47-49), we assessed if this role was conserved in *A. fumigatus*. The capability of the Δ*pptA* strain to generate secondary metabolites was assessed by analysing LC-MS absorbance spectra from 7-day old culture supernatants. Several non-medium derived peaks, which correspond to the major metabolites, including gliotoxin, fumiglavine C, fumiquinazole A, fumiquinazoline C, pyripyroprene A and fumagillin, were observed in extracts from the parental strain grown on Czapek-dox (figure 2.4A) and SAB (figure 2.4B) medium. None of these peaks were identified in supernatant extracts from the *pptA* null isolate which shows an apparent lack of secondary metabolite production. The metabolic profile of the *pptA* null isolate resembles the media only control profile under tested conditions. The metabolite profile of the reconstituted isolate was consistent with that of the parental isolate.

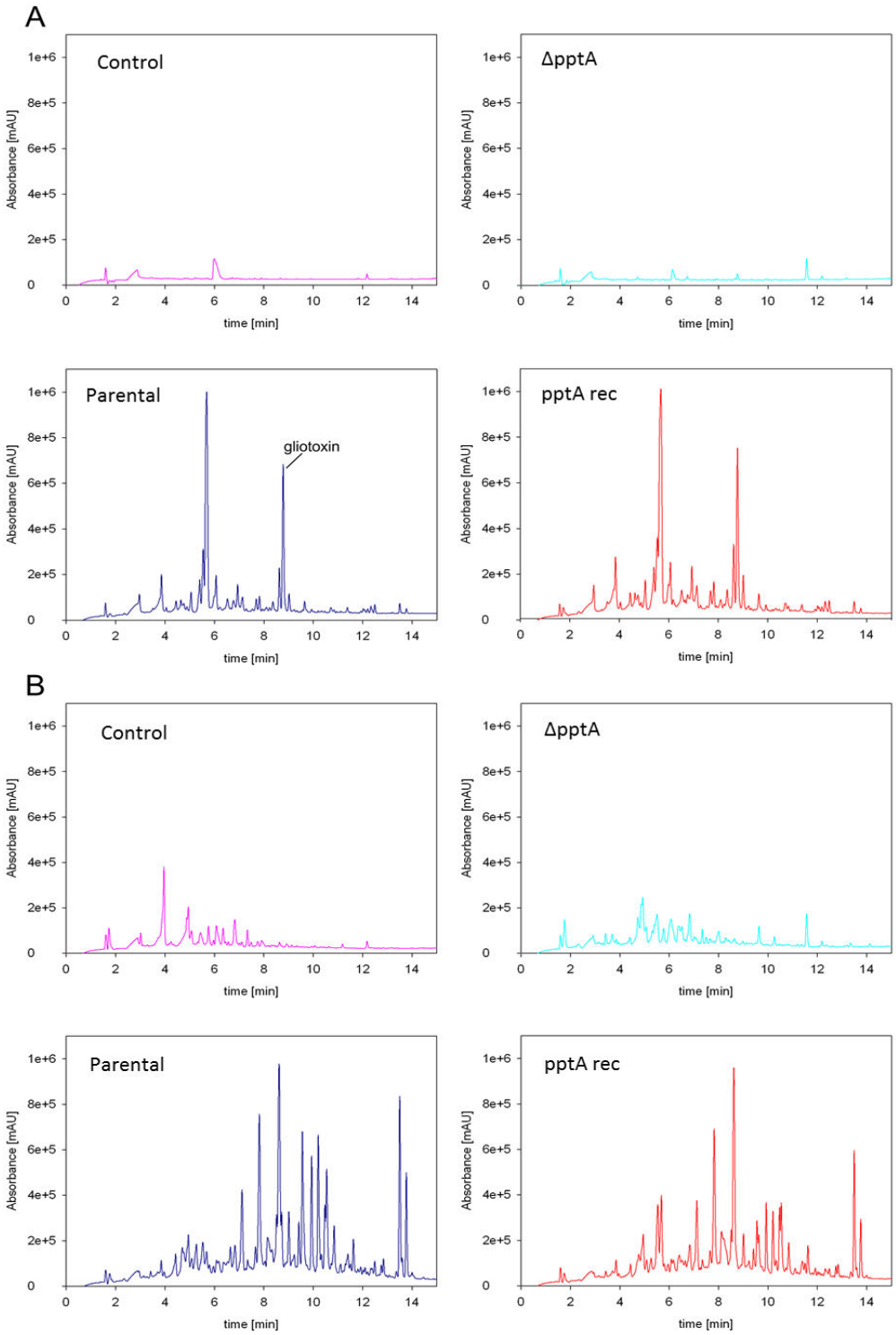

Figure 2.4: Analysis of secondary metabolite production: $1x10^7$ spores were grown for 7 days. The culture supernatant was extracted with an equal volume of ethyl acetate. The organic phase was recovered and dried. The residuum was dissolved in 1 ml methanol and analysed by LC-MS. A) In Czapek-Dox medium, the parental strain and reconstituted isolate produced gliotoxin as well as other metabolites, whereas the *pptA* null did not. B) In Sabouraud medium, the parental strain and reconstituted isolate produced fumiglavine C (RT 8.20), fumiquinazole A (RT9.56) fumiquinazoline C (RT 9.9), pyripyroprene A (RT 11.28), fumagillin (RT 13.50) and traces of triacetylfusarinine C among other metabolites. The *pptA* null showed abrogation of secondary metabolite production.

2.3.5. PptA an important factor in host response

It has been shown that a loss of DHN-melanin biosynthesis in *pksP* mutants of *A. fumigatus* leads to an amorphous and hydrophilic coating of protein around the conidia which coincides with an increase in host recognition, enhanced inflammation and increased phagocytosis (22, 25-27). As the Δ*pptA* isolate lacks the ability to produce melanin we hypothesised that it would be detected more readily by human DCs than an isogenic control isolate (parental strain, A1160p+). We generated a *pksP* null strain, Δ*pksP* as a non-pigmented control for this study. Fixed spores of A1160p+, Δ*pptA*, *pptA* rec and Δ*pksP* strains were used to challenge human dendritic cells. An increase in relative expression of proinflammatory cytokines IL-1β and IL-6 in the DCs was observed when challenged with both Δ*pptA* and Δ*pksP* (P value < 0.01) when compared to the parental strain. Interestingly, the level of response to the *pptA* null isolate was significantly greater (P< 0.01) than that to the Δ*pksP* (figure 2.5).

A. fumigatus conidia and melanin ghosts can inhibit the acidification of phagolysosomes of alveolar macrophages, monocyte-derived macrophages, and human neutrophil granulocytes whereas strains lacking melanin cannot (25). To assess if a similar observation is made with the non-pigmented Δ*pptA* isolate, acidification of phagolysosomes was measured using LysoTracker, a dye which shows red fluorescence in an acidic compartment (figure 2.6). 76% of the Δ*pptA* conidia were found residing in acidified compartments compared to 25% of the parental strain, A1160p+. The level of increase in acidification is similar between Δ*pptA* (76 %) and Δ*pksP* (74 %) which suggests melanin as the main factor in prevention of phagolysosomal acidification.

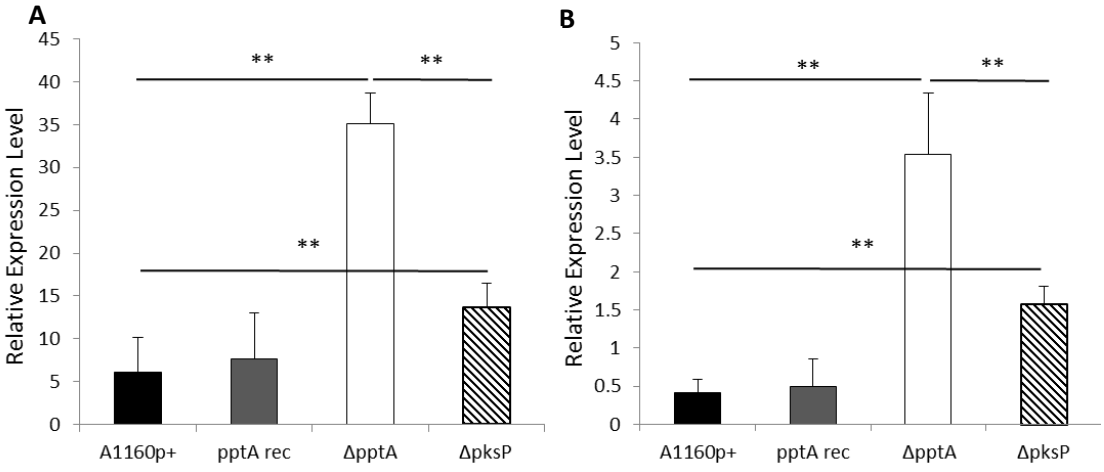

Figure 2.5: Immune response to different Aspergillus mutant strains. White mutant strains elicit an increased inflammatory response. DCs were cultured with fixed conidia for 24 hours. Total RNA of DC cells was extracted and the relative expression of A) IL-1β and B) IL-6 was assessed by QRT-PCR. Data represent the mean of 3 replicates and error bars signify the standard deviation. P values were determined using a student's t-test. ** P value < 0.01.

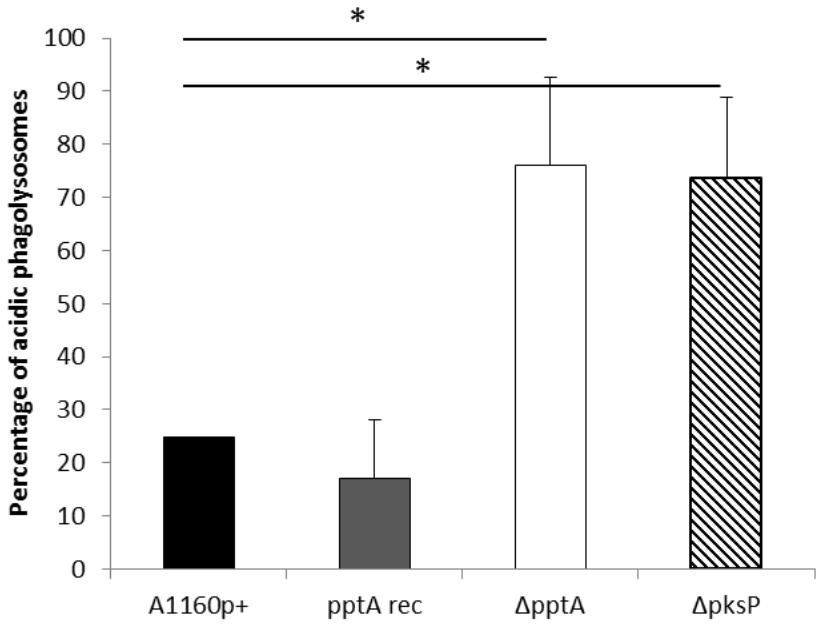

Figure 2.6: Detection of conidia in acidified compartments after phagocytosis by RAW264.7 macrophages. The ratio of conidia present in acidic phagolysosomes to the total number of ingested conidia. Calcofluor white (CFW)-labeled conidia were intracellularly colocalized with LysoTracker Red-DND99. Data represent the mean values and SD of three experiments. P values were determined using a student's t-test.

2.3.6. PptA is vital for virulence of *A. fumigatus*

The significant growth defects *in vitro* and lack of secondary metabolite production indicates that the *pptA* null strain may lack the ability to establish an infection. To test this hypothesis, we first assessed the virulence of Δ*pptA* in the *Galleria mellonella* wax moth virulence model (50). The control isolate A1160p+ caused 100% mortality 4 days post infection whereas all larvae survived in the *pptA* null pool (figure 2.7A).

To assess the underlying cause of this loss of virulence, the pathogenicity of additional isogenic strains lacking either the ability to produce siderophores (Δ*sidA*), lysine (Δ*aarA*) and melanin (Δ*pksP*) was assessed. A significant difference in virulence was observed only for Δ*sidA* (P-value <0.0001 vs the control isolate) (figure 2.7A). This suggests, at least in the larval model, siderophore biosynthesis but not lysine or the biosynthesis of other secondary metabolites is the primary cause of loss of virulence in the *pptA* mutant. To further confirm this, larvae infected with A1160p+, Δ*pptA* and Δ*sidA* were given iron treatments every day for the length of the study. Under these conditions virulence was increased to a higher level than the untreated parental strain in both Δ*pptA* (P value<0.0001) and Δ*sidA* (P value<0.05) deletion strains. Interestingly, there is also an increase in parental strain virulence when supplemental iron is given increasing the rate of total mortality from 4 to 1 day (P value<0.001) (figure 2.7B). 100% survival was observed in larvae that received iron treatment without infection.

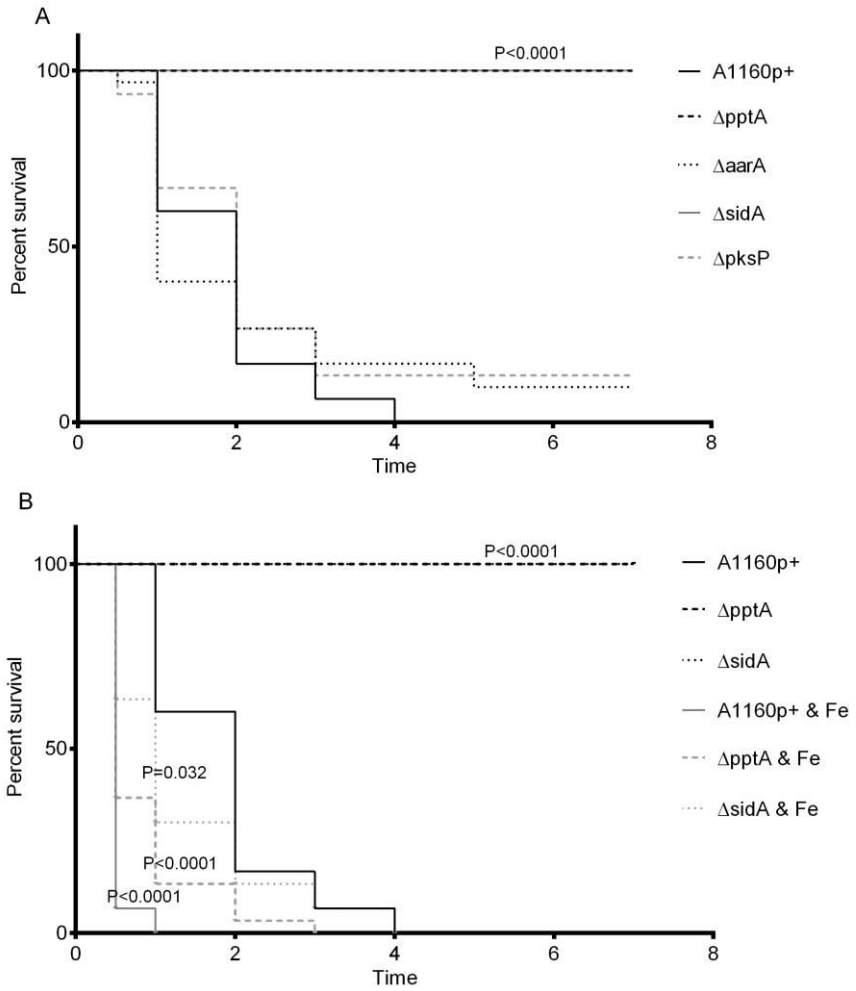

Figure 2.7: The effects of A) a series of KO mutants of *A. fumigatus* on the mortality of the larvae and B) an iron treatment on the pathogenicity of Δ*pptA* and Δ*sidA* in a larvae model. A) Larvae were inoculated with 1x104 spores with the following strains; Δ*pptA*, Δ*aarA*, Δ*pksP*, Δ*sidA*, A1160p+ and CEA10. Percentage larvae survival was plotted in a kaplan meier survival curve. Δ*pptA* and Δ*sidA* showed complete avirulence. B) Larvae were inoculated with 1x104 of the following strains; Δ*pptA*, Δ*sidA* and A1160p+. Half of the larvae from each group were given a daily treatment of 1.5mM $FeSO_4$. A mean value was determined for the control larvae. Larvae survival was plotted against time post infection. Δ*pptA* and Δ*sidA* showed completely restored pathogenicity when treated with iron. P values were calculated through Log Rank analysis.

For a more clinically relevant assessment of both pulmonary (figure 2.8A) and disseminated disease (figure 2.8C) we carried out intranasal and intravenous infection models with Δ*pptA* in leukopenic mice. All mice infected with the parental strain had succumbed to disease and were sacrificed before the end of the study. In keeping with the results from the larval virulence study, 100% survival was seen in the cohort infected with Δ*pptA* isolate in both models. The virulence of the reconstituted isolate was indistinguishable from the parental isolate (P value = 0.3043 and 0.1750 for intranasal and intravenous infections respectively). Additionally we carried out a further pulmonary infection using mice treated with cortisone acetate which retain the ability to recruit neutrophils and monocytes (figure 2.8B). 80% of mice infected with Δ*pptA* survived until the end of the study. Histopathology of the lungs from those mice that

died did not reveal any evidence of fungal hyphae indicating other factors but not infection by the *pptA* isolate were responsible for the observed mortality. Histopathology from mice that survive to day 14 indicate that the Δ*pptA* mutant has been totally cleared from the lung (figure 2.8D).

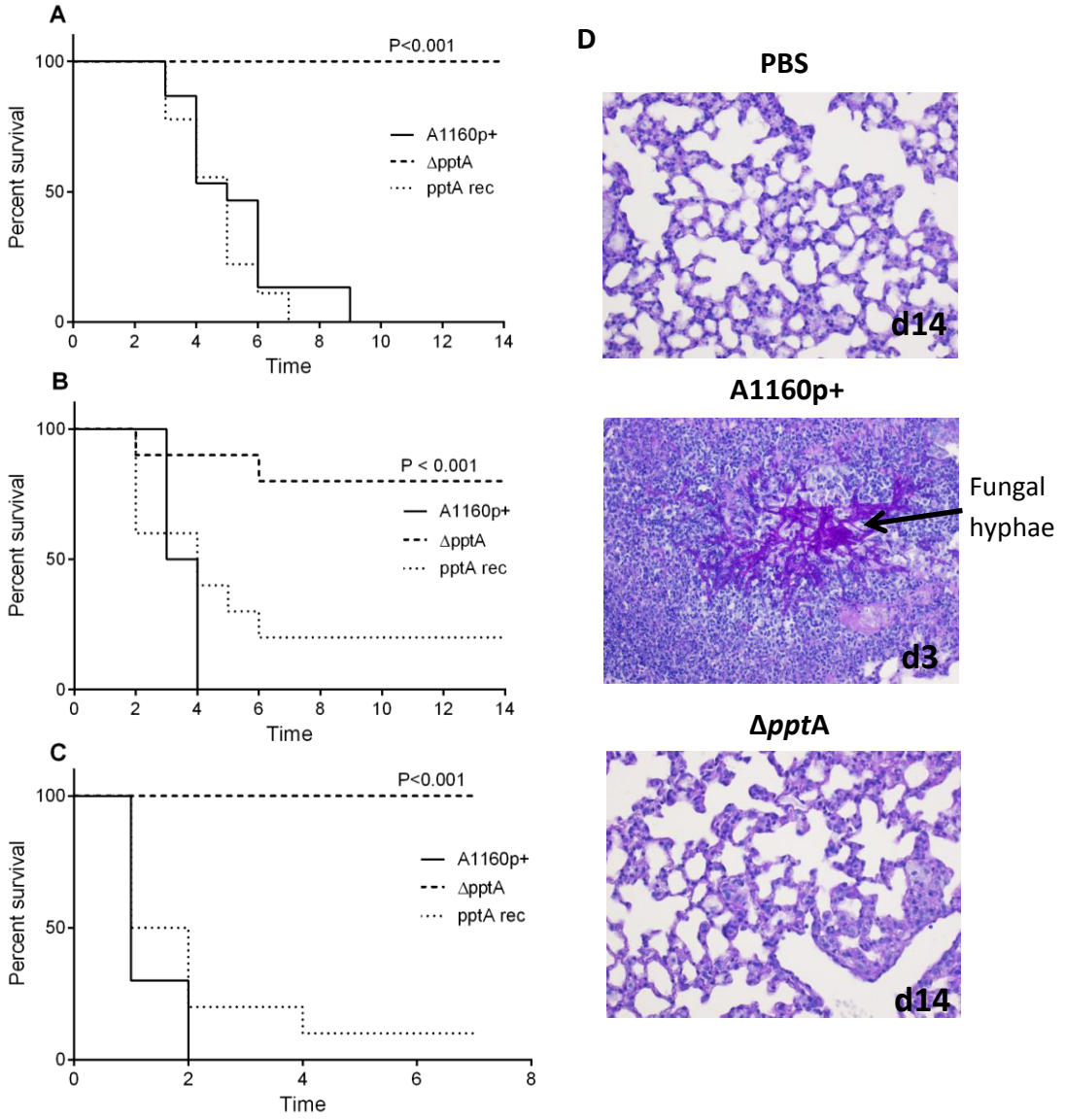

Figure 2.8: Kaplan-Meier curve and histology for murine survival. A) Intranasal infection with 2×10^4 spores. The *pptA* null was avirulent. Log rank analysis was used to compare Δ*pptA* infection to the parental strain (A1160p+) P value <0.001. B) Intranasal infection with 2×10^5 spores in cortisone acetate treated mice. The *pptA* null showed attenuated virulence. Log rank analysis was used to compare Δ*pptA* infection to the parental strain (A1160p+) P value <0.001. C) Intravenous infection with 1.3×10^5 spores. The *pptA* null was avirulent. Log rank analysis was used to compare Δ*pptA* infection to the parental strain (A1160p+) P value of <0.001. D) Histopathology of representative sections of lungs from *A. fumigatus* infected mice. The presence of invasive fungal hyphae (pink), destructed lung tissue, and infiltration of immune cells (purple nuclei) was confirmed in lungs of mice infected with conidia from parental strain, the *pptA* null isolate and the reconstituted isolate. The lung section of a PBS-infected mouse is shown as control (PBS). P values were calculated through Log Rank analysis.

2.3.7. A high throughput screen to determine PptA activity

The activity of AFPptA has previously been assessed by monitoring the transfer of a fluorescently labelled phosphopantetheinyl group from CoA using gel shift assay (15) however this is unsuitable for high-throughput screening of chemical inhibitors. We therefore assessed an alternative strategy, using fluorescence polarization (FP) to monitor the transfer of the labelled phosphopantetheinyl group to an acceptor protein (figure 2.10A; schematic representation of the assay).

An N-terminal GST-tagged derivative of AFPptA and an N-terminal HIS-tagged derivative of PptA and cognate acceptor protein AFAarA were expressed in *E. coli* (figure 2.9). Purified AFPptA and AFAarA proteins were isolated with estimated masses of 65 kDa (including GST-tag) and 150 kDa which correlated well with their predicted masses.

We were able to demonstrate that the recombinant AFPptA could pantothenalyate AFAarA using the BODIPY TMR-labelled substrate (Figure 2.10B). Optimal conditions where FP was maximised whilst retaining a linear increase in FP over a 30 minute period was achieved with 100 ng PptA and 750 ng AarA (figure S2.8). Reproducibility of the assay was high, producing a Z' value of 0.76, which is well within an acceptable range for a high throughput assay.

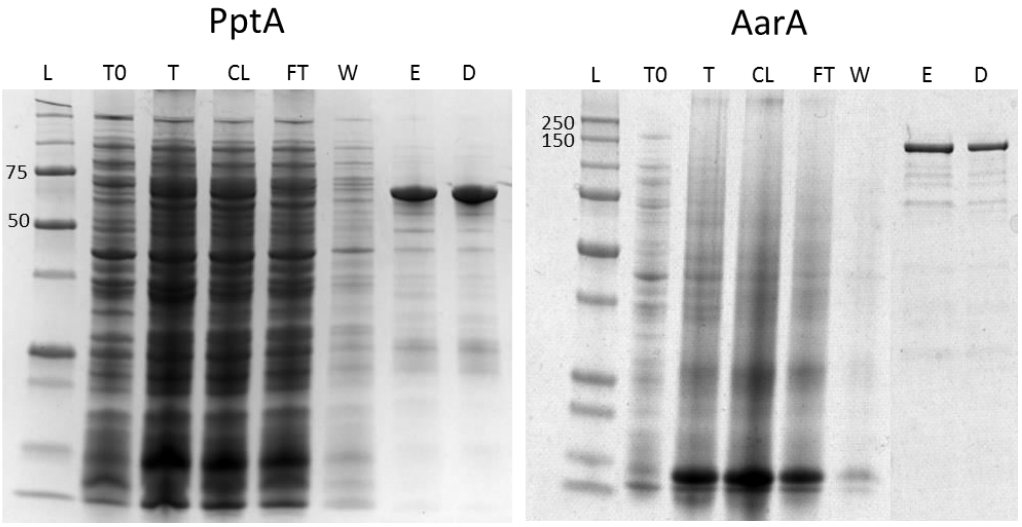

Figure 2.9: PptA-GST and AarA-pManHis protein expression and purification. *E. coli* BL21 DE3 cells were transformed with pGEX6P1_PptA and pManHis_AarA, grown until OD600 >0.5 and then incubated in the presence and absence of 0.5 mM IPTG for 18 h at 18°C. PptA and AarA were purified from the bacterial lysate using glutathione sepharose resin affinity chromatography and NI-NTA His Bind resin affinity chromatography respectively. Protein fractions were separated by polyacrylamide gel electrophoresis on Mini-PROTEAN® TGX Stain-Free™ gels (Life Technologies) followed by staining with InstantBlue sreagent (Expedeon). The molecular weights in kilo Daltons of a precision plus protein ladder (L) are marked. Lane T0, *E. coli* cell lysate; Lane T, *E. coli* cell lysate following IPTG induction; Lane CL, *E. coli* cell lysate following IPTG induction from supernatant; Lane FT, flow through the affinity chromatography; Lane W, wash to remove unbound proteins; Lane E, PptA and AarA purified by affinity chromatography; Lane D, PptA and AarA protein desalted by Sephadex G-25 (PD10 columns, GE Healthcare Life Sciences). PptA-GST and AarA-pManHis show strong bands at ~65kDa and 156kDa respectively.

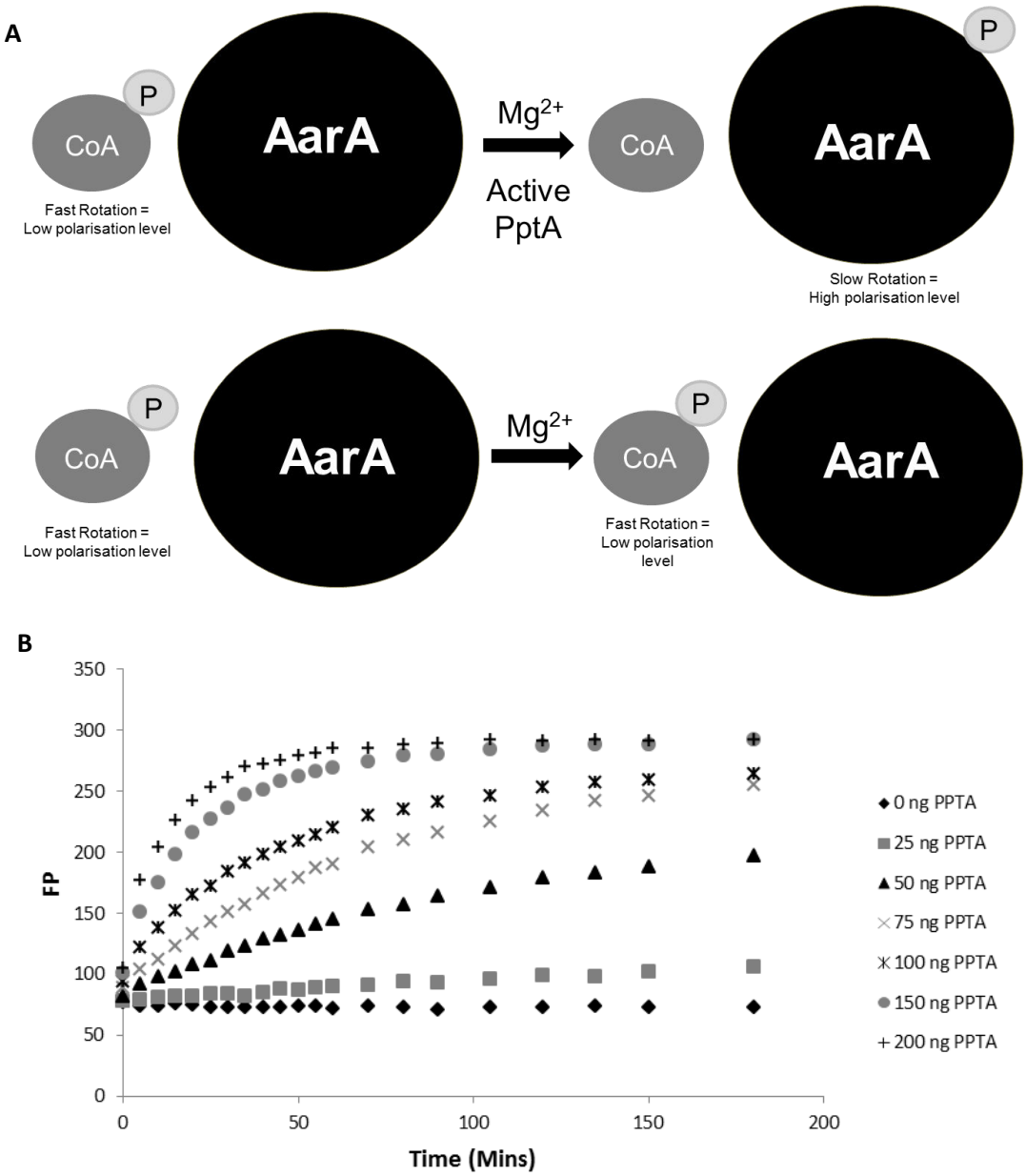

Figure 2.10: A) Fluorescence polarization (FP) Schematic. The BODIPY-TMR labelled phosphopantethiene group (P) on CoA is transferred to AarA in the presence of PptA and Mg2+. When the large BODIPY-TMR labelled AarA complex is excited by polarised light, it begins to rotate at a slow pace. This causes the light to remain polarised and therefore a high polarisation level is observed. If the BODIPY-TMR labelled phosphopantethiene remains on the small CoA (in the absence of PptA), excitation by polarised light will lead to rapid rotation. This in turn depolarises the light and leads to a low polarisation level. B) Titration of PptA (0-200ng per reaction) in the fluorescent polarisation assay.

2.4. Discussion

Many of the antifungals used to treat invasive disease are blighted by significant pharmacological shortcomings, these combined with high rates of mortality and the emergence of resistance, particularly to the azoles, has stimulated the search for new antifungals with novel mechanisms of action (2, 4, 5). In this study we have demonstrated the Sfp-PPTase, PptA of *A. fumigatus* has the potential to be used as a therapeutic target.

Recently, the sole Sfp-type PPTase of *Mycobacterium tuberculosis*, PptT, has been identified as a potential drug target for combating tuberculosis infection. PptT is required for the biosynthesis of mycobactins, mycolic acids, other polyketide derived lipids and siderophores and was found to be essential for viability and persistence in murine infection models (51). The role of the *A. fumigatus* Sfp-PPTase is somewhat similar to that of the *M. tuberculosis* enzyme. We have demonstrated that a *pptA* null is unable to produce any detectable secondary metabolites, leading to amongst other phenotypic defects; loss of spore pigmentation and an inability to grow in iron limiting environments. This is consistent with the proposed role of PptA in activation of the polyketide synthase PksP responsible for the first step in melanin biosynthesis and the non-ribosomal peptide synthases SidC and SidD, required for siderophore biosynthesis. The role of PptA extends beyond that of the mycobacterium PPTase in that it is required for the activation of the fungal specific enzyme α-aminoadipate reductase AarA, a key component in the lysine biosynthetic pathway ((15); and this study) and in keeping with this role, the *pptA* null is unable to grow without supplemental lysine. Sfp-type PPTases have also been identified as essential virulence factors in a range of fungal plant pathogens (19, 52, 53) but this is the first study to show this in a human fungal pathogen.

It has been suggested that antifungal targets should be sufficiently similar to a range of fungal pathogens to provide some confidence that any antifungal compound developed would have a broad spectrum of activity whilst still being sufficiently dissimilar from any host enzyme, to allow selective targeting of the pathogen. There are three known classes of PPTase; type I or AcpS-Type, type II or Sfp-Type and type III Fas-Type. Our phylogenetic analysis of Sfp-type PPTases have shown they are evolutionary distinct from the other types of PPTases. When examining the proteins found within this group it is clear that there is reasonable conservation between AFPptA and those in many other pathogenic fungi including *Aspergillus flavus* (64% ID), and the causative agents of coccidioidomycosis (*Coccidioides posadassi*; 55% ID) and histoplasmosis (*Histoplasma capsulatum;* 49% ID). The relationship between AFPptA and the orthologues in other significant pathogens is less compelling. No significant similarity is found when performing BlastP analysis between PptA and the Sfp-PPTase from *Candida albicans*

(EntD) (ClustalW alignment score of 6.38%) and the *Cryptoccoccus neoformans* (CNAG_03174) (ClustalW alignment score of 14.02%). AFPptA however is evolutionarily distant from the human Sfp-PPTase, Aminoadipate-Semialdehyde Dehydrogenase-Phosphopantetheinyl Transferase (AASDHPPT) and shares low amino acid conservation (26% ID, 61% cover). We conclude from our bioinformatics analyses that antifungals directed against PptA have the potential to be selective however may be limited in their spectrum of activity.

The value of narrow spectrum drug targets should not be discounted. Over the last two decades significant progress has been made in the development of rapid diagnostic methods to identify the causative agent in fungal diseases, allowing clinicians to tailor their therapeutic approach. Treatment regimen already differs depending on the infective agent and site of infection, for example, the echinocandins are increasing used for the treatment of disseminated candidiasis however the azoles are preferred for the treatment of aspergillosis (4). Several clinicians and commercial bodies have also advocated the development of new antifungal classes that have activity restricted to either *Aspergillus* or *Candida* species (4, 54).

PptA has a role in the biosynthesis of numerous factors that have been directly associated with virulence including lysine (28, 29); the siderophores ferricrocin (FC) and triacetylfusarinine C (TAFC) (13, 16), DHN-melanin (24, 55), and gliotoxin (56). This combined with our preliminary dose response studies, indicating that the *pptA* null is unable to grow effectively at clinically relevant levels of lysine and iron, mean that it is unsurprising that our results have demonstrated that the strain is also avirulent in mouse and larval models of *Aspergillus* infection. The roles of all of the above factors in the virulence of the *pptA* null however do not appear to be equally weighted. We have demonstrated that the predominant factor for virulence of the *pptA* null in the larval model is its lack of ability to sequester iron, as virulence of *pksP* and *aarA* knockout mutants are indistinguishable from the isogenic host. This is further exemplified as the virulence defect of the *pptA* null can be rescued by supplying iron during infection. In addition results from a *sidA* null, which lacks TAFC and FC biosynthetic capability behaves in a similar manner to the *pptA* mutant. Interestingly, our finding for pksP is somewhat in conflict with a previous study which indicated that an *A. fumigatus pksP* null had increased virulence in a *Galleria mellonella* model compared to the wildtype however this could reflect the different host strains used in the infection studies (57).

The loss of virulence of the Δ*pptA* strain in a murine infection model is likely to be multi-factorial and complicated by the various challenges experienced by the mutant depending on which organ is infected. Our study reveals that *pptA* is required for virulence in both bronchopulmonary and disseminated murine infection models. The role of lysine biosynthesis

in virulence has been assessed in a number of studies. Strains lacking the ability to synthesise lysine are only avirulent in bronchopulmonary models (28, 29) and are thought to be able to overcome their deficiency in an established infection by liberating lysine via the degradative action of proteases on surrounding tissues. Targeting lysine biosynthesis alone is therefore not likely to resolve a pre-existing infection. A previous study has shown that a *sidA* null is avirulent in a brochopulmonary infection model (13, 16) however no data exists in relation to its ability to cause an infection in a disseminated model. As the level of free iron found in human hosts is extremely low (10^{-21} mM to 10^{-15} mM) as the majority is found tightly bound to other molecules (44, 45), therefore it is unlikely that *A. fumigatus* will be able to overcome the loss of siderophores and therefore *pptA* in an established infection.

The impact on virulence of the *pptA* null may be further compounded by its lack of ability to produce DHN-melanin. Not only have previous studies shown melanin deficient *A. fumigatus* have reduced virulence (24, 55), melanin has also been shown to play a key role in avoiding host detection and have a protective effect against host killing (22-26). Our data shows that the *pptA* null behaves in a similar manner to the *pksP* null by the inability to prevent phagolysosome acidification. Interestingly, the *pptA* null elicits an increased pro-inflammatory response when exposed to human dendritic cells significantly higher than the *pksP* null. It has been shown that a lack of melanin leads to an amorphous and hydrophilic coating of protein surrounding the conidia (58). A difference in the consistency of this protein layer could be responsible for the diverging effects between the 2 melanin deficient strains. Further to this the lack of secondary metabolites produced by the *pptA* null mutant could also be implicated. One such secondary metabolite that has been postulated to play a role in host detection is gliotoxin.

Gliotoxin has been associated with the suppression of the adaptive immune response, the increase of polymorphonuclear-mediated inflammation and the prevention of respiratory burst in human polymorphonuclear leukocytes (56, 59, 60). We have shown gliotoxin is not produced by the *pptA* deficient isolate so therefore could explain the hyper-immune response compared to the *pksP* null mutant. Gliotoxin has also been postulated to play a role in fungal virulence (59-64). The first step of gliotoxin biogenesis requires the action of the NRPS GliP (61, 62). Although the lack of gliotoxin in *gliP* null isolates did not affect the virulence of *A. fumigatus* using neutropenic mice treated with cyclophosphomide and hydrocortisone (61, 62), attenuated virulence was observed in non-neutropenic mice immunosuppressed with corticosteroids (63, 64). Taken together the loss of these other virulence factors in the Δ*pptA* suggest that it will have reduced capabilities for infection establishment within its host, beyond that of a siderophore deficient strain.

The validation of a potential drug target is the first step in the development of a novel antifungal agent, yet without the ability to assess the activity of a target in a high-throughput assay it is unlikely that compounds that can inhibit the function of the target will ever be found. In this study, we have therefore developed a 384-well fluorescent polarisation assay to monitor the activity of PptA. The assay is highly reproducible with sufficient signal window to permit high-throughput screening. We calculated the Z' factor, a parameter used to assess the suitability of high throughput screens, to be 0.76. Typically assays with Z' values greater than or equal to 0.5 are considered suitable for HTS. We also determined that after stopping the reaction, the assay signal was stable for at least a week, (mean FP max at 24 hrs = 205; CV 3.7; mean FP max at 1 week = 205; CV 2.7).

In conclusion PptA is a nexus, linking the biosynthesis of the siderophores TAFC and FC, lysine, DHN-melanin, gliotoxin and all NRPSs, PKSs derived secondary metabolites. Loss of AF*pptA* results in significant virulence defects in both bronchopulmonary and disseminated models of infection and an altered immune response. The lack of similarity between PptA and its human orthologue AASDHPPT along with our ability to monitor its activity in a high throughput screen makes it an excellent antifungal drug target.

2.5. Acknowledgements

A.J. was funded by BBSRC CASE studentship. This project has also received funding from the European Union's Seventh Framework Programme for research, technological development and demonstration under Grant Agreement No. HEALTH-F3-2013-601963.

2.6. References

1. Havlickova B, Czaika VA, Friedrich M. Epidemiological trends in skin mycoses worldwide. Mycoses. 2008;51:2-15.
2. Brown GD, Denning DW, Gow NA, Levitz SM, Netea MG, White TC. Hidden killers: human fungal infections. Science translational medicine. 2012;4(165):165rv13. Epub 2012/12/21.
3. Richardson MD. Changing patterns and trends in systemic fungal infections. The Journal of antimicrobial chemotherapy. 2005;56 Suppl 1:i5-i11. Epub 2005/08/27.
4. Denning DW, Hope WW. Therapy for fungal diseases: opportunities and priorities. Trends in microbiology. 2010;18(5):195-204. Epub 2010/03/09.
5. Denning DW, Bromley MJ. How to bolster the antifungal pipeline. Science. 2015;347(6229):1414-6.
6. Walsh CT, Gehring AM, Weinreb PH, Quadri LE, Flugel RS. Post-translational modification of polyketide and nonribosomal peptide synthases. Current opinion in chemical biology. 1997;1(3):309-15. Epub 1998/07/17.
7. Lambalot RH, Gehring AM, Flugel RS, Zuber P, LaCelle M, Marahiel MA, et al. A new enzyme superfamily - the phosphopantetheinyl transferases. Chemistry & biology. 1996;3(11):923-36. Epub 1996/11/01.
8. Beld J, Sonnenschein EC, Vickery CR, Noel JP, Burkart MD. The phosphopantetheinyl transferases: catalysis of a post-translational modification crucial for life. Natural product reports. 2014;31(1):61-108. Epub 2013/12/03.
9. Crawford JM, Vagstad AL, Ehrlich KC, Udwary DW, Townsend CA. Acyl-carrier protein-phosphopantetheinyltransferase partnerships in fungal fatty acid synthases. Chembiochem : a European journal of chemical biology. 2008;9(10):1559-63. Epub 2008/06/14.
10. Neville C, Murphy A, Kavanagh K, Doyle S. A 4'-phosphopantetheinyl transferase mediates non-ribosomal peptide synthetase activation in *Aspergillus fumigatus*. Chembiochem : a European journal of chemical biology. 2005;6(4):679-85. Epub 2005/02/19.
11. Oberegger H, Eisendle M, Schrettl M, Graessle S, Haas H. 4'-Phosphopantetheinyl transferase-encoding npgA is essential for siderophore biosynthesis in *Aspergillus nidulans*. Current Genetetics. 2003;44(4):211-5.
12. Mayorga ME, Timberlake WE. The developmentally regulated *Aspergillus nidulans wA* gene encodes a polypeptide homologous to polyketide and fatty acid synthases. Molecular & general genetics : MGG. 1992;235(2-3):205-12. Epub 1992/11/01.
13. Schrettl M, Bignell E, Kragl C, Sabiha Y, Loss O, Eisendle M, et al. Distinct roles for intra- and extracellular siderophores during *Aspergillus fumigatus* infection. PLoS pathogens. 2007;3(9):1195-207. Epub 2007/09/12.
14. Abad A, Victoria Fernández-Molina J, Bikandi J, Ramírez A, Margareto J, Sendino J, et al. What makes *Aspergillus fumigatus* a successful pathogen? Genes and molecules involved in invasive aspergillosis. Revista Iberoamericana de Micología. 2010;27(4):155-82.
15. Allen G, Bromley M, Kaye SJ, Keszenman-Pereyra D, Zucchi TD, Price J, et al. Functional analysis of a mitochondrial phosphopantetheinyl transferase (PPTase) gene pptB in *Aspergillus fumigatus*. Fungal genetics and biology : FG & B. 2011;48(4):456-64. Epub 2011/01/05.
16. Schrettl M, Bignell E, Kragl C, Joechl C, Rogers T, Arst HN, et al. Siderophore Biosynthesis But Not Reductive Iron Assimilation Is Essential for *Aspergillus fumigatus* Virulence. The Journal of Experimental Medicine. 2004;200(9):1213-9.
17. Kwon-Chung KJ, Sugui JA. *Aspergillus fumigatus* - What Makes the Species a Ubiquitous Human Fungal Pathogen? PLoS pathogens. 2013;9(12):e1003743.

18. Johnson L. Iron and siderophores in fungal–host interactions. Mycological Research. 2008;112(2):170-83.
19. Horbach R, Graf A, Weihmann F, Antelo L, Mathea S, Liermann JC, et al. Sfp-Type 4'-Phosphopantetheinyl Transferase Is Indispensable for Fungal Pathogenicity. The Plant Cell. 2009;21(10):3379-96.
20. Howard RJ, Ferrari MA, Roach DH, Money NP. Penetration of hard substrates by a fungus employing enormous turgor pressures. Proceedings of the National Academy of Sciences of the United States of America. 1991;88(24):11281-4. Epub 1991/12/15.
21. Deising HB, Werner S, Wernitz M. The role of fungal appressoria in plant infection. Microbes and infection / Institut Pasteur. 2000;2(13):1631-41. Epub 2000/12/13.
22. Volling K, Thywissen A, Brakhage AA, Saluz HP. Phagocytosis of melanized *Aspergillus* conidia by macrophages exerts cytoprotective effects by sustained PI3K/Akt signalling. Cellular Microbiology. 2011;13(8):1130-48.
23. Chai LYA, Netea MG, Sugui J, Vonk AG, van de Sande WWJ, Warris A, et al. *Aspergillus fumigatus* Conidial Melanin Modulates Host Cytokine Response. Immunobiology. 2010;215(11):915-20.
24. Langfelder K, Jahn B, Gehringer H, Schmidt A, Wanner G, Brakhage AA. Identification of a polyketide synthase gene (pksP) of *Aspergillus fumigatus* involved in conidial pigment biosynthesis and virulence. Medical Microbiology and Immunology. 1998;187(2):79-89.
25. Thywissen A, Heinekamp T, Dahse HM, Schmaler-Ripcke J, Nietzsche S, Zipfel PF, et al. Conidial Dihydroxynaphthalene Melanin of the Human Pathogenic Fungus *Aspergillus fumigatus* Interferes with the Host Endocytosis Pathway. Frontiers in microbiology. 2011;2:96. Epub 2011/07/13.
26. Luther K, Torosantucci A, Brakhage AA, Heesemann J, Ebel F. Phagocytosis of *Aspergillus fumigatus* conidia by murine macrophages involves recognition by the dectin-1 beta-glucan receptor and Toll-like receptor 2. Cellular Microbiology. 2007;9(2):368-81.
27. Bayry J, Beaussart A, Dufrêne YF, Sharma M, Bansal K, Kniemeyer O, et al. Surface Structure Characterization of *Aspergillus fumigatus* Conidia Mutated in the Melanin Synthesis Pathway and Their Human Cellular Immune Response. Infection and immunity. 2014;82(8):3141-53.
28. Schöbel F, Jacobsen ID, Brock M. Evaluation of Lysine Biosynthesis as an Antifungal Drug Target: Biochemical Characterization of *Aspergillus fumigatus* Homocitrate Synthase and Virulence Studies. Eukaryotic Cell. 2010;9(6):878-93.
29. Liebmann B, Muhleisen TW, Muller M, Hecht M, Weidner G, Braun A, et al. Deletion of the *Aspergillus fumigatus* lysine biosynthesis gene lysF encoding homoaconitase leads to attenuated virulence in a low-dose mouse infection model of invasive aspergillosis. Archives of microbiology. 2004;181(5):378-83. Epub 2004/03/31.
30. Fraczek MG, Bromley M, Buied A, Moore CB, Rajendran R, Rautemaa R, et al. The cdr1B efflux transporter is associated with non-cyp51a-mediated itraconazole resistance in *Aspergillus fumigatus*. Journal of Antimicrobial Chemotherapy. 2013;68(7):1486-96.
31. Kragl C, Schrettl M, Abt B, Sarg B, Lindner HH, Haas H. EstB-mediated hydrolysis of the siderophore triacetylfusarinine C optimizes iron uptake of *Aspergillus fumigatus*. Eukaryotic Cell. 2007;6(8):1278-85. Epub 2007/06/26.
32. Szewczyk E, Nayak T, Oakley CE, Edgerton H, Xiong Y, Taheri-Talesh N, et al. Fusion PCR and gene targeting in *Aspergillus nidulans*. Nature Protocols. 2007;1(6):3111-20.
33. Punt PJ, Oliver RP, Dingemanse MA, Pouwels PH, van den Hondel CAMJJ. Transformation of *Aspergillus* based on the hygromycin B resistance marker from Escherichia coli. Gene. 1987;56(1):117-24.
34. Vogel HJ. A convenient growth medium for *Neurospora* (medium N). Microbial genetics bulletin. 1956;13:42-3.

35. Tamura K, Stecher G, Peterson D, Filipski A, Kumar S. MEGA6: Molecular Evolutionary Genetics Analysis version 6.0. Molecular biology and evolution. 2013;30(12):2725-9. Epub 2013/10/18.
36. Jones DT, Taylor WR, Thornton JM. The rapid generation of mutation data matrices from protein sequences. Computer applications in the biosciences : CABIOS. 1992;8(3):275-82. Epub 1992/06/01.
37. Chomczynski P. A reagent for the single-step simultaneous isolation of RNA, DNA and proteins from cell and tissue samples. BioTechniques. 1993;15(3):532-4, 6-7. Epub 1993/09/01.
38. Jasper MJ, Tremellen KP, Robertson SA. Primary unexplained infertility is associated with reduced expression of the T-regulatory cell transcription factor Foxp3 in endometrial tissue. Molecular Human Reproduction. 2006;12(5):301-8.
39. Cove DJ. The induction and repression of nitrate reductase in the fungus *Aspergillus nidulans*. Biochimica et biophysica acta. 1966;113(1):51-6. Epub 1966/01/11.
40. Brooks HB, Geeganage S, Kahl SD, Montrose C, Sittampalam S, Smith MC, et al. Basics of Enzymatic Assays for HTS. In: Sittampalam GS, Coussens NP, Nelson H, Arkin M, Auld D, Austin C, et al., editors. Assay Guidance Manual. Bethesda (MD)2004.
41. Asghar AH, Shastri S, Dave E, Wowk I, Agnoli K, Cook AM, et al. The pobA gene of Burkholderia cenocepacia encodes a group I Sfp-type phosphopantetheinyltransferase required for biosynthesis of the siderophores ornibactin and pyochelin. Microbiology. 2011;157(Pt 2):349-61. Epub 2010/10/23.
42. Mc MR, Lund CC, Oncley JL. Unbound amino acid concentrations in human blood plasmas. The Journal of clinical investigation. 1957;36(12):1672-9. Epub 1957/12/01.
43. Zhao QH, Cao Y, Wang Y, Hu CL, Hu AL, Ruan L, et al. Plasma and tissue free amino acid profiles and their concentration correlation in patients with lung cancer. Asia Pacific Journal of Clinical Nutrition. 2014;23(3):429-36.
44. Costerton JW, Balaban N. Control of Biofilm Infections by Signal Manipulation: Springer Berlin Heidelberg; 2007.
45. Raymond KN, Dertz EA, Kim SS. Enterobactin: an archetype for microbial iron transport. Proceedings of the National Academy of Sciences of the United States of America. 2003;100(7):3584-8. Epub 2003/03/26.
46. Márquez-Fernández O, Trigos Á, Ramos-Balderas JL, Viniegra-González G, Deising HB, Aguirre J. Phosphopantetheinyl transferase CfwA/NpgA is required for *Aspergillus nidulans* secondary metabolism and asexual development. Eukaryotic Cell. 2007;6(4):710-20.
47. Bohnert HU, Fudal I, Dioh W, Tharreau D, Notteghem JL, Lebrun MH. A putative polyketide synthase/peptide synthetase from Magnaporthe grisea signals pathogen attack to resistant rice. Plant Cell. 2004;16(9):2499-513. Epub 2004/08/21.
48. Thines E, Aguirre J, Foster A, Deising H. Genetics of phytopathology: Secondary metabolites as virulence determinants of fungal plant pathogens. In: Esser K, Lüttge U, Beyschlag W, Murata J, editors. Progress in Botany: Springer Berlin Heidelberg; 2006. p. 134-61.
49. Yu JH, Keller N. Regulation of secondary metabolism in filamentous fungi. Annual review of phytopathology. 2005;43:437-58. Epub 2005/08/05.
50. Slater JL, Gregson L, Denning DW, Warn PA. Pathogenicity of *Aspergillus fumigatus* mutants assessed in *Galleria mellonella* matches that in mice. Medical Mycology. 2011;49(S1):S107-S13.
51. Leblanc C, Prudhomme T, Tabouret G, Ray A, Burbaud S, Cabantous S, et al. 4'-Phosphopantetheinyl transferase PptT, a new drug target required for *Mycobacterium tuberculosis* growth and persistence in vivo. PLoS pathogens. 2012;8(12):e1003097. Epub 2013/01/12.

52. Wiemann P, Albermann S, Niehaus EM, Studt L, von Bargen KW, Brock NL, et al. The Sfp-Type 4 '-Phosphopantetheinyl transferase Ppt1 of *Fusarium fujikuroi* controls development, secondary metabolism and pathogenicity. PloS one. 2012;7(5).
53. Mohd Zainudin NA, Condon B, De Bruyne L, Poucke CV, Bi Q, Li W, et al. Virulence, host selective toxin production, and development of three *Cochliobolus* phytopathogens lacking the Sfp-type 4'-phosphopantetheinyl transferase Ppt1. Molecular plant-microbe interactions. 2015. Epub 2015/07/15.
54. Therapeutic areas and technologies. Merck Sharp & Dohme Corp, 2012.
55. Tsai HF, Chang YC, Washburn RG, Wheeler MH, Kwon-Chung KJ. The developmentally regulated *alb1* gene of *Aspergillus fumigatus*: its role in modulation of conidial morphology and virulence. Journal of Bacteriology. 1998;180(12):3031-8. Epub 1998/06/11.
56. Tsunawaki S, Yoshida LS, Nishida S, Kobayashi T, Shimoyama T. Fungal metabolite gliotoxin inhibits assembly of the human respiratory burst NADPH oxidase. Infection and immunity. 2004;72(6):3373-82.
57. Jackson JC, Higgins LA, Lin X. Conidiation color mutants of *Aspergillus fumigatus* are highly pathogenic to the heterologous insect host *Galleria mellonella*. PloS one. 2009;4(1):e4224. Epub 2009/01/22.
58. Bayry J, Beaussart A, Dufrene YF, Sharma M, Bansal K, Kniemeyer O, et al. Surface structure characterization of *Aspergillus fumigatus* conidia mutated in the melanin synthesis pathway and their human cellular immune response. Infection and immunity. 2014;82(8):3141-53.
59. Stanzani M, Orciuolo E, Lewis R, Kontoyiannis DP, Martins SL, St John LS, et al. *Aspergillus fumigatus* suppresses the human cellular immune response via gliotoxin-mediated apoptosis of monocytes. Blood. 2005;105(6):2258-65. Epub 2004/11/18.
60. Orciuolo E, Stanzani M, Canestraro M, Galimberti S, Carulli G, Lewis R, et al. Effects of *Aspergillus fumigatus* gliotoxin and methylprednisolone on human neutrophils: implications for the pathogenesis of invasive aspergillosis. Journal of leukocyte biology. 2007;82(4):839-48.
61. Kupfahl C, Heinekamp T, Geginat G, Ruppert T, Hartl A, Hof H, et al. Deletion of the *gliP* gene of *Aspergillus fumigatus* results in loss of gliotoxin production but has no effect on virulence of the fungus in a low-dose mouse infection model. Molecular microbiology. 2006;62(1):292-302.
62. Cramer RA, Gamcsik MP, Brooking RM, Najvar LK, Kirkpatrick WR, Patterson TF, et al. Disruption of a nonribosomal peptide synthetase in *Aspergillus fumigatus* eliminates gliotoxin production. Eukaryotic Cell. 2006;5(6):972-80.
63. Spikes S, Xu R, Nguyen CK, Chamilos G, Kontoyiannis DP, Jacobson RH, et al. Gliotoxin production in *Aspergillus fumigatus* contributes to host-specific differences in virulence. The Journal of infectious diseases. 2008;197(3):479-86. Epub 2008/01/18.
64. Sugui JA, Pardo J, Chang YC, Zarember KA, Nardone G, Galvez EM, et al. Gliotoxin is a virulence factor of *Aspergillus fumigatus*: *gliP* deletion attenuates virulence in mice immunosuppressed with hydrocortisone. Eukaryotic Cell. 2007;6(9):1562-9.

2.7. Supplementary data

Table S2.2: Primers for pptA, aarA, sidA and pksP gene knock out and reconstitution constructs

Gene	Application	Primer	Sequence
Hph/bleo	**Application**	HPHF	CCGGCTCGGTAACAGAACTAACGGCGTAACCAAAAGTCAC
		HPHR	GGGAGCATATCGTTCAGAGCTCTTGACGACCGTTGATCTG
pptA	**2 step fusion PCR**	pptA_P1	CCGGTCTCTTTCTCTGCATC
		pptA_P2	TAGTTCTGTTACCGAGCCGGTCAAACGAGGGAGGAGTCAG
		pptA_P3	GCTCTGAACGATATGCTCCCCCATGCAATATTCCACAGGA
		pptA_P4	CGGCGTACAGTTCGACATTA
		pptA_P5	CGTCCACCTGGATACCTTGT
		pptA_P6	TCTTCATTGGCAACCATCAG
	Amplification Validation	pptAF	ACCACCTCAGGGACAGACAC
		pptAR	CTCCTTGAGAGCCCAGTACG
aarA	**2 step fusion PCR**	aara_P1	ATCACCGTGAATGGATTCGT
		aara_P2	TAGTTCTGTTACCGAGCCGGAACTCTTGTTTGGGCACTCG
		aara_P3	GCTCTGAACGATATGCTCCCGCGATTTTCAGAGACACACG
		aara_P4	TTAAGCTGACGGCAGAGGTT
		aara_P5	TCATCGAGAGTGATGGACGA
		aara_P6	CGCGGTAACAGCCTCATTAT
	Amplification Validation	aarAF	TTCATCACGCTTTCTTCGTG
		aarAR	TCAGCACGTCCAGAACACTC
sidA	**2 step fusion PCR**	sidA_P1	CCTGCTCCAGGGTAGGTGTA
		sidA_P2	TAGTTCTGTTACCGAGCCGGAGAGATGTGGGAGGAGCAG
		sidA_P3	GCTCTGAACGATATGCTCCCGCCATTTCTCTGACAACACG
		sidA_P4	GCCGTCTGTTACATCCAGGT
		sidA_P5	CAGATGAGATGGGCACACTG
		sidA_P6	AGCAATTGTCTGTGCAAACG
	Amplification Validation	sidAF	TTCTGTGTGTTGGGTTTGGA
		sidAR	CCGATTGCAATAACGACCTT
	Reconstituted strain	sidArec_P1	CCTGCTCCAGGGTAGGTGTA
		sidArec_P2	TAGTTCTGTTACCGAGCCGGTTGACTGCGCCAGAATAGT
		sidArec_P3	GCTCTGAACGATATGCTCCCCGTTGTAAAGCTTTCATGGAG
		sidArec_P4	CGATGTAGTAAAGCGGCAAC
pksP	**2 step fusion PCR**	pksP_P1	CACCCTCATAACGACCCAAC
		pksP_P2	TAGTTCTGTTACCGAGCCGGGCCGTGACTGCAAGGAGTAG
		pksP_P3	GCTCTGAACGATATGCTCCCTTGTTCACAGCCTTGGTCAG
		pksP_P4	TCACATCCAGCAATGTGTCA
		pksP_P5	ATGCAACATGCAACCCTACA
		pksP_P6	TGTCTCATCTTCCCCTCAGC
	Amplification Validation	pksPF	GACCGTACAGCTTTGGTGGT
		pksPR	GACAACTCCTTCGCCTTCTG

Table S2.3: Primers for host response RT-PCR

Gene	Primer	Sequence
IL-1β	IL1β_F	GCTGATGGCCCTAAACAGATG
	IL1β_R	TAGTGGTGGTCGGAGATTCGT
IL-6	IL6_F	ACTCACCTCTTCAGAACG
	IL6_R	GGCTTGTTCCTCACTACT
ACTβ	ACTβ_F	GTGATGGTGGGCATGGGTC
	ACTβ_R	ACACGCAGCTCATTGTA

Table S2.4: Primers for recombinant protein production

Protein	Primer	Sequence
PptA	PptA_F	TATGGATCCGCACAAAACGAGAGGATACC
	PptA _R_pManHis	TATGGATCCCTACTAGGGCTGTTTTTTTGTACACTGACAGA
	PptA _R_pGEX	TATGGATCCCTACTAATGATGATGATGATGATGGGGCTGTTTTTTTGTACACTGACAGA
AarA	AarA_F	TATGGATCCGGTGTTGAAACAGCCTCCTT
	AarA _R	ATGAATTCCTACTAAGAAGTGCCCCCACGTCCAC

Table S2.5: List of Clustal W pairwise alignment scores and BlastP analysis against *A. fumigatus* PptA. N/A represents no significant similarity found. Shading represents Clustal W pairwise alignment scores > 50%.

Organism	Gene Name	Sequence length	ClustalW alignment score	BlastP	
				Identity	Query Cover
Aspergillus clavatus	npgA	346	73.12	72	99
Aspergillus flavus	npgA	343	66.76	64	99
Aspergillus terreus	npgA	324	60.8	56	99
Coccidioides immitis	npgA	328	57.32	56	96
Coccidioides posadasii	npgA	334	56.59	55	96
Blastomyces dematitidis	npgA	355	52.11	53	95
Aspergillus niger	npgA	308	53.9	51	96
Paracoccidioides lutzii	npgA	328	47.87	48	96
Arthroderma benhamiae	npgA	311	53.7	50	96
Trichophyton rubrum	npgA	313	52.72	49	96
Arthroderma otae	npgA	284	50.0	47	84
Microsporum gypseum	npgA	311	50.8	47	96
Histoplasma capsulatum	npgA	311	50.8	49	94
Saccharomyces cerevisiae	lys5	272	14.71	31	24
Cryptococcus neoformans	CNAG_03174	264	14.02	N/A	N/A
Magnaporthe oryzae	MGG_17878	325	32.92	32	87
Candida albicans	lys5	329	6.38	N/A	N/A
Mycobacterium tuberculosis	pptT	227	5.29	N/A	N/A
Bacillus subtilis	ppt1	224	16.96	N/A	N/A
Escherichia coli	entD	256	1.56	N/A	N/A
Homo sapiens	AASDHPPT	309	21.04	26	61
Mus musculus	AASDHPPT	309	17.8	26	62

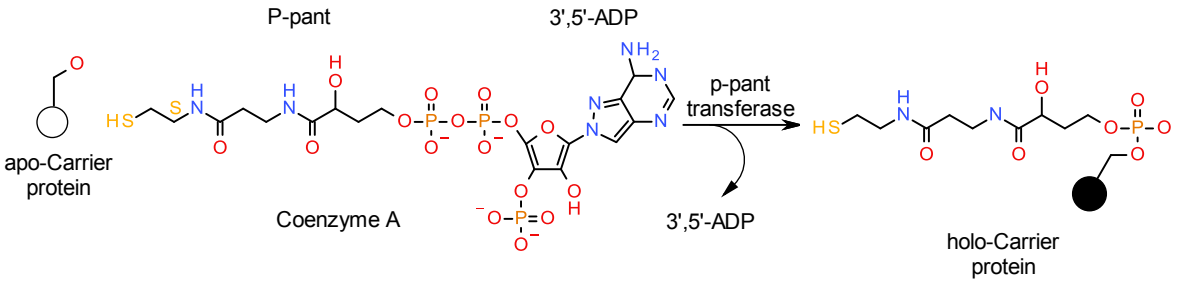

Figure S2.1: Phosphopantetheinylation. The 4'-phosphopantetheine (P-pant) group within Coenzyme A is transferred to a conserved serine residue in the peptidyl carrier domain of the inactive apo-carrier protein to create an active holo-carrier protein. This process is facilitated by 4'-Phosphopantetheinyl transferase (4'-PPTase) (adapted from (6)).

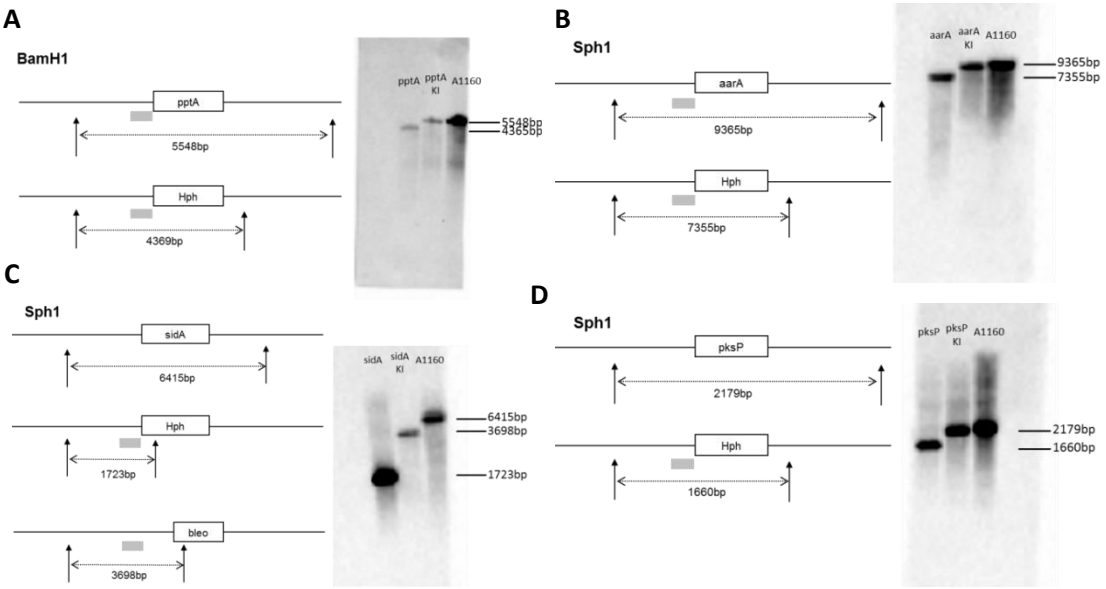

Figure S2.2: Southern blot analysis was used to confirm single intergration of knock out and reconstitution cassettes in mutant strains. The fusion PCR forward flanking sequence was used as a probe generated with gene specific primers P1 and P2. A) ΔpptA DNA was digested with BamH1. The parental strain gave a predicted band of 5.5kb while the ΔpptA strain gave a band at 4.4kb, signifying a single insertion of the replacement construct into the pptA locus. Using the same Southern blot probe a single construct band of 5.5kb was present in pptA rec verifying the reintroduction of pptA into the genome. DNA from the remaining strains; ΔaarA, ΔsidA and ΔpksP was digested using Sph1. B) The ΔaarA strain gave a band at 7.4kb while the parental and reconstituted strain gave a predicted band of 9.4kB. C) The ΔsidA strain gave a band at 1.7kb while the parental strain gave a predicted band of 6.4kB. A single construct band of 3.7kb was present in sidA rec. D) The ΔpksP strain gave a band at 1.7kb while the parental and reconstituted strain gave a predicted band of 2.2kB. Bands present in all gene deletion and reconstitution strains show correct, single insertion of mutation cassettes.

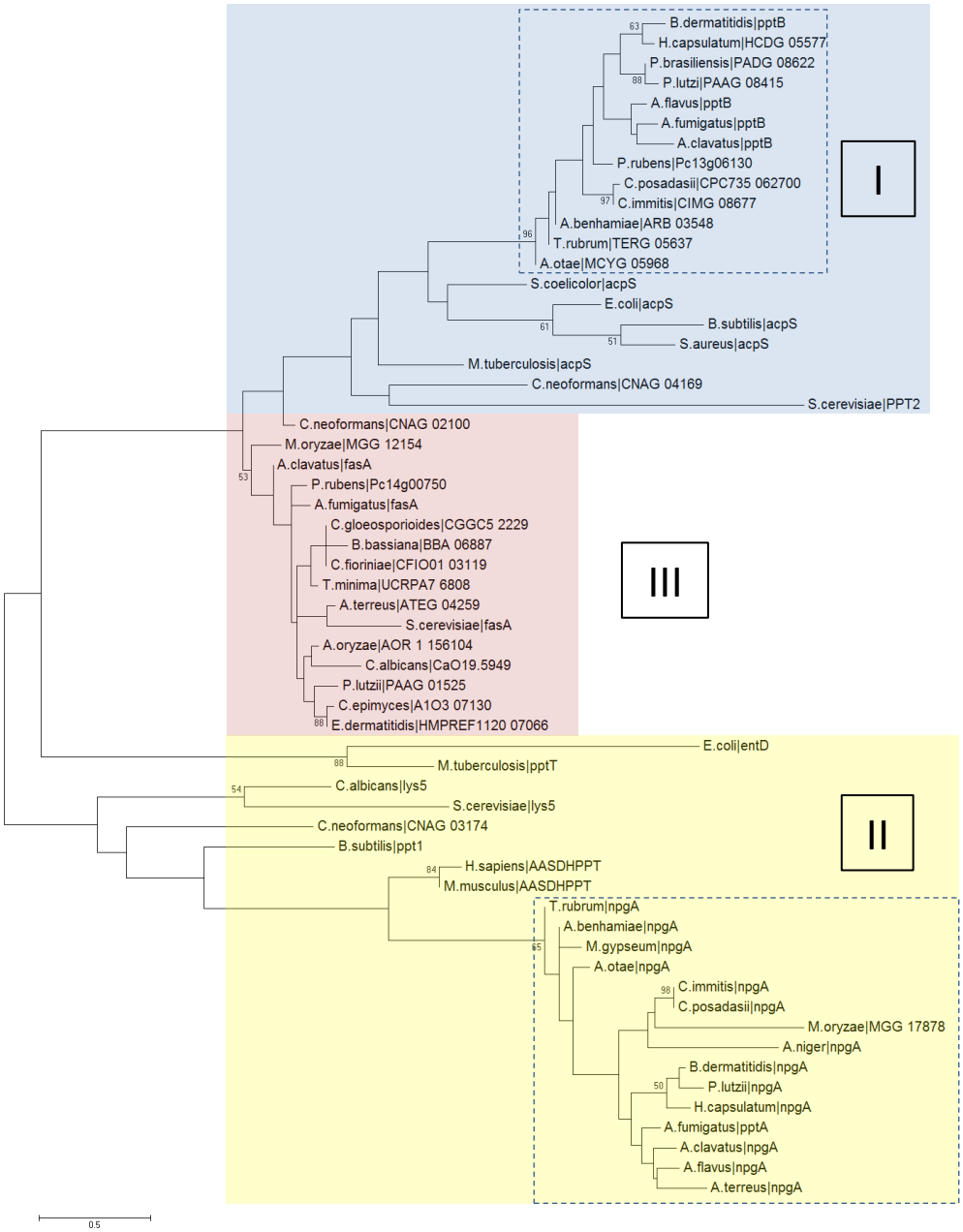

Figure S2.3: Molecular Phylogenetic analysis by Maximum Likelihood method. The evolutionary history was inferred by using the Maximum Likelihood method based on the JTT matrix-based model. The percentage of trees in which the associated taxa clustered together is shown next to the branches. Initial tree(s) for the heuristic search were obtained by applying the Neighbor-Joining method to a matrix of pairwise distances estimated using a JTT model. The tree is drawn to scale, with branch lengths measured in the number of substitutions per site. Evolutionary analyses were conducted in MEGA6. Type I, II and III PPTase are highlighted blue, yellow and red respectively. Dashed boxes show highly conserved PPTase within groups I and II.

Figure S2.4: Fungal Sfp-PPTases signature. Fungal Sfp-PPTases can be identified based on the modified signature (I/V/L)G(I/V/A/T)D(I/V/L)(x)n(F/W)(A/S/T/C)x(K/R)E(S/A)h(h/S)K(M/L/A/F) where n is 41-107 aa. Grey shading indicates conserved signature.

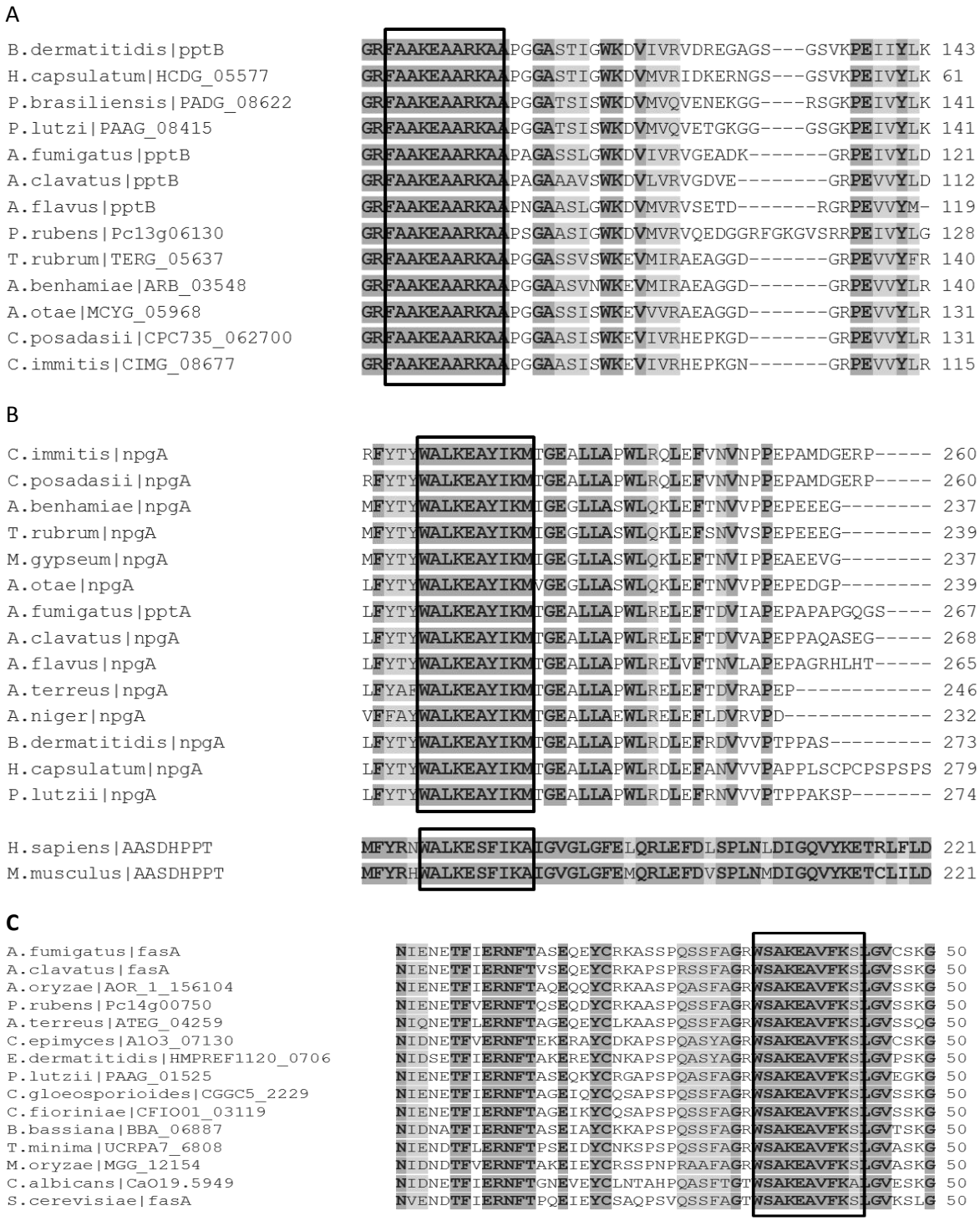

Figure S2.5: Partial sequence alignment of a selection of fungal A) AcpS-type, B) Sfp-type and C) FAS-type PPTases. Dark grey shading and bold lettering indicates positions which have a single, fully conserved residue. Light grey shading indicates conservation between groups of strongly similar properties - scoring > 0.5 in the Gonnet PAM 250 matrix. Black boxes indicate the partial conserved motif; (F/W)(A/S/T/C)x(K/R)E(S/A)h(h/S)K(M/L/A/F/S).

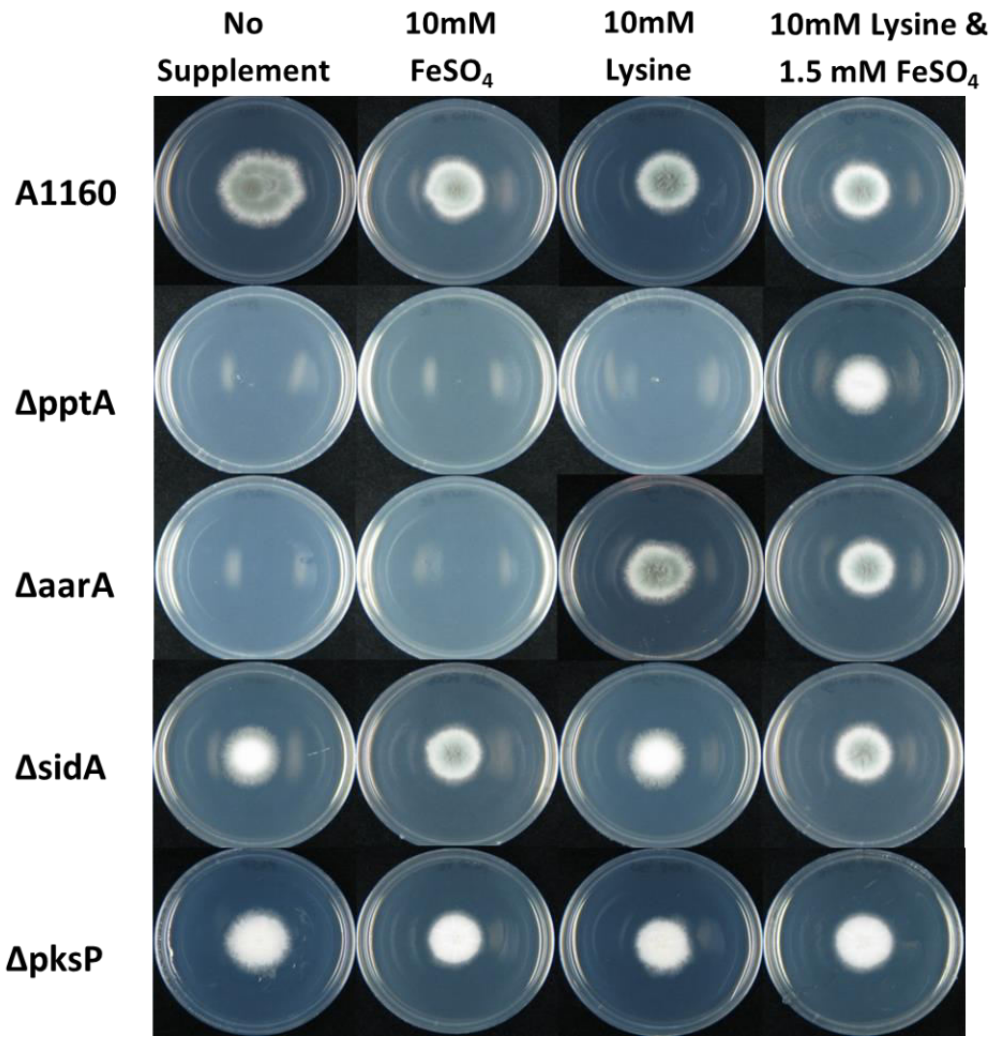

Figure S2.6: Spot analysis of deleted genes. 1x10^4 spores from ΔpptA, ΔaarA, ΔsidA and ΔpksP strains were spotted on to VMM cotaining; no supplement, 1.5 mM supplemental iron ($FeSO_4$), 10mM supplemental lysine, iron and lysine. Cultures were grown at 37°C for 48 hours. As expected ΔpptA only grew on media containing both supplements, ΔaarA will only grow in the presence of supplemental lysine, ΔsidA requires supplemental iron for sporulation and ΔpksP does not require any supplementation but has the same white phenotype as ΔpptA.

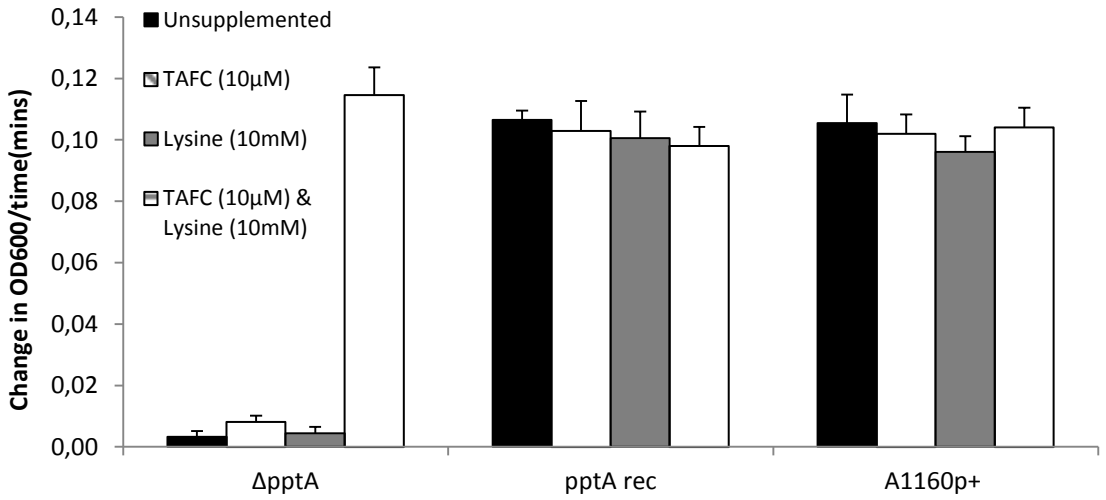

Figure S2.7: Growth rate measurements in 96 well plate. A. fumigatus strains were grown in RPMI media that was either; unsupplemented, supplemented with 10 µM TAFC, supplemented with 10mM lysine or supplemented with both TAFC and Lysine. OD600 was measured every 10 minutes over 48 hours and used to find the kinetic velocity. The mean value for each strain was plotted into a bar graph. Error bars indicate standard deviation. ΔpptA requires both supplemental TAFC and lysine to restore growth to WT.

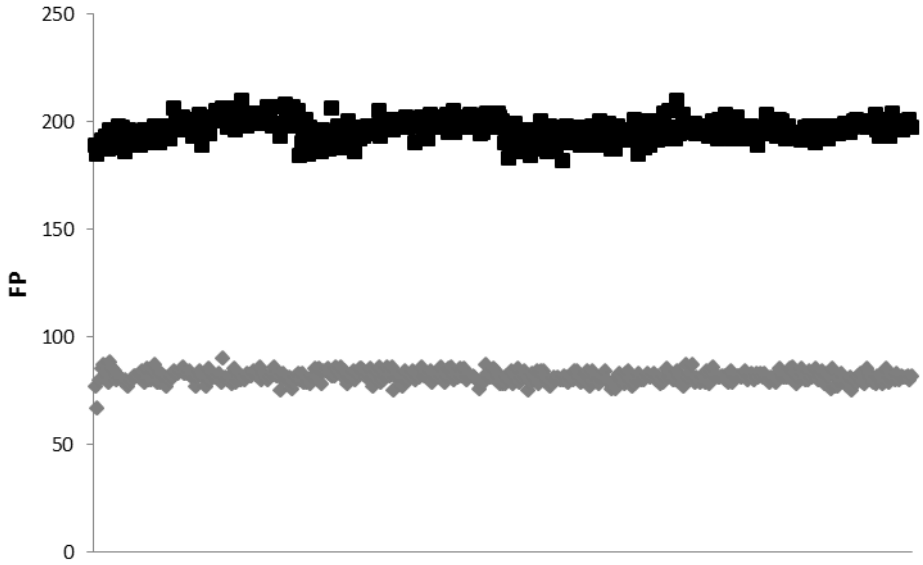

Figure S2.8: Repeatability determination of AFPptA assay over 384 well plate. Each point represents the FP value obtained from the assay in the presence (black) or absence (grey) of the metal chelator and assay inhibitor EDTA

Chapter 3

Inducible cell fusion in the human pathogenic fungus *Aspergillus fumigatus* permits use of parallel fitness analyses to determine the mechanism of action of antifungal compounds

Anna Johns, Darel Macdonald, Adriana Contreras Valenzuela, Jane Mabey Gilsenan, Max Erble, Paul Bowyer, David Denning, Nick Read, Michael Bromley

3. Inducible cell fusion in the human pathogenic fungus *Aspergillus fumigatus* permits use of parallel fitness analyses to determine the mechanism of action of antifungal compounds

Anna Johns, Darel Macdonald, Adriana Contreras Valenzuela, Jane Mabey Gilsenan, Max Erble, Paul Bowyer, David Denning, Nick Read, Michael Bromley

Abstract

Aspergillus fumigatus is the leading cause of invasive aspergillosis, a disease that causes life threatening infections in the immunocompromised population. Due to the pharmacological shortcomings surrounding the current therapeutic options to treat fungal disease such as; toxicity, drug-drug interactions and poor bioavailability, combined with the increasing incidence of antifungal resistance, there is an urgent need to develop a novel class of antifungal drugs. This study validates the use of a chemical genomics approach based on chemically induced haploinsufficiency profiling in *A. fumigatus* to identify either novel drug targets or the mechanism of action of antifungal compounds. We have combated several issues that have previously prevented this technology being used with *A. fumigatus*, including; developing a stable diploid as well as a high throughput gene knockout methodology to generate a suitable library of deletion mutants. Furthermore we have shown that vegetative cell fusion, which would be detrimental to this technology, occurs infrequently under normal cultural conditions in *A. fumigatus*. This study demonstrates the use of parallel fitness profiling along with next generation sequencing based barcode strategy to confirm the mechanism of action of the antifungal agents, itraconazole and brefeldin A.

3.1. Introduction

Fungal diseases are estimated to kill between 1.5 and 2 million people each year which exceeds global mortality estimates for either tuberculosis or malaria (1). A significant proportion of these deaths are the result of invasive and chronic mould infections caused by *Aspergillus* species. The current antifungal armamentarium for the treatment of these infections is limited to four classes of agents which all suffer pharmacological shortcomings including toxicity, drug-drug interactions and poor bioavailability. With the exception of 5-flucytosine, which is not recommended for the treatment of invasive diseases, all commercially available antifungals target and disrupt the integrity of the fungal cell. The azole class of antifungals is the current first line therapy for the treatment of *Aspergillus* infections. However, the development of resistance to this antifungal class is an emerging problem particularly in the Netherlands and UK (2, 3). For individuals infected with a resistant isolate mortality exceeds 88% (2, 3). Novel drugs that act via different mechanisms of action are desperately needed. Since the development of the echinocandin class of antifungals in the 1990s there has been a lack of agents with novel drug targets reaching clinical trials. Recent high profile and relatively late stage antifungal development failures, such as Mycograb and MGCD290, have been disappointing and currently only three antifungal compounds for the treatment of systemic disease are in clinical trials (4).

Standard genomics-driven anti-infective drug target discovery has failed to deliver on its promise to revolutionise the pathway to drug development. This was exemplified by an honest and stark review of antibacterial drug discovery by Payne et al (5) who described how GlaxoSmithKline, over a period of 7 years, invested in excess of $70 million, extensively validating 67 drug targets and carrying out HTS campaigns concluding that the development of anti-bacterials via this route was financially inviable. One key problem with this approach was that it was not possible to assess the targets for 'druggability' i.e. agents that are potent against the isolated target in a HTS screen are able to show anti-proliferative activity.

Successful strides have been made to improve the way genomics is used in drug discovery, relying on it less as a driver to identify novel targets and more to facilitate the identification of the mechanism of action of drugs identified through more traditional screening approaches. Chemical genomics technologies, such as haploinsufficiency profiling in *Saccharomyces cerevisiae* (6-8) and the *Candida albicans* fitness test (CaFT) (9), employ potent, drug-like chemicals that lack mammalian toxicity to identify targets that are druggable and selective. The principle of these approaches is based on chemically induced haploinsufficiency whereby

deletion of a single allele of a drug target in a diploid organism renders the strain more sensitive to that drug. Cognate targets of drugs with an unknown mechanism of action can be identified by screening large, genetically barcoded libraries of mutant isolates. Strains that exhibit fitness defects in a pooled culture at sub-inhibitory drug concentrations are potential targets of drug action. This technology greatly facilitated the determination of the mode of action of the actinomycete derived natural product parnafungin in *C. albicans* (10). Subsequently the presumptive mechanisms of action of over 60 antifungal agents have been identified (11). Recently these technologies have been improved further using barcode analysis by sequencing (Bar-seq), a method that employs next generation sequencing (NGS), to directly count specific barcodes in each strain to allow a more rapid, and higher throughput method for the screening of inhibitory chemical compounds (12) .

While the ability to identify novel druggable targets in yeasts has been successfully addressed, the changing disease landscape, and more particularly our understanding of the significance of mould-based infections, requires similar technologies to be developed in filamentous fungi. A number of issues have inhibited this technology being used with *A. fumigatus* including the fact that it is haploid and that a high throughput gene knockout methodology has not been previously available to generate a suitable library of deletion mutants. In addition filamentous fungi, unlike yeasts, commonly undergo prolific vegetative cell fusion which permits the exchange of cell components including genetic material (13, 14) that would ultimately prevent the successful analysis of parallel fitness of individual genetic isolates in a pooled culture. Vegetative cell fusion is very common and occurs constitutively in diverse filamentous fungi, and has been most extensively investigated in the model *Neurospora crassa* (15, 16).

In this study we show that vegetative cell fusion occurs exceptionally infrequently under normal cultural conditions in *A. fumigatus* but can be induced by environmental stress, involving nitrogen starvation or prolonged exposure to antifungal drugs. Using a non-homologous, end joining deficient diploid isolate of *A. fumigatus,* and a rapid allelic replacement strategy, we have generated a library of 46 heterozygous knockouts of essential genes. By exploiting the lack of significant constitutive cell fusion under our experimental conditions, we have used this library to conduct parallel fitness profiling along with an NGS-based barcode-sequencing strategy to confirm the mechanism of action of the antifungal agents, itraconazole and brefeldin A, and have identified a novel route to resistance against brefeldin A.

3.2. Materials and Methods

3.2.1. Strains

Strains used in this study are listed in table S3.1.

3.2.2. Strain construction

To aid studies of cell fusion in *A. fumigatus,* strains were generated which constitutively expressed GFP (Strain ID: AfGFP) or the RFP Katushka (Turbo 635) (Strain ID: AfRFP) in the cytoplasm. These fluorescent proteins were expressed under the control of the β-tubulin gene promoter (AFUB_086810) or the glyceraldehyde-3-phosphate dehydrogenase (*gpdA*) gene promoter (AFUB_050490), respectively. Fluorescent protein expression cassettes, which encoded *A. fumigatus pyrG* (AFUB_024310) as a selectable marker, were generated via fusion PCR (described elsewhere (17)) and transformed into a stable *pyrG*$^{-}$ derivative of A1160. Selection of AfGFP and AfRFP on chlorate-containing medium permitted the isolation of strains unable to use nitrate as the sole source of nitrogen. Mutations in the molybdene cofactor (*cnx*) and nitrate reductase gene (*niaD*) were confirmed by growth on minimal medium supplemented with different nitrogen sources (described in (18)). These strains were designated AfGFPcnx, AfGFPniaD, AfRFPcnx and AfRFPniaD.

With the aim of generating a library of heterozygous gene knock out *A. fumigatus* strains, a stable diploid strain was engineered as the parent for mutant construction. Briefly, c*nx* and *niaD* mutants of strain A1160p- were isolated by the method described above and these nitrate non-utilising mutants were crossed to generate a stable diploid termed AFMB3 (*pyrG*$^{-/-}$*, cnxABC*$^{+/-}$*, niaD*$^{-/+}$*, Ku80*$^{-/-}$). 46 targeted gene disruption cassettes were generated by fusion PCR and transformed into AFMB3 (described elsewhere (19)) to generate heterozygous knock out strains (*pyrG*$^{+/-}$*, cnxABC*$^{+/-}$*, niaD*$^{-/+}$*, Ku80*$^{-/-}$, targeted gene$^{+/-}$). Duplicate clones of these heterozygote strains were validated and designated StrainID: -1 and StrainID: -2

Strains were grown and maintained on Sabouraud agar or nitrate *Aspergillus* minimal media ($AMMNO_3$) (20). Media was supplemented with 10 mM uridine and 1 mM uracil or 600 mM $KClO_3$ for growth of AFMB3 and cnx/niaD deficient strains respectively. All cultures were incubated at 37°C. Liquid and solid $AMMNO_3$, Vogel's medium (21) or RPMI 1640 medium (Sigma) were used for assessment of hyphal fusion experiments. Parallel fitness profiling was performed in RPMI 1640 (Sigma).

3.2.3. Assessment of cell fusion

The conidia of different paired strains were mixed in a 1:1 ratio (final concentration 1 x 10^6 conidia per ml) and this suspension was used to inoculate assay media. Static liquid cultures were performed in 200-400 µl of culture media or alternatively 50 ml cultures were set up with 2.5 x 10^5 conidia per ml in a 250 ml conical flask with shaking at 200 rpm. The centre of an agar plate was inoculated with 1 µl of a mixed 1 x 10^6 conidia per ml suspension. Cultures were observed at regular intervals (indicated in results) using a Leica TCS SP8 inverted confocal microscope equipped with a tuneable white light laser. Images were captured using a Leica 63 x (1.2 numerical aperture) water immersion objective and very sensitive HyD hybrid detectors. The sequential method of image acquisition was used to avoid bleed through. The tile scan function was used to adjoin adjacent image z stacks to visualize large fields of view for the analysis of cell fusion. Images with a minimum image area of 1.30 mm^2 and depth of 6.4 µm were captured from three different colonies or ten different pellets were screened for fusion. Co-localisation of GFP and RFP in a single cell profile which appeared yellow after merging the green and red channels confirmed cell fusion. Imaris Coloc software (Bitplane) was used to generate a new co-localisation colour channel.

3.2.4. Parallel fitness profiling

Equal numbers of conidia of each heterozygote strain designated -1 were pooled and grown in 50 ml cultures (final inoculum of 2.5 × 10^5 conidia per ml) in the presence and absence of drug in triplicate. The cultures were grown at 200 rpm for 48 hours and total DNA extracted from the biomass using an optimised cetyl trimethyl ammonium bromide (CTAB) method. Briefly, mycelia were snap frozen in liquid nitrogen and ground to a fine powder. The mycelial powder was then transferred to a screw cap tube, suspended in an equal volume of extraction buffer (2% CTAB, 100 mM Tris, 1.4 M NaCl and 10 mM EDTA, pH 8.0) and incubated for 10 min at 65°C. DNA was isolated as previously described (22).

To generate the NGS library, approximately 30 µg DNA was sheered by sonication to generate fragment sizes of 100-400 bp. DNA end repair reactions (100 µl) contained 30 µl of sheared DNA sample, 1× T4 DNA-ligase buffer, 10 mM dNTPs, 15 units of T4 DNA polymerase, 5 units of Klenow DNA polymerase and 50 units of T4 polynucleotide kinase, were incubated at 20°C for 30 minutes. The blunt phosphorylated end repaired DNA fragments were purified using a QIAquick PCR purification kit following the manufacturer's instructions and the DNA eluted in 32 µl of buffer EB. A single adenine base was added (A-tailing) to the 3' end of the end-repaired DNA fragments in a 50 µl reaction containing 1× Klenow buffer, 200 µM dATP, 15

units of Klenow exo- (3’ to 5’ exo minus) and incubated for 30 min at 37°C. A-tailed DNA fragments were cleaned using a QIAquick MiniElute PCR purification kit following the manufacturer's instructions and DNA eluted in 10 µl EB buffer. Paired-end adapter oligonucleotides (Illumina) PEad1 (5’ P-GATCGGAAGAGCGGTTCAGCAGGAATGCCGAG) and PEad2 (5’ ACACTCTTTCCCTACACGACGCTCTTCCGATCT) were annealed in a 100 µl reaction containing 1 x annealing buffer (10 mM Tris pH 7.5, 50 mM NaCl, 1 mM EDTA) and 15 µM of each adapter oligonucleotide. This was incubated at 95°C for 2 min then ramped down to 25°C over 45 minutes. These annealed adapters were ligated to the A-tailed DNA fragments in a 50 µl reaction containing 10 µl of DNA sample, 1× Quick DNA ligase buffer, 10 µl of annealed adapter oligonucleotide mixture, 5 µl of Quick T4 DNA ligase (NEB) and incubated at room temperature for 15 minutes. The sample was gel purified using a QIAquick Gel Extraction Kit following the manufacturer's instructions. DNA fragments between 150-300 bp were excised from the gel. The 3’ sequences flanking the KO-cassette (*pyrG*) were enriched from the adapter ligated DNA fragment by PCR amplification using primers PE2.0 (5’-CAAGCAGAAGACGGCATACGAGATCGGTCTCGGCATTCCTGCTGAACCGCTCTTCCGATCT-3’) and PE1ANpyrG (5’-AATGATACGGCGACCACCGAGATCTACACTCTTTCCCTACACGACGCTCTTCCGATCT NNNNNNCAGTATGCCATAGTTCTGTTACCG-3’) where NNNNNN denotes the unique index that identifies the sample condition (table S3.2) and facilitates pooling of the DNA from multiple cultures. A PCR reaction contained 1x ABsolute qPCR SYBR Green Mix (Thermo Scientific), 200 nM of each primer and 5 ng of total DNA and was performed on an Applied Biosystems® 7500 Real-Time PCR System using MxPro3005P V4.01 (Stratagene). The PCR program began with 15 minute hot-start incubation at 95°C followed by 35 cycles of denaturation at 95°C for 15 seconds, annealing at 60°C for 30 seconds and elongation at 72°C for 30 seconds. The reaction was stopped before the amplification curve reached the plateau stage. Equal amounts of the PCR amplicons were pooled and this library was run on a single lane of an Illumina MiSeq using the standard Illumina sequencing primer (5’-ACACTCTTTCCCTACACGACGCTCTTCCGATCT-3’).

FASTQ files generated by the Illumina sequencer were sorted according to the 6 base (NNNNNN) unique index that identifies the sample condition (table S3.2) using FASTX-Toolkit Barcode Splitter (http://hannonlab.cshl.edu/fastx_toolkit). FASTX-Toolkit FASTQ Quality Filter (http://hannonlab.cshl.edu/fastx_toolkit) was applied to the sorted FASTQ files (parameters: q = 20, p = 99.9) to remove poor quality reads. Each mutant strain possesses a unique gene identifier of 20 bp (table S3.3), FASTX-Toolkit FASTQ/A Trimmer (http://hannonlab.cshl.edu/fastx_toolkit) was used to trim away the adaptors leaving only the unique gene identifier. Sequence reads were mapped to the set of unique gene identifiers with

the program Bowtie (23). Bowtie parameters were set such that reads could contain 3 mismatches. Counts for each gene identifier were calculated. Data was normalised by equalising to the total number of sequenced reads per condition. Pearson correlation and overall standard deviation was calculated between each technical and biological replicate using Microsoft Excel software. Counts for each strain were subsequently normalised to counts from T=0 and then Log2 values were calculated using Microsoft Excel.

3.2.5. Real time PCR fitness assessment

Any strain appearing deficient in these experiments was verified by growth in individual cultures. To confirm the output of the parallel fitness study, quantitative analysis of DNA was also assessed using real-time (RT) PCR. Primers were designed which amplified ~200 bp from the *A. nidulans pyrG* selectable marker (using common primer AnidpyrG_RT) out into the 5' genomic flanking region generating unique sequences for each heterozygote analysed (table S3.4). RT-PCR reactions were carried out using ABsolute QPCR SYBR Green Mix (Thermo Scientific) in a total reaction volume of 25 µl. The final reaction mixture included 1x ABsolute qPCR SYBR Green Mix, 200 nM of each primer and 5 ng of total DNA. All reactions began with 15 minute hot-start incubation at 95°C followed by 30 cycles of denaturation at 95°C for 15 seconds, annealing at 55°C for 30 seconds and elongation at 72°C for 30 seconds. A melting (dissociation) curve to verify single product amplification completed the PCR program and was determined using the following conditions: 1 minute at 95°C, 30 seconds at 55°C and 30 seconds at 95°C. The optimal cycle threshold (Ct) was set automatically by the PCR software (MxPro3005P V4.01, Stratagene). For each pooled culture, each unique sequence was amplified in triplicate and relative strain fitness was determined using the comparative Ct method (ΔΔCt method) using Relative Expression Software Tool (REST) 2009 (Qiagen).

3.2.6. Individual growth assays for fitness assessment

1 x 10^4 conidia from select strains were inoculated on the centre of an AMMNO3 agar plate containing varying concentrations of drug as stated in the results section. Cultures were grown at 37°C and photographed 48 hours after inoculation.

The knock out strains were grown on glucose minimal media in filtered culture flasks at 37°C, after 5-7 days growth the spores were harvested and counted. The spore suspensions from each strain were added to RPMI media in the presence and absence of drug and dispensed into individual wells in a 96 well plate to give a final concentration of 5x10^4 conidia per well. The plate was sealed with a "Breathe Easy" covering membrane (Sigma-Aldrich) and placed on

a microplate scanning spectrophotometer (BIO TEK® Synergy HT). The temperature was set at 37°C and KC4 v3.02 software was used to measure the optical density at 600nm every 10 minutes over a 48 hour time period. Fungal growth was determined by calculating the velocity of the linear phase of the growth curve. The average of 3 replicates was used to derive the mean for each strain and data was normalised to the average growth rate from all strains. Data was plotted into a Tukey box and whisper diagram using GraphPad Prism software.

3.3. Results

3.3.1. Conidial anastomosis tubes are not produced by *A. fumigatus*

The conidia and germ tubes of *N. crassa* and many other filamentous ascomycetes undergo cell fusion during colony initiation by means of specialized cell protrusions called conidial anastomosis tubes that permit the exchange of organelles (including nuclei) and nutrients (24, 25). The early onset of frequent cell fusion would be detrimental to the assessment of the fitness of mutant strains in a pooled culture because it facilitates nuclear exchange between conidial germlings (13, 14). To assess if cell fusion occurs in a similar manner in *A. fumigatus*, we generated CEA10 strains expressing either the green fluorescent protein (Strain ID: AfGFP) or the red fluorescing protein Katuska (Strain ID: AfRFP) in the cytoplasm. Strains were co-inoculated by equally mixing conidia of the 2 strains at a final concentration of 1 x 10^6 conidia per ml in liquid AMM medium supplemented with sodium nitrate ($AMMNO_3$ medium) contained within eight well cell culture chambers. They were then incubated at 37°C and analysed by confocal microscopy after 8 hours and at 4 hourly intervals up to 20 hours. No evidence of cell fusion was detected in 8 cultures despite screening a minimum area of 3.66 mm^2 with a depth of 6.4 µm that contained over 10,000 germinated conidia in each culture (figure 3.1).

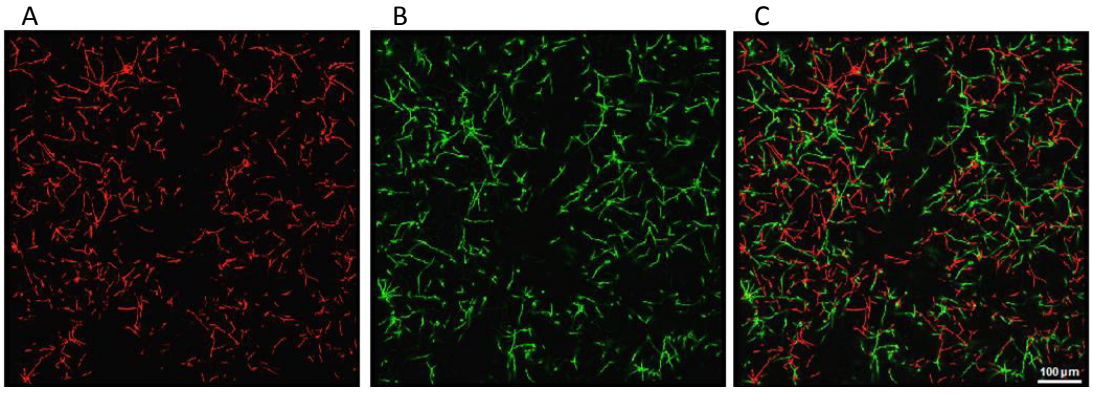

Figure 3.1: Static liquid co-culture of RFP and GFP expressing strains (AfRFP and AfGFP) in AMMNO3 liquid medium. Images derive from merged z-stacks demonstrating the lack of co-localisation of GFP and RFP of a co-inoculated culture after 20 hours (731 mm^2 area over a depth of 6.4 µm). Figures A, B and C show the red (RFP expressing strain), green (GFP expressing strain) and merged channels respectively.

Attempts to evaluate fusion of the 2 strains beyond 20 hours using this approach was not possible as the cells became too densely populated to see anything other than the upper layer of fungal biomass. To assess whether hyphal fusion occurs in more mature colonies, the strains were co-inoculated on solid $AMMNO_3$ medium. Cultures were incubated at 37°C for up to 6

days and checked for hyphal fusion after 12 hours and at 8 hourly intervals. Different regions of the colony were assessed including the central site of inoculation, the periphery and sub-peripheral regions. Evidence of cell fusion, as determined by co-localisation within single cells of green and red fluorescent signals, was observed at 28 hours post inoculation but the percentage cell fusion was low. No more than 10 heterokaryotic hyphal compartments in cultures of this age were observed in a 1.30 mm^2 region of a colony with a depth of 6.4 μm. However cell fusion was not observed in every colony at this stage and when present, co-localisation of red and green signals was clustered in particular regions of the colony (figure 3.2).

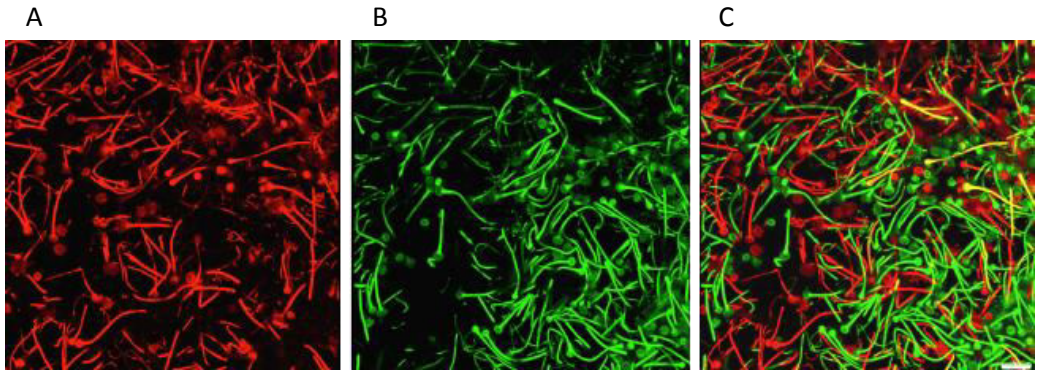

Figure 3.2: Co-localisation of GFP and RFP strains when co-inoculated on solid AMMNO3. A typical field of view of A) red (RFP expressing strain), B) green (GFP expressing strain) and C) merged channels of prototrophic GFP and RFP strains with no stress (1.30 mm^2 area over a depth of 6.4 μm).

3.3.2. Cell fusion is enhanced between complementing auxotrophic mutants

Phenotypic evidence of cell fusion and the formation of diploids via the parasexual cycle were previously described in *A. fumigatus* (26). However, all examples of such events have occurred between auxotrophic strains with different nutritional deficiencies when placed under selective pressure that forces phenotypic complementation. There are no records in the literature providing microscopic evidence of the presumed cell fusion occurring and frequency of these events is unknown. To assess if cell fusion is increased in strains lacking the ability to grow on nitrate as a sole nitrogen source, stable mutants (reversion rate < 1 per 10^7 conidia) lacking functional *niaD* and *cnx* genes were isolated from the GFP and RFP expressing strains to produce the following strains: AfGFPniaD, AfRFPniaD, AfGFPcnx and AfRFPcnx.

Complementary strains (i.e. AfGFPniaD with AfRFPcnx and AfRFPniaD with AfGFPcnx) were co-inoculated in eight well chambers containing liquid $AMMNO_3$ medium, incubated at 37°C and observed microscopically after 8 hours and at 4 hourly intervals up to 32 hours. Signs of cell

fusion were observed after approximately 24 hours by microscopy. Figure 3.3 shows a 731 mm^2 region of a colony with a depth of 6.4 μm that contained 2,089 germinated conidia with equal cells expressing GFP and RFP. A single instance of cell fusion was evident in this colony region (i.e. involving 0.1% of the germlings). The actual level of fusion observed was significantly lower than this as no other fusion events were observed in seven other similarly sized colony samples. Increasing the incubation time to 32 hours did not result in the observation of more fusion. Reliable measurements of fusion beyond this point were not possible because of the high density of growth.

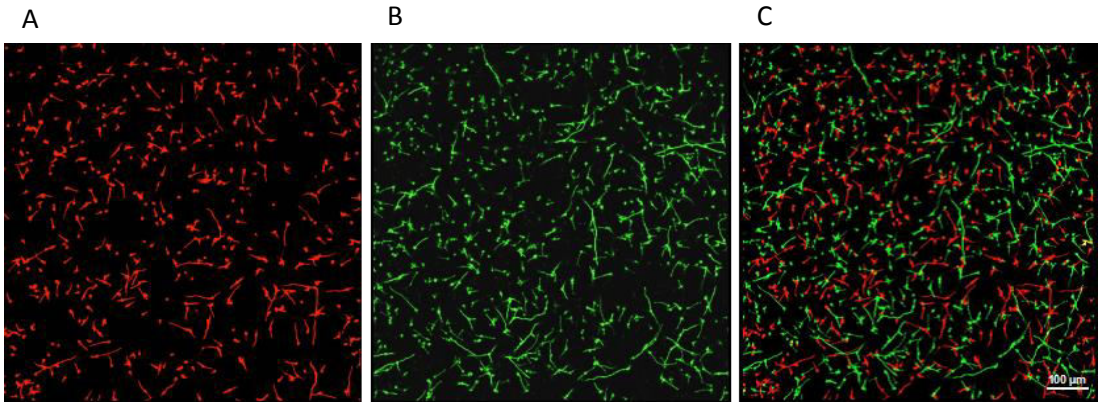

Figure 3.3: Static liquid co-culture of nitrogen starved RFP and GFP expressing strains (AfRFPniaD and AfGFPcnx) in $AMMNO_3$ liquid medium. Images are merged z-stacks demonstrating the lack of co-localisation of GFP and RFP of a co-inoculated culture after 20 hours (731 mm^2 area over a depth of 6.4 μm). Figures A, B and C show the red (RFP expressing strain), green (GFP expressing strain) and merged channels respectively.

The ability of the auxotrophic strains to fuse was assessed over a longer period of time in cultures grown on solid media. The strains were co-inoculated onto $AMMNO_3$ agar plates and incubated at 37°C for up to 6 days. These plates were checked for fusion after 12 hours and at 8 hourly intervals. Signs of cell fusion were observed after approximately 40 hours by microscopy. Fusion occurred most abundantly under these conditions with nearly all hyphae exhibiting co-localisation of GFP and RFP after 92 hours in the 1.30 mm^2 region of a colony with a depth of 6.4 μm (figure 3.4A).

Interestingly, when the same experiments were carried out using one auxotrophic GFP strain lacking the ability to grow on nitrate and an auxotrophic RFP strain competent for growth on nitrate (or vice versa), the competent strain dominated the culture and no hyphal fusion was seen. Taken together our data suggests that cell fusion occurs infrequently in *A. fumigatus* under normal conditions, fusion is greatly enhanced when strains are placed under strong

selective pressure when nitrogen starved. However, this dramatic increase in fusion is not apparent if only one fusion partner is exposed to the selection pressure.

3.3.3. Cell fusion was not observed in shake flask culture

To represent the growth conditions that will be used in parallel fitness experiments, we assessed if cell fusion could occur in shake flask cultures. Strains AfGFPniaD and AfRFPcnx were co-inoculated at a density of 2.5 x 10^6 conidia per ml in $AMMNO_3$ liquid medium and incubated at 37^{o}C with shaking. Fungal pellets that were recovered from 48 hour cultures were examined microscopically. A minimum of ten pellets were screened for cell fusion but none was observed (Figure S3.1).

3.3.4. Cell fusion is induced by exposure to antifungal stress

As cell fusion increased when complementing auxotrophic mutants were placed under nutritional stress (nitrogen starvation) (figure 3.4A), we hypothesised that cell fusion may be induced by other types of environmental stress such as exposure to sub-lethal doses of antifungal drugs. To test this, the prototrophic GFP and RFP expressing strains were co-inoculated on solid $AMMNO_3$ in the presence of sub-lethal concentrations of itraconazole (0.5 μg/ml), brefeldin A (6.25 μg/ml), tunicamycin (25 μg/ml); cerulenin (25 μg/ml), and amphotericin B (0.39 μg/ml) (figure 5B). In each instance, fusion occurred more frequently under stress conditions (figure 3.4B).

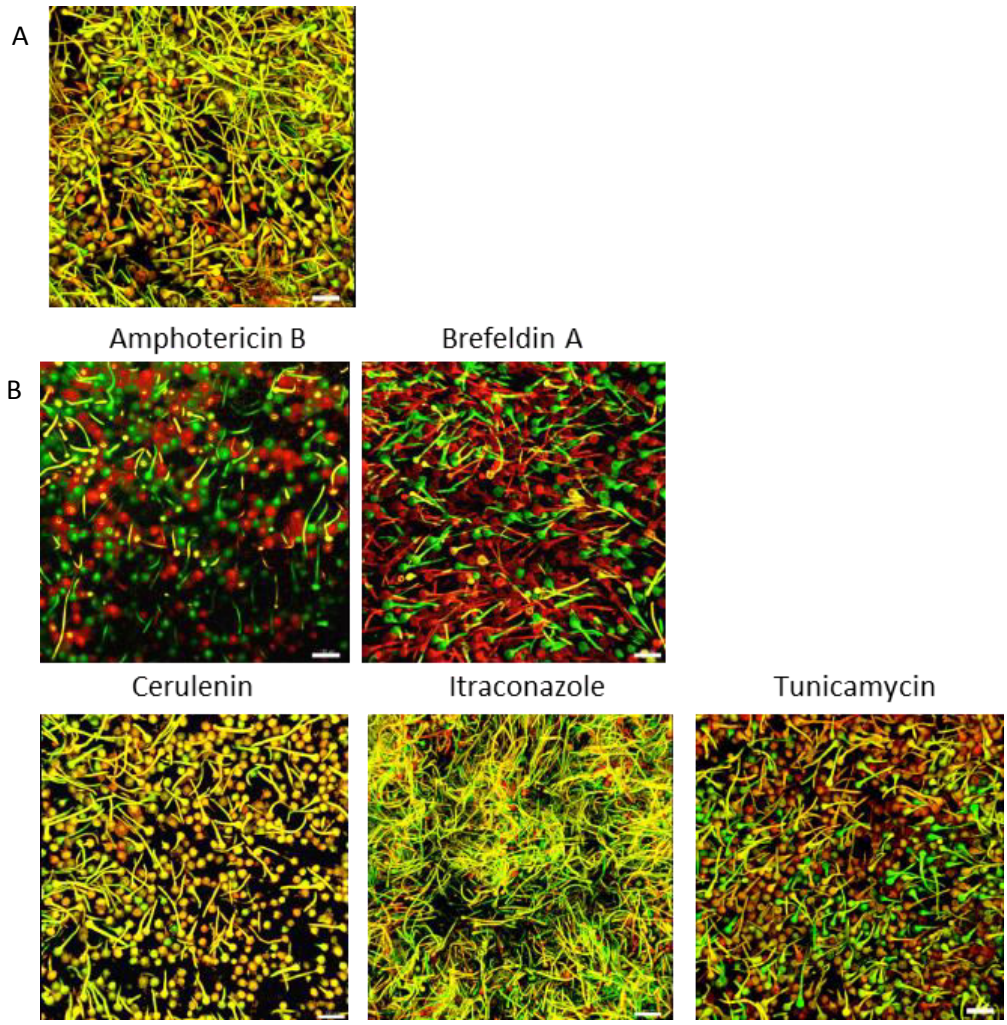

Figure 3.4: Co-localisation of GFP and RFP strains when co-inoculated on solid AMMNO3 in the presence of stress. A typical field of view of merged images (1.30 mm2 area over a depth of 6.4 µm) when in the presence of stressors including A) auxotrophs AfRFPniaD and AfGFPcnx grown under nitrogen starvation conditions and B) prototrophic AfGFP and AfRFP grown in the presence of sub-lethal levels of amphotericin B (0.39 µg/ml); brefeldin A (6.25 µg/ml); cerulenin (25 µg/ml); itraconazole (0.5 µg/ml) or tunicamycin (25 µg/ml). Scale bars in figures A and B represent 100 µm.

3.3.5. Low levels/absence of cell fusion in *A. fumigatus* permits parallel fitness profiling of heterozygous diploid strains

We have determined that cell fusion is absent (or possibly occurs at a low undetectable frequency) even when strains are placed under significant stress and selection pressure in liquid shake culture after growth for 48 hours. Therefore we concluded that this experimental setup could be used for parallel fitness profiling of multiple strains of *A. fumigatus*. With a view to generating a library that can be used in a chemical genomic study and to test this hypothesis we generated a library of 46 gene deletion mutants in a diploid KU80 *A. fumigatus* isolate (AFMB3) using an optimised 96-well plate based, high-throughput gene knockout strategy (Figure 3.5). The genes disrupted in the library were selected as they were either known drug targets or essential for viability. Each knockout cassette was transformed in duplicate ((27); table S3.1). We successfully obtained and validated duplicate clones (designated StrainID: -1 and StrainID: -2) for all strains.

The 46 null mutants with the -1 designation were used in a parallel fitness study to assess if any strains showed a chemically induced haploinsufficient phenotype in response to the antifungal agents itraconazole and brefeldin A. The library was grown in RPMI medium for 40 hours at 37°C with shaking in the presence and absence of sub-lethal levels of drug (0.05 µg/ml itraconazole and 12.5 µg/ml brefeldin A). During this time it would be expected that strains exhibiting chemically induced haploinsufficiency will decrease in relative frequency. The change in the relative abundance of each strain was determined by comparing *en mass* sequencing of the regions flanking the boundary between the ANpyrG selectable marker and the terminator of the gene disrupted (see figure 3.5 which shows a schematic representation of methodology). The changes in the number of sequence reads were then used to calculate relative fitness. Overall, sufficient data was gathered to assess all but two of the genes in the pool for which sequence reads were too low in the overall population to allow meaningful analysis.

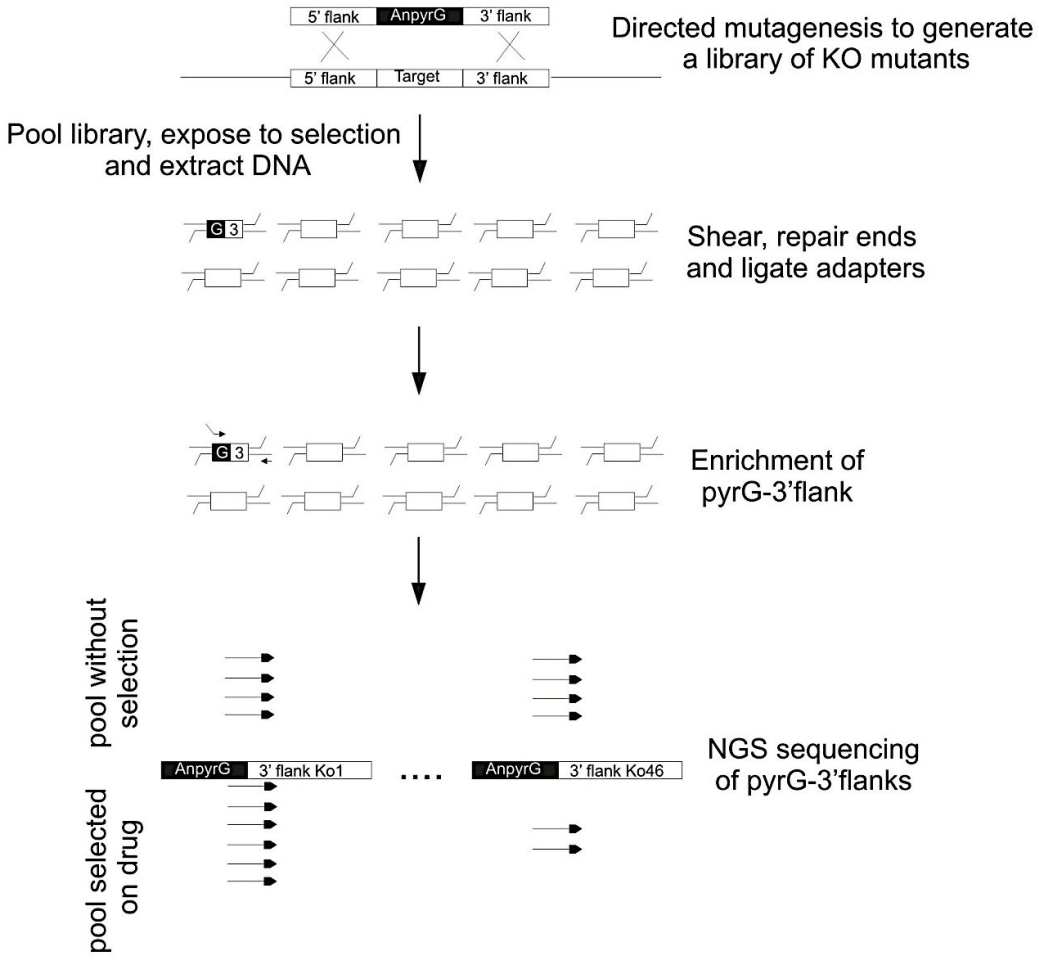

Figure 3.5: Schematic representation of the chemical genomics methodology employed in this study. A library of knockout mutants was generated in the *A. fumigatus* diploid isolate AFMB3. The library was pooled and grown in the presence and absence of an antifungal agent. Genomic DNA was extracted from the pooled library and sheared by sonication. Illumina asymetric linkers are ligated to the sheared DNA. The KO-cassette (pyrG) – 3' target flanks are enriched by PCR amplification. The primers used for amplification anneal to the selectable marker and the non-complementary region of the asymmetric linker. The universal forward primer incorporates the illumina sequencing primer site and the reverse primer incorporates a unique index which will allow sample identification. After sequencing reads are mapped to a reference library that includes the 3' flank regions of all mutants in the library. Relative counts per flank are used to establish the fitness of each strain.

To assess the reproducibility of the chemical genomics assay for the remaining 44 isolates, biological replicates were performed (brefeldin A n = 2; itraconazole n = 3). The reproducibility was high with Pearson correlation coefficients ranging from 0.92 to 0.66 and an overall relative standard deviation for the itraconazole data of 7.9% (standard deviations for the brefeldin A data ranged 21% to 0.4%).

Under both conditions a single outlying strain exhibiting a significant reduction in fitness was identified. These mutants had a decreased gene dosage of the respective drug target *arf2*$^{+/-}$ in

the presence of brefeldin A and *erg11a*$^{+/-}$ in the presence of itraconazole. Additionally, 2 strains with significantly enhanced abundance in the presence of brefeldin A were identified (*atp17*$^{+/-}$ and *mrpl49*$^{+/-}$) (figure 3.6).

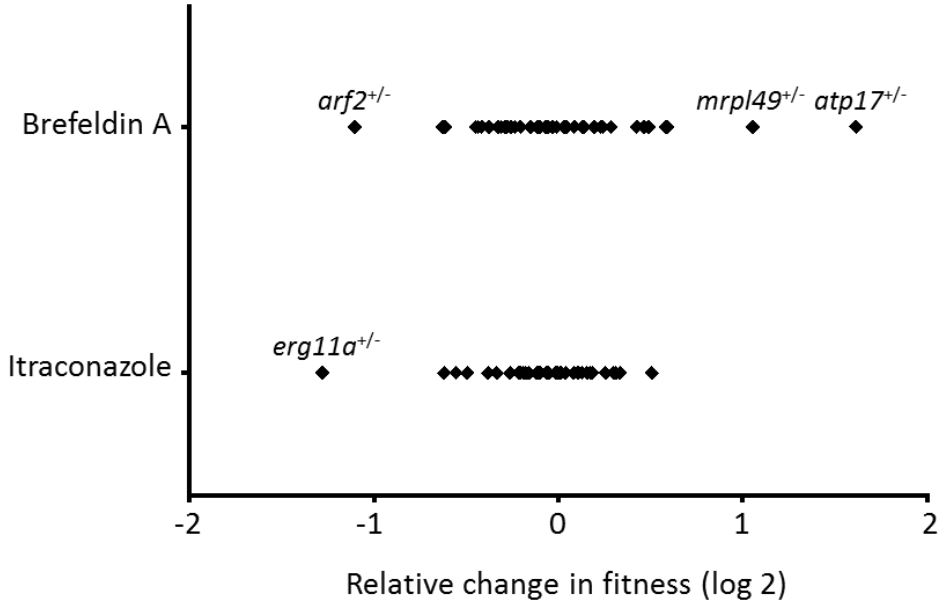

Figure 3.6: Alligned scatter diagram of relative change in fitness (Log 2). A decrease in gene dosage of the respective drug target *arf2*$^{+/-}$ in the presence of brefeldin A and *erg11a*$^{+/-}$ in the presence of itraconazole is shown. Additionally, 2 strains were identified (*atp17*$^{+/-}$ and *mrpl49*$^{+/-}$) with enhanced abundance in the presence of brefeldin A.

To confirm the output of the parallel fitness study, quantitative analysis of the DNA analysed by *en mass* sequencing was assessed using RT PCR. For the selection of strains included in analysis the RT quantification confirmed the accuracy of the NGS analysis (figure 3.7). To further ensure the validity of the parallel fitness profiling data, an additional RT PCR experiment was carried out from brefeldin A cultures inoculated with freshly prepared spore stocks. On this occasion the results for strain *mrpl49*$^{+/-}$ were not replicated (figure S3.2) so this strain was eliminated from further investigation.

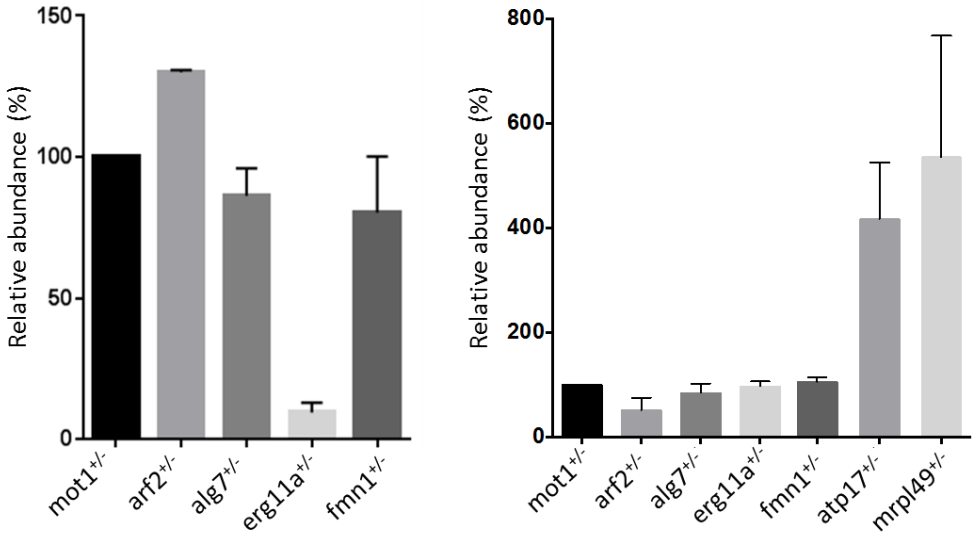

Figure 3.7: Real-time PCR quantitative analysis of the DNA analysed by en mass sequencing. A) DNA isolated from cultures grown in the presence of itraconazole, the strain with the relevant disrupted drug target, erg11a$^{+/-}$, shows the lowest relative abundance. B) DNA isolated from cultures grown in the presence of brefeldin A. The strain with the relevant disrupted drug target arf2$^{+/-}$, shows the lowest relative abundance, atp17$^{+/-}$ and mrpl49$^{+/-}$ show enhanced abundance similar to the NGS results. Analyses were made using *mot1*$^{+/-}$ as the reference strain. Error bars represent standard deviation.

The phenotypes of the *arf2*$^{+/-}$, *erg11a*$^{+/-}$ and *atp17*$^{+/-}$ isolates were further validated by assessing strains in growth assays in the presence and absence of drug on solid $AMMNO_3$ agar medium (figure 3.8A and B) for select strains or all strains in RPMI 1640 liquid media (figure 3.8C). In solid itraconazole cultures *erg11a*$^{+/-}$ exhibits very poor growth compared to the control strain at all concentrations (figure 3.8A). A similar reduction in growth is observed for *erg11a*$^{+/-}$ when all strains are grown individually in the presence of itraconazole in liquid RPMI media (figure 3.8C). The *arf2*$^{+/-}$ strain shows poor growth compared to the control strain, *mot1*$^{+/-}$, in the presence of the lowest concentration of brefeldin A in solid and liquid media, whereas the possible resistant strain *atp17*$^{+/-}$ shows an increased growth (figure 3.8B/C). These individual growth assays coincides with the parallel growth analysis.

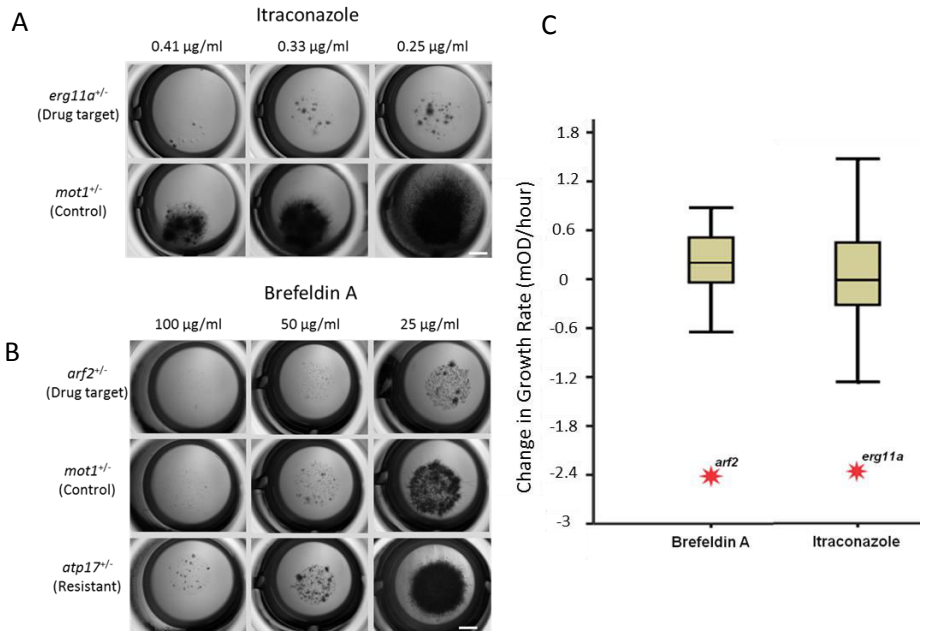

Figure 3.8: Fitness assessment of strains in growth assays on solid AMMNO$_3$ agar medium (A and B) and (C) liquid RPMI 1640 media in the presence and absence of drug. A) *erg11a*$^{+/-}$ exhibits poor growth at all concentrations of itraconazole (0.25 – 0.41 µg/ml) compared to the control strain *mot1*$^{+/-}$ which shows increasing growth as itraconazole concentration decreases. B) *arf2*$^{+/-}$ exhibits no/poor growth at all concentrations of brefeldin A (25 – 100 µg/ml) compared to the control strain *mot1*$^{+/-}$ which shows increasing growth as brefeldin A concentration decreases. *atp17*$^{+/-}$ appears to grow better than the control strain. C) Box and whisper diagram showing *erg11a*$^{+/-}$ and *arf2*$^{+/-}$ exhibit a reduction in growth rate when compared to all other strains when grown individually in the presence of itraconazole and brefeldin A respectively in liquid RPMI media.

3.4. Discussion

Our study shows for the first time that vegetative cell fusion in filamentous fungi can be primarily an inducible phenomenon. We have demonstrated this in the human pathogenic fungus, *A. fumigatus*, and have exploited this discovery to perform parallel fitness analyses to determine the mechanism of action of antifungal compounds.

Filamentous fungi commonly undergo constitutive vegetative cell fusion, which permits the exchange of cell components including nutrients, water, signal molecules and genetic material (13, 15, 16, 28). Vegetative cell fusion has been most extensively studied in the model *N. crassa* (15, 16). In contrast to what occurs in *N. crassa*, our results showed that cell fusion rarely occurs in *A. fumigatus* under normal conditions on a range of standard liquid and solid growth media. Prior to our study, evidence for cell fusion in *A. fumigatus* came from research involving the use of parasexual genetics with this organism. The parasexual cycle, is a non-sexual mechanism for non-meiotic genetic recombination. It involves the formation of a heterokaryon by cell fusion that leads to the formation of a diploid nucleus (karyogamy), which is believed to be unstable and can produce genetic segregants by recombination involving mitotic crossing-over and/or haploidization. It has been employed in several studies with *A. fumigatus* (26). Heterokaryon formation in these studies involves complementing auxotrophic mutants under selection pressure. We demonstrated that significant cell fusion occurred after mixing complementing nitrate auxotrophs expressing either GFP or RFP. We hypothesized that the induction of cell fusion might be due to nutritional stress (nitrogen starvation in the nitrate auxotrophs). In support of this hypothesis we found that exposure to environmental stress from sub-lethal concentrations of commercial antifungal drugs (itraconazole and amphotericin B) and other inhibitory drugs (brefeldin A, tunicamycin and cerulenin) also induced cell fusion.

How inducible cell fusion is regulated in *A. fumigatus* is not clear. Neither is it clear why fungi such as *A. fumigatus* do not undergo cell fusion under non-stressed conditions whilst many other filamentous fungi do. However, there must be a selective advantage for having this different mechanism of cell fusion. For example, it may be that it is advantageous to *A. fumigatus* not to expend large amounts of energy in undergoing cell fusion when environmental conditions are favourable. However, when the environmental conditions cease to be favourable cell fusion is induced to facilitate non-meiotic recombination via the parasexual cycle in order to increase the genetic fitness of the fungus. Sexual reproduction of *A. fumigatus* has not been observed in the wild although it has been demonstrated in culture (29). Thus non-meiotic recombination may be important for generating genetic variation in the predominately asexually reproducing fungus in the natural environment. Cell fusion may also

play roles in the spread of antifungal drug resistance or virulence factors by means of gene transfer (14, 30) in the environment and/or the human host. Increased gene dosage resulting from gene transfer may also increase fitness against certain environmental challenges, and particularly exposure to drugs.

The lack of efficacy, significant toxicity and emergence of resistance associated with the limited antifungal agents currently in clinical use highlights the need for the development of antifungal drugs against novel targets (4). Significant advances have been made in the application of functional genomics tools to drug discovery in the yeasts *Candida albicans* and *Saccharomyces cerevisiae* through the use of chemical genomics. The power of chemical genomics comes from the fact that targets identified through this approach can be defined as both druggable and selective so long as the compounds used in the screen are potent against the pathogen of interest and lack significant toxicity against the host species. Despite its obvious usefulness, limited progress has been made in filamentous fungi particularly because of the technical hurdles in constructing a suitable library of mutants to permit the adoption of similar technologies. This study addresses these problems and demonstrates a chemical genomics system that can be used in a cost effective manner to rapidly and reproducibly identify the mechanism of action of antifungal compounds that are active against filamentous fungi.

Previous studies have demonstrated that strains lacking non-homologous end-joining by virtue of mutations in Ku80, Ku70 or Lig4 (31, 32) can be used to facilitate high efficiency homologous recombination in filamentous fungi. Even in these strains, however, effective gene replacement requires the generation of gene disruption cassettes with around 1 kb of complementary sequence flanking the gene of interest. Methods to generate cassettes rapidly and cheaply using a PCR approach to fuse two gene flanking regions to a selectable marker have been described (33). However adoption of this technology has been limited due to difficulties in reproducibly generating cassettes for different targets. We hypothesised that the use a common linker sequence would allow us to generate cassettes in a reproducible manner. We successfully generated 46 knockout cassettes indicating that this method is highly reproducible.

A key factor in chemical genomics technologies is the requirement to assess the fitness of multiple strains in parallel. Whereas parallel fitness of yeast strains has been the cornerstone of functional genomics technologies, many filamentous fungi undergo vegetative cell fusion which can allow the exchange of genetic material between cells (15). In the context of pooled

fitness profiling such exchanges would clearly be detrimental resulting in the masking of fitness deficiencies. The lack of cell fusion in *A. fumigatus,* particularly in liquid shake culture, indicated that parallel assessment of fitness using multiple strains should be possible in *A. fumigatus*. We demonstrated this by using chemical genomics to confirm the target of action of the well characterised antifungal agents brefeldin A as the Arf GTPase, Arf2 and itraconazole as lanosterol 14 alpha demethylase, Erg11a (Cyp51A). The reproducibility of experimental replicates was high (Pearson correlation coefficients ranging from 0.92 to 0.66). However, we were unable to replicate the apparent comparative increase in growth rate for 1 strain (*mrlp1*$^{+/-}$) grown in the presence of brefeldin A. When this strain was analysed individually it was clear it did not exhibit increased tolerance to brefeldin A indicating a false positive result was obtained in our initial experiment. The cause of this false positive result was not obvious but may be related to technical error. Others have indicated that the performance of similar complex methodologies improves with technical experience and our subsequent results indicate that our performance has improved likewise (12).

In this study we identified that a heterozygous *atp17*$^{+/-}$ isolate displayed increased tolerance against brefeldin A. The a*tp17* gene encodes the f-subunit of the mitochondrial F1F0 ATP synthase and is essential for ATP synthase (complex V) activity (34) and mitochondrial maintenance. In the comparable HIP assay in *S. cerevisiae* (35) the ATP17 heterozygote was assessed in two independent screens with brefeldin A. However, no conclusive fitness result was obtained although one screen indicated that Atp17 may have a modest but not statistical increase in fitness. The mechanism behind the link between the Atp17 haploinsufficiency and brefeldin A resistance was not determined in this study but one may hypothesise that cells deficient in ATP synthase activity accumulate ADP. This in turn may affect cellular metabolic flux, promoting the formation of guanine nucleotides and ultimately GTP, the substrate for ARF2, at the expense of adenosine nucleotides. Indeed deficiencies in adenylosuccinate synthase, the enzyme that catalyses the first step in the formation of ADP from inosine monophosphate (also the precursor for guanine nucleotides) has been shown to lead to significant increases in GTP (36).

In order to maximise the usefulness of this chemical genomics screen, a library will need to be generated that includes strains representing heterozygous mutants in the majority of the essential genes from *A. fumigatus*. Several studies have been carried out to directly identify the essential gene set in *A. fumigatus*. Hu *et al.* (37) identified 35 genes critical for survival using a conditional promoter replacement strategy and we have previously identified 96 essential loci using a transposon mutagenesis approach (27). However with estimated 1000 -

2000 essential genes in *A. fumigatus* we are far short of a comprehensive understanding in this area. The whole genome knock out project in *N. crassa* has identified around 1600 genes (nearly 14% of the genome) that can only be isolated as heterokaryons, presumably because most are essential for viability. This set represents a useful start point to investigate the essential set in *A. fumigatus* using our high throughput gene KO approach. However, the finding that only around 60% of the essential genes are common between the yeasts *S. cerevisiae* and *C. albicans* suggests that the differences between *N. crassa* and *A. fumigatus* may be significant.

This study takes on further significance because of the potential additional applications of the parallel fitness methodologies. Haploinsufficiency profiling has been used recently in an attempt to assign functional relevance to genes that have not previously been functionally characterised in *S. cerevisiae*. Following the screen, a functional role for at least 97% of the genome was found. To date around 45% of the *A. fumigatus* genome is annotated on the Aspergillus genome database (38) as having no known molecular function and where annotation has been given the majority of proposed functions have come from data acquired from other organisms. We are currently involved in an *A. fumigatus* genome wide knockout project. Once completed these strains could be assessed in a similar manner.

In the gram-positive bacteria *Streptococcus pneumonia*, parallel fitness profiling of a library of 10-25,000 transposon mutants has enabled the identification of the fitness defect caused by the loss of each gene in the genome and multiple networks of interacting genes (39). In a similar study in the pathogenic gram-negative bacteria *Haemophilus influenzae,* fitness profiling was carried out in a murine infection model resulting in the identification, in a quantitative manner, of 136 genes that were essential to maintain full virulence (40). Given the exceptionally low number of genes that have been associated with a reduction of virulence in *A. fumigatus,* this technology presents the opportunity to evaluate the effects of mutations in a massively parallel way in an infection model.

3.5. Acknowledgements

A.C.V was funded by a ConaCyt PhD studentship from the Mexican government. A.J was funded by BBSRC CASE studentship.

3.6. References

1. Brown GD, Denning DW, Gow NAR, Levitz SM, Netea MG, White TC. Hidden Killers: Human Fungal Infections. Science Translational Medicine. 2012;4(165).
2. Bueid A, Howard SJ, Moore CB, Richardson MD, Harrison E, Bowyer P, et al. Azole antifungal resistance in *Aspergillus fumigatus*: 2008 and 2009. Journal of Antimicrobial Chemotherapy. 2010;65(10):2116-8.
3. Van der Linden JWM, Snelders E, Kampinga GA, Rijnders BJA, Mattsson E, Debets-Ossenkopp YJ, et al. Clinical Implications of Azole Resistance in *Aspergillus fumigatus*, the Netherlands, 2007-2009. Emerging Infectious Diseases. 2011;17(10):1846-54.
4. Denning DW, Bromley MJ. How to bolster the antifungal pipeline. Science. 2015;347(6229):1414-6.
5. Payne DJ, Gwynn MN, Holmes DJ, Pompliano DL. Drugs for bad bugs: confronting the challenges of antibacterial discovery. Nature Reviews Drug Discovery. 2007;6(1):29-40.
6. Giaever G, Shoemaker DD, Jones TW, Liang H, Winzeler EA, Astromoff A, et al. Genomic profiling of drug sensitivities via induced haploinsufficiency. Nature Genetics. 1999;21(3):278-83.
7. Giaever G, Flaherty P, Kumm J, Proctor M, Nislow C, Jaramillo DF, et al. Chemogenomic profiling: Identifying the functional interactions of small molecules in yeast. Proceedings of the National Academy of Sciences of the United States of America. 2004;101(3):793-8.
8. Lum PY, Armour CD, Stepaniants SB, Cavet G, Wolf MK, Butler JS, et al. Discovering modes of action for therapeutic compounds using a genome-wide screen of yeast heterozygotes. Cell. 2004;116(1):121-37.
9. Xu DM, Jiang B, Ketela T, Lemieux S, Veillette K, Martel N, et al. Genome-wide fitness test and mechanism-of-action studies of inhibitory compounds in *Candida albicans*. PloS Pathogens. 2007;3(6):835-48.
10. Bills GF, Platas G, Overy DP, Collado J, Fillola A, Jimenez MR, et al. Discovery of the parnafungins, antifungal metabolites that inhibit mRNA polyadenylation, from the Fusarium larvarum complex and other Hypocrealean fungi. Mycologia. 2009;101(4):449-72.
11. Roemer T, Xu DM, Singh SB, Parish CA, Harris G, Wang H, et al. Confronting the Challenges of Natural Product-Based Antifungal Discovery. Chemistry & Biology. 2011;18(2):148-64.
12. Smith AM, Heisler LE, Mellor J, Kaper F, Thompson MJ, Chee M, et al. Quantitative phenotyping via deep barcode sequencing. Genome research. 2009;19(10):1836-42. Epub 2009/07/23.
13. Roca MG, Kuo HC, Lichius A, Freitag M, Read ND. Nuclear dynamics, mitosis, and the cytoskeleton during the early stages of colony initiation in *Neurospora crassa*. Eukaryotic Cell. 2010;9(8):1171-83.
14. Ishikawa FH, Souza EA, Shoji JY, Connolly L, Freitag M, Read ND, et al. Heterokaryon incompatibility is suppressed following conidial anastomosis tube fusion in a fungal Plant Pathogen. PloS one. 2012;7(2).
15. Read ND, Fleißner A, Roca GM, Glass NL. Hyphal Fusion. In: Borkovich KA, Ebbole D, editors. Cellular and Molecular Biology of Filamentous Fungi: American Society of Microbiology; 2010. p. 260-73.
16. Read ND, Goryachev AB, Lichius A. The mechanistic basis of self-fusion between conidial anastomosis tubes during fungal colony initiation. Fungal Biology Reviews. 2012;26(1):1-11.

17. Kuwayama H, Obara S, Morio T, Katoh M, Urushihara H, Tanaka Y. PCR-mediated generation of a gene disruption construct without the use of DNA ligase and plasmid vectors. Nucleic Acids Research. 2002;30(2):e2.
18. Cove DJ. Chlorate toxicity in Aspergillus nidulans. Studies of mutants altered in nitrate assimilation. Mol Genomics and Genetics. 1976;146(2):147-59.
19. Oliver JD, Kaye SJ, Tuckwell D, Johns AE, Macdonald DA, Livermore J, et al. The *Aspergillus fumigatus* dihydroxyacid dehydratase Ilv3A/IlvC is required for full virulence. PLoS ONE. 2012;7(9):e43559.
20. Rowlands RT, Turner G. Nuclear and extranuclear inheritance of oligomycin resistance in *Aspergillus nidulans*. Molecular & general genetics : MGG. 1973;126(3):201-16. Epub 1973/11/12.
21. Vogel HJ. A convenient growth medium for *Neurospora* (medium N). Microbial genetics bulletin. 1956;13:42-3.
22. Fraczek MG, Bromley M, Buied A, Moore CB, Rajendran R, Rautemaa R, et al. The cdr1B efflux transporter is associated with non-cyp51a-mediated itraconazole resistance in *Aspergillus fumigatus*. Journal of Antimicrobial Chemotherapy. 2013;68(7):1486-96.
23. Langmead B, Trapnell C, Pop M, Salzberg SL. Ultrafast and memory-efficient alignment of short DNA sequences to the human genome. Genome Biology. 2009;10(3).
24. Roca MG, Read ND, Wheals AE. Conidial anastomosis tubes in filamentous fungi. Fems Microbiol Lett. 2005;249(2):191-8.
25. Roca MG, Arlt J, Jeffree CE, Read ND. Cell biology of conidial anastomosis tubes in Neurospora crassa. Eukaryotic Cell. 2005;4(5):911-9.
26. Berg CM, Garber ED. A genetic analysis of color mutants of *Aspergillus fumigatus*. Genetics. 1962;47(9):1139-&.
27. Carr PD, Tuckwell D, Hey PM, Simon L, d'Enfert C, Birch M, et al. The transposon *impala* is activated by low temperatures: use of a controlled transposition system to identify genes critical for viability of *Aspergillus fumigatus.* Eukaryotic Cell. 2010;9(3):438-48.
28. Ishikawa K, Ito K, Inoue J, Semba K. Cell growth control by stable Rbg2/Gir2 complex formation under amino acid starvation. Genes Cells. 2013;18(10):859-72.
29. O'Gorman CM, Fuller HT, Dyer PS. Discovery of a sexual cycle in the opportunistic fungal pathogen *Aspergillus fumigatus*. Nature. 2009;457(7228):471-U5.
30. Ma LJ, van der Does HC, Borkovich KA, Coleman JJ, Daboussi MJ, Di Pietro A, et al. Comparative genomics reveals mobile pathogenicity chromosomes in *Fusarium.* Nature. 2010;464(7287):367-73.
31. Ninomiya Y, Suzuki K, Ishii C, Inoue H. Highly efficient gene replacements in *Neurospora* strains deficient for nonhomologous end-joining. Proceedings of the National Academy of Sciences of the United States of America. 2004;101(33):12248-53.
32. Ishibashi K, Suzuki K, Ando Y, Takakura C, Inoue H. Nonhomologous chromosomal integration of foreign DNA is completely dependent on MUS-53 (human Lig4 homolog) in *Neurospora*. Proceedings of the National Academy of Sciences of the United States of America. 2006;103(40):14871-6.
33. Kuwayama H, Obara S, Morio T, Katoh M, Urushihara H, Tanaka Y. PCR-mediated generation of a gene disruption construct without the use of DNA ligase and plasmid vectors. Nucleic Acids Research. 2002;30(2).
34. Devenish RJ, Prescott M, Roucou X, Nagley P. Insights into ATP synthase assembly and function through the molecular genetic manipulation of subunits of the yeast mitochondrial enzyme complex. Bba-Bioenergetics. 2000;1458(2-3):428-42.
35. Hillenmeyer ME, Fung E, Wildenhain J, Pierce SE, Hoon S, Lee W, et al. The chemical genomic portrait of yeast: uncovering a phenotype for all genes. Science. 2008;320(5874):362-5. Epub 2008/04/19.

36. Ullman B, Wormsted MA, Cohen MB, Martin DW, Jr. Purine oversecretion in cultured murine lymphoma cells deficient in adenylosuccinate synthetase: genetic model for inherited hyperuricemia and gout. Proceedings of the National Academy of Sciences of the United States of America. 1982;79(17):5127-31. Epub 1982/09/01.
37. Hu W, Sillaots S, Lemieux S, Davison J, Kauffman S, Breton A, et al. Essential gene identification and drug target prioritization in *Aspergillus fumigatus*. PLoS pathogens. 2007;3(3):e24.
38. Cerqueira GC, Arnaud MB, Inglis DO, Skrzypek MS, Binkley G, Simison M, et al. The *Aspergillus* Genome Database: multispecies curation and incorporation of RNA-Seq data to improve structural gene annotations. Nucleic Acids Research. 2014;42(D1):D705-D10.
39. van Opijnen T, Bodi KL, Camilli A. Tn-seq: high-throughput parallel sequencing for fitness and genetic interaction studies in microorganisms. Nature Methods. 2009;6(10):767-U21.
40. Gawronski JD, Wong SMS, Giannoukos G, Ward DV, Akerley BJ. Tracking insertion mutants within libraries by deep sequencing and a genome-wide screen for Haemophilus genes required in the lung. Proceedings of the National Academy of Sciences of the United States of America. 2009;106(38):16422-7.

3.7. Supplementary data

Table S3.1: Strains used in this study

Strain	Description	Source
CEA10	Clinical isolate	FGSC
A1160p-	Derived from CEA10, Ku80^{-}, pyrG^{-}	FGSC
AFMB3	Derived from A1160p^{-}, diploid, pyrG$^{-/-}$, cnxABC$^{+/-}$, niaD$^{-/+}$, Ku80$^{-/-}$	This study
AfGFP	A1160p-, *pyrG*$^{-}$, GFP^{+}	This study
AfRFP	A1160p-, *pyrG*$^{-}$, RFP^{+}	This study
AfGFPcnx	A1160p-, *pyrG*$^{-}$, GFP^{+}, cnx^{-}	This study
AfGFPniaD	A1160p-, *pyrG*$^{-}$, GFP^{+}, niaD^{-}	This study
AfRFPcnx	A1160p-, *pyrG*$^{-}$, RFP+, cnx^{-}	This study
AfRFPniaD	A1160p-, *pyrG*$^{-}$, RFP+, niaD^{-}	This study
A2-1/-2	Diploid, pyrG$^{+/-}$, cnxABC$^{+/-}$, niaD$^{-/+}$, Ku80$^{-/-}$, Afua_1g04840$^{+/-}$ (*mrd1*$^{+/-}$)	This study
A3-1/-2	Diploid, pyrG$^{+/-}$, cnxABC$^{+/-}$, niaD$^{-/+}$, Ku80$^{-/-}$, Afua_1g05830$^{+/-}$ (*mot1*$^{+/-}$)	This study
A4-1/-2	Diploid, pyrG$^{+/-}$, cnxABC$^{+/-}$, niaD$^{-/+}$, Ku80$^{-/-}$, Afua_1g09690$^{+/-}$ (*trl1*$^{+/-}$)	This study
A5-1/-2	Diploid, pyrG$^{+/-}$, cnxABC$^{+/-}$, niaD$^{-/+}$, Ku80$^{-/-}$, Afua_1g11730$^{+/-}$ (*arf2*$^{+/-}$)	This study
A6-1/-2	Diploid, pyrG$^{+/-}$, cnxABC$^{+/-}$, niaD$^{-/+}$, Ku80$^{-/-}$, Afua_1g13100$^{+/-}$ (*nup188*$^{+}$)$^{/-}$	This study
A7-1/-2	Diploid, pyrG$^{+/-}$, cnxABC$^{+/-}$, niaD$^{-/+}$, Ku80$^{-/-}$, Afua_1g13200$^{+/-}$ (*urb2*$^{+/-}$)	This study
A8-1/-2	Diploid, pyrG$^{+/-}$, cnxABC$^{+/-}$, niaD$^{-/+}$, Ku80$^{-/-}$, Afua_1g13420$^{+/-}$ (*rrd2*$^{+/-}$)	This study
A9-1/-2	Diploid, pyrG$^{+/-}$, cnxABC$^{+/-}$, niaD$^{-/+}$, Ku80$^{-/-}$, Afua_1g13790$^{+/-}$ (*hht1*$^{+/-}$)	This study
A10-1/-2	Diploid, pyrG$^{+/-}$, cnxABC$^{+/-}$, niaD$^{-/+}$, Ku80$^{-/-}$, Afua_1g13910$^{+/-}$ (*rad3*$^{+/-}$)	This study
A11-1/-2	Diploid, pyrG$^{+/-}$, cnxABC$^{+/-}$, niaD$^{-/+}$, Ku80$^{-/-}$, Afua_1g14740$^{+/-}$ (*toa1*$^{+/-}$)	This study
A12-1/-2	Diploid, pyrG$^{+/-}$, cnxABC$^{+/-}$, niaD$^{-/+}$, Ku80$^{-/-}$, Afua_2g01330$^{+/-}$ (*rrp46*$^{+/-}$)	This study
B1-1/-2	Diploid, pyrG$^{+/-}$, cnxABC$^{+/-}$, niaD$^{-/+}$, Ku80$^{-/-}$, Afua_2g01570$^{+/-}$ (*aps1*$^{+/-}$)	This study
B2-1/-2	Diploid, pyrG$^{+/-}$, cnxABC$^{+/-}$, niaD$^{-/+}$, Ku80$^{-/-}$, Afua_2g02510$^{+/-}$ (*kog1*$^{+/-}$)	This study
B3-1/-2	Diploid, pyrG$^{+/-}$, cnxABC$^{+/-}$, niaD$^{-/+}$, Ku80$^{-/-}$, Afua_2g03310$^{+/-}$ (*nsp1*$^{+/-}$)	This study
B4-1/-2	Diploid, pyrG$^{+/-}$, cnxABC$^{+/-}$, niaD$^{-/+}$, Ku80$^{-/-}$, Afua_2g03640$^{+/-}$ (*iqg1*$^{+/-}$)	This study
B5-1/-2	Diploid, pyrG$^{+/-}$, cnxABC$^{+/-}$, niaD$^{-/+}$, Ku80$^{-/-}$, Afua_2g05510$^{+/-}$ (*atp17*$^{+/-}$)	This study
B6-1/-2	Diploid, pyrG$^{+/-}$, cnxABC$^{+/-}$, niaD$^{-/+}$, Ku80$^{-/-}$, Afua_2g05820$^{+/-}$ (*fmn1*$^{+/-}$)	This study
B7-1/-2	Diploid, pyrG$^{+/-}$, cnxABC$^{+/-}$, niaD$^{-/+}$, Ku80$^{-/-}$, Afua_2g06060$^{+/-}$ (*hfi1*$^{+/-}$)	This study
B8-1/-2	Diploid, pyrG$^{+/-}$, cnxABC$^{+/-}$, niaD$^{-/+}$, Ku80$^{-/-}$, Afua_2g06150$^{+/-}$ (*pdi1*$^{+/-}$)	This study
B9-1/-2	Diploid, pyrG$^{+/-}$, cnxABC$^{+/-}$, niaD$^{-/+}$, Ku80$^{-/-}$, Afua_2g08550$^{+/-}$ (*ess1*$^{+/-}$)	This study
B10-1/-2	Diploid, pyrG$^{+/-}$, cnxABC$^{+/-}$, niaD$^{-/+}$, Ku80$^{-/-}$, Afua_2g08860$^{+/-}$ (*rrp45*$^{+/-}$)	This study
B11-1/-2	Diploid, pyrG$^{+/-}$, cnxABC$^{+/-}$, niaD$^{-/+}$, Ku80$^{-/-}$, Afua_2g09060$^{+/-}$ (*cdc54*$^{+/-}$)	This study

B12-1/-2	Diploid, pyrG$^{+/-}$, cnxABC$^{+/-}$, niaD$^{-/+}$, Ku80$^{-/-}$, Afua_2g10300$^{+/-}$ (*rps17a*$^{+/-}$)	This study
C1-1/-2	Diploid, pyrG$^{+/-}$, cnxABC$^{+/-}$, niaD$^{-/+}$, Ku80$^{-/-}$, Afua_2g10870$^{+/-}$ (*rrn11*$^{+/-}$)	This study
C2-1/-2	Diploid, pyrG$^{+/-}$, cnxABC$^{+/-}$, niaD$^{-/+}$, Ku80$^{-/-}$, Afua_2g11010$^{+/-}$ (*pyrE*$^{+/-}$)	This study
C3-1/-2	Diploid, pyrG$^{+/-}$, cnxABC$^{+/-}$, niaD$^{-/+}$, Ku80$^{-/-}$, Afua_2g11240$^{+/-}$ (*alg7*$^{+/-}$)	This study
C4-1/-2	Diploid, pyrG$^{+/-}$, cnxABC$^{+/-}$, niaD$^{-/+}$, Ku80$^{-/-}$, Afua_2g11810$^{+/-}$ (*rrp12*$^{+/-}$)	This study
C5-1/-2	Diploid, pyrG$^{+/-}$, cnxABC$^{+/-}$, niaD$^{-/+}$, Ku80$^{-/-}$, Afua_2g12250$^{+/-}$ (*rfc5*$^{+/-}$)	This study
C6-1/-2	Diploid, pyrG$^{+/-}$, cnxABC$^{+/-}$, niaD$^{-/+}$, Ku80$^{-/-}$, Afua_2g12370$^{+/-}$ (*ynl213c*$^{+/-}$)	This study
C7-1/-2	Diploid, pyrG$^{+/-}$, cnxABC$^{+/-}$, niaD$^{-/+}$, Ku80$^{-/-}$, Afua_2g13450$^{+/-}$ (*uso1*$^{+/-}$)	This study
C8-1/-2	Diploid, pyrG$^{+/-}$, cnxABC$^{+/-}$, niaD$^{-/+}$, Ku80$^{-/-}$, Afua_2g16040$^{+/-}$ (*rrp5*$^{+/-}$)	This study
C9-1/-2	Diploid, pyrG$^{+/-}$, cnxABC$^{+/-}$, niaD$^{-/+}$, Ku80$^{-/-}$, Afua_2g16300$^{+/-}$ (*ilv3a*$^{+/-}$)	This study
C10-1/-2	Diploid, pyrG$^{+/-}$, cnxABC$^{+/-}$, niaD$^{-/+}$, Ku80$^{-/-}$, Afua_2g16600$^{+/-}$ (*pol3*$^{+/-}$)	This study
C11-1/-2	Diploid, pyrG$^{+/-}$, cnxABC$^{+/-}$, niaD$^{-/+}$, Ku80$^{-/-}$, Afua_2g16710$^{+/-}$	This study
C12-1/-2	Diploid, pyrG$^{+/-}$, cnxABC$^{+/-}$, niaD$^{-/+}$, Ku80$^{-/-}$, Afua_3g04210$^{+/-}$ (*fas2*$^{+/-}$)	This study
D2-1/-2	Diploid, pyrG$^{+/-}$, cnxABC$^{+/-}$, niaD$^{-/+}$, Ku80$^{-/-}$, Afua_3g07170$^{+/-}$ (*gpi2*$^{+/-}$)	This study
D3-1/-2	Diploid, pyrG$^{+/-}$, cnxABC$^{+/-}$, niaD$^{-/+}$, Ku80$^{-/-}$, Afua_3g08080$^{+/-}$ (*mrpl49*$^{+/-}$)	This study
D4-1/-2	Diploid, pyrG$^{+/-}$, cnxABC$^{+/-}$, niaD$^{-/+}$, Ku80$^{-/-}$, Afua_3g08470$^{+/-}$ (*zwf1*$^{+/-}$)	This study
D5-1/-2	Diploid, pyrG$^{+/-}$, cnxABC$^{+/-}$, niaD$^{-/+}$, Ku80$^{-/-}$, Afua_3g08840$^{+/-}$ (*cop1*$^{+/-}$)	This study
D6-1/-2	Diploid, pyrG$^{+/-}$, cnxABC$^{+/-}$, niaD$^{-/+}$, Ku80$^{-/-}$, Afua_3g09960$^{+/-}$ (*aur1*$^{+/-}$)	This study
D7-1/-2	Diploid, pyrG$^{+/-}$, cnxABC$^{+/-}$, niaD$^{-/+}$, Ku80$^{-/-}$, Afua_3g10450$^{+/-}$	This study
D8-1/-2	Diploid, pyrG$^{+/-}$, cnxABC$^{+/-}$, niaD$^{-/+}$, Ku80$^{-/-}$, Afua_3g12290$^{+/-}$ (*dib1*$^{+/-}$)	This study
D9-1/-2	Diploid, pyrG$^{+/-}$, cnxABC$^{+/-}$, niaD$^{-/+}$, Ku80$^{-/-}$, Afua_3g12300$^{+/-}$ (*rpl22a*$^{+/-}$)	This study
D10-1/-2	Diploid, pyrG$^{+/-}$, cnxABC$^{+/-}$, niaD$^{-/+}$, Ku80$^{-/-}$, Afua_4g04040$^{+/-}$ (*pptb*$^{+/-}$)	This study
D11-1/-2	Diploid, pyrG$^{+/-}$, cnxABC$^{+/-}$, niaD$^{-/+}$, Ku80$^{-/-}$, Afua_4g04630$^{+/-}$ (*yip1*$^{+/-}$)	This study
D12-1/-2	Diploid, pyrG$^{+/-}$, cnxABC$^{+/-}$, niaD$^{-/+}$, Ku80$^{-/-}$, Afua_4g06890$^{+/-}$ (*erg11a*$^{+/-}$)	This study

Table S3.2: Experimental indexing sequences used in this study

Indexing Sequences
CGTGAT
ACATCG
GCCTAA
TGGTCA
CACTGT
ATTGGC
GATCTG
TCAAGT
CTGATC
AAGCTA
GTAGCC
TACAAG
ATCACG

Table S3.3: Unique strain identifier

Strain	Gene ID	Unique Identifier
A2-1	AFUA_1G04840	CAGGCACTCATCTCGTTCAA
A3-1	AFUA_1G05830	CGTCTTGGATCATCGACCTT
A4-1	AFUA_1G09690	TGGACTCGACCCTTATTTGG
A5-1	AFUA_1G11730	AGGATGGAGTAGCAGGCAGA
A6-1	AFUA_1G13100	CCGATCTCGTTGACCATTCT
A7-1	AFUA_1G13200	TCGCTTCTTCGTCTCCTCAT
A8-1	AFUA_1G13420	CATGGTCGATGTGAAACCTG
A9-1	AFUA_1G13790	TGGTCGAGATGACGAAAGTG
A10-1	AFUA_1G13910	AAACTGTCGCCCATTCACTC
A11-1	AFUA_1G14740	GAAGGTGTTGTGTCGGGTCT
A12-1	AFUA_2G01330	GCACTAACCTGCAGCATTCA
B1-1	AFUA_2G01570	GTCGCTCTGCCATCTAAACC
B2-1	AFUA_2G02510	GCGTCACCGTAAGAAAGGAG
B3-1	AFUA_2G03310	CTTTCTTTGGGGAGGGAAAC
B4-1	AFUA_2G03640	AGTGCCTGACTGCTTTTGGT
B5-1	AFUA_2G05510	CAGCTCCTTAATTCGCAAGG
B6-1	AFUA_2G05820	GGATCGTCTTGCTGAGAAGC
B7-1	AFUA_2G06060	GGAAGTGGGGAGAACTAGGC
B8-1	AFUA_2G06150	GATGAGAGCGATGGGAAGAG
B9-1	AFUA_2G08550	GCAAGCCTTGACTGGATCTC
B10-1	AFUA_2G08860	ACCAGCTTACCACCAACGAC
B11-1	AFUA_2G09060	ATCTGGACAACGCGAATACC
B12-1	AFUA_2G10300	TCGAGCTTGGCTTCTGGTAT
C1-1	AFUA_2G10870	AGCAGGAAACCAAGGGAGAT

C2-1	AFUA_2G11010	CGTCAAAGATCGACACATGG
C3-1	AFUA_2G11240	GGCGGTGAGTGATTGACATA
C4-1	AFUA_2G11810	TCAGAGAGGTGCGATGATTG
C5-1	AFUA_2G12250	TACATGGAGGGGATGCTTTC
C6-1	AFUA_2G12370	CGTAGGGGTTGGGTAAAGGT
C7-1	AFUA_2G13450	GCCAAAGGACACAGAAAAGC
C8-1	AFUA_2G16040	TGAAGAGTCCACCGCCTACT
C9-1	AFUA_2G16300	CCAGGCAGAGAGAAAGGATG
C10-1	AFUA_2G16600	ATTCGGGAAGTCGTGTTCTG
C11-1	AFUA_2G16710	CTTCCTTTTCAGCCTTGACG
C12-1	AFUA_3G04210	TGAAAGGTATAGGCGGCAAC
D2-1	AFUA_3G07170	GTGGCGCTAAAATACCTGGA
D3-1	AFUA_3G08080	GCTGGGTTGGACTTGTTGTT
D4-1	AFUA_3G08470	GCGAGGCAGAACTATGGAAG
D5-1	AFUA_3G08840	AAGGGTTGTGTGGCTACGTC
D6-1	AFUA_3G09960	GAGGAAGGGCGAGAAGAGTT
D7-1	AFUA_3G10450	GCTGCAATCAAGAGGCTACC
D8-1	AFUA_3G12290	GGGTAGTGTAAGCCCGATGA
D9-1	AFUA_3G12300	TCGCTAGCAGTGGAGTCTCA
D10-1	AFUA_4G04040	GGTCCTCAGGGGAAGATAGC
D11-1	AFUA_4G04630	TAGTCAGACAGCCCCAGCTT
D12-1	AFUA_4G06890	ACTTTCATTCGGCTCAGCAC

Table S3.4: Real-time PCR primers used to quantify strain abundance in parallel fitness studies.

Heterozygous Gene Name	Primer Name	Primer Sequence
arf2$^{+/-}$	AFUA_1g11730_RT	5’-TTCCAACACCGACAAAACAAG-3’
alg7$^{+/-}$	AFUA_2g11240_RT	5’-CCAGGTTGATTCGACTGGAT-3’
erg11a$^{+/-}$	AFUA_4g06890_RT	5’-TTCTGAAACACGTGCGTAGC-3’
mrpl49$^{+/-}$	AFUA_3g08080_RT	5'-GACGCCCATCAACAACAAGT-3'
atp17$^{+/-}$	AFUA_2g05510_RT	5’-GCGTCTCCTTGCGAATTAAG-3’
mot1$^{+/-}$	AFUA_1g05830_RT	5'-TGACCTCGAGAGGAGGAAAA-3'
fmn1$^{+/-}$	AFUA_2g05820_RT	5'-TTCTAACCCGTCGTGACTCC-3'
	AnidpyrG_RT	5’-CTATGGCGTGATAGCGTTGA-3’

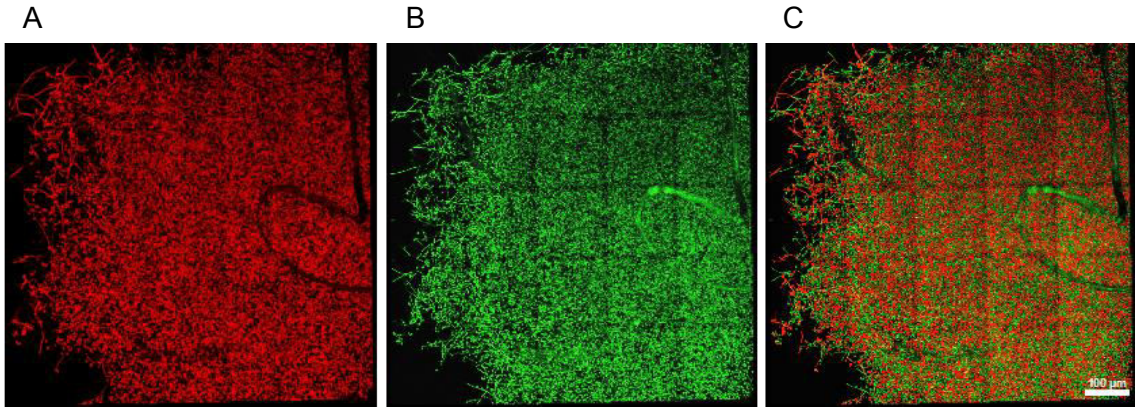

Figure S3.2: Shake flask co-culture of nitrogen starved RFP and GFP expressing strains (AfRFPcnx and AfGFPniaD) in liquid AMMNO3 medium. Images are merged z-stacks demonstrating the lack of co-localisation of GFP and RFP of a co-inoculated culture after 48 hours (731 mm^2 area over a depth of 6.4 µm). Figures A, B and C show the red (RFP expressing strain), green (GFP expressing strain) and merged channels respectively

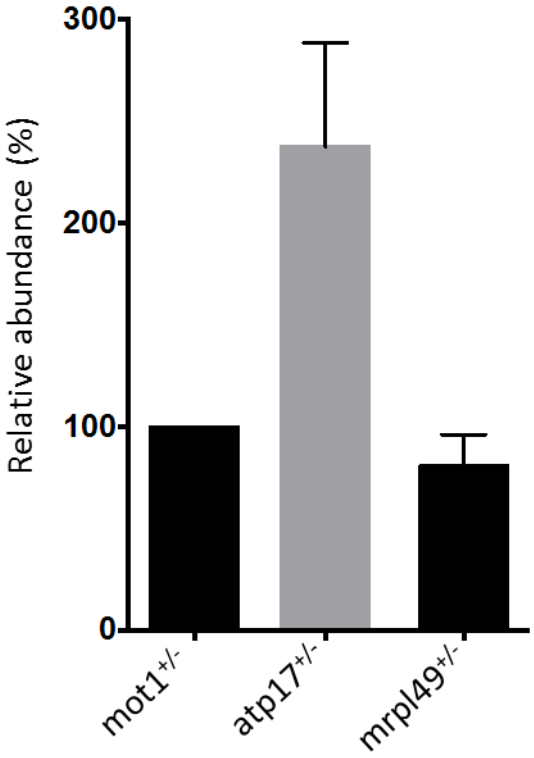

Figure S3.3: Real-time PCR quantitative analysis of the DNA analysed by en mass sequencing. A) DNA isolated from cultures inoculated with freshly prepared spore stocks grown in the presence of brefeldin A. *mrpl49*$^{+/-}$ no longer shows enhanced abundance however *atp17*$^{+/-}$ does. Analyses were made using mot1$^{+/-}$ as the reference strain. Error bars represent standard deviation.

Chapter 4

Exploring the *Aspergillus fumigatus* phosphatome for potential drug targets

Anna Johns, Lydia Tabenero and Mike Bromley

4. Exploring the *Aspergillus fumigatus* phosphatome for potential drug targets

Anna Johns, Lydia Tabenero and Mike Bromley.

Abstract

Aspergillus fumigatus is the leading cause of invasive aspergillosis a fungal disease which poses as a serious threat to patients with a weakened immune response due to disorders such as leukaemia, HIV, AIDS and also persons undergoing chemotherapy treatments. In *Aspergillus fumigatus* and all other fungal species phosphatase mediated reversible protein phosphorylation is an important regulatory mechanism of cell cycle and homeostasis maintenance. Therefore phosphatase genes are considered to be an attractive target for novel drugs. In this study we used an ontology based classification tool and published literature to identify 38 phosphatases in the genome of *A. fumigatus*. Bioinformatic analysis allowed the identification of several fungal specific enzymes. Deletion strains were generated for all phosphatase genes and phenotypic analysis was carried out. A method to assess parallel fitness using next generation sequencing was validated and used to identify strains exhibiting reduced fitness. Our analyses show there are three candidates; NimT, NemA and PtcB, which have the potential of becoming novel antifungal targets for the pathogen *A. fumigatus.* These phosphatases have both significant effects on fungal fitness but are also highly divergent from human proteins.

4.1. Introduction

Aspergillus fumigatus is a filamentous, opportunistic fungal pathogen. It is the leading cause of aspergillosis, an invasive fungal disease that can see mortality rates of up to 95% even after treatment (1). The risks associated with current medications such as adverse side effects in patients, drug-drug interactions and increasing antifungal resistance (2) have made it necessary for a novel class of drugs to be discovered. The availability of the *A. fumigatus* genome makes it possible to analyse whole gene families with the aim to identify new antifungal targets.

Cycles involving phosphorylation and dephosphorylation post-translational modification occur in eukaryotes as a mechanism to deal with internal or external cellular signals (3). These cycles can result in different reversible cellular processes such as; signal proliferation, differentiation or cell arrest (4). In filamentous fungi these cellular processes could play an important role in secondary metabolism, virulence and pathogenic development. Phosphorylation and dephosphorylation are mediated by kinases and phosphatases respectively.

Protein phosphatases are structurally and mechanistically evolutionary distinct (5). Based on substrate specificity they have been grouped into two families, the serine/threonine phosphatases (STP) including aspartate based catalysis phosphatases and the tyrosine-specific phosphatases (PTP) (6) (Figure S4.1).

STPs share very high similarity at the catalytic centre although they have very poor amino acid sequence homology (7) and can be grouped based on whether they require metal-ions as well as their substrate specificity (7, 8). Three distinct families have been classified; phosphoprotein phosphatases (PPPs), metal-dependent protein phosphatases (PPMs) and aspartate based phosphatases (FCP/SCP). Classical PPPs are involved in chromosome condensation, chromatid cohesion and immune response (9-12). PPMs are dependent on Mg^{2+}/Mn^{2+} and are made up of PP2C type phosphatases. Aspartate based phosphatases are defined by a signature motif DXDXT/V found in their catalytic domain. They include; FCP, SCP and the mammalian protein Dullard which all show catalytic activity towards the TFIIF-interacting C-terminal domain of RNA polymerase II. Dullard phosphatases are also included in this group.

Protein tyrosine phosphatases are the largest family of protein phosphatases, recognised by a conserved CX_5R motif located in the catalytic domain. All members perform nucleophilic attacks on the targeted phosphate group via a catalytic cysteine residue (6). As a diverse family of proteins they can be further divided into subfamilies which include the classical PTPs, low molecular weight PTPs (LMW-PTP), dual specificity PTPs and Cdc25 phosphatases. PTPs have

roles in cell adhesion, cytokinesis, PIP_3 signalling, mitosis regulation as well as many unknown functions (5, 9, 13, 14).

Protein phosphatases are becoming more recognised as attractive targets for novel drugs with many PTPs, DSPs and lipid phosphatases being studied as potential targets for the treatment of diabetes, obesity and cancer (6, 15, 16). However the only FDA approved phosphatase targeting drugs are cyclosporine A and FK506 which both inhibit the PPP phosphatase, PP2B, and cause immunosuppression (6). As well as in human disease potential phosphatase targets are also being identified in pathogens. Three phosphatases in Mycobaterium tuberculosis have shown to be essential for pathogen virulence. These include; *ptpA* involved in V-ATPase trafficking inhibition and phagosome-lysosome fusion blocking; *ptpB* which promotes host cell survival by activating the Akt pathway and also blocks p38 mediated IL-6 and ERK1/2 production (17, 18) and *sapM* which inhibits the production of phosphatidylinositol 3-phosphate (PI3P), vital for phagosome biogenesis (19). *Yersinia pestis,* the pathogen responsible for bubonic plague, encodes a PTP (YopH) responsible for inhibition of phagocytosis, production of reactive oxygen species and cytoskeletal rearrangements, abolishment of this gene leads to avirulence *in vivo* (20). LipA a lipid and tryrosine phosphatase found in *Listeria monocytogenes,* the pathogen causing listeriosis infection, has an unknown function but causes drastically reduced pathogenicity *in vivo* (21). The causative agent of African sleeping sickness, *Trypanosoma brucei,* possesses a phosphatase Ptp1 that prevents sporadic differentiation of life cycle forms which is vital for transmissibility of the parasite (22).

This study will exploit the knowledge on domain structure and conserved catalytic signatures to identify all the protein phosphatases in *Aspergillus fumigatus.* Deletion of each phosphatase will allow us to identify the effect on growth and virulence in an attempt to identify novel drug targets. We present a pooled fitness technique in *Aspergillus fumigatus* similar to an approach taken in *S. pneumoniae* (23) that will allow us to quantitatively measure growth rate of all phosphatase deletion strains by the use of next generation sequencing. During the preparation of this manuscript work was published by another research group which also explores the phosphatases of *A. fumigatus* (24, 25), similarities and/or differences between our data set and theirs will be deliberated in the discussion section.

4.2. Materials and Methods

4.2.1. Bioinformatics

A classification tool, based on knowledge of conserved phosphatase motifs (26), was used to identify and classify phosphatases in *A. fumigatus*, *A. niger*, *A. nidulans*, C. albicans and *S. cerevisiae*. Each protein identified was inspected to discover any false positives. For all species, literature searching and NCBI BLASTp analysis (http://blast.ncbi.nlm.nih.gov/blast) against well classified phosphatases allowed the identification of further phosphatases.

4.2.2. Phylogenetic Analysis

Phosphatase protein sequences for *Aspergillus spp* were taken from the Aspergillus genome database (http://www.aspgd.org), *S. cerevisiae* sequences were obtained from Saccharomyces genome database (http://www.yeastgenome.org), *C. albicans* sequences from the Candida genome database (http://www.candidagenome.org), the human sequences were obtained from DEPOD - the human DEPhOsphorylation Database (version 1.1) (http://www.koehnlab.de/depod/index.php). Phosphatase domain analysis was carried out using InterPro: protein sequence analysis & classification (http://www.ebi.ac.uk/interpro/). MEGA6 software was used to generate phylograms. This software uses ClustalW to perform the alignment. Maximum likelihood method was used to convey evolutionary links, with 1000 bootstrap replicates.

4.2.3. Phosphatase knockout generation

Gene knockout cassettes were generated using a modified PCR fusion approach (27, 28) (figure S4.2). Approximately 1 kb of 5' and 3' flanking regions of gene of interest were amplified by PCR from fungal genomic DNA using long amp DNA polymerase. All primers can be found in table S4.1. Primers P1 and P2 were used to amplify the 5' and P3 and P4 were used to amplify the 3' non-coding regions of the gene. The hygromycin B phosphotransferase resistant gene (hph) was amplified from pAN7-1 (29) incorporating P2 and P3 overhangs for preparation of all deletion constructs. Additionally a mme1 restriction enzyme site was incorporated into fusion primer P3 for downstream NGS library preparation. PCR primer design software Primer 3 (http://frodo.wi.mit.edu/) was used to aid primer design and all primers were supplied by Eurofins MWG Operon. The process consists of 3 rounds of PCR reactions previously published by Frazeck, *et al* (2013).

A. fumigatus mycelia were treated with 5% Glucanex (Novozymes) solution (made up in 0.6M KCl/50mM $CaCl_2$ solution) for 2–3 h at 30°C to produce protoplasts. DNA was transformed into protoplasts by PEG-mediated transformation. 200µg/ml hygromycin was used for selection.

To confirm the success of the gene knockout, diagnostic PCR reactions were performed on DNA extracted from purified transformant isolates. The purified null mutant DNA was isolated and checked to ensure the selective marker gene had been inserted into the correct location. It involved two PCR reactions: i) amplification across the 5' flanking region and selective marker gene; ii) amplification across the 3' flanking region and selective marker gene (figure S4.3).

4.2.4. Parallel Fitness Profiling

Equal numbers of spores of each strain were pooled and grown in 50 ml cultures of liquid vogels minimal media (VMM) (30) (final inoculum of 2.5×10^5 spores/ml). The cultures were grown at 200 rpm for 48 hours and total DNA was extracted from the biomass using an optimised cetyl trimethyl ammonium bromide (CTAB) method. Fungal mycelia were snap frozen in liquid nitrogen and ground to a fine powder using a pestle and mortar. The mycelial powder was then transferred to a screw cap tube, resuspended in an equal volume of extraction buffer (2% CTAB, 100 mM Tris, 1.4 M NaCl and 10 mM EDTA, pH 8.0) and incubated for 10 min at 65°C. DNA extraction was then performed previously described (27). For the T0 samples, DNA was extracted from the original pooled spore stock by resuspending spores in 1ml extraction buffer (2% CTAB, 100 mM Tris, 1.4 M NaCl and 10 mM EDTA, pH 8.0) and transferring to a screw cap tube containing glass beads. 6 cycles of bead beating using mpbio fastprep instrument, followed by incubation for 10 min at 65°C were applied to the samples. DNA extraction was then performed as previously described (27).

4.2.5. NGS library preparation

100 µg DNA was digested using type 2 restriction enzyme mme1, each reaction contained 30 µl DNA, 1 x CutSmart™ Buffer, 50 µM S-adenosylmethionine and were incubated at 37°C for 2 hours. Reactions were then heat inactivated for 20 minutes at 65°C. To prevent re-ligation 5' phosphate group was removed by the addition of 1 unit of shrimp alkaline phosphatase (NEB) and incubate at 37°C for 30 minutes. DNA was column purified using a QIAquick PCR purification kit following the manufacturer's instructions and eluted in 30 µl of molecular grade H_2O. Paired-end adapter oligonucleotides PEad1 (5' PHO-AGATCGGAAGAGCGGTTCAGCAGGAATGCCGAG) and PEad2 (5' ACACTCTTTCCCTACACGACGCTCTTCCGATCTnN) were annealed in a 100 µl reaction containing 1 x annealing buffer (10 mM Tris pH 7.5, 50 mM NaCl, 1 mM EDTA) and 15 µM of each adapter oligonucleotide. This was incubated at 95°C for 2 min then ramped to 25°C over 45 minutes. These annealed adapters were ligated to the digested DNA fragments in a 50 µl reaction containing 10 µl of DNA sample, 1× Quick DNA ligase buffer, 5 µl of annealed adapter oligonucleotide mixture, 1 µl of Quick T4 DNA ligase (NEB) and incubated at 14°C overnight.

Ligated samples were diluted (1in20) and used in a first round PCR enrichment reaction containing; diluted ligated DNA, 1 x LongAmp *Taq* reaction buffer, 300µM dNTPs, 0.2µM AdaptF (ATCGTTGGTGTCGATGTCAG),0.2µM AdaptR (GCATTCCTGCTGAACCGCTC) and 5 units LongAmp *Taq* DNA polymerase. PCR reaction involved a hot start of 95°C for 2 min followed by 35 cycles of denaturing (95°C for 15 seconds), annealing (58°C for 20 seconds) and elongation (68°C for 40 seconds), finally an elongation step of 68°C for 5 min was performed. PCR products (368bp) were column purified using a QIAquick PCR purification kit following the manufacturer's instructions and eluted in 30 µl of molecular grade H_2O. A second round of PCR enrichment followed using primers PEmme2.0 (5'-CCTCTCTATGGGCAGTCGGTGATCTCGGCATTCCTGCTGAACCGCTCTTCCGATCT-3') and PE1mme1 (5'- CCATCTCATCCCTGCGTGTCTCCGACTCAGNNNNNNNNNNGATAGCAGATCAACGGTCGTCAAGA GCTCTGA-3') where NNNNNNNNNN denotes the unique index that identifies the condition of the experiment and facilitates pooling of the DNA from multiple cultures. The indexing sequences used in this study can be found in table S4.2. The PCR amplification conditions are the same as round 1. PCR products were gel purified using a QIAquick Gel Extraction Kit following the manufacturer's instructions and DNA bands of 145bp were excised from the gel. Figure 4.1 shows a schematic for this process.

All DNA samples were quantified and normalised to 0.03ng/ul in molecular grade water. The samples were pooled in equal volumes into one tube and mixed thoroughly by vortexing. Purified and pooled barcoded libraries were stored at -20 until required.

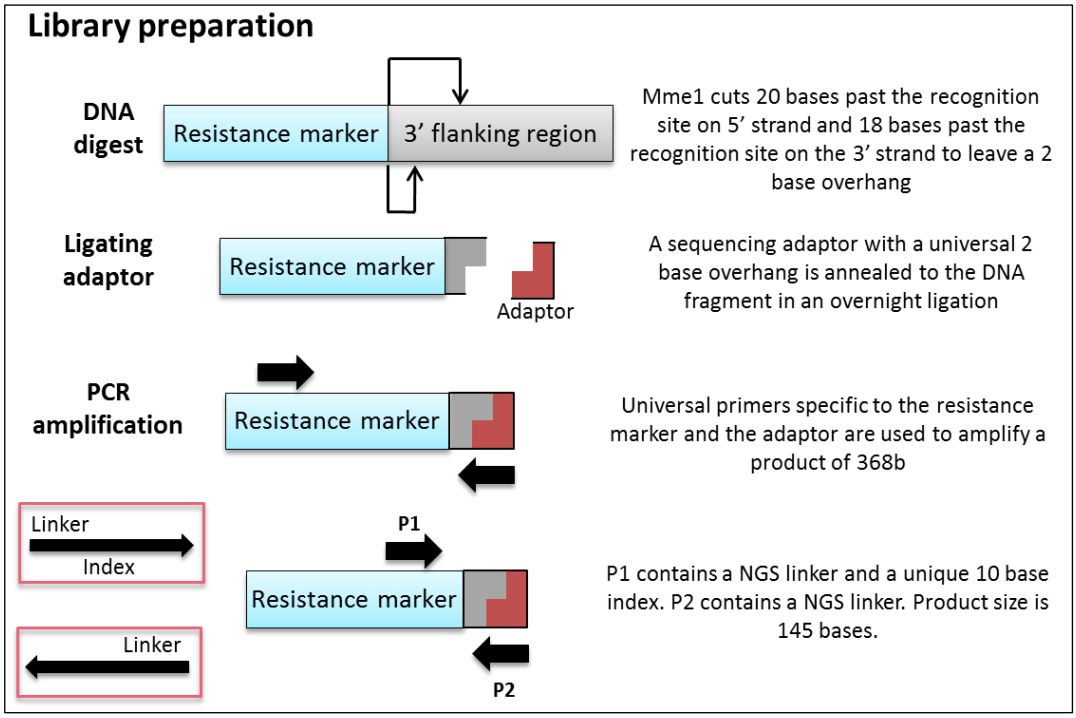

Figure 4.1: Schematic of DNA preparation for NGS.

4.2.6. Ion Personal Genome Machine (PGM) system preparation

The barcoded library underwent emulsification to create a microreactor containing a single DNA fragment, 1 ion sphere particle (ISP) and PCR reagents. Emulsion PCR is used to amplify the DNA fragment millions of times so that each ISP contains millions of copies of the same fragment. An ION PGM Template OT2 200 Kit (Life Technologies™) and a One Touch 2 System was used according to manufacturing guidelines. The positive ISPs then underwent quality control using an ION PGM Quality Control Kit (Life Technologies™) and a Qubit Fluorometer to assess the percentage of template ISPs according to manufacturing guidelines. 2 probes are used Alexa Fluor 488 which binds to all ISPs and Alexa Fluor 647 which binds to the attached DNA fragment. The ratio of Alexa Fluor 647 fluorescence (template ISPs) to Alexa Fluor 488 fluorescence (all ISPs) gives the total percentage of template ISPs. The optimum level of Templated ISPs for sequencing is 10-30%.

Next the template positive ISPs were enriched by removing non-template ISPs using an ION PGM Template OT2 200 Kit (Life Technologies™), Dynabeads MyOne Streptavidin C1 beads (Life Technologies™) and an Ion OneTouch ES machine according to manufacturing guidelines.

The Ion PGM system was cleaned and initialised using ION PGM Sequencing 200 Solutions Kit (Life Technologies™), ION PGM Sequencing Reagents 200 Kit (Life Technologies™) and a Cleaning Chip (Life Technologies™) according to manufacturing guidelines. A sequencing primer and Ion PGM Sequencing 200 polymerase (Life Technologies™) were added to the positive ISP solution before it was loaded on a 318 Chip V2 (Life Technologies™). The 318 Chip V2 was then placed in the Ion PGM system and calibrated before a 16S Targeted Sequencing with 500 flows protocol was applied to sequence the DNA fragments.

4.2.7. NGS data processing

Ion PGM technology sorts sequenced reads according to the 10bp unique index and organises the sequences in FASTQ files ready to be exported. Each strain possesses a unique strain identifier of 15bp (table S4.3), FASTX-Toolkit FASTQ/A Trimmer (http://hannonlab.cshl.edu/fastx_toolkit/) was used to trim away the adaptors leaving only the unique strain identifier. Sequence reads were mapped to the set of unique gene identifiers with the program Bowtie (31). Bowtie parameters were set such that reads could contain 3 mismatches. Counts for each gene identifier were calculated. Data was normalised by equalising to the total number of sequenced reads per condition. The pairwise comparisons; Pearson correlation and coefficient of determination were calculated between each technical and biological replicate using Microsoft Excel software. Counts for each strain were subsequently normalised to counts from T=0 and then Log2 values were calculated using

Microsoft Excel software and plotted into an aligned scatter graph using GraphPad Prism 6 software.

4.2.8. Individual growth rate assessment

The knock out strains were grown on VMM in filtered culture flasks at 37°C, after 5-7 days growth the spores were harvested and counted. The spore suspensions from each strain were added to liquid VMM and dispensed into individual wells in a 96 well plate to give a final concentration of $5x10^4$ conidia per well. The plate was sealed with a "Breathe Easy" covering membrane (Sigma-Aldrich) and placed on a microplate scanning spectrophotometer (BIO TEK® Synergy HT). The temperature was set at 37°C and KC4 v3.02 software was used to measure the optical density at 600nm every 10 minutes over a 48 hour time period. Fungal growth was determined by calculating the velocity of the linear phase of the growth curve. The average of 3 replicates was used to derive the mean for each strain and data was normalised to the average growth rate from all strains. The Log2 values were calculated using Microsoft Excel software and plotted into an aligned scatter diagram using GraphPad Prism software.

$1x10^4$ spores from each strain as well as the parental strain (A1160p+) were spotted VMM agar and incubated for 4 days at 37°C. Horizontal and vertical diameter measurements were taken daily. Growth rates were calculated and normalised to the mean growth rate. The Log2 values were calculated using Microsoft Excel software and plotted into an aligned scatter graph using GraphPad Prism 6 software.

4.3. Results

4.3.1. There is high similarity between phosphatase types in fungal species

Phosphatases are increasingly being recognised as potential drug targets in a range of human pathogens. As such we have explored the phosphatome of the fungal pathogen *A. fumigatus* as well as other fungal species in the hope of identifying novel fungal specific drug candidates. A classification tool, based on knowledge of conserved phosphatase motifs (26), was used to identify and classify 32 phosphatases in *A. fumigatus.* Identified proteins Pub1 (Afu1g12000) and Afu2g03420 appeared not to be phosphatases when comparing to orthologues in a range of other species. Literature searching and NCBI BLASTp analysis against well classified phosphatases allowed an additional 8 phosphatases in *A. fumigatus* to be identified giving 38 phosphatases in total. The same methodology was also applied to other fungal species and total protein phosphatases found were; 40 in *A. niger*, 36 in *A. nidulans*, 40 in *S.cerevisiae* and 37 in *C. albicans* (WO1). Each species contains a representative for each of the main classes of phosphatase; protein tyrosine (PTP), dual-specificity (DSP), phosphatase and tensin homolog (PTEN), myotubularin (MTMs) and serine/threonine (STP). It was found that the majority (>50%) of phosphatases in each species belonged to the STP group and the least populated groups were MTM and PTEN phosphatases. This is in contrast to the types of phosphatases found in humans which have an even spread of STPs, PTPs and DSPs (figure 4.2A).

To gain a further understanding of how well conserved the phosphatase proteins are between the *Aspergillus* species, Interpro: protein sequence analysis and classification was used explore the similarity of their domain architecture (figure 4.2B). Conserved architectural structure between the phosphatases from each species was observed, however there were differences in the number of certain sub families of phosphatases. These included classic PTPs (*A. fumigatus*; 4, *A. nidulans*; 6, *A. niger;* 5), DSPs (*A. fumigatus*; 5, *A. nidulans*; 4, *A. niger;* 5), PPPs (*A. fumigatus*; 9, *A. nidulans*; 9, *A. niger*; 11) and PPMs (*A. fumigatus*; 8, *A. nidulans*; 5, *A. niger;* 6).

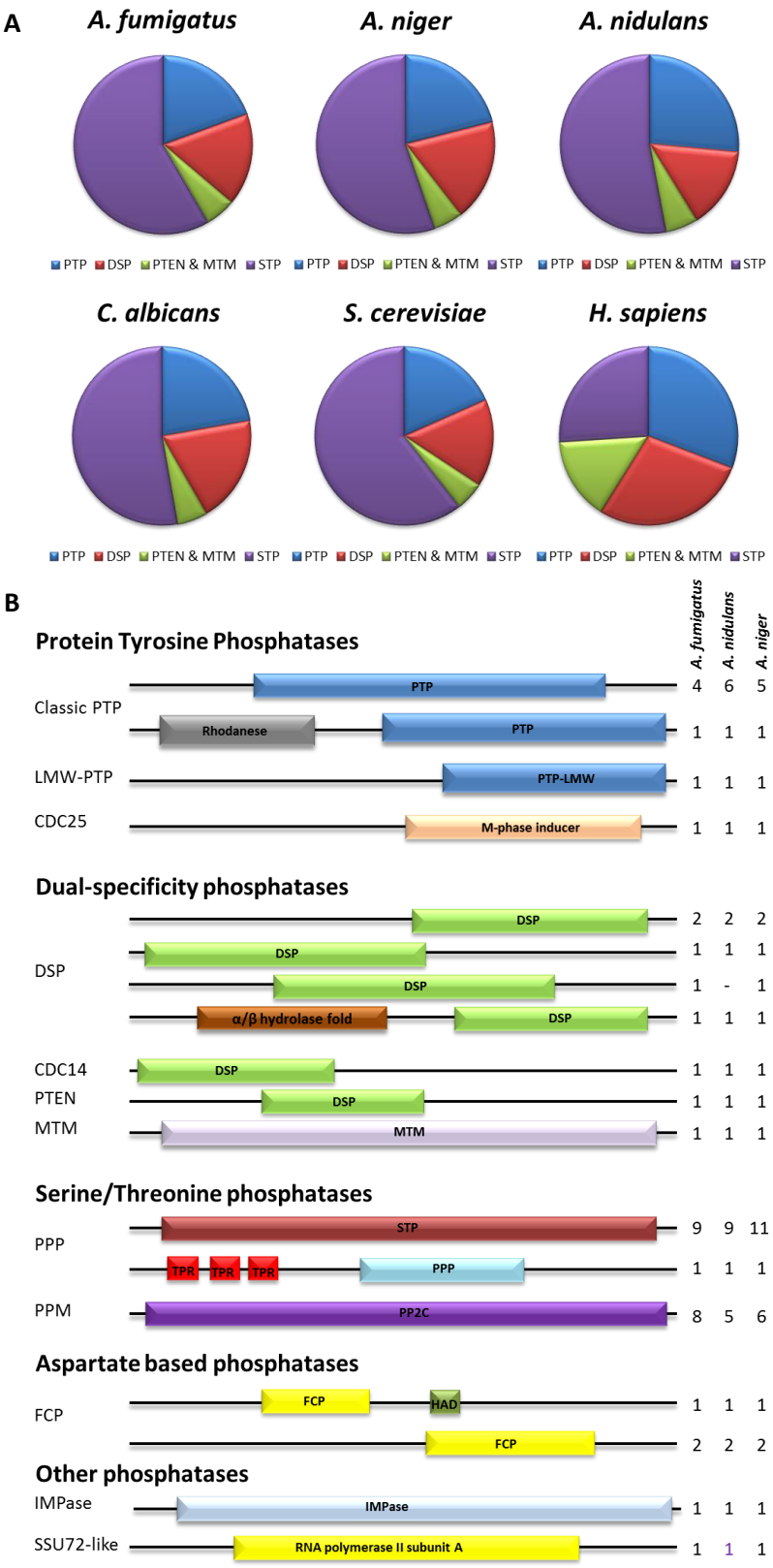

Figure 4.2: Comparison of the protein phosphatase in different fungal species. A) Pie charts to show the distribution of phosphatases in *A. fumigatus, A. niger, A. nidulans, C. albicans, S. cerevisiae and H. sapiens.* B) Domain organisation of the *Aspergilli* protein phosphatases. One domain is represented for regions where InterPro gave variations/overlaps representing the same biological role. PTP, protein tyrosine phosphatase; DSP, dual-specificity phosphatase; TPR, Tetratricopeptide repeat; HAD, HAD-superfamily phosphatases; MTM, myotubularin; PTEN, phosphatase and tensin homolog; IMPase, inositol monophosphatase.

4.3.2. Fungal specific phosphatase groups are found in many phosphatase families

Ideally a fungal specific drug target will show significant divergence from any host orthologue to avoid cross inhibition with the target. In the hope of identifying similarities and differences between human and fungal phosphatases and more precisely fungal specific groupings we have constructed a series of phylogenetic trees using phosphatase protein sequences from *A. fumigatus, A. nidulans, A. niger, S. cerevisiae, C. albicans* and *H. sapiens*. In the majority of clades found in the constructed phylograms the human phosphatases cluster together as do the *Aspergilli* proteins. The yeast species; *S. cerevisiae* and *C. albicans* also commonly group together.

4.3.2.1. Phosphoprotein Phosphatases (PPP)

The PPP phylogram can be separated into 8 subfamilies which are clearly displayed as separate clades (figure 4.3). The majority of clades contain representatives from each fungal species, however there are no fungal phosphatase representatives found in the PPEF (PP7) clade. This is confirmed as the domain analyses revealed no PPPs containing EF-hands (a domain typically found in PPEF phosphatases) in the *Aspergillus* phosphatases (figure 4.2B), furthermore BLASTp analysis between the human PPEF phosphatases and the fungal genomes revealed no PPEF-like orthologues. More importantly for this study we have identified 2 clusters of *Aspergillus* specific phosphatases which could be potential *Aspergillus* specific drug targets. The long branch-lengths of the phosphatases in this group show that they have diverged far more through evolution than the others. All phosphatases within these groups have yet to be characterised but they all have predicted phosphatase domain architecture (figure 4.2B). Each cluster contains 1 phosphatase per *Aspergillus spp.* BLASTp analysis using the *A. fumigatus* protein (Afu5g08620) from cluster I identifies the human phosphatase, PPEF1 as the closest match although there is very low conservation (25% identity, 34% coverage). The second cluster contains the *A. fumigatus* protein (Afu1g14840), which shows no similarity to any human protein.

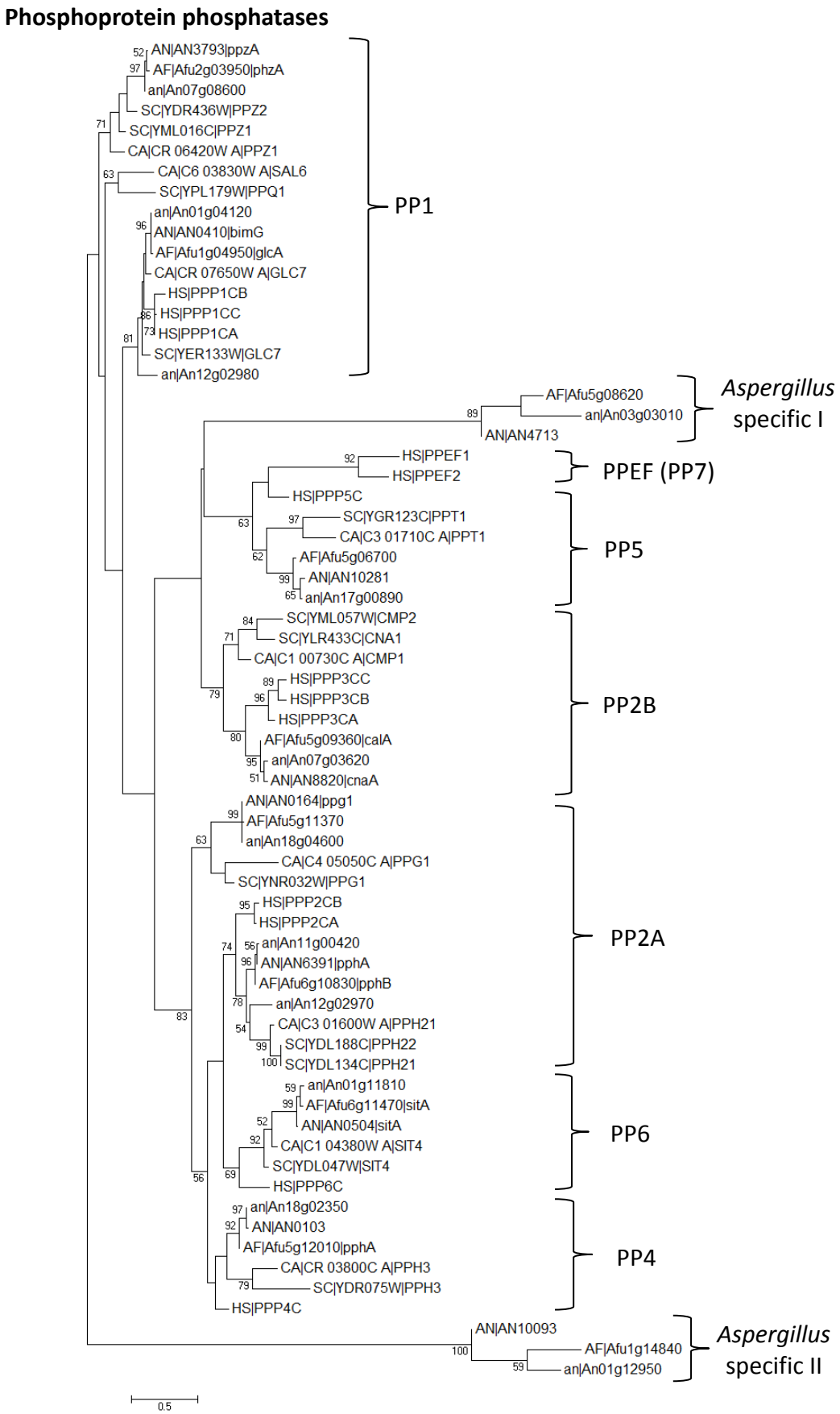

Figure 4.3: Phylogram of PPP. The evolutionary history was inferred using the Maximum Likelihood method based on the JTT matrix-based model. The bootstrap consensus tree inferred from 1000 replicates is taken to represent the evolutionary history of the taxa analysed (*A. fumigatus* (AF), *A. niger* (an), *A. nidulans* (AN), *S. cerevisiae* (SC), *C. albicans* (CA), *Human* (HS). Evolutionary analyses were conducted in MEGA6.

4.3.2.2. Metal-dependent protein phosphatases (PPM)

The second category of serine/threonine phosphatases are PPM which are dependent on Mg^{2+}/Mn^{2+} and they all contain the PP2C domain. There are several clusters of fungal phosphatases (figure 4.4). Clusters I-IV contain representatives from all fungal species as well as human. Again the *Aspergillus* phosphatases appear to be closely related within each cluster however cluster III reveals significant evolutionary divergence between the *Aspergillus* species with 3 phosphatase representatives from *A. fumigatus* (PtcH, PtcD and PtcE) and 1 uncharacterised phosphatase from both *A. niger* and *A. nidulans*. Interestingly there are 2 fungal specific clusters found in this phylogram. Fungal specific cluster I contains phosphatase PtcA from *A. fumigatus* which shares some sequence conservation with the human protein PPM1K (36% identity, 20% coverage) as well as PTC6 from *C. albicans* and *S. cerevisiae*. Cluster II contains PtcF from *A. fumigatus* which shows similarity to the human protein PDP1 (31% identity, 70% coverage), PTC5 from *C. albicans* and *S. cerevisiae,* 2 uncharacterised phosphatases from *A. niger* and 1 from *A. nidulans.*

4.3.2.3. Aspartate based phosphatases

Aspartate based phosphatases contain FCP, SCP and Dullard phosphatases. The tree can be separated into 3 clades (figure S4.4). A single representative from each fungal species is found in the Dullard and FCP clade. The SCP clade contains 2 phosphatases from *S. cerevisiae*, PSR1 and PSR2 which have derived from a gene duplication event and 1 each from the remaining fungal species. There are no fungal specific clusters found in this sub-family of phosphatases.

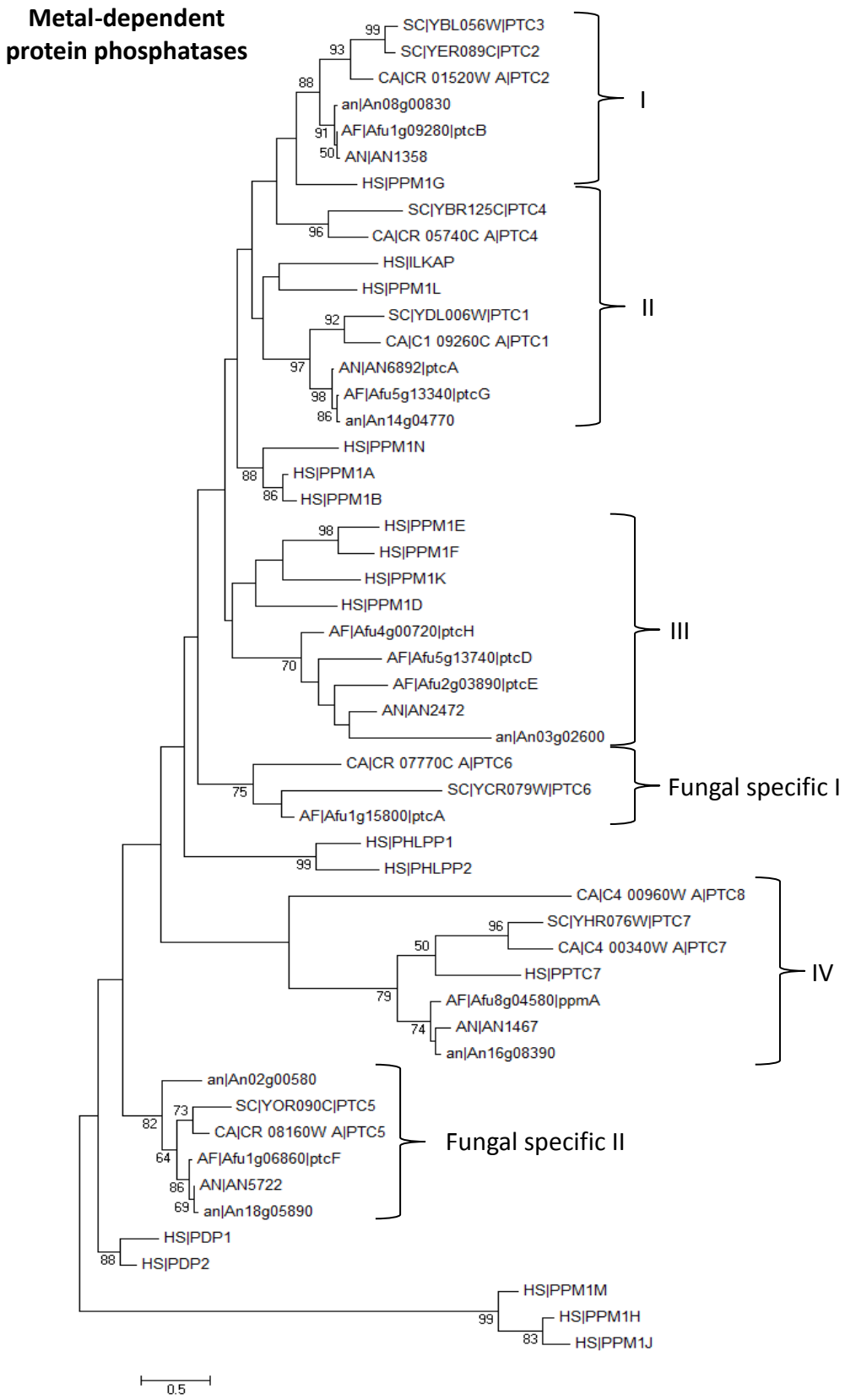

Figure 4.4: Phylogram of PPM. The evolutionary history was inferred using the Maximum Likelihood method based on the JTT matrix-based model. The bootstrap consensus tree inferred from 1000 replicates is taken to represent the evolutionary history of the taxa analysed (*A. fumigatus* (AF), *A. niger* (an), *A. nidulans* (AN), *S. cerevisiae* (SC), *C. albicans* (CA), *Human* (HS). Evolutionary analyses were conducted in MEGA6.

4.3.2.4. Protein tyrosine phosphatases (PTP)

Protein tyrosine phosphatases are the largest family of protein phosphatases. They have been subdivided into 3 phylogenetic trees in this section; classic PTPs (including CDC25s and LMW-PTP phosphatases), dual specificity phosphatases (DSP) and MTM and PTEN phosphatases.

Phylogenetic analysis of PTPs has led to several distinct clades (figure 4.5). There is an *Aspergillus* clade for the CDC25 phosphatases, interestingly the *Candida* and *Saccharomyces* CDC25 are not found in this grouping indicating evolutionary divergence between fungal species. There is a human specific cluster of receptor PTPs and eyes absent phosphatases (EYAs) which contain no fungal proteins. The lack of fungal EYAs phosphatases was confirmed through reciprocal BLASTp analysis against the human EYAs, furthermore no fungal phosphatases contained EYA domains (figure 4.2B). The PTP subfamily contains 2 fungal specific clusters found in this group (I and II). Cluster I contains PtyA and Afu4g10270 from *A. fumigatus.* PtyA shows sequence conservation with the human non-receptor PTP, PTPN6 (36% identity, 12% coverage). It also appears to share a close relationship with uncharacterised proteins AN5767 and An18g06400 from *A. nidulans* and *A. niger* respectively. The uncharacterised protein from *A. fumigatus,* Afu4g10270, shares sequence conservation with the human protein; very-long-chain (3R)-3-hydroxyacyl-CoA dehydratase 2 (29% identity, 94% coverage). The second fungal specific cluster contains 1 protein from each fungal species which are all orthologues to the *S. cerevisiae* SIW14 protein. The *A. fumigatus* protein has been characterised as YphA which is similar to the human CDC14 phosphatase (27% identity, 36% coverage). The low conservation between the human proteins and *A. fumigatus* proteins found in both fungal specific clusters again prove promising for potential drug targets.

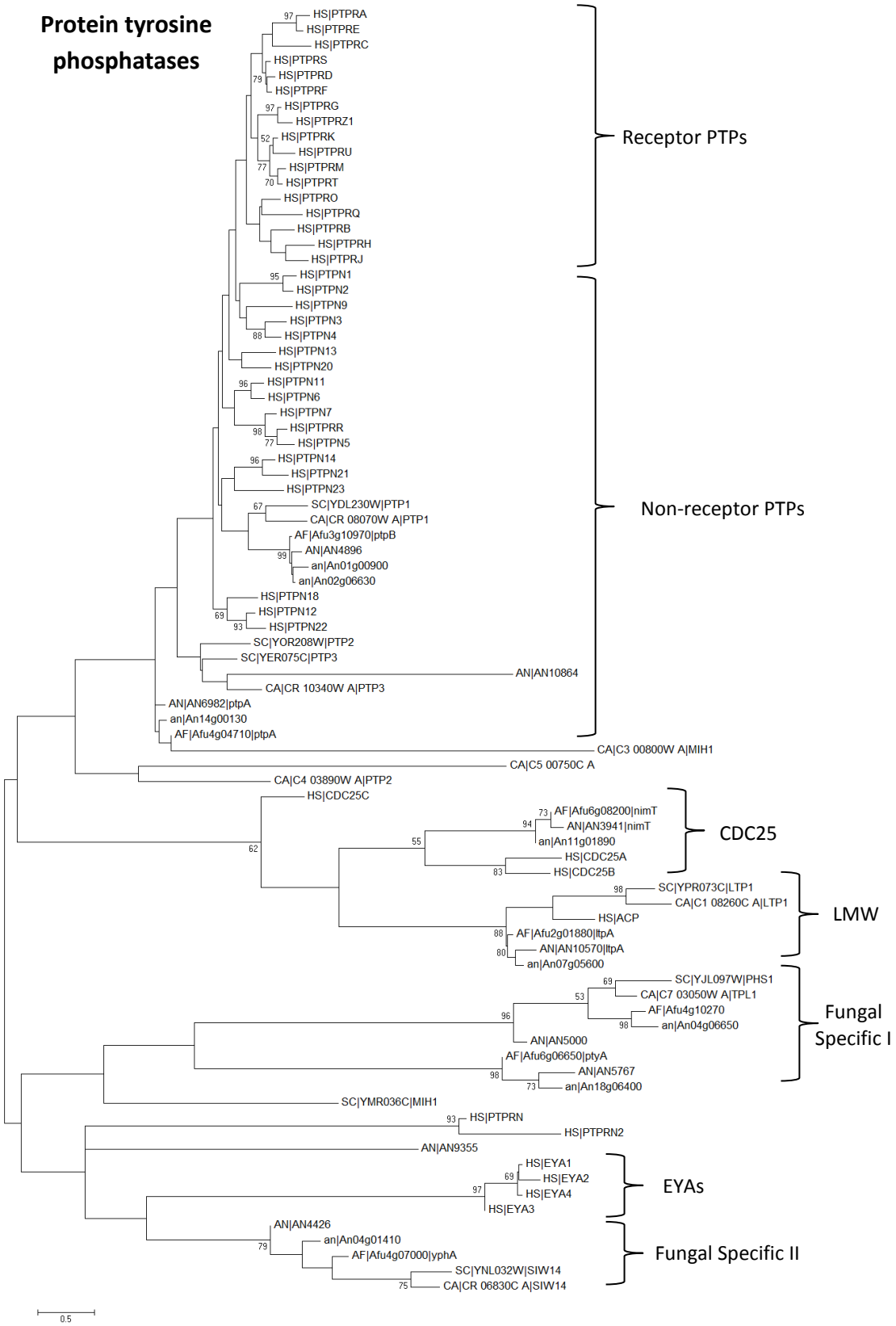

Figure 4.5: Phylogram of PTP. The evolutionary history was inferred using the Maximum Likelihood method based on the JTT matrix-based model. The bootstrap consensus tree inferred from 1000 replicates is taken to represent the evolutionary history of the taxa analysed (*A. fumigatus* (AF), *A. niger* (an), *A. nidulans* (AN), *S. cerevisiae* (SC, *C. albicans* (CA), *Human* (HS)). Classic PTP, CDC25 and LMW-PTP phosphatases were included in this analysis. Evolutionary analyses were conducted in MEGA6.

4.3.2.5. Dual-specificity phosphatases (DSP)

DSPs show specificity to tyrosine as well as serine/threonine. There are several clades included in this phylogram (figure 4.6). As seen previously the *Aspergilli* protein phosphatases show a very close relationship within each cluster, as do the *S. cerevisiae* and *C. albicans.* There are no *Aspergilli* representatives within the MKP clusters, however YVH1 from *C. albicans* and *S. cerevisiae* are found within this group. 2 out of the 3 groups of atypical DSPs contain fungal phosphatases, however the final group is human specific. There are 2 fungal specific clusters of proteins that appear evolutionary distinct from human DSPs within this phylogram. The first includes a single phosphatase from each species which are orthologues to *S. cerevisiae* PPS1. The *A. fumigatus* protein Pps1 shows low conservation with the human MKPs protein DUSP1, with an identity of only 34% (25% coverage). The second includes OCA1 from *S. cerevisiae* which has been defined as a Plant and Fungi Atypical DSPs (PFA-DSP) (32). PFA-DSPs are a group of atypical DSPs found in plants, fungi, kinetoplastids, and slime moulds. The *A. fumigatus* protein in this cluster has been defined as DspB, it shares 30% identity (22% coverage) with the human atypical DSP, RNGTT. As this group appears divergent from human proteins they should be considered as potential drug targets.

4.3.2.6. MTM and PTEN phosphatases

The lipid phosphatases are smallest subgroup of PTPs, they contain only 1 PTEN and 1 MTM phosphatase from each fungal species. This tree can be split into 2 clades (figure S4.5). The first clade contains all MTM proteins from humans and fungal species. There are far more human MTM phosphatases compared to those found in fungal species. The second clade contains all the PTEN phosphatases from human and each fungal species.

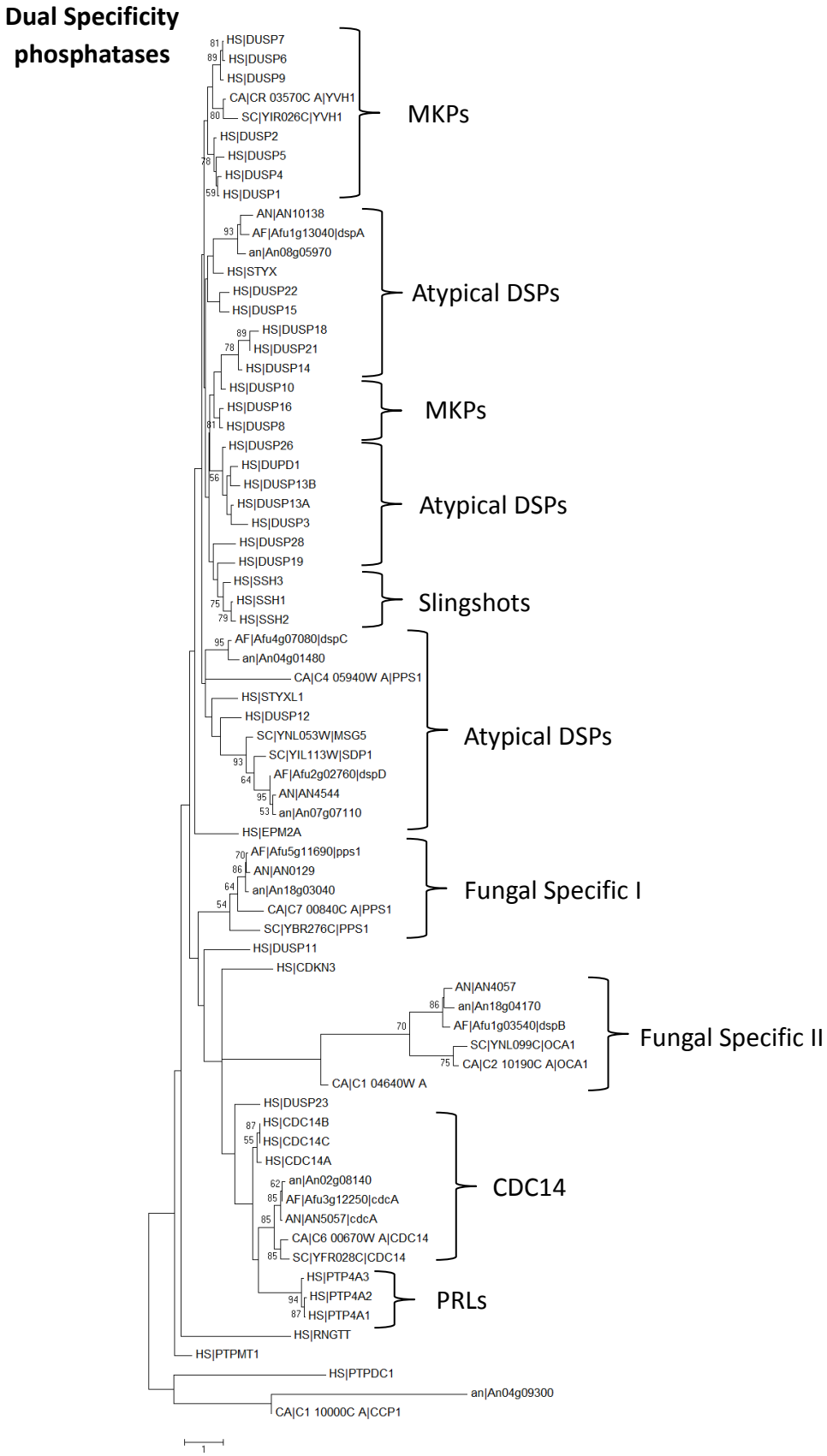

Figure 4.6: Phylogram of DSPs. The evolutionary history was inferred using the Maximum Likelihood method based on the JTT matrix-based model. The bootstrap consensus tree inferred from 1000 replicates is taken to represent the evolutionary history of the taxa analysed (*A. fumigatus* (AF), *A. niger* (an), *A. nidulans* (AN), *S. cerevisiae* (SC), *C. albicans* (CA), *Human* (HS)). Evolutionary analyses were conducted in MEGA6.

4.3.3. Parallel fitness profiling in *A. fumigatus* allows high throughput drug target identification

Parallel fitness studies using libraries of knock out mutants, would allow the high throughput identification of slow growing stains, subsequently this would allow the genes important in fungal fitness to be identified. Proteins encoded by these genes could then be classified as potential drug targets. With a view to generating a knock out library that can be used in a parallel fitness study and to identify potential drug targets we created a library of 38 phosphatase gene deletion mutants in the *A. fumigatus* isolate, A1160p+, using an optimised 96-well plate based, high-throughput gene knockout strategy (figure S4.2). Each strain was validated by PCR (figure S4.3). Mutant strains were numbered according to table S4.4 and are displayed in figure 4.7. Upon strain purification it was determined that 5 out of the 38 genes (*nimT* (Afu6g08200), *glcA* (Afu1g04950), *fcp1* (Afu3g11410), *ssuA* (Afu2g03760) and *pphB* (Afu6g10830)) were essential to viability due to the inability of transformant colonies to grow when streaked on selective media. BLASTp analysis and database searching revealed that the orthologues of these genes were also essential for viability in *A. nidulans* and in most cases *S. cerevisiae* (table S4.5).

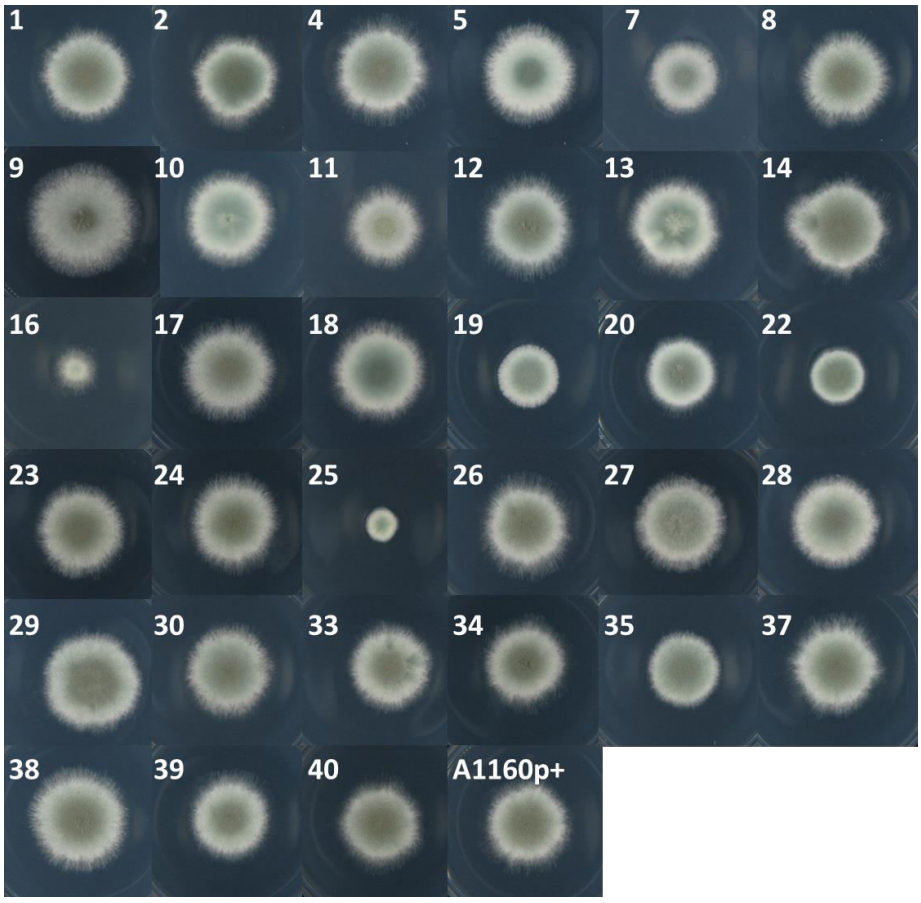

Figure 4.7: 33 non-essential phosphatase knockout strains generated. Parental strain, A1160p+ is also included. Strains 16 and 25 show significantly reduced growth. Strains were grown on VMM for 48 hours at 37°C.

The 33 non-essential mutants were used in a parallel fitness study to assess if any strains showed a reduced fitness phenotype. The mutant library was grown in liquid VMM (3 biological replicates were included) for 48 hours at 37°C with shaking, DNA was extracted. During incubation time it would be expected that strains that exhibit reduced growth will decrease in relative frequency. The change in the relative abundance of each strain was determined by comparing *en mass* sequencing of the unique strain identifier. This allowed differences in relative abundance of each strain to be determined. The changes in the number of sequence reads were then used to calculate relative fitness (see methods section).

To assess the reproducibility of the parallel fitness experimental technical and biological replicates were evaluated. The counts for each strain were normalised to the total number of sequenced reads per condition. Technical replicates compared the same DNA libraries from 2 separate NGS runs and showed high reproducibility with a Pearson correlation coefficient of 0.997 and a coefficient of determination of 0.994 (figure 4.8A). Biological replicate pairwise comparisons also showed similar reproducibility (figure 4.8B). This data shows that using NGS for *A. fumigatus* parallel fitness studies is highly reproducible.

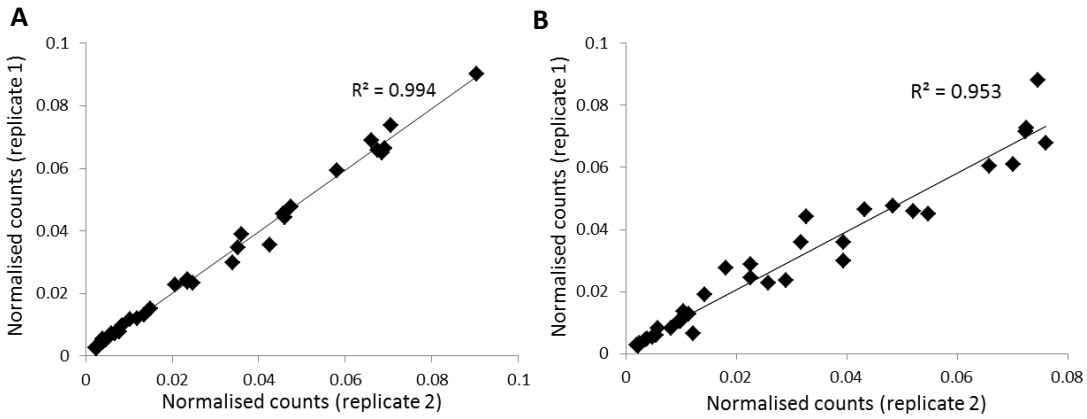

Figure 4.8: Pairwise comparisons of A) technical and B) biological replicates. R^2 = coefficient of determination.

The sequencing counts for each strain were further normalised to the T=0 count and the log2 values were calculated. The data points were plotted in an aligned scatter diagram, the mean is represented by the vertical line (figure 4.9). 4 outliers (35, 22, 19 and 29) with reduced fitness were identified as well a strain exhibiting increased fitness (strain 9).

To confirm the output of the parallel fitness study the phenotypes of the knock out mutant isolates were further validated by assessing strains in growth assays in liquid VMM (figure 4.9). In keeping with the results obtained from the parallel fitness study strains 35, 22 and 19 also exhibited slow growth and strain 9 an increase in growth. Although strain 29 did not display as

much of a fitness defect when grown individually as it did in the parallel fitness study it still appears to grow much slower than the mean growth rate.

The phenotypes of the mutant strains were further validated by performing radial growth rate analysis on solid VMM. Again consistent with the parallel fitness study strains 35, 22 and 19 exhibited slow growth whereas strain 9 displayed an increase in growth (figure S4.6). Interestingly, strain 25 exhibited a severe fitness defect on solid media that was not identified in the parallel fitness study or the growth rate study in liquid media.

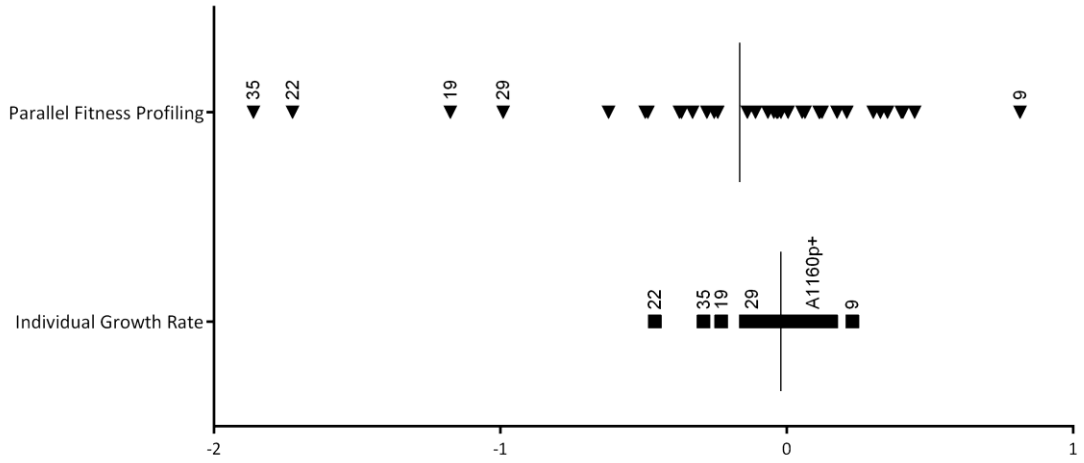

Figure 4.9: Alligned scatter diagram including all the Log2 data points from the parallel fitness and the individual growth rate studies. The mean is represented by the vertical line.

4.4. Discussion

Phosphorylation and dephosphorylation cycles mediated by kinases and phosphatases respectively are important in eukaryotes as a method to either propagate or terminate internal or external cellular signals (3). The correct regulation of phosphatases and kinases is vital to ensure the equilibrium of phosphorylation cycles is maintained. As such phosphatases are necessary for cellular homeostasis (4). Therefore it is unsurprising that phosphatases have been identified as drug targets for a range of human diseases (6, 15, 16) as well as potential antibacterials (18, 20, 21, 33-35). This study involves a bioinformatics approach to identify fungal or *Aspergillus* specific phosphatases as well as the validation of a NGS process to study parallel fitness of a library *A. fumigatus* phosphatase null mutants.

This study identified 38 phosphatases produced by *A. fumigatus,* which is in contrast to the 32 recently identified in the Winkelströter, *et al* study (25). We have carried out a comprehensive phylogenetic analysis which has allowed the identification of various fungal specific clusters for many specific types of phosphatases. There are 2 *Aspergillus* specific clusters found in the PPP phylogram which appear highly divergent from the other phosphatases. Each cluster contains 1 uncharacterised *A. fumigatus* phosphatase which display the domain architecture expected of PPPs. Interestingly, neither of these proteins were identified as phosphatases in the Winkelströter (2015) study (25). The amino acid sequence of Afu5g08620 shows low conservation to the human phosphatase, PPEF1 (25% identity, 34% coverage) whereas protein, Afu1g14840, shows no similarity to any human protein. However, as the corresponding null mutants show no obvious phenotypic defects, neither protein can be considered promising drug target candidates.

The PPM phylogram contained 2 fungal specific phosphatase clusters. 2 *A. fumigatus* proteins were found within this; PtcA (Afu1g15800) and PtcF (Afu1g06860). PtcA is an orthologue to PTC6 in *S. cerevisiae* which under cell wall stress conditions is involved in the down regulation of Slt2 phosphorylation and changes to the vacuole (36). PtcA shares 36% identity (20% coverage) with the human PP2C phosphatase, PPM1K. Our phenotypic analysis showed that loss of Afu1g15800 (strain 34) had no effect on fungal fitness. A similar observation is observed in the Winkelströter (2015) study (24). As fungal viability is not affected by the loss of PtcA it should not be pursued as a drug target. PtcF is an orthologue to *S. cerevisiae,* PTC5 which is responsible for the dephosphorylation of the Pda1p subunit which subsequently regulates pyruvate dehydrogenase activity (37). In the Winkelströter (2015) study the *ptcF* null mutant displayed increased sensitivity when grown at higher temperatures (44°C) and under iron starvation conditions, however the most drastic growth reduction was observed when the

strain was grown in the presence of geldanamycin (GEL) which prevents heat shock protein 90 (Hsp90) activity (24). Our studies have found there is no effect on fitness when *ptcF* null (strain 34) is grown in parallel or individually. Further phenotypic analysis would be required to determine the suitability of PtcF as a drug target for *A. fumigatus* infection.

The PTP phosphatases also showed 2 fungal specific clusters, which included 3 *A. fumigatus* proteins; PtyA (Afu6g06650), Afu4g10270 and YphA (Afu4g07000). Winkelströter, *et al,* classified PtyA as fungal specific (25) and showed a null mutant grew significantly less than the wild type in iron starvation conditions (24), our studies have shown that no effect to fitness is observed when the strain (strain 4) is grown individually or in parallel. Similarly to PtyA, YphA was also classified as a fungal specific phosphatase (25). It is an orthologue to *S. cerevisiae*, SIW14 which has been shown to control localisation GLN3 in combination with protein kinase NPR1 (38). Again this null mutant (strain 11) exhibited unaltered fitness in our studies but the Winkelströter (2015) study showed reduced growth when Hsp90 was inactivated (24). The uncharacterised PTP protein, Afu4g10270, shows low similarity to the non-phosphatase human protein; (3R)-3-hydroxyacyl-CoA dehydratase 2 (29% identity, 94% coverage). This null mutant (strain 39) again shows no effect on fungal growth in our studies and was not identified as a phosphatase in the Winkelströter (2015) study (25).

The DSPs also possess a fungal specific cluster which appear evolutionary distinct from other phosphatases. The *A. fumigatus* protein included in this group is named DspB, and is clustered together with the plant and fungi atypical DSP (PFA-DSP), OCA1, found in *S. cerevisiae*. BLASTp analysis shows it shares 30% identity (22% coverage) with the human atypical DSP, RNGTT. In keeping with our study Winkelströter, *et al,* showed a *dspB* null isolate had no effect on growth under standard conditions however did display reduced viability in iron starvation conditions (24).

Although the fungal specific groups of phosphatases share low conservation with their human proteins, they do not appear to have an effect on *A. fumigatus* growth under standard conditions however Winkelströter, *et al,* have shown some are sensitive to iron starvation conditions. As iron starvation is a common feature in a human host environment it would be beneficial to carry out virulence studies with these iron implicated mutants before they are excluded as potential antifungal targets.

Null mutant construction allowed the identification of 5 essential phosphatase genes; *nimT* (Afu6g08200), *glcA* (Afu1g04950), *fcpA* (Afu3g11410), *ssuA* (Afu2g03760) and *pphB* (Afu6g10830). Comparing these proteins to proteins found in humans allows the prioritisation of drug target development based on sequence conservation. GlcA, PphB and FcpA were also

found to be essential to viability in *A. fumigatus* in the Winkelströter, *et al,* study (24). When comparing GlcA, PphB and FcpA to human proteins they were found to be highly conserved between the 2 species (table S4.4). The high similarity between the fungal and human proteins makes them low priority in the pursuit of developing drug targets, as it is likely an inhibiting agent would interfere with the human protein also. Another essential gene encoded by the protein SsuA, has also shown to be essential to the yeast *S. cerevisiae* (39). When comparing the *A. fumigatus* protein to the human orthologue SSU72 it displayed 45% identity (73% coverage). Again, the high identity across the majority of the proteins decreases the priority of developing an SsuA inhibitor. Finally, the *nimT* gene encodes the CDC25 phosphatase; its orthologue has been shown to be essential in *A. nidulans* (40). When BLASTp analysis is used to compare it to the human genome it appears to be similar to CDC25B. The 2 proteins share 43% identity (26% coverage). Although the identity suggests the proteins are similar it is only over a quarter of the sequence, therefore it should be considered as a high priority for inhibitor development, however more structural analysis of NimT would be beneficial. Winkelströter, *et al,* were unable to construct *ssuA* and *nimT* null mutants but were postulated as essential due to effects their orthologues have in other strains. In contrast to the Winkelströter, *et al,* study we did not find genes *dspA* and *ppgA* essential for viability.

We have shown that PGM Ion Torrent NGS can be used to assess the *in vitro* fitness of strains grown in parallel with high levels of reproducibility. We have shown the parallel fitness results are consistent with individual growth studies, with strains; 19, 22 and 35 exhibiting slow growth and strain 9 showing increased growth in all phenotypic assessments.

Ultimately parallel fitness data could be used to identify potential drug targets for *A. fumigatus* infection. We identified 3 strains (strains 19, 22 and 35) with a consistent fitness reduction across all assessments. Strain 19 is deficient in *ppgA* (Afu5g11370), a PPP encoding gene. The Winkelströter (2015) study was unable to obtain a knockout strain for this mutant so a phenotypic comparison cannot be made (24). A parallel fitness study using *S. cerevisiae* mutants found that the orthologue PPG1 also displayed reduced fitness (41). However, PpgA shares high conservation (55% identity, 91% coverage) with the human protein PPP4C. Strain 22 has a null *sitA* (Afu6g11470) gene, which encodes a PPP phosphatase. SitA has been shown to have a reduction in MpkA phosphorylation, protein kinase C activity and biofilm formation (42). The *sitA* null is also avirulent in a murine model of invasive pulmonary aspergillosis (42) however the SitA protein shares 67% identity (74% coverage) with the human PPP6C protein. The similarity between PpgA and SitA with human proteins suggests there would be a high risk of an inhibitor agent working against not only the fungal protein but the human protein as well, which in turn could lead to adverse side effects. Strain 35 has a *nemA* (Afu1g09460)

deletion, which encodes a FCP phosphatase. The Winkelströter (2015) study showed their *nemA* null isolate had reduced conidial production at 44°C, reduced growth under both iron starvation conditions and also when in the presence of cell wall damaging agents. Furthermore, growth is impaired when Hsp90 activity is inhibited. Clearly this indicates *nemA* is involved in a range of cellular activity. NemA shares 48% identity (36% coverage) of the human FCP, CTDNEP1. As the identity is only over 36% of the protein it might be possible to develop it as a fungal specific drug target. More analysis into its structure would be required.

Interestingly, strain 25 showed the slowest growth when grown individually on solid media, however when grown in parallel and individually in liquid media this was not the case. Strain 25 has a null mutation in *ptcB* (Afu1g09280). PtcB has been identified as a component involved in the high osmolarity glycerol response pathway through the regulation of the kinase SakA (25). Winkelströter (2015) showed PtcB was a vital component to virulence in a murine model of invasive pulmonary aspergillosis (25) and is sensitive to cell wall damaging agents and gliotoxin (24, 25). A study involving the fungal strain *Botrytis cinerea* has shown when its PtcB orthologue is removed the strain becomes far more sensitive to osmotic stress (43). Therefore it is possible that the different phenotypic growth observed in this strain is due to differing osmotic pressures between the media types. In a comparison to human proteins it was found to share 36% identity (66% coverage) with PPM1A. This low similarity, the effect on growth and virulence may prove promising in the development of a novel antifungal agent.

This study has identified there are fungal specific phosphatases found in both STP and PTP families. These phosphatases share low conservation with human proteins, but none of them have been identified as being required for growth in standard laboratory conditions so therefore cannot be prioritised as potential drug targets. Out of the 5 essential phosphatases identified in this study only NimT shows significant divergence from a human protein to be considered as a high priority for potential inhibitor development. The *in vitro* fitness analysis gave 2 potential drug target candidates NemA and PtcB which cause a reduction in fitness in their absence and also significant divergence from human proteins. Development of *in vivo* parallel fitness analysis may reveal more potential phosphatases that could be targeted by inhibiting agents.

4.5. Acknowledgements

Thanks to the BBSRC for providing A.J. with a CASE studentship.

4.6. References

1. Brown GD, Denning DW, Gow NA, Levitz SM, Netea MG, White TC. Hidden killers: human fungal infections. Science translational medicine. 2012;4(165):165rv13. Epub 2012/12/21.
2. Denning DW, Hope WW. Therapy for fungal diseases: opportunities and priorities. Trends in microbiology. 2010;18(5):195-204. Epub 2010/03/09.
3. Dickman MB, Yarden O. Serine/threonine protein kinases and phosphatases in filamentious fungi. Fungal Genetics and Biology. 1999;26(2):99-117.
4. Bauman AL, Scott JD. Kinase- and phosphatase-anchoring proteins: harnessing the dynamic duo. Nature cell biology. 2002;4(8):E203-6. Epub 2002/08/01.
5. Tonks NK. Protein tyrosine phosphatases: from genes, to function, to disease. Nature Reviews Molecular Cell Biology. 2006;7(11):833-46.
6. McConnell JL, Wadzinski BE. Targeting protein serine/threonine phosphatases for drug development. Molecular Pharmacology. 2009;75(6):1249-61.
7. Moorhead Greg BG, De Wever V, Templeton G, Kerk D. Evolution of protein phosphatases in plants and animals. Biochemical Journal. 2009;401-9 p.
8. Shi YG. Serine/Threonine Phosphatases: Mechanism through structure. Cell. 2009;139(3):468-84.
9. Trinkle-Mulcahy L, Lamond AI. Mitotic phosphatases: no longer silent partners. Current Opinion in Cell Biology. 2006;18(6):623-31.
10. Sagara J, Higuchi T, Hattori Y, Moriya M, Sarvotham H, Shima H, et al. Scapinin, a Putative protein phosphatase-1 regulatory subunit associated with the nuclear nonchromatin structure. Journal of Biological Chemistry. 2003;278(46):45611-9.
11. Kitajima TS, Sakuno T, Ishiguro K, Iemura S, Natsume T, Kawashima SA, et al. Shugoshin collaborates with protein phosphatase 2A to protect cohesin. Nature. 2006;441(7089):46-52. Epub 2006/03/17.
12. Loh C, Shaw KT, Carew J, Viola JP, Luo C, Perrino BA, et al. Calcineurin binds the transcription factor NFAT1 and reversibly regulates its activity. The Journal of biological chemistry. 1996;271(18):10884-91. Epub 1996/05/03.
13. Robinson FL, Dixon JE. Myotubularin phosphatases: policing 3-phosphoinositides. Trends in cell biology. 2006;16(8):403-12. Epub 2006/07/11.
14. Alonso A, Sasin J, Bottini N, Friedberg I, Friedberg I, Osterman A, et al. Protein tyrosine phosphatases in the human genome. Cell. 2004;117(6):699-711.
15. Nunes-Xavier C, Roma-Mateo C, Rios P, Tarrega C, Cejudo-Marin R, Tabernero L, et al. Dual-specificity map kinase phosphatases as targets of cancer treatment. Anti-Cancer Agents in Medicinal Chemistry. 2011;11(1):109-32.
16. Ríos P, Nunes-Xavier CE, Tabernero L, Köhn M, Pulido R. Dual-specificity phosphatases as molecular targets for inhibition in human disease. Antioxidants & Redox Signaling. 2013;20(14):2251-73.
17. Silva AP, Tabernero L. New strategies in fighting TB: targeting *Mycobacterium tuberculosis*-secreted phosphatases MptpA & MptpB. Future medicinal chemistry. 2010;2(8):1325-37. Epub 2011/03/24.
18. Beresford N, Patel S, Armstrong J, Szoor B, Fordham-Skelton AP, Tabernero L. MptpB, a virulence factor from *Mycobacterium tuberculosis*, exhibits triple-specificity phosphatase activity. Biochem J. 2007;406:527.
19. Vergne I, Chua J, Lee HH, Lucas M, Belisle J, Deretic V. Mechanism of phagolysosome biogenesis block by viable *Mycobacterium tuberculosis*. Proceedings of the National Academy of Sciences of the United States of America. 2005;102(11):4033-8. Epub 2005/03/09.
20. Bliska JB, Guan KL, Dixon JE, Falkow S. Tyrosine phosphate hydrolysis of host proteins by an essential *Yersinia* virulence determinant. Proceedings of the National Academy of Sciences of the United States of America. 1991;88(4):1187-91. Epub 1991/02/15.

21. Kastner R, Dussurget O, Archambaud C, Kernbauer E, Soulat D, Cossart P, et al. LipA, a tyrosine and lipid phosphatase involved in the virulence of *Listeria monocytogenes*. Infection and immunity. 2011;79(6):2489-98.
22. Szoor B, Wilson J, McElhinney H, Tabernero L, Matthews KR. Protein tyrosine phosphatase TbPTP1: a molecular switch controlling life cycle differentiation in *trypanosomes*. Journal of Cell Biology. 2006;175(2):293-303.
23. van Opijnen T, Bodi KL, Camilli A. Tn-seq: high-throughput parallel sequencing for fitness and genetic interaction studies in microorganisms. Nature Methods. 2009;6(10):767-U21.
24. Winkelströter LK, Dolan SK, Fernanda dos Reis T, Bom VLP, Alves de Castro P, Hagiwara D, et al. Systematic Global analysis of genes encoding protein phosphatases in *Aspergillus fumigatus*. G3: Genes|Genomes|Genetics. 2015;5(7):1525-39.
25. Winkelstroter LK, Bom VLP, de Castro PA, Ramalho LNZ, Goldman MHS, Brown NA, et al. High osmolarity glycerol response PtcB phosphatase is important for *Aspergillus fumigatus* virulence. Molecular microbiology. 2015;96(1):42-54.
26. Brenchley R, Tariq H, McElhinney H, Szoor B, Huxley-Jones J, Stevens R, et al. The TriTryp Phosphatome: analysis of the protein phosphatase catalytic domains. BMC Genomics. 2007;8.
27. Fraczek MG, Bromley M, Buied A, Moore CB, Rajendran R, Rautemaa R, et al. The cdr1B efflux transporter is associated with non-cyp51a-mediated itraconazole resistance in *Aspergillus fumigatus*. Journal of Antimicrobial Chemotherapy. 2013;68(7):1486-96.
28. Szewczyk E, Nayak T, Oakley CE, Edgerton H, Xiong Y, Taheri-Talesh N, et al. Fusion PCR and gene targeting in *Aspergillus nidulans*. Nature protocols. 2006;1(6):3111-20. Epub 2007/04/05.
29. Punt PJ, Oliver RP, Dingemanse MA, Pouwels PH, van den Hondel CAMJJ. Transformation of *Aspergillus* based on the hygromycin B resistance marker from Escherichia coli. Gene. 1987;56(1):117-24.
30. Vogel HJ. A convenient growth medium for *Neurospora* (medium N). Microbial genetics bulletin. 1956;13:42-3.
31. Langmead B, Trapnell C, Pop M, Salzberg SL. Ultrafast and memory-efficient alignment of short DNA sequences to the human genome. Genome Biology. 2009;10(3).
32. Roma-Mateo C, Rios P, Tabernero L, Attwood TK, Pulido R. A novel phosphatase family, structurally related to dual-specificity phosphatases, that displays unique amino acid sequence and substrate specificity. Journal of Molecular Biology. 2007;374(4):899-909.
33. Bach H, Papavinasasundaram KG, Wong D, Hmama Z, Av-Gay Y. Mycobacterium tuberculosis virulence is mediated by PtpA dephosphorylation of human vacuolar protein sorting 33B. Cell Host Microbe. 2008;3(5):316-22.
34. Singh R, Rao V, Shakila H, Gupta R, Khera A, Dhar N, et al. Disruption of mptpB impairs the ability of *Mycobacterium tuberculosis* to survive in guinea pigs. Molecular microbiology. 2003;50(3):751-62.
35. Fu Y, Galan JE. A *salmonella* protein antagonizes Rac-1 and Cdc42 to mediate host-cell recovery after bacterial invasion. Nature. 1999;401(6750):293-7. Epub 1999/09/28.
36. Sharmin D, Sasano Y, Sugiyama M, Harashima S. Type 2C protein phosphatase Ptc6 participates in activation of the Slt2-mediated cell wall integrity pathway in *Saccharomyces cerevisiae*. J Biosci Bioeng. 2015;119(4):392-8.
37. Krause-Buchholz U, Gey U, Wunschmann J, Becker S, Rodel G. YIL042c and YOR090c encode the kinase and phosphatase of the *Saccharomyces cerevisiae* pyruvate dehydrogenase complex. Febs Lett. 2006;580(11):2553-60.
38. Hirasaki M, Kaneko Y, Harashima S. Protein phosphatase Siw14 controls intracellular localization of Gln3 in cooperation with Npr1 kinase in *Saccharomyces cerevisiae.* Gene. 2008;409(1-2):34-43.

39. Sun ZW, Hampsey M. Synthetic enhancement of a TFIIB defect by a mutation in SSU72, an essential yeast gene encoding a novel protein that affects transcription start site selection in vivo. Molecular and Cell Biology. 1996;16(4):1557-66.
40. Son S, Osmani SA. Analysis of All Protein Phosphatase Genes in *Aspergillus nidulans* Identifies a New Mitotic Regulator, Fcp1. Eukaryotic Cell. 2009;8(4):573-85.
41. Qian W, Ma D, Xiao C, Wang Z, Zhang J. The genomic landscape and evolutionary resolution of antagonistic pleiotropy in yeast. Cell reports. 2012;2(5):1399-410. Epub 2012/10/30.
42. Bom VLP, de Castro PA, Winkelströter LK, Marine M, Hori JI, Ramalho LNZ, et al. *Aspergillus fumigatus sitA* phosphatase homologue is important for adhesion, cell wall integrity, biofilm formation and virulence. Eukaryotic Cell. 2015.
43. Yang Q, Yu F, Yin Y, Ma Z. Involvement of protein tyrosine phosphatases BcPtpA and BcPtpB in regulation of vegetative development, virulence and multi-stress tolerance in *Botrytis cinerea*. PloS one. 2013;8(4):e61307. Epub 2013/04/16.
44. Russell P, Moreno S, Reed SI. Conservation of mitotic controls in fission and budding yeasts. Cell. 1989;57(2):295-303. Epub 1989/04/21.
45. Feng ZH, Wilson SE, Peng ZY, Schlender KK, Reimann EM, Trumbly RJ. The Yeast Glc7-gene required for glycogen accumulation encodes a type-1 protein phosphatase. Journal of Biological Chemistry. 1991;266(35):23796-801.
46. Giaever G, Chu AM, Ni L, Connelly C, Riles L, Veronneau S, et al. Functional profiling of the *Saccharomyces cerevisiae* genome. Nature. 2002;418(6896):387-91.
47. Zhang DW, Mosley AL, Ramisetty SR, Rodriguez-Molina JB, Washburn MP, Ansari AZ. Ssu72 Phosphatase-dependent erasure of phospho-Ser7 marks on the RNA polymerase II C-terminal domain is essential for viability and transcription termination. Journal of Biological Chemistry. 2012;287(11):8541-51.
48. Ronne H, Carlberg M, Hu GZ, Nehlin JO. Protein phosphatase-2a in *Saccharomyces-Cerevisiae* - effects on cell-growth and bud morphogenesis. Molecular and Cell Biology. 1991;11(10):4876-84.

4.7. Supplementary Data

Table S4.1: Primers used to generate knockout cassette. A mme1 restriction enzyme site has been incorporated into primer 3 (red lettering).

	KO #	oligoname	sequence
Primer 1	1	Afu2g11990P1	GGGTTCAACACTACGTGCAA
	2	Afu1g11600P1	CTTGACGCGTGTTGTTCATT
	4	Afu6g06650P1	GGGTTCGACTTCAATCAGGA
	5	Afu1g05640P1	GGGTAACCACACTACTGCCG
	6	Afu6g08200P1	ATGGACTATGGAGTCGTCCG
	7	Afu3g12250P1	CCACCGTTCGTATTGATTCC
	8	Afu1g03540P1	ATCGCGATTCAAGAGCATGT
	9	Afu2g02760P1	CTTCTGGCTTACTGGGGTCA
	10	Afu4g07080P1	GGCTAAGAGACCGTCACCAA
	11	Afu4g07000P1	TTGCGAGGCGTAGGTTATTC
	12	Afu3g10970P1	AACAGAGTTTCGCCTCCAGA
	13	Afu4g04710P1	CCCACCCATAACGTCATACC
	14	Afu2g01880P1	GACGTTGCTCGTATGCTTCA
	15	Afu1g04950P1	GCTTCATCCTGGAGGTGAATAA
	16	Afu2g03950P1	GCACACTGGGATAGGAAATGA
	17	Afu5g06700P1	AGGAGCAAAACTCCAGCGTA
	18	Afu5g09360P1	GGAGGAAGAGTTGATGGCAC
	19	Afu5g11370P1	ATGTGACCGAAAGAGCGACT
	20	Afu5g12010P1	CGGTAAGGTGTCATTCAATCAT
	21	Afu6g10830P1	TGAATGACTTGATTGGGCTG
	22	Afu6g11470P1	ATTTGGACTCCTTCTCGCCT
	23	Afu5g08620P1	GTACCGATGACCCTCTGTCG
	24	Afu1g06860P1	CCACTGGGCAGCTTTTCTAC
	25	Afu1g09280P1	CTCCTCGTTCCTAGGTGAGC
	26	Afu2g03890P1	TCCGGGACTTAGTGATGAGG
	27	Afu5g13340P1	TGTTCAGCCACCGTTTATCA
	28	Afu5g13740P1	TAGAATCAACCTCGCCATCC
	29	Afu8G04580P1	TGCCCATTTCCGTATCCTAA
	30	Afu1g04790P1	TTCCCGCTTGATCTGATACC
	32	Afu3g11410P1	TCACTCTGGCTGGTCACAAC
	33	Afu5g11690P1	CTGGTGATACGGGGTTTGCT
	34	Afu1g15800P1	GATCCCAACTCTCAAGGCGA
	35	Afu1g09460P1	GACGCGAAGGAGAAGGTAGG
	36	Afu2g03760P1	CGGTGGGCAGAAATCTTCCT
	37	Afu1g13040P1	CGACTTTGTTCTCGTTGCCC
	38	Afu4g00720P1	TGATCCTGCTTGACCGTGTC
	39	Afu4g10270P1	CAGCAACAGCAACAGCATGT
	40	Afu1g14840P1	TGCTACTCCTCTGTCGTTCG
Primer 2	1	Afu2g11990P2	TAGTTCTGTTACCGAGCCGGGATGGGAGAGGAAGAAAGGG
	2	Afu1g11600P2	TAGTTCTGTTACCGAGCCGGTGCAGATTGGGAGGGTAGAC
	4	Afu6g06650P2	TAGTTCTGTTACCGAGCCGGGCTTTTGCCGTCCATACATC
	5	Afu1g05640P2	TAGTTCTGTTACCGAGCCGGCAAACCTTAGCGATCCGTGT
	6	Afu6g08200P2	TAGTTCTGTTACCGAGCCGGGGGATTTCCTCGGTAAAGGA
	7	Afu3g12250P2	TAGTTCTGTTACCGAGCCGGGATGGCAAAAACTCGAAAGC
	8	Afu1g03540P2	TAGTTCTGTTACCGAGCCGGATGCGAGAGTCCAGAGATCC
	9	Afu2g02760P2	TAGTTCTGTTACCGAGCCGGGCGGCTGTAAGGAGTGAGAC
	10	Afu4g07080P2	TAGTTCTGTTACCGAGCCGGGATGCCACGTTATAGCCGAT
	11	Afu4g07000P2	TAGTTCTGTTACCGAGCCGGGCTCCCTTGTTCGAAGAGAA
	12	Afu3g10970P2	TAGTTCTGTTACCGAGCCGGGAGTTGAAGCAAGCTTTCGG
	13	Afu4g04710P2	TAGTTCTGTTACCGAGCCGGCAGATCTACCGATCCTCCCA
	14	Afu2g01880P2	TAGTTCTGTTACCGAGCCGGCAGGTGTGCAGATTACTCGCT

	15	Afu1g04950P2	TAGTTCTGTTACCGAGCCGGAAAAGAAGGACGAGGGGAGA
	16	Afu2g03950P2	TAGTTCTGTTACCGAGCCGGGATACGAAGTTCTGGGCTCG
	17	Afu5g06700P2	TAGTTCTGTTACCGAGCCGGGTGCGATGGAATCGGTAGAT
	18	Afu5g09360P2	TAGTTCTGTTACCGAGCCGGTTGCGCAGTGTGAACTAAGG
	19	Afu5g11370P2	TAGTTCTGTTACCGAGCCGGAATGGACAACGTGCCAAACT
	20	Afu5g12010P2	TAGTTCTGTTACCGAGCCGGGAAGGGGGCCCTGTAGTAAC
	21	Afu6g10830P2	TAGTTCTGTTACCGAGCCGGAGGCTGACCAGGGATTTTCT
	22	Afu6g11470P2	TAGTTCTGTTACCGAGCCGGGAGCTAGCAGAACGGCAGAT
	23	Afu5g08620P2	TAGTTCTGTTACCGAGCCGGGCAAGGTCGGAGATTTCGTA
	24	Afu1g06860P2	TAGTTCTGTTACCGAGCCGGGGCTGGTACGGAAAAACAGA
	25	Afu1g09280P2	TAGTTCTGTTACCGAGCCGGACCAGAAGACCTCAGACGGA
	26	Afu2g03890P2	TAGTTCTGTTACCGAGCCGGATCACCTCGGAAAGATGCTC
	27	Afu5g13340P2	TAGTTCTGTTACCGAGCCGGCCCTTTGGGAAGGAAAGAAG
	28	Afu5g13740P2	TAGTTCTGTTACCGAGCCGGTTGCTGTTTGCTCTGAGGAG
	29	Afu8G04580P2	TAGTTCTGTTACCGAGCCGGCCCTGTCCCTCAGAATACCA
	30	Afu1g04790P2	TAGTTCTGTTACCGAGCCGGCGGAATTCAAAAGGCGTAGA
	32	Afu3g11410P2	TAGTTCTGTTACCGAGCCGGCTAGCCTCTTATCCGACCCC
	33	Afu5g11690P2	TAGTTCTGTTACCGAGCCGGATGACAGCTGTGCAGTTCGA
	34	Afu1g15800P2	TAGTTCTGTTACCGAGCCGGAAGATTCAGGGTGTGCGTGG
	35	Afu1g09460P2	TAGTTCTGTTACCGAGCCGGCTGGCGCAGTTATCTACAGGA
	36	Afu2g03760P2	TAGTTCTGTTACCGAGCCGGGGAAGTGACAGAGTGGGAGC
	37	Afu1g13040P2	TAGTTCTGTTACCGAGCCGGGCGGAACAGTCTTTTCGAGC
	38	Afu4g00720P2	TAGTTCTGTTACCGAGCCGGTATTGATCCTGCTGCGAGGG
	39	Afu4g10270P2	TAGTTCTGTTACCGAGCCGGAAAAGGGTCAGCTAGTCGGC
	40	Afu1g14840P2	TAGTTCTGTTACCGAGCCGGCCTGGACTACGAATCAATGCG
Primer 3	1	Afu2g11990P3	GCTCTGAACGATATGC**TCCAAC**ACCAAGCTTGTTCGTCGTTT
	2	Afu1g11600P3	GCTCTGAACGATATGC**TCCAAC**AAATTTGACTTGGACGGCAC
	4	Afu6g06650P3	GCTCTGAACGATATGC**TCCAAC**ATTATGGGCGGATACAATGG
	5	Afu1g05640P3	GCTCTGAACGATATGC**TCCAAC**TGCGACGATTACAACAAAGG
	6	Afu6g08200P3	GCTCTGAACGATATGC**TCCAAC**AGCCGGTTGACTTTCCTTTT
	7	Afu3g12250P3	GCTCTGAACGATATGC**TCCAAC**TCATTTTCTTGGTCTTGGGC
	8	Afu1g03540P3	GCTCTGAACGATATGC**TCCAAC**ACGAATAATGATTCCGCGAC
	9	Afu2g02760P3	GCTCTGAACGATATGC**TCCAAC**TTAAGGCAGCCTGTCTCTGC
	10	Afu4g07080P3	GCTCTGAACGATATGC**TCCAAC**CTCTCCAAGAACATTTGGGC
	11	Afu4g07000P3	GCTCTGAACGATATGC**TCCAAC**TGGAGGACTGGATAACCTCG
	12	Afu3g10970P3	GCTCTGAACGATATGC**TCCAAC**CAGGAAATTCGAGCATGGAT
	13	Afu4g04710P3	GCTCTGAACGATATGC**TCCAAC**GCTCTACGGGTGACTGAAGG
	14	Afu2g01880P3	GCTCTGAACGATATGC**TCCAAC**GGATGGCATACTGCGTTCTT
	15	Afu1g04950P3	GCTCTGAACGATATGC**TCCAAC**ATCCCACATTCGTCAACACA
	16	Afu2g03950P3	GCTCTGAACGATATGC**TCCAAC**ATTCATCCGCCAAGAAATTG
	17	Afu5g06700P3	GCTCTGAACGATATGC**TCCAAC**GCTTATGCGCAGAACTCCAT
	18	Afu5g09360P3	GCTCTGAACGATATGC**TCCAAC**TCACGTCCATGTTGTGCTTT
	19	Afu5g11370P3	GCTCTGAACGATATGC**TCCAAC**AGTACTTCCCGATGCAGAGC
	20	Afu5g12010P3	GCTCTGAACGATATGC**TCCAAC**CGGCCCAATCAATGACTACT
	21	Afu6g10830P3	GCTCTGAACGATATGC**TCCAAC**GACCCTTCGAGAGGGCTACT
	22	Afu6g11470P3	GCTCTGAACGATATGC**TCCAAC**ATACCTCTTTCGCGCTCTCC
	23	Afu5g08620P3	GCTCTGAACGATATGC**TCCAAC**GGTGTTTGGGCGTCTACAAT
	24	Afu1g06860P3	GCTCTGAACGATATGC**TCCAAC**GAGGATACCGTCGGATGAAA
	25	Afu1g09280P3	GCTCTGAACGATATGC**TCCAAC**TCCTCCTCGATCTGGTCTTG
	26	Afu2g03890P3	GCTCTGAACGATATGC**TCCAAC**GCAGAGCAGGCCTCTAAAAA
	27	Afu5g13340P3	GCTCTGAACGATATGC**TCCAAC**TCATCCCACGACGTGATAAA
	28	Afu5g13740P3	GCTCTGAACGATATGC**TCCAAC**AGCAGCTCCCAGACTATGGA
	29	Afu8G04580P3	GCTCTGAACGATATGC**TCCAAC**AAAATGGGTGTTCCTTGTGC
	30	Afu1g04790P3	GCTCTGAACGATATGC**TCCAAC**TTAACTGTTCCCGGCATTTC
	32	Afu3g11410P3	GCTCTGAACGATATGC**TCCAAC**AATCGATTTTCTGTGCGGTT
	33	Afu5g11690P3	GCTCTGAACGATATGC**TCCAAC**AAAGGGAAGCAGGATGGAGC

	34	Afu1g15800P3	GCTCTGAACGATATGC**TCCAAC**TGGGACCCTTTGAATCCTGC
	35	Afu1g09460P3	GCTCTGAACGATATGC**TCCAAC**TTTCCTGTAAAGCGAGCCGA
	36	Afu2g03760P3	GCTCTGAACGATATGC**TCCAAC**AACTCCAACTAAGCAAAAGGGT
	37	Afu1g13040P3	GCTCTGAACGATATGC**TCCAAC**TGTGCTGCGTTAACATTCTGC
	38	Afu4g00720P3	GCTCTGAACGATATGC**TCCAAC**GCCCGCATTCACAGTAAACG
	39	Afu4g10270P3	GCTCTGAACGATATGC**TCCAAC**ATTTCTTTCGCTCGCTCTCC
	40	Afu1g14840P3	GCTCTGAACGATATGC**TCCAAC**GGCCAAATTCGGGTTATAGCG
Primer 4	1	Afu2g11990P4	GAGTATCTCCGGCTCATGGA
	2	Afu1g11600P4	AGTACCCCAATGTCCAGCAG
	4	Afu6g06650P4	GCAGTTCATTTTGACGCTGA
	5	Afu1g05640P4	CTTGAGCAGATTCCCCAAAG
	6	Afu6g08200P4	CGATGCCTCAGGTTTTCTTC
	7	Afu3g12250P4	AGTTTCTCAAGCGGTGTGCT
	8	Afu1g03540P4	GATAGAGCGTCAGCTTTGCC
	9	Afu2g02760P4	CGAGAGTTCGGGCGTAGTAG
	10	Afu4g07080P4	TCCATTTCAGATGGGGCTAC
	11	Afu4g07000P4	TTTGCAAAGCAGAATCAACG
	12	Afu3g10970P4	ATTCGACCCCTTCGACATC
	13	Afu4g04710P4	CGTTAACGCCTCCTTCTCTG
	14	Afu2g01880P4	TTGGACCACCTCGGAATATC
	15	Afu1g04950P4	GGGTATCAGGTGGCTGTCTC
	16	Afu2g03950P4	AGAGATTGCTCCTGGGTTGA
	17	Afu5g06700P4	CCAGTTCTTCGACAGTGCAA
	18	Afu5g09360P4	ATACATCCTCCCAGGGTTCC
	19	Afu5g11370P4	GATCTCGTTGCCTCGAAGAC
	20	Afu5g12010P4	CTGAAGCTTCGAGCGTCTTT
	21	Afu6g10830P4	ATCGGTACGAGGGAGGAGAT
	22	Afu6g11470P4	CCCAGACAGCATCAGTGCTA
	23	Afu5g08620P4	TGCTCTCACTTTCCATCACG
	24	Afu1g06860P4	TCTCAACTGGCAAGATCACG
	25	Afu1g09280P4	TGTACTGGGTATGAGGCGCT
	26	Afu2g03890P4	CAGCAAAAGGACGGAAAAGA
	27	Afu5g13340P4	GCTGGCTGATGGAGAAGAAA
	28	Afu5g13740P4	AAAAGACCTACCCCAAACGG
	29	Afu8G04580P4	GAGGAGTTTCAGTTCCGTCG
	30	Afu1g04790P4	GCTTGCAGGTGGTGATGATT
	32	Afu3g11410P4	TATTCCTCCATGCATCGTCA
	33	Afu5g11690P4	GGATCATACCCTCTGCAGCC
	34	Afu1g15800P4	GCTTGTAGTTGTCACGTCGC
	35	Afu1g09460P4	AACAAGCCCTCCTACTTCGC
	36	Afu2g03760P4	TTGGCCTGAACATCACCTCG
	37	Afu1g13040P4	TCCTCGCGTTCCTTTTCTCC
	38	Afu4g00720P4	ATGCCCTTGTACCTTGGCTG
	39	Afu4g10270P4	CCAGACGGCGACAGATGAAC
	40	Afu1g14840P4	CGCAAAGACGATGAACACCC
Primer 5	1	Afu2g11990P5	CATCTTCCATGCGGAACTTT
	2	Afu1g11600P5	CACATGTTCCACAGCAACCT
	4	Afu6g06650P5	ATATTCCAGCGACGATCCAG
	5	Afu1g05640P5	TTAATCCCTACCGAACGACG
	6	Afu6g08200P5	GCGCCCTACCTACGTAACAA
	7	Afu3g12250P5	ACAATGGGAGAAGAATTGCG
	8	Afu1g03540P5	ACATTGGCAGCCATTATTCC
	9	Afu2g02760P5	TTCCAATCACTTTTGGCTCC
	10	Afu4g07080P5	TCTGGTTCAGTCGCACAGAC
	11	Afu4g07000P5	CTTTGGCCACTAAGGAGCTG
	12	Afu3g10970P5	CGTTGTCTTTCTCCCTCTCCT

	13	Afu4g04710P5	ATTCGCTATTTCCATGTCGG
	14	Afu2g01880P5	TGTTTCTCACAGTTGGCTGC
	15	Afu1g04950P5	CCTTTTCTCTTCCCTCACCC
	16	Afu2g03950P5	CTTGGGGCAATTCTTCGATA
	17	Afu5g06700P5	AAGCCGGTCAGTATCACCAC
	18	Afu5g09360P5	TGGGAGAAATCGGAGTATCG
	19	Afu5g11370P5	GGCGAAGACTAAAACGCTTG
	20	Afu5g12010P5	AGGGTATGAAGATTGCACGG
	21	Afu6g10830P5	ACAAGAAAGGCCACCACAAC
	22	Afu6g11470P5	GTCAGACTTTCGAGGAACGC
	23	Afu5g08620P5	GCTGTTTTCGGATACACGGT
	24	Afu1g06860P5	ACTCTCCAACACGACGTTCC
	25	Afu1g09280P5	GAGATTTGCACACGCCACTA
	26	Afu2g03890P5	CGCTTGAAGTGACAGATCCA
	27	Afu5g13340P5	TCTGCACTGAGGGCTCCTAT
	28	Afu5g13740P5	TGCGCCATACTTGTTCTCTG
	29	Afu8G04580P5	CGAGAAGACGAGGACCAGAG
	30	Afu1g04790P5	AGTCCAGACCAATGCAGCTT
	32	Afu3g11410P5	TTGGTCCCCTTGCTATTTTG
	33	Afu5g11690P5	GGAGATTGACGTTGGAGGGG
	34	Afu1g15800P5	CCATCAAGGGTCTCAACGGT
	35	Afu1g09460P5	AGAACGGTAGCTCCTTGTGC
	36	Afu2g03760P5	TCATGAGTTAGGCGTGACGG
	37	Afu1g13040P5	TGAGTGGGGTTTCTGGATCTG
	38	Afu4g00720P5	CTGGAGCTGCGATGTCATGA
	39	Afu4g10270P5	AAGTGGAGAATGGGTCAGCC
	40	Afu1g14840P5	TGGCAGAAGTCTTGGTGTCC
Primer 6	1	Afu2g11990P6	GCTTTCTGTCGTGGATGGAT
	2	Afu1g11600P6	CAGAAACCTACCCTCCACCA
	4	Afu6g06650P6	GTCGCTTCGATATTCTTCGC
	5	Afu1g05640P6	CCGCTCTCCATGATGAATCT
	6	Afu6g08200P6	CCCAATTTTCTCGCCAAATA
	7	Afu3g12250P6	CCCATCTTCGTCATCTTCGT
	8	Afu1g03540P6	GACCTTCCGATTCTGAACCA
	9	Afu2g02760P6	GCTTCAATTAGCAAGCGGAC
	10	Afu4g07080P6	CGATGACATGAGGCAAGCTA
	11	Afu4g07000P6	TACAGAGGAGCCGAAGAGGA
	12	Afu3g10970P6	AGGTCGACAATTGGGATGAG
	13	Afu4g04710P6	CCTTGGCCTGGAGAACATAA
	14	Afu2g01880P6	CTCGACTTTCTCGTTCCGTC
	15	Afu1g04950P6	ATACCCCATCGGTCCCTATC
	16	Afu2g03950P6	GAGAGCGGCCTACAACAGAC
	17	Afu5g06700P6	TTCTGAGAACAACCACGACG
	18	Afu5g09360P6	CCGGCTGATATTGACCTGTT
	19	Afu5g11370P6	ACCAGAATGACGAATCCCTG
	20	Afu5g12010P6	CCCAGGAGGAGCATCAATAA
	21	Afu6g10830P6	AAAGCCGAATCAAAAGGGAT
	22	Afu6g11470P6	CTTCCCGTTTTTCTCAGCAG
	23	Afu5g08620P6	TATTTCTGCGTCAGGCACAC
	24	Afu1g06860P6	TCAGCTGGACAAGGTGTCTG
	25	Afu1g09280P6	TACCCAGGTGGGTTCTATCG
	26	Afu2g03890P6	TTCCTCGAAGACTGGCAGAT
	27	Afu5g13340P6	CGAGGAAGAAGGAACACGAG
	28	Afu5g13740P6	AGTCAAACGAACCCACCTTG
	29	Afu8G04580P6	AGAAGCTCCTGAATCAGCCA
	30	Afu1g04790P6	GCACGCATTTATGTCCACTG

	32	Afu3g11410P6	CATCTGGATCATCATCGTGC
	33	Afu5g11690P6	TGCATCAACGAGACAACTGGA
	34	Afu1g15800P6	TCGTTCTGGCGCTCATAATGA
	35	Afu1g09460P6	GCTATACACGCCCAGACCTC
	36	Afu2g03760P6	ACTGGAACCCTTCGCATGAC
	37	Afu1g13040P6	ACCATCCGTAGTGTTGGCTG
	38	Afu4g00720P6	GCCATTGTTGACAGGACAGG
	39	Afu4g10270P6	CACAGACAGCAGGAGAAGGG
	40	Afu1g14840P6	TTCAGCTTGTACCCATCCGC

Table S4.2: Unique index that identifies the condition of the experiment

Condition	Index
T0 1	CTAAGGTAAC
T0 2	TAAGGAGAAC
T0 3	AAGAGGATTC
VMM 1	TTCGTGATTC
VMM 2	TTCCGATAAC
VMM 3	TGAGCGGAAC

Table S4.3: Unique strain identifier

Strain Number	Null Gene	Identifier
1	Afu2g11990	ACCAAGCTTGTTCGT
2	Afu1g11600	AAATTTGACTTGGAC
4	Afu6g06650	ATTATGGGCGGATAC
5	Afu1g05640	TGCGACGATTACAAC
7	Afu3g12250	TCATTTTCTTGGTCT
8	Afu1g03540	ACGAATAATGATTCC
9	Afu2g02760	TTAAGGCAGCCTGTC
10	Afu4g07080	CTCTCCAAGAACATT
11	Afu4g07000	TGGAGGACTGGATAA
12	Afu3g10970	CAGGAAATTCGAGCG
13	Afu4g04710	GCTCTACGGGTGACT
14	Afu2g01880	GGATGGCATACTGCG
16	Afu2g03950	ATTCATCCGCCAAGA
17	Afu5g06700	GCTTATGCGCAGAAC
18	Afu5g09360	TCACGTCCATGTTGT
19	Afu5g11370	AGTACTTCCCGATGC
20	Afu5g12010	CGGCCCAATCAATGA
22	Afu6g11470	ATACCTCTTTCGCGC
23	Afu5g08620	GGTGTTTGGGCGTCT
24	Afu1g06860	GAGGATACCGTCGGA
25	Afu1g09280	TCCTCCTCGATCTGG
26	Afu2g03890	GCAGAGCAGGCCTCT
27	Afu5g13340	TCATCCCACGACGTG
28	Afu5g13740	AGCAGCTCCCAGACT
29	Afu8g04580	AAAATGGGTGTTCCT
30	Afu1g04790	TTAACTGTTCCCGC
33	Afu5g11690	AAAGGGAAGCAGGAT
34	Afu1g15800	TGGGACCCTTTGAAT
35	Afu1g09460	TTTCCTGTAAAGCGA

37	Afu1g13040	TGTGCTGCGTTAACA
38	Afu4g00720	GCCCGCATTCACAGT
39	Afu4g10270	ATTTCTTTCGCTCGC
40	Afu1g14840	GGCCAAATTCGGGTT

Table S4.4: Table of phosphatase mutants generated. KO # was assigned to each gene that was abolished.

KO #	Gene ID	Phosphatase family	Gene name	Viable	Closest human protein	Phosphatase family	BLASTp analysis	
							% identity	% cover
1	Afu2g11990	PTENS		Y	PTEN	PTEN	35	36
2	Afu1g11600	IMPase		Y	IMPA1	IMPase	34	78
3	Afu1g12000							
4	Afu6g06650	PTP	ptyA	Y	PTPN6	Non receptor PTP	36	12
5	Afu1g05640	MTM		Y	MTMR6	MTM	34	72
6	Afu6g08200	CDC25	nimT	N	CDC25B	CDC25	43	26
7	Afu3g12250	CDC14	cdcA	Y	CDC14A	CDC14	35	62
8	Afu1g03540	DSP	dspB	Y	RNGTT	Atypical DSP	30	22
9	Afu2g02760	DSP	dspD	Y	DUSP9	MKPs	38	11
10	Afu4g07080	DSP	dspC	Y	DUSP12	Atypical DSP	29	85
11	Afu4g07000	PFA	yphA	Y	CDC14A	DSP	27	36
12	Afu3g10970	PTP	ptpB	Y	PTPRO	Receptor PTP	33	65
13	Afu4g04710	PTP	ptpA	Y	PTPN22	Non receptor PTP	30	50
14	Afu2g01880	PTP-LMW	ltpA	Y	ACP1	LMW PTP	42	42
15	Afu1g04950	PPP	glcA	N	PPP1CB	PPP	84	99
16	Afu2g03950	PPP	phzA	Y	PPP1CA	PPP	64	59
17	Afu5g06700	PPP		Y	PPP5C	PPP	51	99
18	Afu5g09360	PPP	calA	Y	PPP3CB	PPP	64	84
19	Afu5g11370	PPP	ppgA	Y	PPP4C	PPP	55	91
20	Afu5g12010	PPP	pphA	Y	PPP4C	PPP	70	83
21	Afu6g10830	PPP	pphB	N	PPP2CB	PPP	84	93
22	Afu6g11470	PPP	sitA	Y	PPP6C	PPP	67	74
23	Afu5g08620	PPP-like		Y	PPEF1	PPP	25	34
24	Afu1g06860	PPM	ptcF	Y	PDP1	PP2C	31	70
25	Afu1g09280	PPM	ptcB	Y	PPM1A	PP2C	36	66
26	Afu2g03890	PPM	ptcE	Y	ILKAP	PP2C	30	83
27	Afu5g13340	PPM	ptcG	Y	PPM1A	PP2C	31	48
28	Afu5g13740	PPM	ptcD	Y	PPM1A	PP2C	26	90
29	Afu8g04580	PPM	ppmA	Y	PPTC7	PP2C	38	43
30	Afu1g04790	SCP	psrA	Y	CTDSP2	FCP/SCP	47	42
31	Afu2g03420	FCP						
32	Afu3g11410	FCP	fcpA	N	CTDP1	FCP/SCP	40	49
33	Afu5g11690	DSP	pps1	Y	DUSP1	MKPs	34	25
34	Afu1g15800	PPM	ptcA	Y	PPM1K	PP2C	36	20
35	Afu1g09460	Dullard	nemA	Y	CTDNEP1	FCP/SCP	48	36
36	Afu2g03760	SSU72	ssuA	N	SSU72	SSU72	45	73
37	Afu1g13040	DSP	dspA	Y	DUSP6	MKPs	33	40
38	Afu4g00720	PPM	ptcH	Y	PPM1A	PP2A	32	65
39	Afu4g10270	PTP		Y	very-long-chain (3R)-3-hydroxyacyl-CoA dehydratase 2		29	94
40	Afu1g14840	PPP-like		Y	N/A	N/A	N/A	N/A

Table S4.5: Essential phosphatases identified in *A. fumigatus* and orthologues

A. fumigatus	***A. nidulans* orthologue**					***S. cerevisiae* orthologue**				
Protein	**Protein**	**BLASTp Analysis**		**Essential**	**Ref**	**Protein**	**BLASTp Analysis**		**Essential**	**Ref**
		ID (%)	**Cover (%)**				**ID (%)**	**Cover (%)**		
NimT	NimT	75	100	Yes	(40)	MIH1	40	29	No	(44)
GlcA	BimG	98	99	Yes	(40)	GLC7	84	99	Yes	(45)
FcpA	PodH	66	100	Yes	(40)	FCP1	37	72	Yes	(46)
SsuA	AN3810	76	100	-	-	SSU72	46	80	Yes	(39, 47)
PphB	PphA	98	100	Yes	(40)	PPH21/ PPH22	75	96	No	(48)

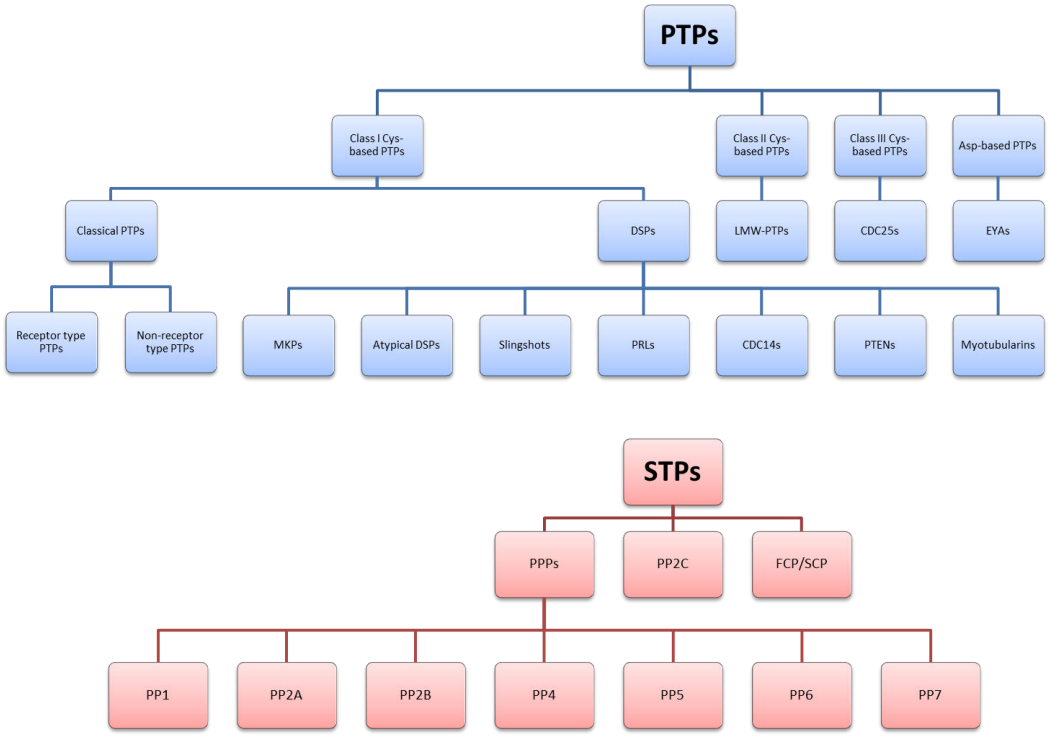

Figure S4.1: 2 families of phosphatases; A) tyrosine-specific phosphatases (PTP) and B) serine/threonine phosphatases (STP). PTPs include; Classical PTPs, dual specificity (DSPs), low molecular weight PTPs (LMW-PTPs), CDC25s, EYAs. The classical PTPs are further divided into receptor and non-receptor type PTPs. The DSPs are subdivided into; Map kinase phosphatases (MKPs), atypical DSPs, slingshots, phosphatase of regenerating liver (PRLs), CDC14s, phosphatase and tensin homolog (PTENs) and Myotubularins (MTMs). STPs include; phosphoprotein phosphatases (PPPs), metal-dependent protein phosphatases (PPMs) and aspartate based phosphatases (FCP/SCP).

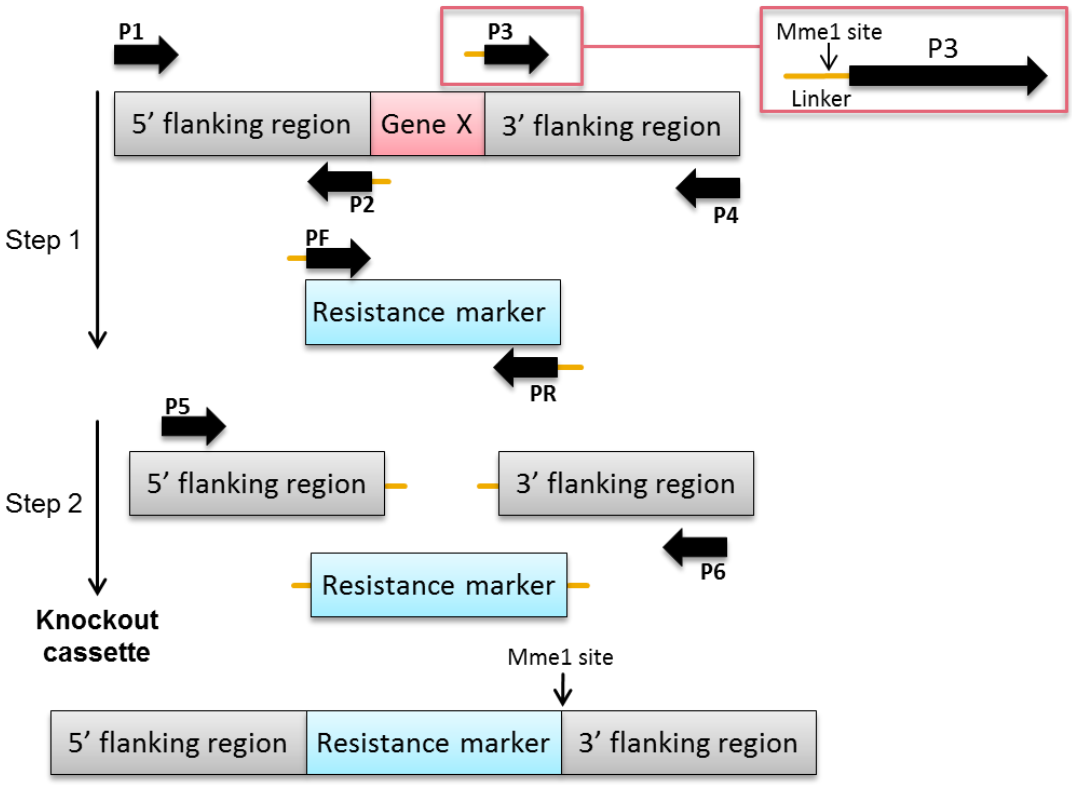

Figure S4.2: Two Step Fusion PCR. Step 1, Using primers P1 and P2 in one reaction and P3 and P4 in another, 2 PCR products of the regions flanking the chosen insertion site are produced. These products contain "tails" which were embedded in P2 and P3. P3 also has an mme1 restriction site incorporated into it which is required for next generation sequencing library preparation. An additional PCR reaction is used to amplify a resistance marker, primers in this reaction contain complementary "tails" to those found in P2 and P3. Excess primers and nucleotides from this reaction are then removed. Step 2, Nested primers P5 and P6 are used to amplify the two flanking regions together with the pre-amplified resistance marker. The PCR product is a linear transforming DNA fragment.

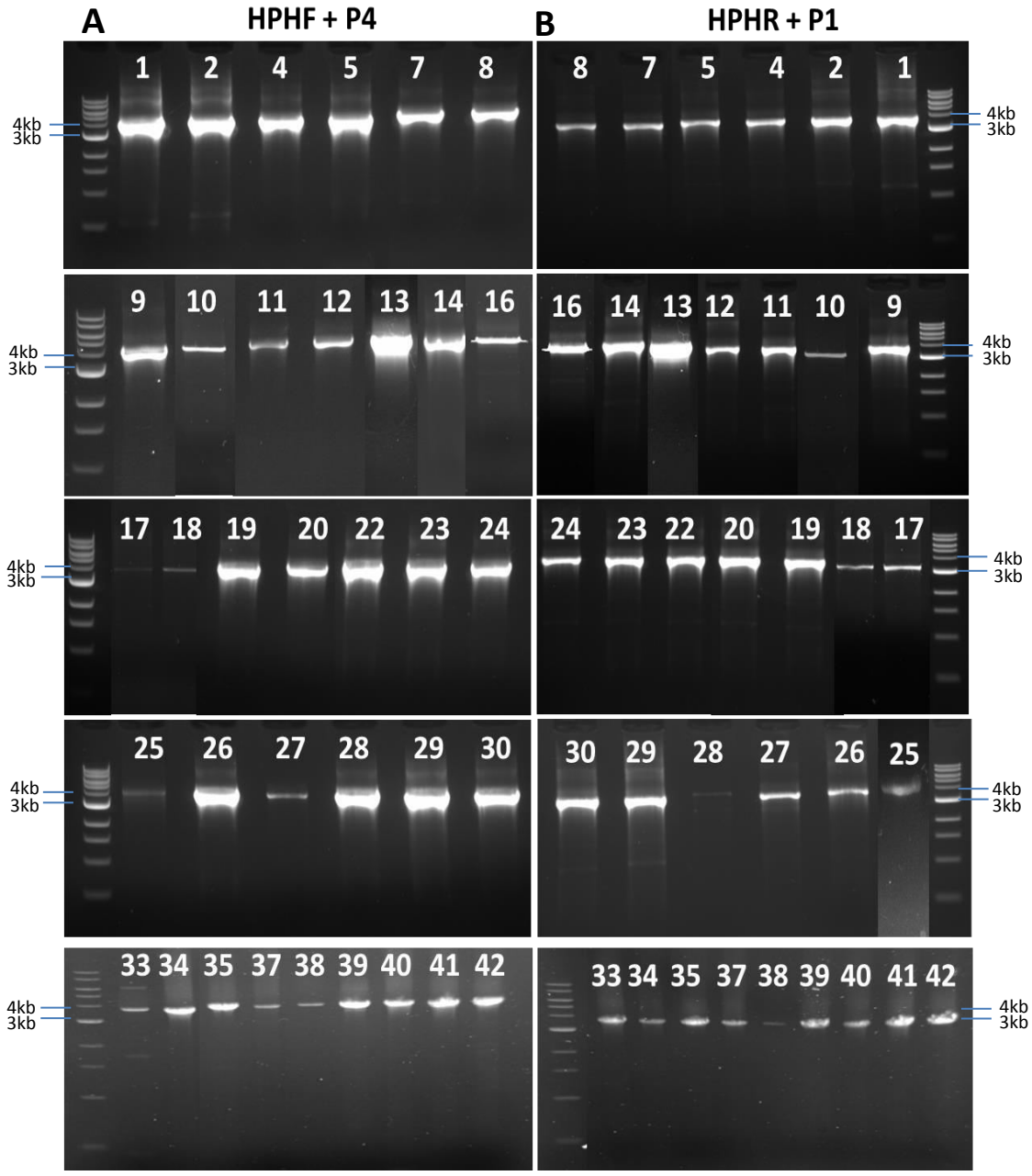

Figure S4.3: PCR validation of phosphatase null mutants. DNA isolated from each strain underwent two PCR validation reactions to produce a product of approximately 3.5kb: A) amplification across the 3' flanking region and selective marker gene (HPHF and P2); B) amplification across the 5' flanking region and selective marker gene (HPHR and P1). A product size of approximately 3.5kb is observed for all strains.

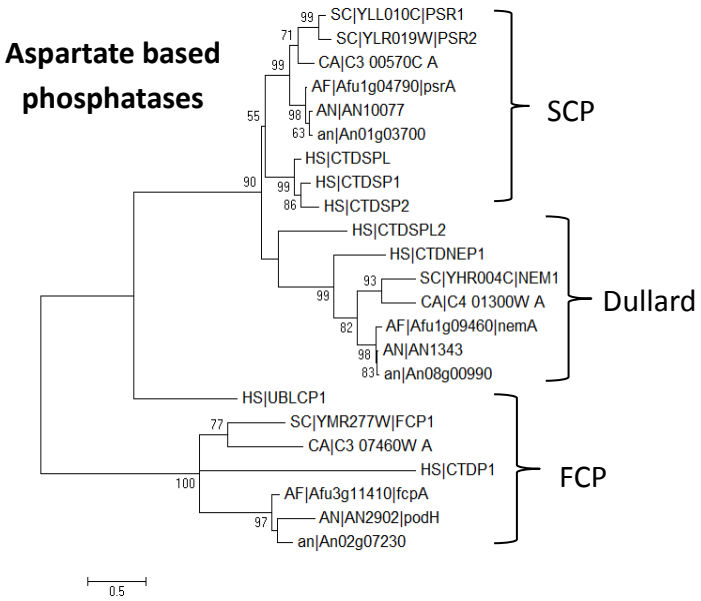

Figure S4.4: Phylogram of aspartate based phosphatases. The evolutionary history was inferred using the Maximum Likelihood method based on the JTT matrix-based model. The bootstrap consensus tree inferred from 1000 replicates is taken to represent the evolutionary history of the taxa analysed (*A. fumigatus* (AF), *A. niger* (an), *A. nidulans* (AN), *S. cerevisiae* (SC, *C. albicans* (CA), *Human* (HS)). Evolutionary analyses were conducted in MEGA6.

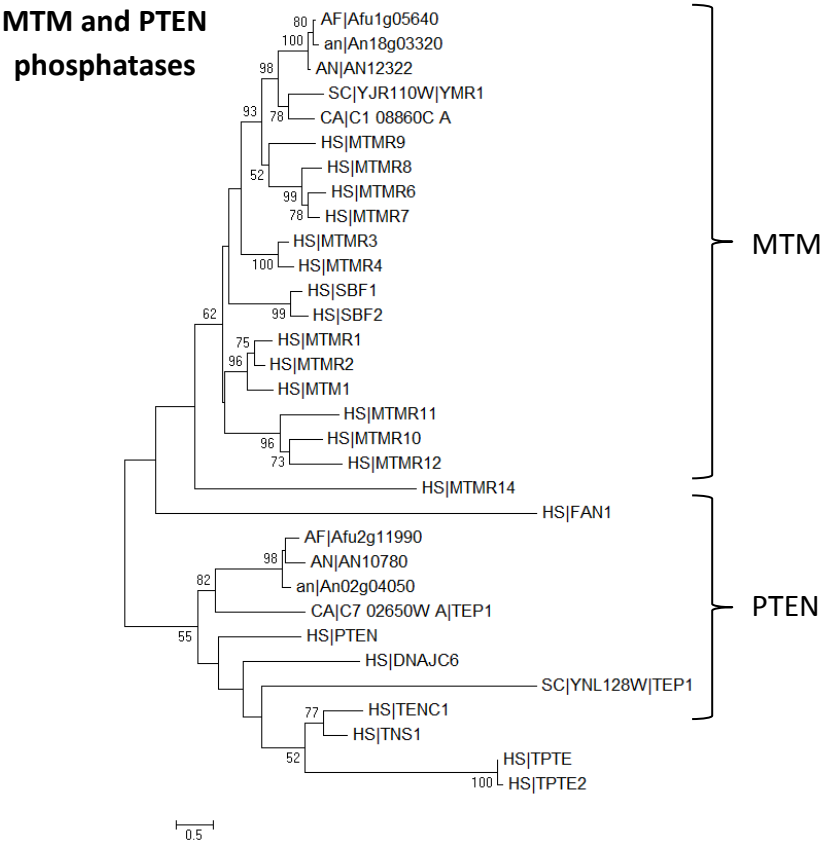

Figure S4.5: Phylogram of MTM and PTEN phosphatases. The evolutionary history was inferred using the Maximum Likelihood method based on the JTT matrix-based model. The bootstrap consensus tree inferred from 1000 replicates is taken to represent the evolutionary history of the taxa analysed (*A. fumigatus* (AF), *A. niger* (an), *A. nidulans* (AN), *S. cerevisiae* (SC), *C. albicans* (CA), *Human* (HS). Evolutionary analyses were conducted in MEGA6.

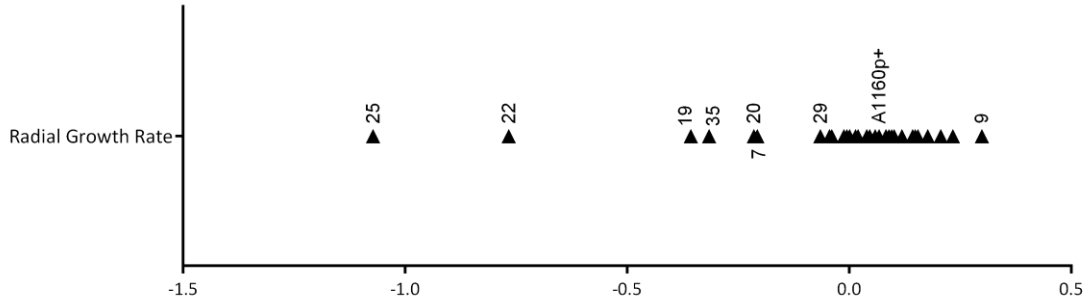

Figure S4.6: Fitness assessment of strains in growth assays on solid VMM.

Chapter 5

Conclusions and Future Work

5. Conclusions and Future Work

The significant pharmacological inadequacies of antifungals as well as emergence of resistance, particularly to the azoles, have stimulated the search for new antifungals with novel mechanisms of action (1, 2). However this is a topic that has been somewhat neglected by the scientific community. With less than 1% of grant applications received by the Medical Research Council between 2007 and 2012 involved in fungal research (3) and pharmaceutical companies focused more on antibiotic development (1) it clearly demonstrates this as an area requiring attention from both academic and industrial settings. As such this thesis strives to close this gap in research by outlining various drug target validation and identification strategies to improve therapeutic options for *Aspergillus fumigatus* infection.

The second chapter of this thesis demonstrates the Sfp-type phosphopantetheinyl transferase (PPTase), PptA of *A. fumigatus* has the potential to be used as a therapeutic target to treat Aspergillosis infection. PPTases are responsible for a reaction known as phosphopantetheinylation, which mediates the transfer and tethering of 4'-phosphopantetheine (P-pant) from coenzymeA (CoA) to a conserved serine residue within a peptidyl carrier domain of a protein substrate (4, 5). This process alters the target protein from an inactive apo-enzyme into an active holo-enzyme permitting attachment of substrates and intermediates for a range of enzymes involved in both primary and secondary metabolism. This project has shown the *A. fumigatus* PptA plays a role in a variety of biosynthesis pathways including; siderophores triacetylfusarinine C (TAFC) and ferricrocin (FC), lysine, DHN-melanin, gliotoxin and all NRPSs and PKSs derived secondary metabolites. It is this combination of roles that makes PptA such an attractive drug target. Removal of *pptA* results in significant viability as well as virulence defects in both bronchopulmonary and disseminated models of infection. Furthermore it leads to an altered immune response in host cells ultimately leaving the fungus far more vulnerable. The low conservation between PptA and its human orthologue AASDHPPT as well as the development of a high throughput screening assay heightens the potential of developing a successful selective inhibiting agent. In the future, the assay should be used to screen inhibitor libraries. Additionally the crystal structure of PptA should be solved and used in *in silico* modelling to aid the identification or development of potential inhibitors.

The third chapter of this thesis focuses on the validation of chemically induced haploinsufficiency profiling in *A. fumigatus.* Currently the majority of drug discovery involves high throughput *in vitro* screening of various compounds against a preselected drug target. Drugs found in this manner can be successful however a prior knowledge of potential drug targets is required. Another problem facing drug development is the unknown mode of action

of current pipeline drugs. Knowing the mode of action can also allow further potential drug discovery options to be exploited such as target crystallisation and *in silico* discovery. Chemically induced haploinsufficiency profiling tackles these issues; as it requires no prior knowledge of specific targets and would assist in identifying the mechanism of action of current pipe line drugs. Additionally, the *in vitro* nature of this profiling technique permits only cell entering drugs that remain significantly un-metabolised to be identified. Past studies have shown that this technique can be successfully used in *S. cerevisiae* and *C. albicans* (6-8). This project aimed to validate the application in the fungal pathogen *A. fumigatus* and demonstrates a chemical genomics system that can be used in a cost effective manner to rapidly and reproducibly identify the mechanism of action of antifungal compounds that are active against filamentous fungi. One of the issues surrounding parallel fitness studies in filamentous fungi is the ability to exchange genetic material between cells through vegetative cell fusion (9) as such exchanges could possibly mask fitness deficiencies. This study revealed *A. fumigatus* undergoes very little cell fusion events especially in liquid shake cultures therefore allowing the parallel assessment of fitness using multiple strains. A library of 46 gene deletion mutants (known drug targets or known to be essential for viability) in a diploid KU80 *A. fumigatus* isolate (AFMB3) were generated using an optimised 96-well plate based, high-throughput gene knockout strategy. The library was grown in sub-lethal levels of itraconazole or brefeldin. DNA was isolated from the cultures and next generation sequencing (NGS) was used to measure the change in relative abundance of each strain. As expected single strains with a mutation in the drug target showed reduced fitness when grown in the presence of that drug *arf2*$^{+/-}$ in the presence of brefeldin A and *erg11a*$^{+/-}$ in the presence of itraconazole. RT-PCR was successfully used to validate the results from NGS. This technique can now be adapted to larger libraries of mutant strains for the high throughput identification of good quality drug targets to enable development of new molecular agents, which inhibit filamentous fungi via a novel mechanism of action.

Chapter 4 explores the phosphatome of *A. fumigatus*. Correct regulation of phosphatases and kinases is vital to ensure the equilibrium of phosphorylation cycles are maintained and therefore are both essential components for cellular homeostasis (10). As a result phosphatases have been recognised as potential drug targets not only for human disease but also against human pathogens (11-17). Phosphatase domain analysis and construction of phylograms showed the well conserved nature of phosphatases amongst the *Aspergillus spp.* It also allowed the identification of numerous fungal specific clusters within several families of phosphatases. This chapter also validated an additional method for measuring parallel fitness of mutant strains as a means to identify potential drug targets. A library of 38 mutants with a

single null phosphatase gene in each strain was generated in the haploid KU80 *A. fumigatus* isolate (A1160p+). 5 essential phosphatases were identified in *A. fumigatus* with only 1, NimT, showing enough divergence from a human orthologue to be considered as a high priority for inhibitor development. *In vitro* parallel fitness of the remaining 33 strains was assessed by NGS using an in-house Ion PGM System. Biological and technical replicates showed high reproducibility, proving this technology as a suitable method for *in vitro* fitness measurements. The parallel fitness data was compared to growth rate data of strains grown individually. The *in vitro* fitness analysis gave 2 potential drug target candidates NemA and PtcB which cause a reduction in fitness in their absence and also show significant divergence from human orthologues. Future work should include replicating this work *in vivo.* A successful method to measure *in vivo* parallel fitness could drastically reduce the numbers of animals used in infection experiments, therefore making it very ethically relevant. When attempting *in vivo* parallel fitness profiling very low levels of reproducibility were observed. Therefore it is essential that future work should focus on a better DNA isolation method to separate fungal and host DNA. Moreover, NGS DNA preparation should be optimised to minimise the number of PCR steps and cycles which in turn could reduce the overall error rate in the enriched DNA fragments. Further drug target validation techniques, similar to those found in chapter 2 of this thesis, could now be applied to the 3 high priority potential drug targets, NimT, NemA and PtcB identified in this project. Additionally this technology could be applied to other libraries of mutant strains, such as *A. fumigatus* kinome deletion mutants, in a large scale attempt to identify novel drug targets.

5.1 References

1. Denning DW, Bromley MJ. How to bolster the antifungal pipeline. Science. 2015;347(6229):1414-6.
2. Denning DW, Hope WW. Therapy for fungal diseases: opportunities and priorities. Trends in microbiology. 2010;18(5):195-204. Epub 2010/03/09.
3. MRC strategic review of fungal disease research in the UK. MRC, 2014.
4. Walsh CT, Gehring AM, Weinreb PH, Quadri LE, Flugel RS. Post-translational modification of polyketide and nonribosomal peptide synthases. Current opinion in chemical biology. 1997;1(3):309-15. Epub 1998/07/17.
5. Lambalot RH, Gehring AM, Flugel RS, Zuber P, LaCelle M, Marahiel MA, et al. A new enzyme superfamily - the phosphopantetheinyl transferases. Chemistry & biology. 1996;3(11):923-36. Epub 1996/11/01.
6. Giaever G, Shoemaker DD, Jones TW, Liang H, Winzeler EA, Astromoff A, et al. Genomic profiling of drug sensitivities via induced haploinsufficiency. Nature genetics. 1999;21(3):278-83. Epub 1999/03/18.
7. Xu D, Jiang B, Ketela T, Lemieux S, Veillette K, Martel N, et al. Genome-wide fitness test and mechanism-of-action studies of inhibitory compounds in *Candida albicans*. PLoS pathogens. 2007;3(6):e92. Epub 2007/07/03.
8. Jiang B, Xu D, Allocco J, Parish C, Davison J, Veillette K, et al. PAP inhibitor with in vivo efficacy identified by *Candida albicans* genetic profiling of natural products. Chemistry & biology. 2008;15(4):363-74. Epub 2008/04/19.
9. Read ND, Fleißner A, Roca GM, Glass NL. Hyphal Fusion. In: Borkovich KA, Ebbole D, editors. Cellular and Molecular Biology of Filamentous Fungi: American Society of Microbiology; 2010. p. 260-73.
10. Bauman AL, Scott JD. Kinase- and phosphatase-anchoring proteins: harnessing the dynamic duo. Nature cell biology. 2002;4(8):E203-6. Epub 2002/08/01.
11. McConnell JL, Wadzinski BE. Targeting protein serine/threonine phosphatases for drug development. Molecular Pharmacology. 2009;75(6):1249-61.
12. Nunes-Xavier C, Roma-Mateo C, Rios P, Tarrega C, Cejudo-Marin R, Tabernero L, et al. Dual-specificity map kinase phosphatases as targets of cancer treatment. Anti-Cancer Agents in Medicinal Chemistry. 2011;11(1):109-32.
13. Ríos P, Nunes-Xavier CE, Tabernero L, Köhn M, Pulido R. Dual-specificity phosphatases as molecular targets for inhibition in human disease. Antioxidants & Redox Signaling. 2013;20(14):2251-73.
14. Silva AP, Tabernero L. New strategies in fighting TB: targeting *Mycobacterium tuberculosis*-secreted phosphatases MptpA & MptpB. Future medicinal chemistry. 2010;2(8):1325-37. Epub 2011/03/24.
15. Bliska JB, Guan KL, Dixon JE, Falkow S. Tyrosine phosphate hydrolysis of host proteins by an essential *Yersinia* virulence determinant. Proceedings of the National Academy of Sciences of the United States of America. 1991;88(4):1187-91. Epub 1991/02/15.
16. Kastner R, Dussurget O, Archambaud C, Kernbauer E, Soulat D, Cossart P, et al. LipA, a tyrosine and lipid phosphatase involved in the virulence of *Listeria monocytogenes*. Infection and immunity. 2011;79(6):2489-98.
17. Szoor B, Wilson J, McElhinney H, Tabernero L, Matthews KR. Protein tyrosine phosphatase TbPTP1: a molecular switch controlling life cycle differentiation in *trypanosomes*. J Cell Biol. 2006;175(2):293-303.

6. Appendix

During the course of this PhD it was identified that the PptA null mutant of *A. fumigatus* produced a significant increase of total secreted proteins including the industrial important enzyme, cellulase. This novel finding was explored further as a side project and detailed in the following section of this thesis.

The effect of *pptA* on industrial protein production yields

Anna Johns, Michael Bromley

Abstract

Filamentous fungi have been used in the biotechnological industry to produce enzymes for a large range of applications. Strategies have been continuously employed to improve the yields of proteins made by these organisms. This study has shown that removal of the Sfp-type 4'-Phosphopantetheinyl transferase, PptA, leads to a greater yield of total protein and cellulases produced by *Aspergillus fumigatus* and the industrial relevant strain, *Aspergillus niger.* Furthermore, we identified the gene encoding PptA in *Trichoderma reesei,* a strain commonly utilised to produce high yields of enzyme in the industrial sector. We show that removal of this gene resulted in hyper-growth under certain conditions and also an increase yield of cellulases.

6.1. Introduction

Filamentous fungal hosts have been used for several decades to produce enzymes for biotechnological use with wide applications in the paper, food, brewing, detergent, starchsaccharification and animal feed industries amongst others (1, 2). The popularity of using these hosts is due to a number of factors including; their capability to secrete vast amounts of protein, the ease at which they are grown in well-defined media and the ability to effortlessly scale-up cultures.

In particular, high yield production strains of *Trichoderma reesei* and *Aspergillus niger* are used for the manufacture and secretion of bulk enzymes. With current industrial production strains secreting 100 g/L homologous under optimized fermentation (3). Nonetheless, higher yields and therefore lower enzyme cost is critical if the full economic benefit and potential applications are to be reached. For example, reducing enzyme cost is widely recognized as the single biggest economic barrier to the mass conversion of lignocellose waste for bioethanol production (4). Strategies to achieve this reduced cost include; sourcing low cost fermentation ingredients, fermentation protocol modification and strain improvement. The industrial global market is continuously increasing with an approximate worth of $4.8 billion in 2013 and predictions that it will reach around $7.1 billion by 2018 (5). Some of the leading companies involved in enzyme production include: Novozymes, Roche and Dupont (2). It is a highly competitive industry with each company striving to produce high quality enzymes, maximise performance and to produce a constant stream of inovation (6).

One of the main types enzymes produced by this industry is cellulase. The process of converting cellulosic materials to fermentable sugars is expensive and therefore companies are always searching for a way to improve production (7). *Trichoderma* and *Aspergilli spp*. have been comprehensively studied because of their ability to produce highly active cellulases capable of extensively degrading insoluble cellulose to soluble sugars in vitro (8-10). Several attempts have been made to generate hypercellulase strains, with some success. One example includes several rounds of random mutagenesis to generate Tricoderma strain, RUT-C30 (11-13). RUT-C30 mutants showed approximately 15-20 fold increase in cellulase activity over the wild type QM6a (14). Another example is an *A. niger* strain, NCIM 1207, which showed a hyer-increase in β-glucosidase and β-xylosidas (10, 15).

This study involves a more directed approach to strain development rather than the traditional random mutagenisis approaches previously descibed. We have developed strains with an increase in the production of extracellular proteins in particular cellulases, accomplished by

the deletion of the Sfp-4'-phosphopantetheinyl transferase gene (also known as npgA, pptA and ppt1).

4'-Phosphopantetheinyl Transferase (4'-PPTase) mediates the transfer and covalent tethering of 4'-phosphopantetheine (P-pant) from coenzymeA (CoA) to a conservered serine residue within the peptidyl carrier domain of the protein substrate (16, 17). This process changes the inactive apoenzyme into an active holo-enzyme and is known as phosphopantetheinylation (17) (Figure 5.1). It is a key post-translational step for a range of enzymes involved in both primary and secondary metabolism to give an array of natural products, such as; lysisne biosynthesis, fatty acid biosynthesis, non-ribosomal peptide (NRP) and polyketide (PK) to aid production of metabolites (16-19).

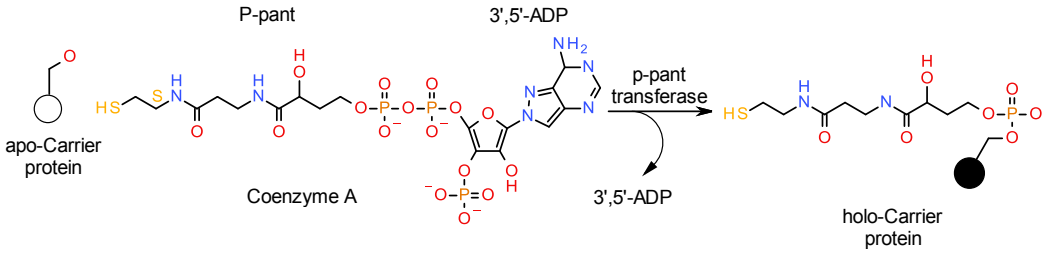

Figure 6.1: Phosphopantetheinylation. The 4'-phosphopantetheine (P-pant) group within Coenzyme A is transferred to a conserved serine residue in the peptidyl carrier domain of the inactive apo-carrier protein to create an active holo-carrier protein. This process is facilitated by 4'-Phosphopantetheinyl transferase (4'-PPTase) (adapted from (17)).

There are three classes of 4'-PPTases; Sfp-type, ACPs-type and one that plays an integral role in fatty acid biosynthesis (20). The Sfp-type (surfactin phosphopantetheinyl transferase) enzyme activates α- aminoadipate reductase which is essential in lysine biosynthesis (21), it also activates PKS and NRPS which are vital in secondary metabolism (17, 22, 23). ACPs-type (acyl carrier protein) enzymes prime apo-acyl carrier proteins, allowing tethering of a growing fatty acyl chain. The final type of 4'-PPTases is an integral domain found at the C-terminal of the fatty acid synthase alpha subunit where is acts to transfer the phosphopantethinyl group to its acyl carrier protein domain to allow assembly of megasynthatase complexes (24).

In *Aspergillus nidulans* the Sfp-type 4'-PPTase gene is known as npgA (18). NpgA has been well characterised, shows a wide array of activity and is responsible for the phosphopantetheinylation of enzymes involved in primary and secondary metabolism (23). This includes polyketide synthase, WA, required for melanin pigment synthesis (25), α-aminoadipate reductase required for lysine biosynthesis, NRPS SidC and SidD, components of intracellular and extracellular siderophore biosynthesis (26, 27) and NRPS δ-(L-α-aminoadipyl)-L-cysteinyl-D-valine synthetase required for penicillin biosynthesis (23). Without

supplementation of the siderophore triacetylfusarinine C (TAFC) and lysine the npgA knockout mutant will not grow (23), therefore making this gene essential to the viability of *A. nidulans*.

The *Aspergillus fumigatus* orthologue of npgA is pptA which also activates several proteins and so has noticeable effects on many similar pathways (18). As in *A. nidulans* the pptA knock out mutant is auxotrophic for lysine and has been shown to activate AARA *in vitro* (28). In contrast to the situation in *A. nidulans* however, *A. fumigatus* is able to acquire free iron without the need for siderophores due to the action of an operative reductive iron assimilatory system (26). The ability to grow when lysine and iron supplementations are present reflect pptA's role in the phosphopantothenylation of AAR and the NRPS SidC (involved in the synthesis of ferrocrocin and hydroxyferricrocin) and potentially SidD (involved in the synthesis of fusarinine C and triacetylfusarinine C) (27). The pptA knockout strain also has albino conidia rather than the normal green colouration. This is due to the lack of pantetheinylation of the polyketide synthase, pksP/alb, which is required for the biosynthesis of WA pigment intermediate (28) which is in turn necessary for the synthesis of PK-derived DHN-melanin pigment. Sfp-PPTase is also found in *Aspergillus niger* and has been called pptA. Consistent with other findings it has been shown to be vital in melanin, lysine and siderophore production with the null mutant growth rescued in the presence of lysine and siderophores and it producing white spores (29). Furthermore the above *Aspergillus spp.* Sfp-PPTase has been confirmed as vital components in secondary metabolite production (22, 29) (chapter 2). A similar observation is made with *Trichoderma virens* Sfp-type 4'-PPTase, ppt1. Ppt1 null mutant is auxotrophic for iron and lysine and produces nonpigmented conidia. Ppt1 is required to activate PKS and NRPS responsible for the production of most secondary metabolites (30).

We hypothesised that the lack of secondary metabolite production in PptA knockout isolates would release energy that could be harnessed to increase growth and extracellular protein production. Abolishing PptA in *A. fumigatus, A. niger* and *T. reesei* causes an increase in external cellulase production but no measurable change in extracellular protein production. This behaviour can be harnessed as a valuable resource for the industrial production of enzymes.

6.2. Methods and Materials

6.2.1. Sfp-PPTase identification

The Sfp-type enzyme of *A. fumigatus*, PptA (AFUB_024520) is well characterised (18, 28)(chapter 2). BLASTp (NCBI), using the PptA amino acid sequenced derived from CADRE (http://www.cadre-genomes.org.uk) was used to identify sfp-type 4'-PPTase genes in *Aspegillus niger* and *Trichoderma reesei.* 100 bases upstream and downstream of predicted proteins identified in each species were searched for an appropriate start and stop codons using Artemis. ClustalW 2.1 was used to align the 3 sequences.

6.2.2. Strains

Strains used are listed in table 5.1. *A. fumigatus* and *A. niger* were cultured on Sabaroud agar at 37°C and 30°C respectively in the dark. *T. reesei* was cultured on potato dextrose agar at 30°C in the light. For *A. fumigatus, T. reesei* and *A. niger pptA* null strains, 0.5 mM $FeSO_4$ and 10 mM lysine supplements were added to the media.

Table 5.1: Strains used in this study

Species	Strains	Source
A. fumigatus	A1160 ($Ku80^-pyrG^+$)	FGSC
	AFΔppta ($Ku80^-/pyrG^+/pptA^-$)	Chapter 2
A. niger	A1180 ($kusA^-$)	FGSC
	ANΔppta ($kusA^-/pptA^-$)	This study
T. reesei	QM6a	FGSC
	TRΔpptA ($pptA^-$)	This study

6.2.3. Deletion of pptA

Approximately 1 kb of 5' and 3' flanking regions of pptA were amplified by PCR from fungal genomic DNA using long amp DNA polymerase. Primers P1 and P2 were used to amplify the 5' non-coding region and P3 and P4 were used to amplify the 3' non-coding regions of the *pptA* gene (Table 5.2). The hygromycin resistant gene (*hph*) was amplified incorporating P2 and P3 overhangs with for preparation of all deletion constructs. The PCR products were purified (Qiaquick PCR purification, Qiagen) and deletion constructs prepared by fusion PCR. The three appropriate fragments were mixed and subjected to fusion PCR using nested primers P5 and P6. Fusion PCR products were purified before being used to transform. Fungal mycelia was treated with Glucanex (Novozymes) for 2–3 h at 30°C to produce protoplasts. DNA was transformed into protoplasts by PEG-mediated transformation. Transformants were screened for homologous recombination by PCR.

Table 6.2: Primers used to generate gene deletion cassette

Primer	Sequence
Aspergillus fumigatus	
AFUB_024520AP1	CCGGTCTCTTTCTCTGCATC
AFUB_024520AP2	TAGTTCTGTTACCGAGCCGGTCAAACGAGGGAGGAGTCAG
AFUB_024520AP3	GCTCTGAACGATATGCTCCCCCATGCAATATTCCACAGGA
AFUB_024520AP4	CGGCGTACAGTTCGACATTA
AFUB_024520AP5	CGTCCACCTGGATACCTTGT
AFUB_024520AP6	TCTTCATTGGCAACCATCAG
Aspergillus niger	
An12g03950_P1	GACCTCCACACTATCTGCCA
An12g03950_P2	TAGTTCTGTTACCGAGCCGGCTGATGTGAGGAGATCGGGC
An12g03950_P3	GCTCTGAACGATATGCTCCCAAAGAAACCCATGGCCTCGT
An12g03950_P4	ATTGTGCTCCGTATCGCTGG
An12g03950_P5	CAGGAAGGGCAAGTCGAGAG
An12g03950_P6	GTTTCAAGTGGGTTATGCGCT
Trichoderma reesei	
ID 41504 _P1	TCGAAAGTCTCGAAACATAAGC
ID 41504 _P2	TAGTTCTGTTACCGAGCCGGTGTCTCTTTGATGGCCTGCA
ID 41504 _P3	GCTCTGAACGATATGCTCCCAACGGGACATCAGATTGCGA
ID 41504 _P4	ACTCTTCTCTTGTTGGCGCA
ID 41504 _P5	CTCCCACAAACCCGTTCTC
ID 41504 _P6	CTCGACGTTCCCATCAAGCT

6.2.4. Radial growth rate

To ensure uniformity between Δ*pptA* and parental strains, growth rate was determined by daily diameter measurements of a single colony grown on solid media were made. 20 ml of molten Vogel's minimal media (VMM) (31) containing 1.5% agar, 1% glucose, 0.5 mM $FeSO_4$, 10 mM lysine was added to 9 cm petri dishes. $1x10^4$ spores of each strain was dispensed on to the centre of the dish. This was done in triplicate. Colony diameter measurements were taken daily.

To obtain photographs of the strains, $1x10^4$ spores of each strain was dispensed on to the centre of the plate containing VMM with 1.5% agar and 1% glucose. Media was either; unsupplemented, supplemented with 0.5 mM $FeSO_4$ or 10 mM lysine or both 0.5 mM $FeSO_4$ and 10 mM lysine. Plates were left to grow for 72 hours. A Canon PowerShot Pro Series digital camera was used to photograph strains.

6.2.5. Determination of grow rates in liquid cultures

To ensure Δ*pptA* and parental strains grew at similar rates in carboxymethyl cellulose (CMC) liquid media a growth assay was performed. VMM containing 1% CMC, 1% glycerol/lactose/glucose and 0.01% tween 20 was either; unsupplemented, supplemented

with 0.5 mM $FeSO_4$ or 10 mM lysine or both 0.5 mM $FeSO_4$ and 10 mM lysine. Each media type was inoculated with $2.5x10^5$ spores/ml of each strain. 200 µl of the media/spore mixture was transferred into a well of a 96-well plate to give $5x10^4$ spores per well. 10 replicates of each strain were included in the plate as well as 2 replicates of a control containing sterile media. The plate was sealed with a "breathe easy" covering membrane (Sigma-Aldrich) and placed on a microplate scanning spectrophotometer (BIO TEK® Synergy HT). The temperature was set at 37°C for *A. fumigatus* or 30°C for *A. niger* and *T. reesei* and KC4 v3.02 software was used to measure the optical density at 600 nm every 10 minutes over a 48 hour time period. Fungal growth was determined by calculating the velocity of the linear phase of the growth curve. A Student's T-test was used to determine differences in fungal strains.

6.2.6. Coomassie (Bradford) protein assay

250 ml conical flasks containing liquid VMM consisting of 1% CMC, 1% glycerol/1% lactose/1% glucose, 0.5 mM $FeSO_4$, 10 mM lysine were inoculated with $2x10^6$ spores/ml of Δ*pptA* and parental strains. Each strain was grown with 4 replicates and a negative control (media only). Cultures were shaken at 200 rpm at 37°C for *A. fumigatus* or 30°C for *A. niger* and *T. reesei*, 1 ml aliquots were taken from the supernatant and filter sterilised daily.

A coomassie protein assay kit (thermo scientific) was used to determine the amount of protein in each sample following the manufacturer's protocol. BSA protein standards were diluted in culture media. Each sample was tested in duplicate/triplicate. The absorbance was measured at 595 nm on a microplate scanning spectrophotometer (BIO TEK® Synergy HT). A standard curve was prepared by plotting the average blank corrected measurement for each standard verses its concentration in µg/ml. A Student's T-test was used to determine differences in fungal strains

6.2.7. Clearance zone assay

10 ml molten VMM agar media consisting of 1.5% agar, 1% glucose, 0.5 mM $FeSO_4$ and 10 mM lysine was poured and allowed to set in 9 cm petri dishes. 6 ml of the same media with 1% CMC was poured on top in an even layer and allowed to set. $1x10^4$ spores of each strain (parental strain and associated Δ*pptA* mutant) was dispensed on to the centre of the plate, in triplicate. The colony was allowed to grow at 37°C for *A. fumigatus* and 30°C for *A. niger* and *T. reesei* for 4 days. The petri dish was flooded with 10ml congo red (0.1%, v/v) solution and left for 25 minutes. The congo red solution was removed and 2 washes with 10 ml dH_2O followed by 2 washes with 1 M NaCl were performed. Diameter and halo width measurements were made and averaged. The colony and clearance zone area were calculated and a ratio of colony: clearance zone was derived. A Student's T-test was used to determine the statistical significance between colony: clearance zone ratios of the different fungal strains.

6.3. Results

6.3.1. Identification of a Sfp-PPTase in *T. reesei*

Contrary to previous findings (30), bioinformatic analysis of the *T. reesei* genome identified an orthologue to *A. fumigatus* PptA (protein ID 41504). An alignment of the *A. fumigatus* PptA protein sequence and orthologues found in *A. niger* and *T. reesei* are shown in Figure 5.3. The 2 *Aspergilli spp* show a relatively high level of sequence conservation with a Clustal W pairwise alignment score of 52.83 and a BLASTp identity of 51% (96% coverage) (table 5.3). When comparing the Aspergillus proteins to *T. reesei,* with Clustal W pairwise alignment scores were less than 30 and BLASTp identities were less than 35% (table 5.3). The conserved motif that distinguishes fungal PPTases, (I/V/L)G(I/V/A/T)D(I/V/L)(x)n(F/W)(A/S/T/C)x (K/R)E(S/A)h(h/S)K(M/L/A/F) where n is 41-107 aa, and 'h' is an amino acid with a hydrophobic side chain (chapter 2), can be found in all species (figure 5.2).

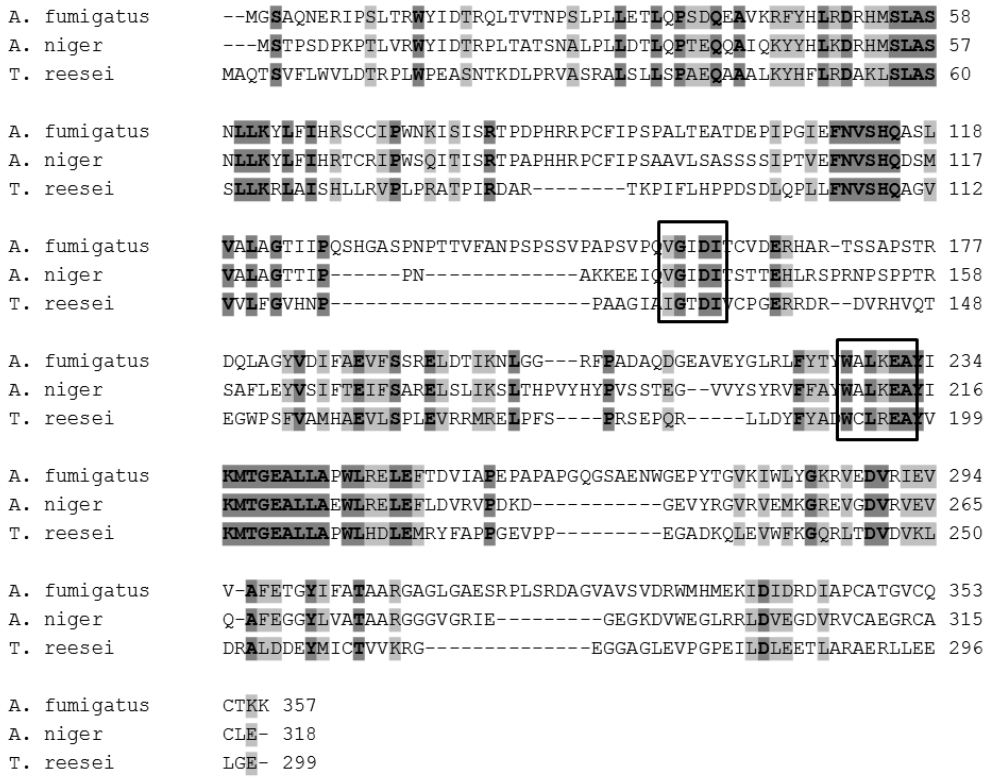

Figure 6.2: Sequence alignment of *A. fumigatus* PptA and the *A. niger* and *T. reesei* orthologues. ClustalW software was used to align sequences. Dark grey shading and bold lettering indicates positions which have a single, fully conserved residue. Light grey shading indicates conservation between groups of strongly similar properties - scoring > 0.5 in the Gonnet PAM 250 matrix. Black boxes indicate a conserved PPTase signature (32).

Table 6.3: List of Clustal W pairwise alignment scores and BLASTp analysis between *A. fumigatus* PptA, *A. niger* PptA and *T. reesei* (protein ID 41504)

Sequence A	Length	Sequence B	Length	ClustalW Alignment Score (%)	BLASTp analysis	
					Identity (%)	Cover (%)
A. fumigatus	357	*A. niger*	318	52.83	51	96
A. fumigatus	357	*T. reesei*	299	26.76	31	89
A. niger	318	*T. reesei*	299	28.76	33	90

6.3.2. Sfp-PPTase is required for normal growth in all species

To establish whether the absence of Sfp-type 4'-PPTase leads to an increase in overall protein production *A. niger* (An12g03950) and *T. reesei* (protein ID 41504) genes were deleted. PCR fusion was used to generate a knock out cassette and a hygromycin resistance gene (*hph*) was used as a selectable marker. Gene replacement was confirmed by PCR. The *A. fumigatus pptA* null mutant was generated in a previous study (Chapter 2). The deletion mutants will be referred to as Δ*pptA* mutants with prefixes AF (*A. fumigatus*); AN (*A. niger*) and TR (*T. reesei*).

All deletion mutants have a white phenotype consistent with the expected defect in the biosynthesis of melanin (figure 5.3). Consistent with previous studies both *Aspergillus spp.* require supplemental lysine and iron to restore growth to parental phenotype. In contrast to this, the *T. reesei pptA* null mutant is able to grow without the need for additional iron. After 48 hours the colony diameter of the *T. reesei* null mutant was much larger than that of the parental host and exhibited a fluffy, white phenotype consistent with PPT1 null mutant of *T. virens* (30).

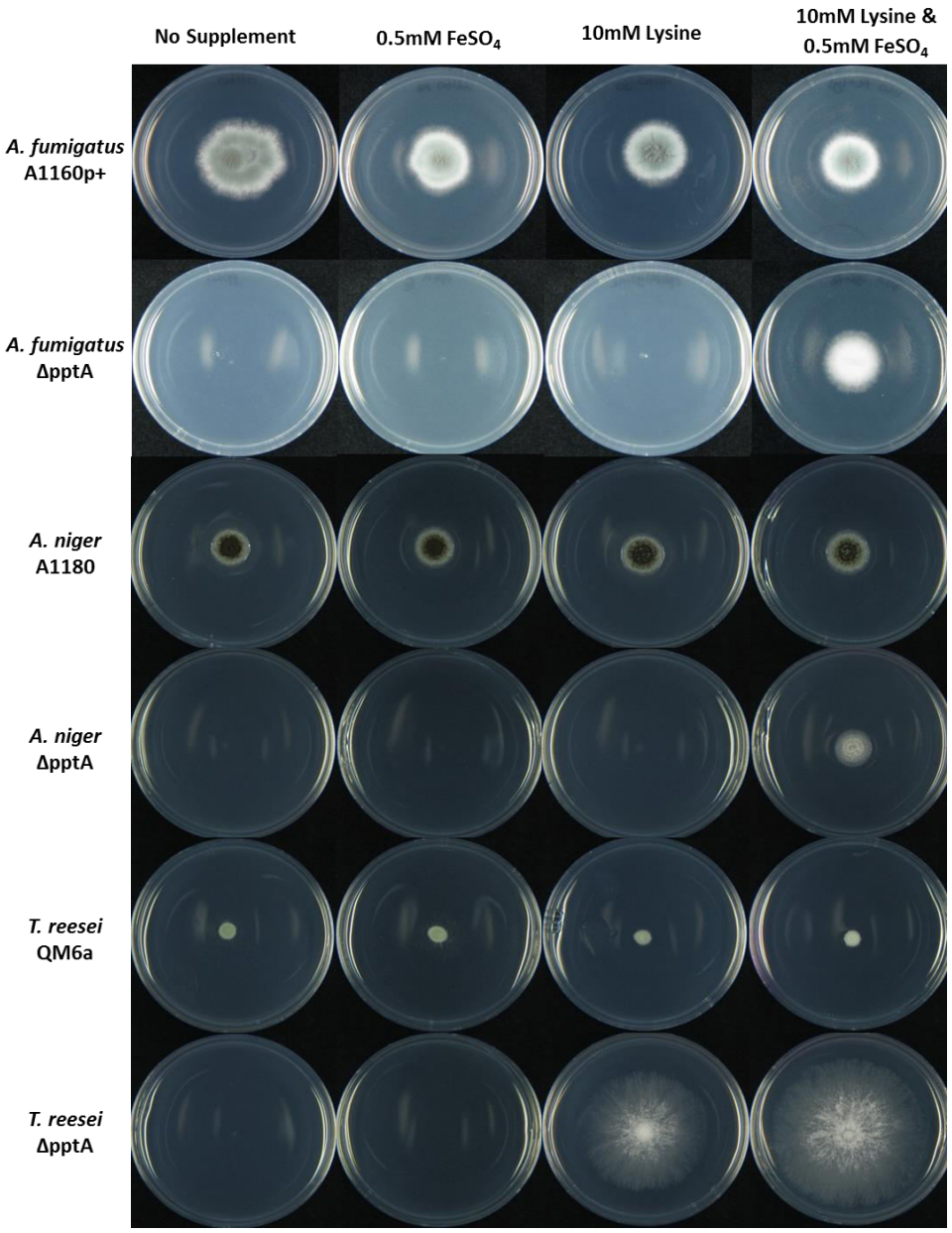

Figure 6.3: Photographs of parental and Δ*pptA* strains. 1x10^4 spores from *A. fumigatus*, *A. niger* and *T. reesei* strains were spotted on to VMM cotaining; no supplement, 0.5 mM supplemental iron ($FeSO_4$), 10 mM supplemental lysine or 0.5 mM supplemental iron ($FeSO_4$) and 10 mM supplemental lysine. Cultures were grown at 37°C for 72 hours. As expected the *Aspergillus spp.* Δ*pptA* mutants only grew on media containing both supplements. *T. reesei* Δ*pptA* mutant required only lysine to restore growth.

6.3.3. *T. reesei* Δ*pptA* exhibits an increased growth rate in the presence of lysine

Radial growth rate measurements of parental and Δ*pptA* isolates were taken on VMM or VMM with supplemental; iron, lysine or both iron and lysine. *A. fumigatus* parental strain, A1160p+, showed similar growth rate in all conditions whereas the Δ*pptA* only grew if both supplements were present (figure 5.4A). *A. niger* strains behaved in a similar manner to the *A. fumigatus* isolates (figure 5.4B). The *T. reesei* parental strain grew at similar rates in all conditions however, strikingly the *T. reesei* Δ*pptA* mutant grew at a much faster rate than the parental strain when lysine or both supplements were present in the media. The TRΔ*pptA* was unable to grow in the absence of lysine supplementation (figure 5.4C).

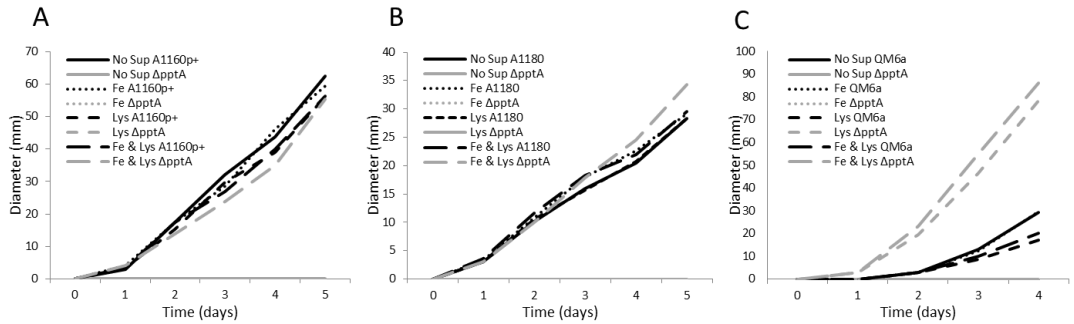

Figure 6.4: Radial growth rates of parental and Δ*pptA* strains. 1x10^4 spores from *A. fumigatus*, *A. niger* and *T. reesei* strains were spotted on to VMM cotaining; no supplement (no sup), 0.5 mM $FeSO_4$ (Fe), 10 mM lysine (lys) or both 0.5 mM $FeSO_4$ and 10 mM lysine (Fe&Lys). A) *A. fumigatus* was grown at 37°C, B) *A. niger* and C) *T. reesei* cultures were grown at 30°C. The diameter was measured daily. The parental strains of each species were unaffected by changes to the media. The *Aspergillus spp*. Δ*pptA* strains required both supplements to restore growth rate to parental strain. The *T. reesei* Δ*pptA* strain required supplemental lysine to restore growth, which led to a much faster growth rate than the parental strain.

To ensure a similar observation is made in liquid media, growth rates were calculated based on a change in OD600 over a 48 hour time period. VMM or VMM supplemented with; iron, lysine or both iron and lysine was used**.** 1% CMC with either 1% glycerol, 1% lactose or 1% glucose was used as the carbon source. The *A. fumigatus* parental strain, A1160p+, showed similar growth rate in all conditions whereas the AFΔ*pptA* only grew if both supplements were present. A reduction in growth rate was observed in the Δ*pptA* isolate even in the presence of both supplements however statistical significance was only achieved in glycerol media (P value < 0.05) (figure 5.5A). As expected the *A. niger* Δ*pptA* required both supplements to restore growth. Interestingly in contrast to what was observed on solid media, the growth rate of ANΔpptA exceeded that of the parental isolate in glycerol media containing iron and lysine (P< 0.05). No significant difference was observed between strains in the lactose or glucose media when both supplements were provided (figure 5.5B). Finally, the *T. reesei* parental strain grew

at the same rate when exposed to different supplements. As with the solid agar, the *TRΔpptA* mutant grew at a much faster rate than the parental strain when lysine or both supplements were present in the media containing glucose (P value < 0.05). However, this was not observed in media containing lactose were the mutant grew at the same rate as the parental strain when lysine or both supplements were present (figure 5.5C). No fungal growth was observed in glycerol media.

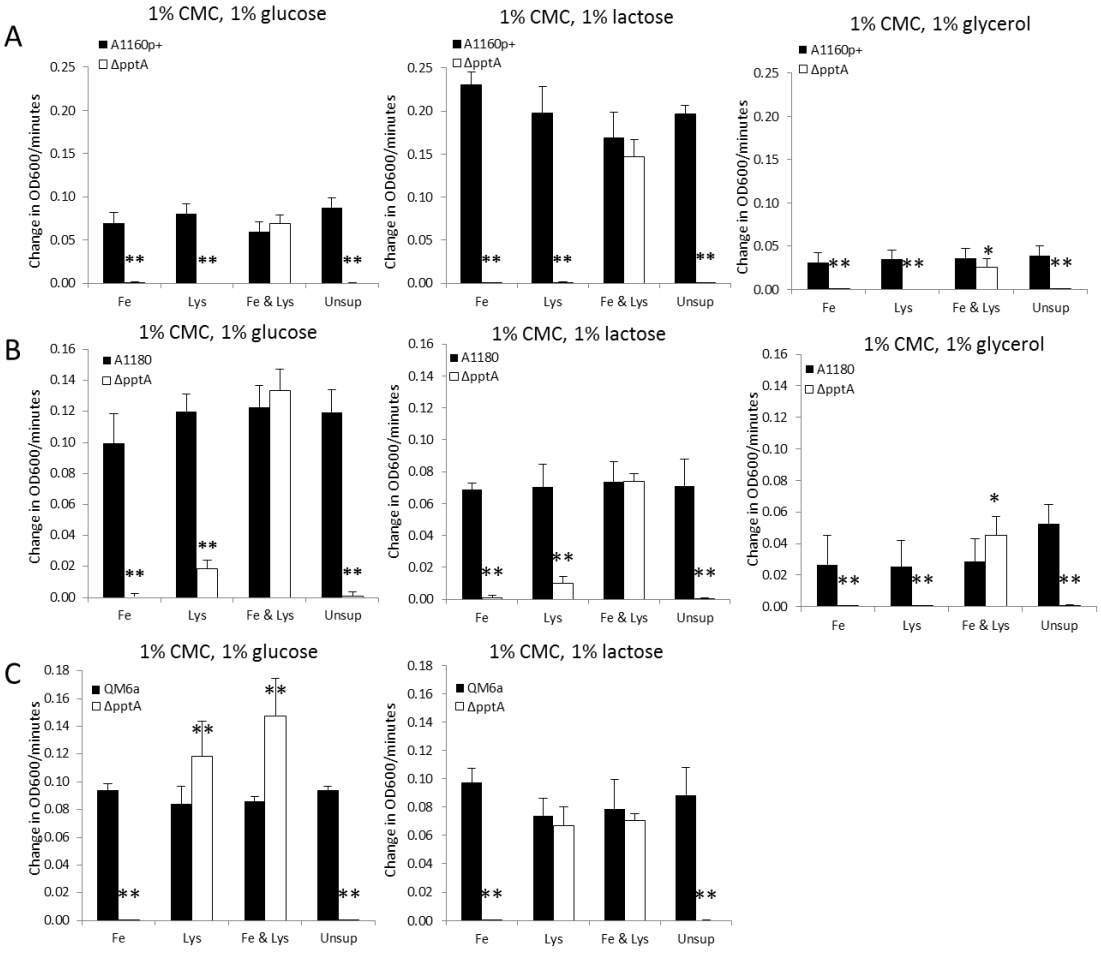

Figure 6.5: Growth rate measurements in 96 well plate. Strains were grown in VMM media that was either; unsupplemented (Unsup), supplemented with 0.5 mM $FeSO_4$ (Fe), supplemented with 10 mM lysine (Lys) or supplemented with both $FeSO_4$ and lysine (Fe & Lys). OD600 was measured every 10 minutes over 48 hours and used to determine the kinetic velocity. The mean value for each strain was plotted into a bar graph. Error bars indicate standard deviation. A) *A. fumigatus* Δ*pptA* and B) *A. niger* Δ*pptA* require both supplements to restore growth. C) *T. reesei* Δ*pptA* requires only lysine. A Student's T-test was used to determine the P value. * P value < 0.05, ** P value < 0.01.

6.3.4. Sfp-PPTases have a significant effect on total protein production under certain conditions

As Sfp-PPTases have an effect on fungal growth we wanted to explore whether they affect total protein production. Strains were grown for 96 hours in supplemented VMM with 1% CMC and either 1% glycerol, 1% lactose or 1% glucose as the carbon source. Samples from the supernatants were taken every 24 hours. A coomassie total protein assay was used to determine the amount of total protein produced by Δ*pptA* strains compared to parental strains. *A. fumigatus* Δ*pptA* produced a significantly higher (P value<0.01) concentration of total protein after 96 hours in media containing glycerol and glucose, however the level of increase was relatively small at 22% and 13% respectively. The opposite is observed for lactose media as the parental strain produces a higher concentration of total protein throughout the time course (P value<0.01 at 48, 72 and 96 hours) (figure 5.6A). *A. niger* Δ*pptA* produces significantly (P value<0.01) more protein at 48-96 hour time points in glycerol media. Significantly (P value<0.01) more protein is produced by ANΔ*pptA* in lactose media up until the 72 hour time point, after which concentrations level off, this may be due to an exhaustion of nutrients. The opposite is observed in glucose media with the *A. niger* parental strain producing more protein up until the 72 hour time point (figure 5.6B). No difference is observed between the *T. reesei* strains in glucose cultures. However, in the lactose media the QM6a strain produced significantly more protein than the Δ*pptA* strain (P value<0.05 at 48 and 72 and P value<0.01 96 hours) (figure 5.6C).

To examine this further in *A. fumigatus,* strains were grown for 120 hours in supplemented VMM with 1% CMC and 1% glycerol as the carbon source. Culture supernatants were taken daily. These were filtered and then run on a protein gel (figure 5.7). Protein bands become more intense as time increases, suggesting an overall increase in total protein however no differentially expressed proteins were observed.

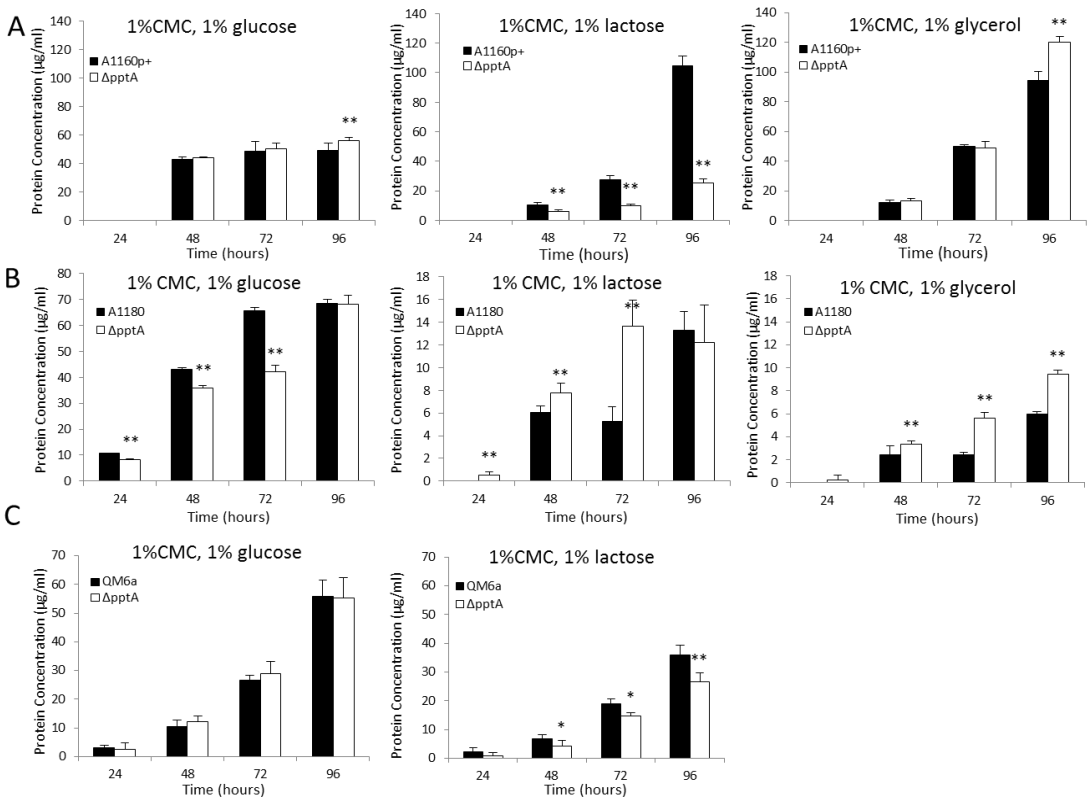

Figure 6.6: Coomassie (Bradford) protein assay. Aliquots from parental and Δ*pptA* cultures were taken daily and used in a coomassie assay to determine total protein concentration. A) *A. fumigatus* cultures show an increase in overall protein production as time increases. In glycerol cultures the Δ*pptA* strain produces significantly more total protein than A1160p+ at 96 hours, however the opposite is observed in lactose cultures. B) *A. niger* Δ*pptA* produces significantly more protein in the glycerol cultures from 48-96 hours. However in lactose cultures the Δ*pptA* produces more protein until 72 hours after which the concentration levels off similar to that A1180. C) *T. reesei* glucose cultures show an increase in overall protein production as time increases but with no real difference between stains. In lactose media the QM6a strain produces significantly more protein. Error bars signify standard deviation. A Student's T-test was used to determine the P value. * P value < 0.05, ** P value < 0.01.

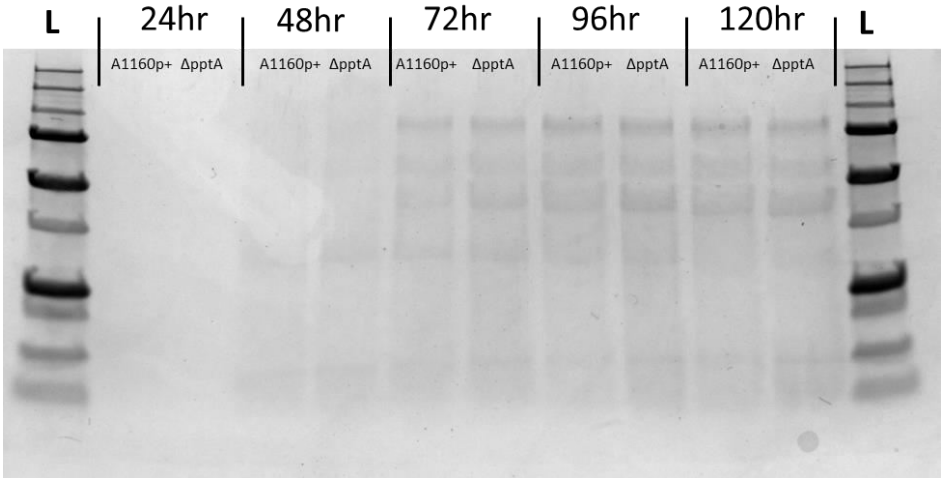

Figure 6.7: Protein gel of *A. fumigatus* supernatants. Aliquots of *A. fumigatus* A1160p+ and Δ*pptA* cultures were taken daily. These were run on a protein gel. The protein bands appear darker as time increases. No difference is observed between strains. A precision plus protein ladder (L) is also loaded on the gel.

6.3.5. An increase cellulase production is caused by Sfp-PPTase deletion

Cellulases are a major enzyme used in the biotechnological sector. It was important to clarify if the Δ*pptA* strains produced a significantly greater amount of the cellulose degrading enzyme. This was determined by performing a cellulose clearance zone assay, where the ratio of clearance zone area to colony area was measured by the addition of congo red. Congo red has a high binding affinity to cellulose, as cellulose is incorporated in the media any area where cellulose degradation has occurred will result in the media remaining unstained. Strains were grown for 96 hours on a thin layer of supplemented VMM with 1% CMC and 1% glucose as the carbon source. In all species a significantly larger clearance zone is observed by Δ*pptA* strains when compared to its parental strain (P value < 0.01) (figure 5.8A-C).

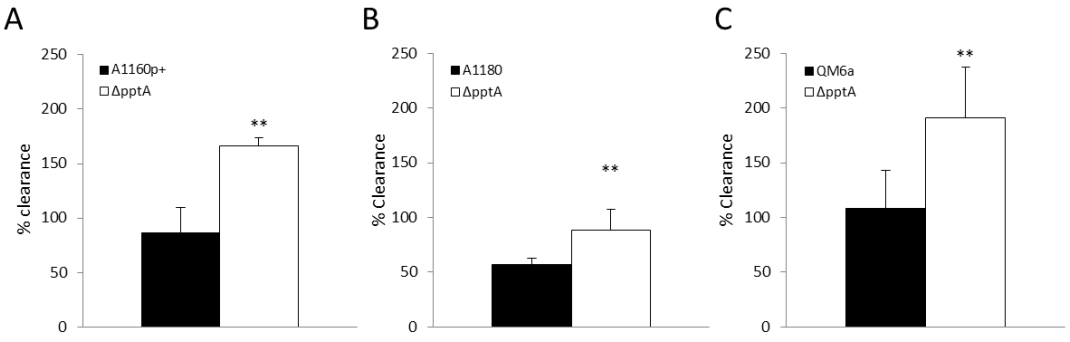

Figure 6.8: Cellulose clearance assay. 1x10^4 spores from A) *A. fumigatus*, B) *A. niger* and C) *T. reesei* strains were spotted on to VMM containing 0.5 mM supplemental iron ($FeSO_4$) and 10 mM supplemental lysine. Cultures were grown for 4 days. Clearance was determined by adding a congo red solution to the plate. The ratio of colony area: clearance zone area was determined for each strain. Error bars signify standard deviation. All Δ*pptA* strains have a significantly greater clearance zone than the parental strains. A Student's T-test was used to determine the P value. ** P value < 0.01.

6.4. Discussion

Over the years many approaches have been taken to increase fungal enzyme yields such as mutagenesis and optimising fermentation processes with the objective to reduce overall costs. In this study we performed a mutation that abolished the Sfp-PPTase which is vital for NRPS and PKS driven secondary metabolism, to test the effect it has on overall protein production in 3 fungal strains, *A. fumigatus, A. niger* and *T. reesei*.

All Δ*pptA* strains required supplementation to grow. *Aspergilli spp.* required both lysine and iron which is consistent with the involvement Sfp-PPTase has in lysine and siderophore synthesis. In contrast *T. reesei* Δ*pptA* strain required only lysine however growth improved with the further addition of iron. The ability of TRΔ*pptA* to grow without supplemental iron, could be explained by low concentrations of iron found in VMM and potentially the lower requirement for iron in *Trichoderma* species compared to *Aspergilli* in the absence of siderophores. It was also observed that *T. reesei* Δ*pptA* strain had a substantial increase in radial growth rate compared to QM6a once supplements had been provided. This was also true in liquid VMM containing 1% CMC and 1% glucose as the carbon source however when glucose was substituted for 1% lactose this was no longer apparent. A similar observation in increased growth has been made in *T. virens* and to a far lesser extent in *A. nidulans* when orthologous Sfp-PPTase was abolished (22, 30). A delay in hyphal branching was postulated to cause this in *A. nidulans* whereas a lack of production of secondary metabolites was hypothesized in *T. virens*. This was further confirmed by the ability to reduce the growth rate of the ppt1 null mutant by growing it in the presence of secondary metabolites produced by the wild type suggesting some of the properties of these metabolites can be detrimental to its growth. This has been seen by one of the antibiotics, Gliovirin, produced by *T. virens*, when overexpression of this gene led to decreased growth compared to the wild type (33). However as the presence of lactose in the media halts the increased growth of the deletion mutant the lack of secondary metabolites may not be the overall cause of this phenomenon or it could be suggested that particular toxins are not produced when the organism is grown in lactose media. Further studies should be carried out to confirm this.

We postulated that the absence of Sfp-PPTase could alter the production of total protein secretions. We grew liquid cultures of parental and Δ*pptA* strains, taking daily samples of their supernatants. A coomassie assay was used to determine total protein concentration. *A. niger* Δ*pptA* strain produced up to 61% and 57% more proteins in lactose and glycerol media. A similar observation was made with *A. fumigatus* Δ*pptA* strain grown in glycerol and glucose

media, where the Δ*pptA* produced 22% and 13% more proteins than A1160p+ at 96 hours respectively.

Cellulases are used in several industries; coffee, textiles, laundry detergents, pulp and paper, pharmaceuticals and biofuels (34). An increase in overall cellulase production in fungal strains would be a valuble assent to any of these industrial sectors. As such we have found that all Δ*pptA* strains produced significantly more cellulase than their parental strain counterpart (P value < 0.01). The *A. fumigatus* Δ*pptA* produced 48% more cellulase whereas *A. niger* and *T. reesei* knock out strains produced 36% and 44% more cellulase respectively than their parental strains.

The ability of Δ*pptA* strains to produce enhanced cellulase yields, and in the case of *Aspergilli spp* increased total protein, we are confident that the mutant is an attractive strain for industrial enzyme production. The only negative for using a Δ*pptA* strain is the added cost of providing supplemental lysine, future work to determine if lower concentrations of lysine are sufficient for fungal growth could drastically limit this expense. This has been shown for AFΔ*pptA* which requires only 2.5mM lysine to restore growth fully, 25% of the concentration used in this study (Chapter 2). Additionally a lysine salt such as L-lysine monohydrochloride could be used as a substitute for pure L-lysine as it can be up to 10 times cheaper (based on pricing on the Sigma website). Futhermore, work to define if any other industry valuable enzymes are produce in greater yields would strengthen the argument of using Δ*pptA* as an industrial strain.

6.5. Acknowledgements

Thanks to the BBSRC for providing A.J. with a CASE studentship.

6.6. References

1. Gerngross TU. Advances in the production of human therapeutic proteins in yeasts and filamentous fungi. Nature Biotech. 2004;22(11):1409-14.
2. Li S, Yang X, Yang S, Zhu M, Wang X. Technology prospecting on enzymes: application, marketing and engineering. Computational and structural biotechnology journal. 2012;2:e201209017. Epub 2012/01/01.
3. Cherry JR, Fidantsef AL. Directed evolution of industrial enzymes: an update. Current Opinions in Biotechnology. 2003;14(4):438-43.
4. Klein-Marcuschamer D, Oleskowicz-Popiel P, Simmons BA, Blanch HW. The challenge of enzyme cost in the production of lignocellulosic biofuels. Biotechnology and Bioengineering. 2012;109(4):1083-7.
5. Global Markets for Enzymes in Industrial Applications. USA: BCC Research, 2014 BIO030H.
6. Adrio JL, Demain AL. Microbial enzymes: tools for biotechnological processes. Biomolecules. 2014;4(1):117-39. Epub 2014/06/28.
7. Eveleigh DE. Cellulase - a Perspective. Philosophical Transactions of the Royal Society A. 1987;321(1561):435-+.
8. Xu F, Wang J, Chen S, Qin W, Yu Z, Zhao H, et al. Strain Improvement for Enhanced Production of Cellulase in *Trichoderma viride*. Applied Biochemistry and Microbiology. 2011;47(1):53-8.
9. Adsul MG, Bastawde KB, Varma AJ, Gokhale DV. Strain improvement of *Penicillium janthinellum* NCIM 1171 for increased cellulase production. Bioresource Technology. 2007;98(7):1467-73.
10. Gokhale DV, Puntambekar US, Vyas AK, Patil SG, Deobagkar D. Hyper production of β-glucosidase by an *Aspergillus* sp. Biotechnology Letters. 1984;6(11):719-22.
11. Montenecourt BS, Eveleigh DE. Semiquantitative plate assay for determination of cellulase production by *Trichoderma viride*. Applied and Environmental Microbiology. 1977;33(1):178-83.
12. Montenecourt BS, Eveleigh DE. Preparation of mutants of *Trichoderma reesei* with enhanced cellulase production. Applied and Environmental Microbiology. 1977;34(6):777-82.
13. Montenecourt BS, Eveleigh DE. Selective screening methods for the isolation of high yielding cellulase mutants of *Trichoderma reesei*. Hydrolysis of cellulose: mechanisms of enzymatic and acid catalysis: American Chemical Society. 1979. p. 289-301.
14. Bisaria VS, Ghose TK. Biodegradation of Cellulosic Materials - Substrates, Microorganisms, Enzymes and Products. Enzyme Microbial Technology. 1981;3(2):90-104.
15. Gokhale DV, Puntambekar US, Deobagkar DN. Xylanase and β-xylosidase production by *Aspergillus niger* NCIM 1207. Biotechnology Letters. 1986;8(2):137-8.
16. Lambalot RH, Gehring AM, Flugel RS, Zuber P, LaCelle M, Marahiel MA, et al. A new enzyme superfamily - the phosphopantetheinyl transferases. Chemistry & biology. 1996;3(11):923-36. Epub 1996/11/01.
17. Walsh CT, Gehring AM, Weinreb PH, Quadri LE, Flugel RS. Post-translational modification of polyketide and nonribosomal peptide synthases. Current opinion in chemical biology. 1997;1(3):309-15. Epub 1998/07/17.
18. Neville C, Murphy A, Kavanagh K, Doyle S. A 4'-phosphopantetheinyl transferase mediates non-ribosomal peptide synthetase activation in *Aspergillus fumigatus*. Chembiochem : a European journal of chemical biology. 2005;6(4):679-85. Epub 2005/02/19.
19. Reuter K, Mofid MR, Marahiel MA, Ficner R. Crystal structure of the surfactin synthetase-activating enzyme Sfp: a prototype of the 4'-phosphopantetheinyl transferase superfamily. 1999. 6823-31 p.

20. Beld J, Sonnenschein EC, Vickery CR, Noel JP, Burkart MD. The phosphopantetheinyl transferases: catalysis of a post-translational modification crucial for life. Natural product reports. 2014;31(1):61-108. Epub 2013/12/03.
21. Ehmann DE, Gehring AM, Walsh CT. Lysine Biosynthesis in *Saccharomyces cerevisiae*: Mechanism of α-Aminoadipate Reductase (Lys2) Involves Posttranslational Phosphopantetheinylation by Lys5. Biochemistry. 1999;38(19):6171-7.
22. Márquez-Fernández O, Trigos Á, Ramos-Balderas JL, Viniegra-González G, Deising HB, Aguirre J. Phosphopantetheinyl transferase CfwA/NpgA Is required for *Aspergillus nidulans* secondary metabolism and asexual development. Eukaryotic Cell. 2007;6(4):710-20.
23. Oberegger H, Eisendle M, Schrettl M, Graessle S, Haas H. 4'-Phosphopantetheinyl transferase-encoding npgA is essential for siderophore biosynthesis in *Aspergillus nidulans*. Current Genetics. 2003;44(4):211-5.
24. Crawford JM, Vagstad AL, Ehrlich KC, Udwary DW, Townsend CA. Acyl-carrier protein-phosphopantetheinyltransferase partnerships in fungal fatty acid synthases. Chembiochem : a European journal of chemical biology. 2008;9(10):1559-63. Epub 2008/06/14.
25. Mayorga ME, Timberlake WE. The developmentally regulated *Aspergillus nidulans wA* gene encodes a polypeptide homologous to polyketide and fatty acid synthases. Molecular & general genetics : MGG. 1992;235(2-3):205-12. Epub 1992/11/01.
26. Schrettl M, Bignell E, Kragl C, Joechl C, Rogers T, Arst HN, et al. Siderophore biosynthesis but not reductive iron assimilation is essential for *Aspergillus fumigatus* virulence. The Journal of Experimental Medicine. 2004;200(9):1213-9.
27. Schrettl M, Bignell E, Kragl C, Sabiha Y, Loss O, Eisendle M, et al. Distinct roles for intra- and extracellular siderophores during *Aspergillus fumigatus* infection. PLoS pathogens. 2007;3(9):1195-207. Epub 2007/09/12.
28. Allen G, Bromley M, Kaye SJ, Keszenman-Pereyra D, Zucchi TD, Price J, et al. Functional analysis of a mitochondrial phosphopantetheinyl transferase (PPTase) gene *pptB* in *Aspergillus fumigatus*. Fungal genetics and biology : FG & B. 2011;48(4):456-64. Epub 2011/01/05.
29. Jørgensen TR, Park J, Arentshorst M, van Welzen AM, Lamers G, vanKuyk PA, et al. The molecular and genetic basis of conidial pigmentation in *Aspergillus niger*. Fungal Genetics and Biology. 2011;48(5):544-53.
30. Velazquez-Robledo R, Contreras-Cornejo HA, Macias-Rodriguez L, Hernandez-Morales A, Aguirre J, Casas-Flores S, et al. Role of the 4-Phosphopantetheinyl transferase of *Trichoderma virens* in secondary metabolism and induction of plant defense responses. Molecular Plant Microbe Interactions Journal. 2011;24(12):1459-71.
31. Vogel HJ. A convenient growth medium for *Neurospora* (medium N). Microbial genetics bulletin. 1956;13:42-3.
32. Asghar AH, Shastri S, Dave E, Wowk I, Agnoli K, Cook AM, et al. The *pobA* gene of *Burkholderia cenocepacia* encodes a group I Sfp-type phosphopantetheinyl transferase required for biosynthesis of the siderophores ornibactin and pyochelin. Microbiology. 2011;157(Pt 2):349-61. Epub 2010/10/23.
33. Howell CR, Stipanovic RD. Gliovirin, a new antibiotic from *Gliocladium virens,* and its role in the biological control of *Pythium ultimum*. Canadian Journal of Microbiology. 1983;29(3):321-4.
34. Kuhad RC, Gupta R, Singh A. Microbial cellulases and their industrial applications. Enzyme Research. 2011;2011:10.